

**INVESTIGATING NOVEL INTERACTION PARTNERS OF AMYLOID PRECURSOR
PROTEIN: THE MECHANISTIC TARGET OF RAPAMYCIN AND PIKFYVE COMPLEX**

BENJAMIN DAVID GUSCOTT

Doctor of Philosophy

ASTON UNIVERSITY

March 2016

© Benjamin Guscott, 2016

Benjamin Guscott asserts his moral right to be identified as the author of this thesis.

This copy of the thesis has been supplied on condition that anyone who consults it is understood to recognise that its copyright rests with its author and that no quotation from the thesis and no information derived from it may be published without appropriate permission or acknowledgement.

**INVESTIGATING NOVEL INTERACTION PARTNERS OF AMYLOID PRECURSOR
PROTEIN: THE MECHANISTIC TARGET OF RAPAMYCIN AND PIKFYVE COMPLEX**

**Benjamin David Guscott
Doctor of Philosophy
2016**

Thesis summary

Previous Work

Although the amyloid precursor protein (APP) is known to have a central role in Alzheimer's disease, its cellular function is poorly characterised.

To better understand the cellular functions of APP, an interactome of APP's intracellular domain (AICD) was generated using a proteo-liposome based assay, which enabled interactions to be identified within a membrane context. In addition to proteins known to bind AICD, novel interactors were identified, including the mechanistic target of rapamycin complex 1 (mTORC1) and the phosphoinositide kinase PIKfyve complex.

Binding of AICD to the two complexes was confirmed by Western blotting of treated AICD-proteoliposomes and pulldowns of purified protein by AICD.

Project Aims

This project aimed to investigate the biological relevance of the APP/mTOR and APP/PIKfyve complex interactions.

Results

Investigation of the APP/mTOR interaction showed mTOR signalling increased in mammalian cells overexpressing APP/AICD, while loss of function studies determined *C. elegans* APP (APL-1) is involved in mTOR ortholog function. The APP/PIKfyve interaction was investigated with APP family knockdown, and TAT-AICD: a new molecular tool to allow acute AICD overexposure within the cell. Knockdown decreased PIKfyve function, while TAT-AICD exposure increased PIKfyve function in mammalian tissue culture.

mTOR and PIKfyve are important to degradative pathway progression, and results suggested APP modulates the activity of these proteins.

Protein degradation is important in human disease, including Alzheimer's disease. Experiments elaborating APP relevance in the lysosome demonstrated that APP degradation is dependent on sorting, endosomal acidification and the inhibition of mTOR. Further experiments linked PIKfyve inhibition to these degradative processes, in particular, to lower organelle acidification and altered late endosome morphology.

Summary

These results suggest an interdependence between APP, mTOR and PIKfyve, where APP appears to impact lysosomal function, while also being dependent upon it for down-regulation.

Key words: Alzheimer's disease, AICD, APP, cell penetrating peptide, mTOR.

Acknowledgements

I would like to thank Alzheimer's Research UK for funding and supporting my studies, and wish to express gratitude to my supervisors Dr Thomas Wassmer and Dr. Zita Balklava for support throughout my study, your enthusiasm, patience and insight have been valuable for my continued growth. I would also like to thank Dr. Stephane Gross and Dr. Alice Rothnie for their comments and encouragement, and Dr Lindsay Marshall for continued support and comments throughout the corrections process.

I would like to show my appreciation to new and old colleagues alike. I'm thankful to those at the University of Birmingham for their understanding, support and advice; while those at the Institute of Aquaculture, University of Stirling started me on the road to further education.

To everyone I've come to know at Aston University, thank you for the good times, for your encouragement and some much needed distraction. I would like to thank my friends among the University of Exeter and Coastal Carolina University alumni, for their continued friendship in spite of my distance and the limited time I've been able to spare. In particular I'm grateful to Daniel Wise, Cora Paine, Ruth Aldred and Rachel Manley for shared laughter, discussions and experiences.

To my family, I would like to thank you for making me who I am, quirks and all.

Finally, I am indebted to Doctor Emily Burns, who has not only been a continued source of support and encouragement, but also pivotal to the completion of this work.

List of Abbreviations

4EBP1 = 4 E binding protein 1
Ac = Acidic domain
ADP = Adenosine diphosphate
AICD = Amyloid precursor protein intracellular domain
Akt = Protein kinase B
ALFY = Autophagy linked FYVE protein
ALS = Amyotrophic lateral sclerosis
Ambra1 = Activating molecule of Beclin 1-regulated autophagy 1
AP = Adaptor protein
APL-1 = Amyloid precursor-like
APLP1 = APP like protein 1
APLP2 = APP like protein 2
APPL = Amyloid precursor protein-like
APOE = apolipoprotein E
APP = Amyloid precursor protein
ATP = Adenosine triphosphate
A β = Amyloid beta
BACE-1 = Beta secretase -1
C. elegans = *Caenorhabditis elegans*
CCV's = Clathrin coated vesicles
CFD = Corneal fleck dystrophy
CFP = Cyan fluorescent protein
CI-MPR = Cation independent mannose-6-phosphate receptor
CME = Clathrin mediated endocytosis
CMT4J = Charcot-Marie-Tooth Neuropathy Type 4J
COPI = Coat protein complex 1
COPII = Coat protein complex 2
CPP = Cell Penetrating Peptide
Crb = Crumbs
CuBD = Copper binding domain
DAG = Diacylglycerol
DEPTOR = DEP domain containing mTOR interacting protein
D. melanogaster = *Drosophila melanogaster*
E1 = Ectodomain 1
E1 enzyme = E1-activating enzyme
E2 = Ectodomain 2
E2 enzyme = E2-conjugating enzyme
ECM = Extracellular matrix
E. coli = *Escherichia coli*
EEA1 = Early endosome antigen 1
EGFR = Epidermal growth factor receptor
ER = Endoplasmic reticulum
ESCRT = Endosomal sorting complexes required for transport
FOXO = Fork head box protein O
GAK = Cyclin G-associated kinase
GAP = GTPase-activating protein
GDP = Guanosine diphosphate
GDI = Rab-GDP dissociation inhibitor
GEF = GDP/GTP exchange factor
GFP = Green fluorescent protein
GTP = Guanosine triphosphate
GVD = Granulovacuolar Degeneration
GWAS = Genome-wide association studies
HBD = heparin binding domain
HEK-293t = Human embryonic kidney 293 cells

HSC70 = heat shock cognate 70
 HPLC = high performance liquid chromatography
 KPI = Kunitz-type protease inhibitor
 LAMP = Lysosomal associated membrane protein
 LC3 = Light chain 3
 LDL = Low density lipoprotein
 LTP = Long term potentiation
 MBP = Maltose binding protein
 ML1N = N-terminal polybasic domain of TRPML-1
 mLST8 = Mammalian lethal SEC13 protein 8
 MMSE = Mini mental status examination
 mSIN1 = Mammalian stress-activated protein kinase interacting protein 1
 mTOR = Mechanistic target of rapamycin
 mTORC1 = mTOR complex 1
 mTORC2 = mTOR complex 2
 MVB = multi vesicular body
 NMR = Nuclear magnetic resonance
 NMDA = *N*-Methyl-D-aspartic acid
 PCR = Polymerase chain reaction
 PDZ domain = Post synaptic density protein (PSD95), *Drosophila* disc large tumor suppressor
 PH = Pleckstrin Homology
 PI = Phosphatidylinositol
 PI(3)P = Phosphatidylinositol 3 phosphate
 PI(3,4)P₂ = Phosphatidylinositol 3,4 bisphosphate
 PI(3,4,5)P₃ = Phosphatidylinositol 3,4,5 triphosphate
 PI(3,5)P₂ = Phosphatidylinositol 3,5 bisphosphate
 PI(4)P = Phosphatidylinositol 4 phosphate
 PI(4,5)P₂ = Phosphatidylinositol 4,5 bisphosphate
 PI3K = Phosphoinositide 3 kinase
 PIP = Phosphoinositide
 PIKfyve = FYVE finger containing phosphoinositide kinase
 PKC = Protein kinase C
 PLC = Phospholipase C
 PROTOR = Protein observed with RICTOR
 PX = Phox Homology
 PTB = Phosphotyrosine binding
 RAPTOR = Regulatory associated protein of mTOR
 RICTOR = rapamycin-insensitive companion of mTOR
 S6K1 = S6 kinase 1
 SDS-PAGE = sodium dodecyl sulphate polyacrylamide gel electrophoresis
 SGK = serum and glucocorticoid-regulated kinase
 SNARE = Soluble N-ethylmaleimide-sensitive factor attachment protein receptors
 SNX = Sorting nexin
 TAT = Trans-Activator of Transcription
 TEV = tobacco etch virus
 TGN = Trans Golgi network.
 TRPML1 = transient receptor potential cation channel, mucolipin subfamily-1
 TSC = Tubular sclerosis complex
 Ub = Ubiquitin
 ULK = Unc-51 like autophagy activating kinase
 VPS = Vacuolar protein sorting
 WIPI = WD-repeat domain phosphoinositide interacting proteins
 YFP = Yellow fluorescent protein

Contents

Thesis Summary.....	2
Acknowledgements.....	3
List of Abbreviations.....	4
Contents.....	6
List of Figures.....	10
List of Tables.....	12
Chapter 1 Introduction.....	13
1.1 Alzheimer's Disease.....	14
1.1.1 Pathology.....	14
1.1.1.1 The Amyloid Precursor Protein and Alzheimer's Disease.....	16
1.1.1.2 The Amyloid Cascade Hypothesis.....	17
1.1.2 Genetics of Alzheimer's Disease.....	17
1.1.3 Alzheimer's Therapy and the Focus of Research.....	20
1.2 The APP Gene Family.....	22
1.2.1.1 Differences of APP, APLP1 and APLP2.....	23
1.2.2 Structure of APP Family Members.....	24
1.2.2.1 Extracellular Domains.....	24
1.2.2.2 Cell Adhesion Model of APP Function.....	25
1.2.2.3 Intracellular Domain.....	26
1.3 The Endosome.....	29
1.3.1 Mechanisms of Intracellular Vesicular Trafficking.....	30
1.3.1.1 Endosomal Identity and Phosphoinositides.....	30
1.3.1.2 Vesicle Formation.....	30
1.3.1.3 Vesicle Targeting, Docking and Fusion.....	32
1.3.2 Intracellular Vesicular Trafficking.....	34
1.3.2.1 Endocytosis and The Early Endosome.....	35
1.3.2.2 Exocytosis.....	35
1.3.3 Degradative Pathways.....	36
1.3.3.1 The Late Endosome.....	37
1.3.3.2 The Ubiquitin-Proteasome System.....	37
1.3.3.3 Autophagy.....	38
1.4 The Mechanistic Target of Rapamycin.....	42
1.4.1 mTOR Structure.....	42
1.4.2 mTOR in Human Health.....	46
1.5 The Phosphoinositide Kinase PIKfyve.....	48
1.5.1 Structure.....	48
1.5.2 Function.....	49
1.5.3 PIKfyve in Human Disease.....	51
1.6 Investigating Novel Interaction Partners of APP.....	52
1.6.1 Confirming and Elaborating the Physical Interaction Between APP and mTOR.....	53
1.6.1.1 Biological Significance of the APP/mTOR Interaction.....	54
1.6.2 Confirming and Elaborating the Physical Interaction Between APP and the PIKfyve Complex.....	54
1.6.3 Challenges in APP Family Research.....	55
1.6.4 Challenges in mTOR Research.....	56
1.6.5 Challenges in PIKfyve Research.....	57
1.6.5.1 Phosphoinositide Probes.....	58
1.6.5.2 TRPML1 and the PI(3,5)P ₂ Probe.....	59
1.6.6 Project Aims.....	60
Chapter 2 Materials and Methods.....	61
2.1 Materials and Methods.....	62
2.1.1 Materials.....	62
2.1.2 General Methods.....	66
2.1.2.1 Creation of Electrocompetent E. coli.....	66

2.1.2.2 Bacterial Transformation of Electrocompetent <i>E. coli</i>	66
2.1.2.3 Plasmid Isolation.....	66
2.1.2.4 Restriction Digests.....	67
2.1.2.5 Cloning.....	67
2.1.2.6 Polymerase Chain Reaction (PCR).....	68
2.1.2.7 Thawing Cell Stocks for Mammalian Tissue Culture.....	68
2.1.2.8 Mammalian Tissue Culture Passage.....	69
2.1.2.9 Mammalian Tissue Culture Transfections.....	69
2.1.2.10 Preparation of Mammalian Tissue Culture Cells for Western Blotting.....	69
2.1.2.11 Sodium Dodecyl Sulphate Polyacrylamide Gel Electrophoresis (SDS-PAGE).....	70
2.1.2.12 Western Blotting.....	71
2.1.2.13 Immunostaining.....	71
2.1.2.14 Microscopy.....	72
2.1.3 Investigation Specific Methods.....	72
2.1.3.1 Construction of AICD, TAT and TAT-AICD.....	72
2.1.3.2 Protein Expression and Purification.....	72
2.1.3.3 TAT Uptake Assay.....	74
2.1.3.4 RNAi Suppression.....	74
2.1.3.5 Vacuole Quantification.....	74
2.1.3.6 Vacuole Quantification in PIKfyve Inhibitor Sensitised Cells.....	74
2.1.3.7 APP Overexpression and mTOR Manipulation in HeLa and SH-SY5Y Cells.....	75
2.1.3.8 <i>C. elegans</i> culture.....	75
2.1.3.9 Lipid Quantification in <i>C. elegans</i> by Oil Red O and BODIPY Staining.....	76
2.1.3.10 LysoTracker Staining.....	77
2.1.3.11 Automated Vesicle Quantification.....	77
Chapter 3 Results	78
3.1 TAT-AICD as a Biochemical Tool.....	79
3.1.1 Introduction.....	79
3.1.1.1 Manipulating APP.....	79
3.1.1.2 Challenges in Overexpressing AICD.....	79
3.1.1.3 TAT.....	80
3.1.1.4 Mechanisms of TAT Entry.....	80
3.1.1.5 Using TAT as a Tool In Molecular Biology.....	82
3.1.2 Results.....	82
3.1.2.1 Confirmation and Characterisation of TAT Uptake transfected HeLa Cells.....	82
3.1.2.2 TAT-AICD Appears to Increase PIKfyve Function.....	86
3.1.2.3 TAT-AICD and mTOR Substrates.....	89
3.1.3 Discussion.....	90
3.1.3.1 Confirming and Describing TAT and TAT-AICD Cellular Uptake.....	90
3.1.3.2 TAT-AICD Colocalises with ML1Nx2-GFP.....	90
3.1.3.3 TAT-AICD Decreases Sensitivity to PIKfyve Inhibition in HeLa Cells.....	91
3.1.3.4 TAT-AICD Increases ML1Nx2-GFP Number and Size.....	91
3.1.3.5 TAT-AICD is a Novel Tool for the Manipulation of PIKfyve Function.....	91
3.1.3.6 TAT-AICD has no Discernable Effect on Several mTOR Substrates.....	92
3.2 Investigating a Functional Interaction Between APP and mTOR.....	94
3.2.1 Introduction.....	94
3.2.1.1 Evidence for mTOR Signalling Lowered in Alzheimer's Disease.....	94
3.2.1.2 Evidence for Upregulated mTOR Signalling in Alzheimer's Disease.....	95
3.2.1.3 Investigating an APP/mTOR Interaction.....	96

3.2.2 Results.....	97
3.2.2.1 APP Overexpression in HeLa and SH-SY5Y Cells Increases Downstream Phosphorylation in Targets of mTORC1 and mTORC2.....	97
3.2.2.2 APL-1 Mutation yn5 Creates an Additive Effect with daf-15 and let-363 Knockdown, Showing Fat Droplet Accumulation as Seen by Oil Red O and BOD.....	101
3.2.2.3 Successful Knockdown of APP Family Proteins, Alone or in Combination Fails to Alter mTOR Signalling.....	103
3.2.3 Discussion.....	104
3.2.3.1 APP Overexpression in HeLa and SH-SY5Y Cells Increases Downstream Phosphorylation in Targets of mTORC1 and mTORC2.....	104
3.2.3.2 APL-1 Mutation yn5 is Additive with daf-15 and let-363 Mutation, Showing Fat Droplet Accumulation as Seen by Oil Red O and BODIPY Staining.....	104
3.2.3.3 Successful Knockdown of APP Family Proteins, Alone or in Combination Fails to Alter mTOR Signalling.....	105
3.3 Investigating a Functional Interaction Between APP and the PIKfyve Complex.....	107
3.3.1 Introduction.....	107
3.3.2 Results.....	109
3.3.2.1 APP/APLP2 Double Knockdown Increases the Percentage of Cells with Vacuolar Structures in HeLa Cells Visible by Light Microscopy.....	109
3.3.2.2 APP/APLP2 Double Knockdown Increases Sensitivity to PIKfyve Inhibition in HeLa Cells.....	110
3.3.2.3 APP/APLP2 Double Knockdown Decreases the Number of ML1Nx2-GFP Positive Vesicles in HeLa Cells.....	111
3.3.3 Discussion.....	113
3.3.3.1 APP/APLP2 Double Knockdown Increases the Percentage of Cells with Intracellular Structures in HeLa Cells Visible by Light Microscopy.....	113
3.3.3.2 APP/APLP2 Double Knockdown Increases Sensitivity to PIKfyve Inhibition in HeLa Cells.....	113
3.3.3.3 APP/APLP2 Double Knockdown Decreases the Number of ML1Nx2-GFP Positive Vesicles in HeLa Cells.....	114
3.4 APP and Lysosomal Acidification.....	115
3.4.1 Introduction.....	115
3.4.2 Results.....	115
3.4.2.1 Rapid Turnover of APP in SH-SY5Y Cells is Induced by Inhibition of mTOR Via Torin 1.....	115
3.4.2.2 APP Turnover by Amino Acid Starvation is Halted by Lysosomal Inhibition.....	117
3.4.2.3 PIKfyve Inhibition Lowers the Number of LysoTracker Positive Structures Mimicking Inhibited Lysosomal Acidification.....	118
3.4.2.4 PIKfyve Inhibition Using Apilimod Reduces LysoTracker and Lamp1 Positive Vesicles.....	120
3.4.3 Discussion.....	123
3.4.3.1 Rapid Turnover of APP in SH-SY5Y Cells is Induced by Inhibition of mTOR Via Torin 1.....	124
3.4.3.2 Amino Acid Starvation Dependent APP Turnover is Halted by Lysosomal Inhibition.....	124
3.4.3.3 PIKfyve Inhibition Lowers the Number of LysoTracker Positive Structures Mimicking Inhibited Lysosomal Acidification.....	125
3.4.3.4 PIKfyve Inhibition Using Apilimod Reduces LysoTracker and Lamp1 Positive Vesicles.....	125
3.4.3.5 Further Evidence for APP/PIKfyve Interdependence.....	126
Chapter 4 Discussion.....	127
4.1 Discussion.....	128

4.1.1 Summary of Findings.....	128
4.1.1.1 Creation and use of TAT-AICD.....	128
4.1.1.2 Testing Prospective APP Interaction Partners.....	129
4.1.1.3 The Relevance of APP in the Endosome: A Result Driven Investigation.....	130
4.1.1.4 Summary.....	131
4.1.2 Significance.....	131
4.1.2.1 A Tool for Mammalian PIKfyve Research.....	131
4.1.2.2 Clues for APP's Cellular Role.....	132
4.1.2.3 Ageing and Human Disease.....	133
4.1.3 Challenges and Limitations.....	134
4.1.3.1 Consoling mTOR and PIKfyve Activation.....	134
4.1.3.2 New Tools: The ML1Nx2-GFP Probe.....	135
4.1.3.3 New Tools: TAT-AICD.....	135
4.1.4 The Future of Alzheimer's Therapy and Research.....	136
4.1.4.1 Approaches to APP Research.....	137
4.1.4.2 Next Steps in APP Research.....	137
References.....	139

List of Figures

Figure 1. The Secretase processing of APP.....	16
Figure 2. Location of Alzheimer’s disease related mutations in APP.....	18
Figure 3. The Evolutionary History of APP family proteins.....	22
Figure 4. Domain structures for APP family members.....	23
Figure 5. Model of APP dimerization.....	26
Figure 6. Road map of the secretory and endocytic pathways.....	29
Figure 7. Clathrin coat assembly.....	31
Figure 8. Rab membrane association and activation.....	33
Figure 9. The Ubiquitin-Proteasome System.....	38
Figure 10. Autophagosome Initiation Dependent on mTORC1 Inactivity.....	39
Figure 11. Development of the Autophagosome.....	40
Figure 12. The structure of mTORC1 and 2.....	43
Figure 13. mTORC1 signalling pathway.....	44
Figure 14. mTORC2 signalling pathway.....	45
Figure 15. Model of PIKfyve arrangement and binding.....	49
Figure 16. AICD Proteo-liposome presentation method.....	52
Figure 17. Example of proposed CPP translocation mechanisms.....	81
Figure 18. Design Expression and Purification of TAT, TAT-AICD, AICD.....	83
Figure 19. Penetration and cellular distribution of TAT and TAT-AICD in GFP-ML1Nx2.....	85
Figure 20. Penetration and cellular distribution of TAT and TAT-AICD in GFP-ML1Nx2.....	86
Figure 21. The effect of TAT-AICD on ML1Nx2-GFP in HeLa cells.....	87
Figure 22. The effect of TAT-AICD on PIKfyve function in HeLa cells.....	88
Figure 23. mTOR signalling in HeLa cells upon treatment with TAT-AICD.....	89
Figure 24. APP drives mTOR signalling via its intracellular domain in HeLa cells.....	99
Figure 25. APP drives mTOR signalling via its intracellular domain in SH-SY5Y cells.....	100
Figure 26. Truncation of the intracellular domain from the <i>C. elegans</i> ortholog of APP, APL-1 (<i>apl-1(yn5)</i>) creates a synthetic increase in lipid deposition when <i>apl-1(yn5)</i> is combined with suppression of <i>C. elegans</i> mTOR function.....	102

Figure 27. Successful knockdown of APP family proteins in HeLa cells, alone or in combination, fails to alter mTOR signaling.....	103
Figure 28. APP family siRNA for the investigation of an APP/PIKfyve interaction.....	109
Figure 29. RNAi suppression of APP and APLP2 increases the number of vacuoles per cell in PIKfyve inhibited HeLa Cells.....	111
Figure 30. APP and APLP2 suppression leads to the reduction of ML1Nx2-GFP positive vesicles.....	112
Figure 31. APP abundance is dependent on mTOR catalytic activity in both SH-SY5Y control cells and those lentivirally overexpressing APP.....	116
Figure 32. mTOR inhibition-induced downregulation of APP is mediated by lysosomal degradation in HeLa cells.....	117
Figure 33. PIKfyve inhibition using YM201636 lowers the number of acidic vesicles.....	119
Figure 34. Inhibition of PIKfyve using apilimod affects acidified organelles.....	121
Figure 35. Inhibition of PIKfyve using apilimod affects endosomes/lysosomes.....	122

List of Tables

Table 1. GWAS hits for Alzheimer's disease.....	19
Table 2. Overview of phosphoinositides: location of enrichment and roles.....	30
Table 3. APP family: mouse knockouts and coresponding phenotypes.....	55
Table 4. Phosphoinositide probes by <i>in vitro</i> specificity.....	59
Table 5. Protein Purification Solutions.....	62
Table 6. Bacterial Culture Solutions and Media.....	62
Table 7. Cloning.....	63
Table 8. Tissue Culture Solutions and Media.....	63
Table 9. SDS-PAGE and Western Blotting Solutions.....	64
Table 10. Antibodies.....	65
Table 11. PCR Reagents.....	68
Table 12. Acrylamide Gel Ingredients (Per Gel).....	70

Chapter 1

Introduction

1.1 Alzheimer's Disease

Alzheimer's disease is named after Alois Alzheimer, who first described the clinical and pathological characteristics of the disease in one of his patients. Alzheimer's disease, a form of dementia characterised by profound memory loss and confusion, is a neurodegenerative disorder primarily related to ageing.

Over 100,000 people are diagnosed with Alzheimer's each year (127,095 between 2013-2014) (HSCIC 2015), with approximately 850,000 people living with dementia in the UK today (Alzheimer's Society 2014). By 2025, the number is expected to exceed 1 million and by 2050 it is projected to include over 2 million people (Lewis *et al.*, 2014). More women than men develop Alzheimer's; in the UK around 62% of cases are female while approximately 38% are male (Lewis *et al.*, 2014) with dementia being the leading cause of death among women in the UK with 12.2% of deaths per year attributable to the disease (ONS 2014). Stemming from the progressive nature of the disease, the patient's condition deteriorates over time, with death occurring several years after diagnosis (Wolfson *et al.*, 2001) and the patient requiring increasing care up until then. Because the degradation is primarily of higher brain function, death occurs indirectly: dehydration, pneumonia and cachexia are the most commonly reported causes (Chandra *et al.*, 1986).

1.1.1 Pathology

Gross pathological changes in Alzheimer's disease include cerebral atrophy, particularly in the cortex and hippocampus, as well as "plaques and tangles"; protein aggregates of amyloid beta (A β) plaques and hyperphosphorylated tau (neurofibrillary tangles).

Alzheimer's disease can exhibit pathological changes of varying severity (Braak and Braak 1991) and at different scales – from visible pathology to microscopic, histological changes. The changes often seen upon visual inspection of the Alzheimer's brain (via neuroimaging or

post-mortem) include generalised atrophy of the cerebral hemisphere, affecting white and grey matter. As might be expected in a neurodegenerative disease, ventricle size can be severely increased, although this is limited to the lateral and third ventricles (de la Monte 1989). Marked atrophy also occurs in the amygdala, hippocampus, and medial temporal lobes (Wenk 2003). In spite of pathology altering the cerebrum, the cerebellum is relatively spared from disease, allowing faculties such as fine motor control to remain, even when cognitive function is lost (Karas *et al.*, 2003).

The main microscopic signs of Alzheimer's disease are protein aggregates characterised by their morphology, staining profile and the specific protein involved in their formation. These can be found alongside more general changes, such as neuron loss and variations in glial cell number and size in affected regions of the brain (West *et al.*, 1994; Mackenzie *et al.*, 1995).

Plaques consist of aggregated A β peptide, these plaques appear as argyrophilic extracellular deposits, varying in size and found in two general forms: diffuse and neuritic. Diffuse plaques are homogeneous masses that do not accumulate congo red stain, while neuritic plaques contain a dense core of A β and cellular material that can be stained with congo red or silver surrounded with a silver stained "halo". Neuritic plaques, as their name suggests, also contain abnormal neuritic and microglial processes. Neurofibrillary tangles are lesions found in the brain consisting of hyperphosphorylated tau protein creating intracellular paired helical fragments (Stelzmann *et al.*, 1995; Kidd 1963; Wischik *et al.*, 1988). Neurofibrillary tangles are seen as silver stained fibrillar flecks formed in the cell body of neurons, they consist of hyperphosphorylated forms of the microtubule associated protein tau. Although the tangles are within living neurons, upon cell death the tangle remains as an insoluble 'ghost' (Reviewed in Perl 2010).

1.1.1.1 The Amyloid Precursor Protein and Alzheimer's Disease

The plaques found in Alzheimer's disease come about through processing of amyloid precursor protein (APP) by secretases. Beta secretase BACE1 (Reviewed in Vassar 2004) and the gamma secretase complex (Reviewed in Iwatsubo 2004) cut APP to release aggregation prone A β peptides, while alpha secretase cleavage produces non-amyloidogenic products (Reviewed in Allinson *et al.*, 2003). In addition to extracellular peptide release, the action of secretases also produce the larger soluble, secreted remnant of the extracellular domain (sAPP) and the intracellular domain of APP (AICD) (**Figure 1**).

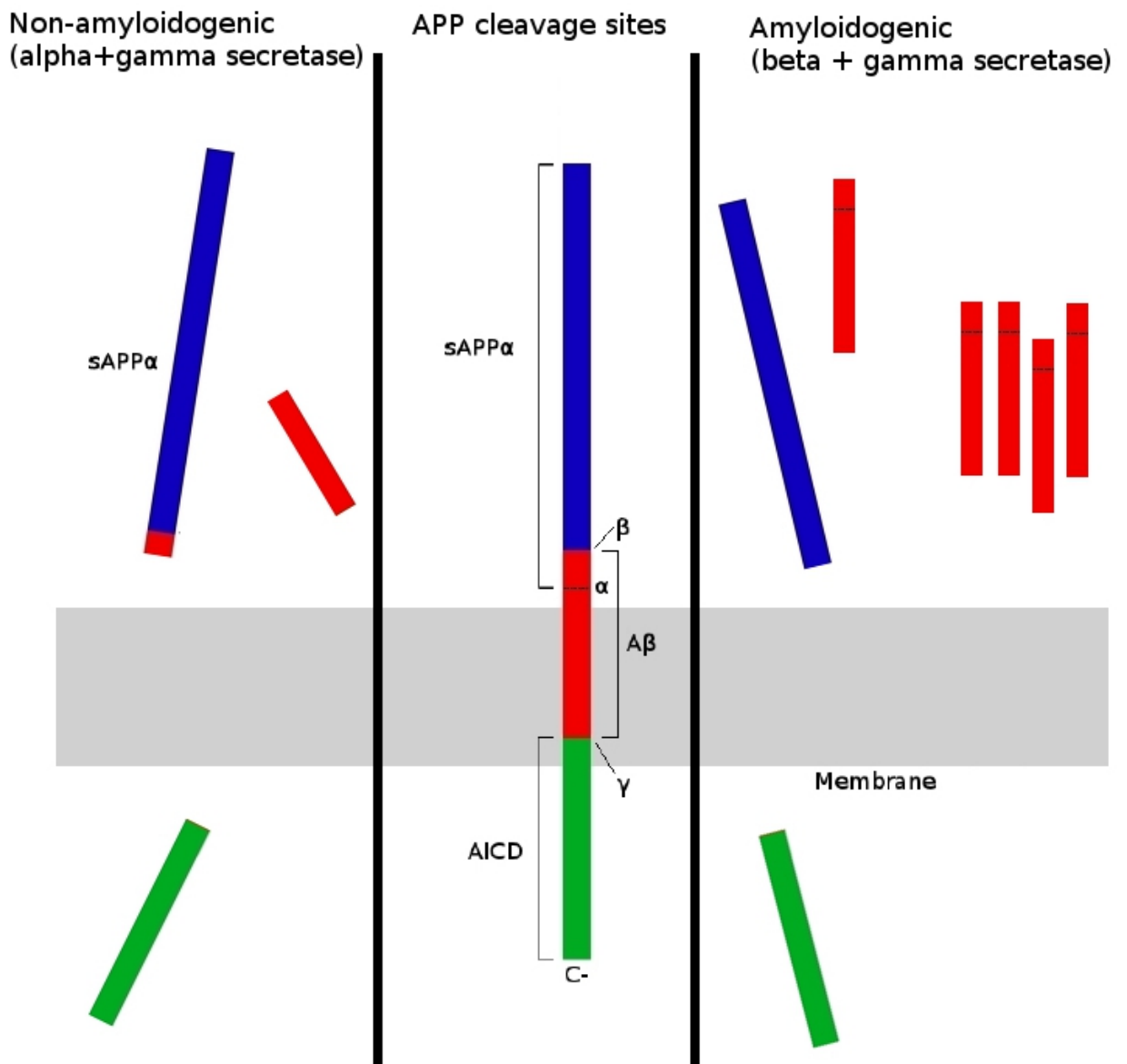


Figure 1.) The Secretase processing of APP. APP is cleaved by secretases to produce secreted APP (sAPP) and APP intracellular domain (AICD), APP may be cut by either alpha or beta secretase. If cut by alpha secretase, the A β stretch of APP is disrupted, leading to a non-amyloidogenic product along with the longer sAPP α after gamma secretase release (left panel). If cut by beta secretase, an aggregation prone product results alongside sAPP β and AICD.

Research into APP continues to focus on the origins and effect of amyloid beta, however, with respect to determining APP's functional roles within the cell, A β is unlikely to be important and is not the most 'interesting' segment of the protein. The A β stretch is not conserved evolutionarily beyond a handful of mammals (Podlisny *et al.*, 1991), while APP orthologues exist in *Drosophila melanogaster* and *Caenorhabditis elegans* (Rosen *et al.*, 1989; Daigle and Li 1993). Several biological roles have been attributed to APP, with the intracellular and extracellular regions of APP designated domains relating to their structure and function.

1.1.1.2 The Amyloid Cascade Hypothesis

The amyloid cascade hypothesis states that A β is the primary cause of Alzheimer's disease: the cleavage of APP leads to the release and aggregation of A β (specifically A β 42), which causes cell death leading to dementia (Hardy and Allsop 1991; Reviewed in Karran *et al.*, 2011). The hypothesis that A β is the primary cause of Alzheimer's has a large body of research supporting it: most familial Alzheimer's mutations increase the amount of A β 42 formed (Tanzi and Bertram 2005) and A β itself appears to exert a neurotoxic effect (Goodman and Mattson 1994). A myriad of effectors have been implicated in A β neurotoxicity, be it interference with insulin signalling (Xie *et al.*, 2002), Wnt (Reviewed by Caricasole *et al.*, 2003), alcohol dehydrogenase (Lustbader *et al.*, 2004), or by altering microglial activation (Reviewed in Bamberger and Landreth 2001).

1.1.2 Genetics of Alzheimer's Disease

The expression and processing of APP is central to the development of Alzheimer's disease. Overexpression of APP is known to lead to early onset Alzheimer's disease, seen clinically in Down's syndrome patients as a result of the extra copy of APP from the trisomy of chromosome 21. A range of APP mutations that alter its processing and cleavage have been found in the majority of familial Alzheimer's disease cases. In addition, other mutations that alter APP processing have been found to predispose individuals to dementia. Known APP mutations include 'Indiana' (V717F), 'London' (V717I) and 'Swedish' (K670N/M671L) (Goate

et al., 1991; Murrel *et al.*, 1991; Mullan *et al.*, 1992; Crews *et al.*, 2010; **Figure 2**). Mutations in the gene encoding gamma secretase protein, which cleaves APP, also leads to familial Alzheimer's disease (Sherrington *et al.*, 1995; Wasco *et al.*, 1995).



Figure 2.) Location of Alzheimer's disease related mutations in APP (from Crews *et al.* 2010). Mutations listed: Swe = Swedish, Lon = London, Ind = Indiana, Iowa, Arc = Arctic, Italian, Dutch, Flemish.

Other than changes in APP and APP processing genes, one of the most well known genetic risk factors for developing Alzheimer's disease is the apolipoprotein E (APOE) 4 allele (Corder *et al.*, 1993). APOE is a gene that codes a transporter of lipoproteins, cholesterol, and fat soluble vitamins. While the role of APOE4 in Alzheimer's pathogenesis is unclear, it has been implicated in a variety of processes relevant to the disease, from the regulation of A β aggregation and deposition to lipid metabolism, synaptic plasticity, and neuroinflammation (Reviewed in Liu *et al.*, 2013). More recently, APOE4 has also been found to be associated with high intracellular calcium levels and apoptosis rates after mechanical injury (Jiang *et al.*, 2015).

Table 1.) GWAS hits for Alzheimer's disease (from Lambert *et al.* 2013). Genome-wide association study hits for Alzheimer's disease showing gene, gene product and biological role(s).

Gene	Gene Product	Role
ABCA7	ATP-binding cassette A, member 7	Cholesterol regulation (Kaminski <i>et al.</i> , 2000).
BIN1	Bridging integrator 1	Membrane dynamics, muscle development (Nicot <i>et al.</i> , 2007; Sakamuro <i>et al.</i> , 1996).
CLU	Clusterin	Complement, apoptosis, lipid transport, cell adhesion, autophagy (Koltai 2014; Sansanwal <i>et al.</i> , 2015). Note that the PTK2B-CLU GWAS signal distinction is unclear.
CR1	Complement receptor 1	Complement regulation (Lida <i>et al.</i> , 1982; Khera and Das 2009).
EPHA1	Ephrin type-A receptor 1	Neuronal migration (Torii <i>et al.</i> , 2009)
MS4A6A-MS4A4E	Membrane-spanning 4-domain sub-family A	Immune cell activation (Stashenko <i>et al.</i> , 1981; Ravetch and Kinet 1991; Proitsi <i>et al.</i> , 2014).
PICALM	Phosphatidylinositol binding clathrin assembly protein	Trafficking (Tebar <i>et al.</i> , 1999).
CD33	Cluster of differentiation 33	Myeloid lineage development (Paul <i>et al.</i> , 2000; Hernández-Caselles <i>et al.</i> , 2006)
HLA-DRB5-DRB1	MHC II DR β 5 and 1	Immunocompetence/histocompatibility (antigen presentation) (Holling <i>et al.</i> , 2004).
SORL1	Sortilin-related receptor L (DLR class) 1	Trafficking (Andersen <i>et al.</i> , 2005).
PTK2B	Protein tyrosine kinase 2 β	MAPK signalling, calcium flux, hippocampal LTP (Lev <i>et al.</i> , 1995). Note that the PTK2B-CLU GWAS signal distinction is unclear.
SLC24A4	Solute carrier family 24 member 4	Sodium/potassium/calcium exchanger, may be involved in neural development, hair and skin pigmentation (Sulem <i>et al.</i> , 2007).
ZCWPW1	Zinc finger, CW type with PWWP domain 1	Epigenetic regulation (He <i>et al.</i> , 2010).
CELF1	CUGBP, Elav-like family member 1	Control of alternative splicing (Gallo <i>et al.</i> , 2010).
NME8	NME/NM23 family member 8	Ciliary function (Duriez <i>et al.</i> , 2007).
FERMT2	Fermitin family member 2	Actin assembly and cell shape modulation, angiogenesis (Pluskota <i>et al.</i> , 2011).
CASS4	Cas scaffolding protein family member 4	Actin dynamics (Kirsch <i>et al.</i> , 1999).
INPP5D	Inositol polyphosphate-5-phosphatase	Negative regulator of myeloid cell proliferation. Interacts with CD2AP; involved in actin remodelling and membrane trafficking (March <i>et al.</i> , 2000).
MEF2C	Myocyte enhancer factor 2	Involved in cardiac and vascular development, neuronal survival (Akhtar <i>et al.</i> , 2012).

Genome-wide association studies (GWAS) are a powerful tool for studying genetic variations and their association with disease. GWAS for late onset Alzheimer's disease has found a host of genes significantly associated with the condition (**Table 1**). GWAS is limited by the ability to pick out a specific gene from a cluster of genes (resolution), indeed Lambert *et al.*

note that the region of interest around ZCWPW1 is large, containing about 10 genes including MADD which is already implicated in Alzheimer's disease (Del Villar and Millar 2004). Another limitation of GWAS is the understanding of how these gene 'hits' may be contributing to the disease. In spite of the limitations, these studies are contributing to an increasingly clear picture of the disease and how it develops. Indeed, when observed in terms of gene product, the Alzheimer's GWAS results show a pattern of genes related to neuronal maintenance, immune function, cytoskeletal dynamics, membrane dynamics and membrane trafficking.

1.1.3 Alzheimer's Therapy and the Focus of Research

The only licensed therapies for Alzheimer's to date are supportive in nature, promoting cholinergic transmission (cholinesterase inhibitors donepezil, galantamine and rivastigmine) or mitigating excitotoxicity using the NMDA receptor antagonist memantine (Kaduszkiewicz *et al.*, 2005; Koch *et al.*, 2008). It could be argued that current research has been driven by the need for an effective, disease modifying therapy for Alzheimer's disease.

In the last 10 years there have been attempts to develop new treatments, but clinical trials have consistently failed to show both efficacy and safety. Immunotherapy was one approach in which amyloid plaques were targeted for removal by the patient's own immune system. Interestingly, even with successful removal of plaques, disease progression continued (Holmes *et al.*, 2008). Another class of drugs that have so far failed were the secretase inhibitors; in theory lowering APP processing should minimise plaque formation and therefore slow disease progression, but these enzymes have multiple biological targets. Gamma secretase cleaves Notch, CD44, cadherins, ephrin-B2 and ErbB4 (De Strooper *et al.*, 1999; Ni *et al.*, 2001; Lammich *et al.*, 2002; Marambaud *et al.*, 2003; Georgakopoulos *et al.*, 2006); BACE1 is required for proper muscle spindle formation and peripheral myelination (Willem *et al.*, 2006; Cheret *et al.*, 2013). With the broad significance of secretase processing,

Inhibition should be expected to have profound effects on an organism, indeed the safety profile of secretase inhibitors in clinical trials has been poor (Svedružić *et al.*, 2013).

The failure to find safe effective therapeutics for Alzheimer's disease only highlights the need for a better understanding of the proteins involved in the condition. Despite being the protein underpinning Alzheimer's disease, research into APP has been neglected relative to its product A β .

1.2 The APP Gene Family

The APP family are all type I transmembrane proteins, with a large extracellular portion made of multiple distinct domains, and a smaller intracellular tail. The APP family appears to have emerged ~900 million years ago in *Bilaterians*, coinciding with the evolution of nervous systems and synapses. Known early examples of APP are found in the nematode (roundworm) *Caenorhabditis elegans* and the fruit fly *Drosophila melanogaster* (expressing a single gene each, APL-1 and APPL, respectively) (Shariati and De Strooper 2013; **Figure 3**). The early emergence and conserved nature of APP suggest an important role in cell biology (Daigle and Li 1993), furthermore, APP family protein isoforms are expressed throughout the organism, not just neuronally, demonstrating that a wider biological role has developed (Sisodia *et al.*, 1993).

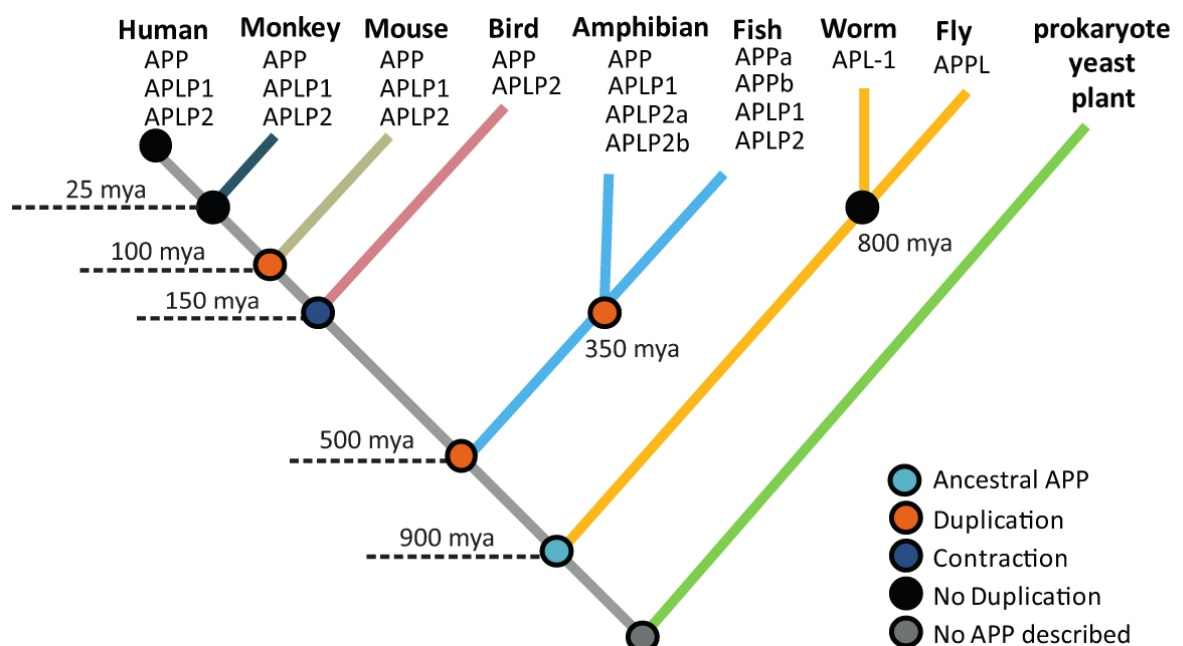


Figure 3.) The Evolutionary History of APP family proteins (from Shariati and De Strooper 2013). The APP family emerged ~900million years ago (mya) with APL-1 and APPL in worms and flies, but has undergone duplication and contraction in divergent species (orange and blue spots, respectively).

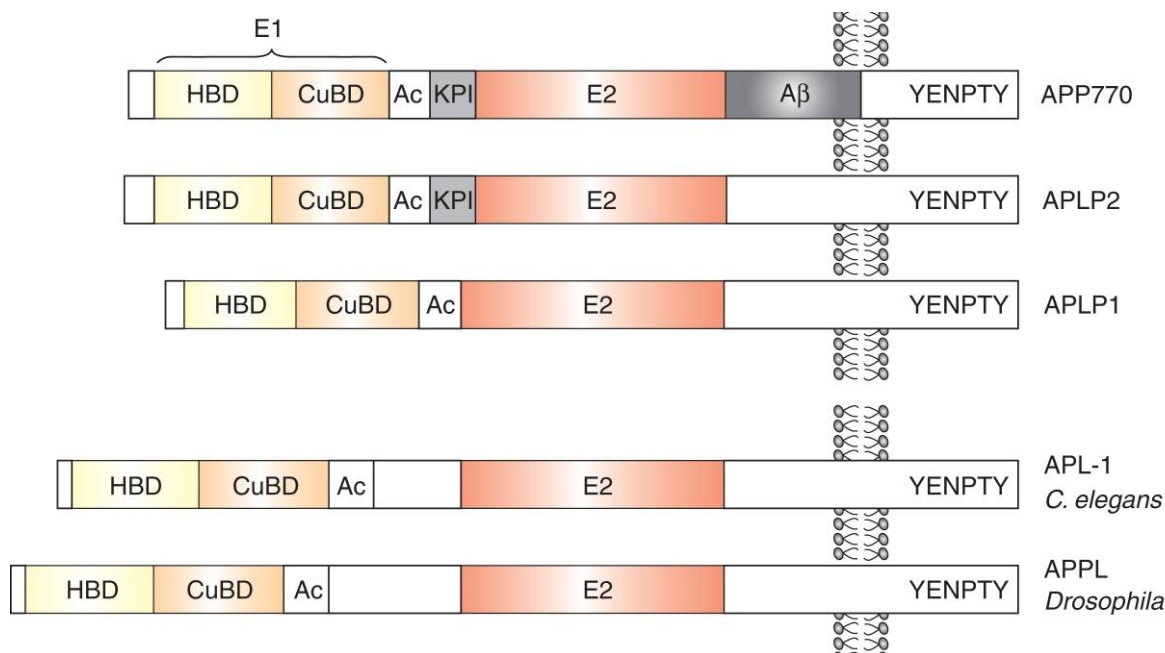


Figure 4.) Domain structures for APP family members (from Müller and Zheng 2012). All members contain conserved, shared features including an acidic domain (Ac), E2 (ectodomain 2) and E1 (ectodomain 1), as well as an intracellular YENPTY motif. APP is unique in containing the A β stretch, while APLP1 and APP's evolutionary ancestors lack a Kunitz-type protease inhibitor (KPI) domain. E1 contains a heparin binding domain (HBD) and copper binding domain (CuBD).

In humans, the APP family consists of APP, and APP like proteins 1 and 2 (APLP1 and 2, respectively). These proteins share many structural elements (**Figure 4**), in particular, an almost identical intracellular domain. In spite of the structural similarities, the APP family proteins have a multitude of isoforms, which through their domain inclusion and/or tissue specificity may dictate very different functions.

1.2.1.1 Differences of APP, APLP1 and APLP2

APLP1, unlike APP and APLP2 is restricted to neurons of the central and peripheral nervous system (Slunt *et al.*, 1994; Lorent *et al.*, 1995), and consists of two almost identical isoforms with 650 and 651 amino acids, respectively (Uniprot.org). APLP1 is also set apart from the other APP family members within the brain by its apparent restriction to post-mitotic cortical plate neurons, while APLP2 can be found in the proliferating ventricular/sub-ventricular zones and APP is expressed in both (Lopez-Sanchez *et al.*, 2005). APLP1 may be even further restricted to post-synaptic membranes (Kim *et al.*, 1995; Lo *et al.*, 1995; Thinakaran *et al.*, 1995; Lyckman *et al.* 1998). While structurally distinct from full length APP and APLP2, APLP1 overlaps somewhat with shorter isoforms lacking a KPI domain (exon 7, present in

APP₇₅₁, APP₇₇₀, APLP2₇₆₃); interestingly these KPI negative isoforms are also neuronally predominant (Kitaguchi *et al.*, 1988; Ponte *et al.*, 1988; Tanzi *et al.*, 1988). While the domain structure of APLP2 appears more similar to APP than APLP1, particularly in light of the shared KPI domain, APLP2 has been proposed to be the most evolutionarily divergent family member (Shariati and De Strooper 2013).

1.2.2 Structure of APP Family Members

1.2.2.1 Extracellular Domains

The extracellular domains of APP family proteins share conserved regions, divided into ectodomain 1 (E1) and ectodomain 2 (E2). The E1 of APP family proteins can be further subdivided into a heparin binding domain and a copper binding domain.

At the N-terminal extremity of APP family proteins is a heparin binding domain (HBD), a site which contains many basic residues on its surface capable of binding extracellular proteoglycans (Small *et al.*, 1994). The HBD also contains a hydrophobic pocket, proposed as a site for dimerisation or protein binding, indeed this site has been suggested as being a ligand binding site or otherwise functioning as a growth factor *in vivo* (Rossjohn *et al.*, 1999).

Neighbouring the HBD is the copper/metal binding domain, a stretch containing a single alpha-helix and beta-sheet, capable of binding metal ions (Bush *et al.*, 1993). This binding appears to be able to reduce copper (II) to copper (I) (Multhaup *et al.*, 1996), the functional significance of this is unclear but has been proposed as a regulator of copper homeostasis (Barnham *et al.*, 2003).

Alternative splicing of APP and APLP2 produces a Kunitz-type protease inhibitor (KPI) domain, this may be significant because serine proteases are implicated in promoting neuronal cell growth (Wang and Reiser 2003). Interestingly, KPI domain isoforms appear to be more common in non-neuronal cells such as astrocytes and a variety of blood cells

(Rohan de Silva *et al.*, 1997; Van Nostrand *et al.*, 1991a; Bush *et al.*, 1990; Gardella *et al.*, 1990; Van Nostrand *et al.*, 1991b). Many potential roles for KPI domains appear to be linked to wound repair and regulating blood clotting through inhibition of serine proteases.

C-terminal to the acidic and KPI domain is the E2 domain; forming multiple alpha-helices, this domain dimerises supporting a model where APP can self-associate. Similar to the E1 domain, the E2 domain has heparin (Clarris *et al.*, 1997) and metal binding capability (Dahms *et al.*, 2012). Within the E2 domain of APP is the “RERMS” motif, which has been found to be sufficient for the growth promoting actions of secreted APP (Rosen *et al.*, 1989; Ninomiya *et al.*, 1993; Roche *et al.*, 1994).

1.2.2.2 Cell Adhesion Model of APP Function

The extracellular domains of APP family proteins are diverse, but are beginning to be understood in the context of cell adhesion. Dimerisation of the extracellular domains has been studied at some length previously in the context of proteolytic processing and cell-cell adhesion (Scheuermann *et al.*, 2001; Soba *et al.*, 2005; Munter *et al.*, 2007), with potential for a role in synaptic adhesion (Baumkötter *et al.*, 2011).

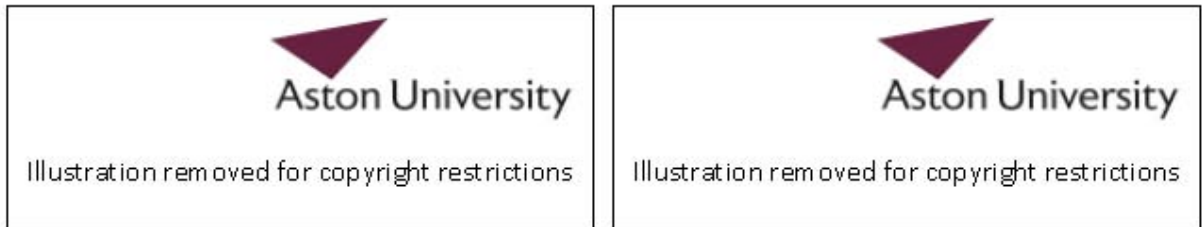


Figure 5.) Model of APP dimerisation (from Hoefgen *et al.*, 2014). Heparin (blue line) induces dimerisation of the E1 domains, if the APP molecules exist in the same cell **(a)** this leads to E2 binding, if the APP molecules exist in different cells **(b)** this leads to cell-cell adhesion.

Understanding of the nature of the APP family's extracellular domain has allowed the formulation of a model for the function in cell adhesion. Extracellular matrix (ECM) induced dimerisation may either bind APP/APLP from the same cell or two separate cells for anchorage (Hoefgen *et al.*, 2014; **Figure 5**). In this model, the maintenance of an extracellular interaction would dictate the intracellular output of APP.

1.2.2.3 Intracellular Domain

The intracellular domain of APP family members is highly conserved (King and Turner 2004), both between members (APP, APLP1, APLP2) and through lineage (APL-1, APPL). Nuclear magnetic resonance (NMR) study has determined that AICD has a dynamic secondary structure (Ramelot *et al.*, 2000). AICD adopts flexible conformation capable of interacting with a wide number of targets in much the same way as α -synuclein, the central protein in Parkinson's disease (Uversky *et al.*, 2003). The intrinsic disorder in peptide sequences like AICD is thought to support molecular recognition in an intracellular signalling context in a multitude of ways. It allows binding of partners transiently, with high specificity but low affinity; the protein also accommodates its own conformation to bind diverse partners. A

protein with dynamic, low complexity structure may also aid its own rapid destruction, a feature particularly useful for important regulatory proteins (Uversky *et al.*, 2005).

Three sequence motifs are known to be of importance to AICD. The YTSI sequence is important in the sorting of APP, obeying the YXX Φ consensus motif for clathrin mediated endocytic sorting (Lai *et al.*, 1998; Bonifacino *et al.*, 2003). The VTPEER motif is the second prominent sequence, allowing the stabilisation of AICD with Fe65 family proteins through the dimeric adaptor protein 14-3-3 γ (Sumioka *et al.*, 2005). The third and perhaps most widely studied feature of AICD is the GYENPTY sequence, containing an NPXY motif. NPXY is found in tyrosine receptor kinases among others (Chen *et al.*, 1990; Bonifacino and Traub 2003; Lemmon and Schlessinger 2010), and is able to regulate endocytosis and trafficking (Lai *et al.*, 1995; Perez *et al.*, 1999; Ring *et al.*, 2007). The GYENPTY motif of APP is important for the function of known interactors that bear a phosphotyrosine binding domain such as X11, Fe65 family proteins (Borg *et al.*, 1996) and JIP (Matsuda *et al.*, 2001). Interestingly, mutation of the GYENPTY sequence alters APP trafficking (Perez *et al.*, 1999), resulting in diminished A β production (Ring *et al.*, 2007).

AICD is released through gamma secretase cleavage much like Notch, a protein that promotes proliferative signalling during neurogenesis via intracellular domain nuclear translocation. Indeed AICD has been shown to regulate gene expression by interacting with Fe65 and Tip60 (Cao and Sudhof 2001). The possibility of AICD being part of a G-coupled receptor signaling-like pathway has been found, where AICD was found to interact with G $_{\alpha o}$ (Nishimoto *et al.*, 1993; Brouillet *et al.*, 1999). AICD G $_{\alpha o}$ interaction has since been proposed as contributing to synaptogenesis (Ashley *et al.*, 2005) or calcium homeostasis (Leissring *et al.*, 2002; Shaked *et al.*, 2009).

Interestingly, Alzheimer's disease-like pathology can be brought about by overexpression of AICD independent of APP (Ghosal *et al.*, 2009). Specifically, AICD overexpression in mice produces memory deficits, widespread neuronal death in the hippocampus and dentate

gyrus, and is associated with prolific tau hyperphosphorylation.

The intracellular domain of APP family proteins has received limited attention regarding mechanistic output and interactions, therefore studying this domain may yield better understanding of APP, its gene family, and perhaps Alzheimer's disease itself.

1.3 The Endosome

Cells are highly ordered and compartmentalised, but the internal structure needs to maintain a balance between import and export of components. The cell must transport cargos to where they are needed and rapidly alter the composition of its membranes in response to changing needs. The cell fulfils the needs of dynamic compartmentalisation through intracellular trafficking: the budding, fission and fusion of membrane enclosed compartments collectively known as the endosome (**Figure 6**).



Figure 6.) Road map of the secretory and endocytic pathways (from Alberts *et al.*, 2008). From the endoplasmic reticulum to the plasma membrane, membranes are important to transport and process cell products and external materials. **A)** Compartments and sites which contribute to intracellular trafficking are as follows: the endoplasmic reticulum, the Golgi apparatus, secretory vesicles, plasma membrane (cell exterior), early endosome, late endosome and lysosome. **B)** Red arrows show secretory pathways, blue arrows denote retrieval (recycling) pathways and green arrows indicate the endocytic pathway.

Many cellular products and specific extracellular materials are either unable to diffuse through the cytoplasm, or are required in a limited range of locations. Some would be harmful if allowed outside of their functional locations. The cell produces and transports products in a way that only exposes them to environments necessary to their movement and function (Cung *et al.*, 1989).

1.3.1 Mechanisms of Intracellular Vesicular Trafficking

1.3.1.1 Endosomal Identity and Phosphoinositides

Phosphoinositides (PIPs) are a class of phospholipids that, although low abundance in cell membranes, have an important role to play in regulating cellular homeostasis. PIPs act as a membrane anchored signal that can communicate the identity of a membrane, ensuring the correct assembly of protein complexes and by extension the behaviour of that component of the cell. There are a number of PIPs, enabling differential labelling, they differ in the presence of phosphate (alone or in combination) on the third, fourth and fifth carbon of the inositol ring. When membrane identity changes occur, phosphate patterns on the inositol head can be rapidly altered through the action of kinases and phosphatases (**Table 2**; Reviewed in Di Paolo and Camilli 2006; Krauss and Haucke 2007). PIPs also act as a pool of secondary messengers: diacylglycerol and cytosol soluble inositol phosphates have their own impact on cell behaviour (Reviewed in Hokin 1985).

Table 2.) Overview of phosphoinositides: location of enrichment and roles (from Paolo and Camilli 2006; Kraub and Haucke 2007). Relevant kinases and phosphatases are also listed.

PIP	Enrichment	Roles	Forming Kinase	Phosphatase
PI(3)P	Early endosome	Protein recruitment for trafficking	Vps34	Myotubularins
PI(3,5)P ₂	Late endosome	Control of fission / fusion events, GLUT4 translocation	PIKfyve	Myotubularins, Fig4
PI(4)P	Golgi	Protein recruitment / destabilisation for trafficking	PI4KA	
PI(4,5)P ₂	Plasma membrane	Protein recruitment for trafficking, Na ion channel opening, actin rearrangement, second messenger pool	PI4P5Ks	Synaptojanin, OCRL
PI(3,4,5)P ₃	Plasma membrane	Positive mTORC2 signal (via PDK1)	PIK3CA (P110a)	PTEN, synaptojanin, SHIP2

1.3.1.2 Vesicle Formation

Transport between endosomal compartments and the plasma membrane requires cargo specific, distinct vesicles to be formed. The formation of vesicles come about through the

recruitment of coat proteins around a membrane, deforming that membrane and 'cutting' it from its source. These coat proteins can be clathrin, COPI or COPII-coated. Clathrin coated vesicles were the first to be identified and demonstrate the principles of vesicle formation common to coat proteins (Reviewed in Traub and Wendland 2010; McMahon and Boucrot 2011). Clathrin is responsible for vesicles shuttling between the plasma membrane and endosome, and between the endosome and outer (*trans*) Golgi network, while COPII is responsible for exporting vesicles from the endoplasmic reticulum (ER). COPI vesicles exist in the early secretory pathway, transporting primarily between Golgi stacks (cisternae), but otherwise from the Golgi to constitutive secreting vesicles or back to the ER (Pearse 1976; Owen *et al.*, 2004; Barlowe *et al.*, 1994; Letourneur *et al.*, 1994; Waters *et al.*, 1991).

Clathrin is composed of three light and three heavy protein chains that together make a 'three-legged' structure (triskelion), this can be recruited to a membrane by specialised adaptor proteins. The progressive recruitment of clathrin then forms a basket-like structure on a membrane, the curvature of which is thought to promote budding of the new vesicle (Lundmark and Carlsson 2010). Overcoming the energy barrier of vesicle fission requires the action of proteins such as dynamin, physically distorting the bud and recruiting lipid modifying enzymes. Upon fission, the coat proteins disassemble to leave a 'naked' transport vesicle.



Figure 7.) Clathrin coat assembly (from McMahon and Boucrot 2011). Five steps of clathrin coat assembly: nucleation, cargo selection, coat assembly, scission, and uncoating.

Clathrin coated vesicle formation can be broken down into five steps: nucleation, cargo selection, coat assembly, scission and uncoating (**Figure 7**; Reviewed in McMahon and Boucrot 2011). Nucleation is the conglomeration of initial coat protein effectors, with PI(4,5)P₂ rich areas of the membrane binding FCH domain only proteins (FCHO 1,2), which in turn aids the recruitment of intersectin and epidermal growth factor receptor (EGFR)

pathway substrate 15 (EPS15) and EPS15 related (EPS15R) (Henne *et al.*, 2010). The presence of PI(4,5)P₂, FCHO proteins and EPS15-EPS15R aids binding of adaptor protein 2 (AP2) and generates some initial membrane curvature, leading to the start of clathrin coating. Cargo selection is made possible by cargo-specific adaptors binding AP2, these include Numb (for Notch recruitment), β-arrestin (recruiting G-protein coupled receptors), and ARH, selecting low density lipoprotein (LDL) receptors (Ferguson *et al.*, 1996; Santolini *et al.*, 2000; Keyel *et al.*, 2006). Coat assembly continues through the progressive recruitment and polymerisation of clathrin triskelions, creating an increasingly spherical bud. Amphiphysin and sorting nexin 9 (SNX9) are BAR-domain containing proteins; they bind AP2 and recruit dynamin to the 'neck' of the budding vesicle; dynamin triggering scission of the vesicle upon GTP hydrolysis (Wigge *et al.*, 1997; Boucrot *et al.*, 2010). Uncoating of the vesicle's clathrin shell is performed by heat shock cognate 70 (HSC70) ATPase, in conjunction with cyclin G-associated kinase (GAK) or auxillin (Schlossman *et al.*, 1984; van der Blik *et al.*, 1993; Sweitzer *et al.*, 1998; Stowell *et al.*, 1999). Phosphatases such as synaptojanin (a curvature sensitive 5' phosphatase) are recruited through the maturation of the clathrin coat, and are capable of dephosphorylating inositol headgroups, in this case the loss of PI(4,5)P₂ changes the identity (protein binding profile) of the vesicle (Cremona *et al.*, 1999; Chang-Ileto *et al.*, 2011).

1.3.1.3 Vesicle Targeting, Docking and Fusion

For a vesicle to recognise a specific destination and begin fusion, targeting is required. Targeting depends on Rab proteins, (small GTPases in the Ras superfamily), complementary Rab effectors and vesicular/target SNARE proteins (soluble N-ethylmaleimide-sensitive factor attachment protein receptors). Rab proteins recognise complimentary Rab effectors, in a docking context these effectors 'tether' vesicles with the target membrane (Reviewed in Bonifacino and Glick 2004). Tethering allows SNARE proteins on the vesicle (v-SNARE) and the target membrane (t-SNARE) to interact, docking the vesicles and catalysing fusion (McNew *et al.*, 2000; Pfeffer 1999; Jahn and Scheller 2006).

The process of vesicle docking and fusion begins with Rab proteins, a diverse group with highly selective distribution (Pereira-Leal and Seabra 2001). Rab proteins cycle between their GTP bound, membrane associated state and GDP bound, cytosolic state. The GDP bound state keeps the Rab inactive and primarily in the cytosol through association with another protein, the Rab-GDP dissociation inhibitor (GDI) (Garrett *et al.*, 1994). Rabs contain a prenylated tail capable of membrane anchoring, but need GDI displacement factor (GDF) and a Rab specific GDP/GTP exchange factor (Rab-GEF) to remove GDI binding and allow interaction with its effector (**Figure 8**; Grosshans *et al.*, 2006). To reverse the behaviour of Rabs, a GTPase-activating protein (GAP) hydrolyses GTP allowing Rab sequestration by GDIs (Ullrich *et al.*, 1993; Ullrich *et al.*, 1994; Soldati *et al.*, 1995; Rak *et al.*, 2003).

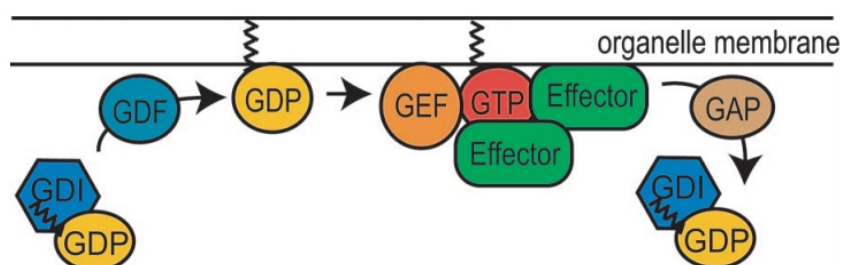


Figure 8.) Rab membrane association and activation (from Grosshans *et al.*, 2006). Prenylated Rab GTPase is soluble and inactive when bound to GDI. GDF allows the Rab GTPase to be released from GDI and attached to the organelle membrane via its isoprenyl anchor. The activation of Rab GTPases involves the GEF mediated exchange of GDP for GTP on the organelle anchored Rab, facilitating the binding and action of specific effectors. Recycling of Rab GTPases occurs through Rab specific GAPs which increase the rate of GTP hydrolysis, the inactive Rab GTPase can then be removed from the membrane by GDI to rejoin the cytosolic pool.

Rab effectors can vary depending on the required function including motor proteins for vesicle transport or tethering proteins for vesicle docking. In the case of vesicle docking, tethering proteins interact with Rabs to allow an initial docking of the vesicle and target membrane (Grosshans *et al.*, 2006). To fuse a vesicle and a target membrane requires both membranes to be effectively touching, exchanging lipids, and for water to be displaced from the surface of each membrane, this energetically unfavourable event requires specialised proteins, SNAREs.

Vesicle fusion occurs when two specific corresponding SNAREs bind to each other: a single stretch v-SNARE and 2-3 member t-SNARE complexes, tightening in a zipper-like fashion (Sutton *et al.*, 1998). Full fusion does not necessarily occur immediately, in the case of

neurotransmitter exocytosis Ca^{2+} triggers the final rapid fusion. After membrane fusion SNAREs must be recycled for reuse; the cell uses a protein called NSF and two accessory proteins to pry the SNAREs apart in an ATP-dependent manner (Söllner *et al.*, 1993).

1.3.2 Intracellular Vesicular Trafficking

The compartments that make up the intracellular trafficking system consist of the ER, the Golgi apparatus, secretory vesicles, plasma membrane (cell exterior), early endosome, late endosome, and lysosome.

By internalising plasma membrane via the process of endocytosis, the cell imports materials such as nutrients, some of which require capture and internalisation by the membrane. Plasma membrane proteins can also be expected to receive damage, lose function or otherwise require removal due to changing cellular needs.

Endocytosed material must be sorted to differentiate between material destined for recycling or degradation; compartments termed early endosomes fulfill this function in retrograde transport. If not retrieved from early endosomes to be translocated or recycled, a transition to late endosomes occurs via multivesicular bodies, so named for their highly invaginated, vesiculated morphology (Reviewed in Katzmann *et al.*, 2002; Gruenberg and Stenmark 2004).

Multivesicular bodies process deeper into the cell via microtubule mediated transport (Nielsen *et al.*, 1999) where protein composition and the internal environment of the compartment changes: inactive degradative proenzymes build up and the progressive acidification of the lumen takes place through the action of V-type ATPase proton pumps. Fusion of existing lysosomes introduces active hydrolases, in turn activating the proenzymes present (Reviewed in Huotari and Helenius 2011).

1.3.2.1 Endocytosis and the Early Endosome

The internalisation of plasma membrane during endocytosis results in vesicles consisting of plasma membrane and the proteins associated with it, in addition, any materials associated with this protein is also internalised. The cell must make "decisions" about the fate of this material, it does this in the early endosome. LDL, transferrin and EGF receptors are representative of how the early endosome sorts endocytosed material. The main method of cholesterol transport in the body is in protein bound form (LDL). LDL receptors on the cell surface sequester LDL, which is then internalised by the cell via clathrin mediated endocytosis. The resulting vesicles join with the early endosome where the mildly acidic environment dissociates the LDL cargo from its receptor (Anderson *et al.*, 1977). The early endosome membrane tubulates around the free receptors, enriching them away from lumen soluble material, these tubules then bud off, being recycled back to the plasma membrane. Transferrin receptors bind the iron transport molecule transferrin, and upon binding follows the same route as LDL into the early endosome. The transferrin receptor differs in that it is only the iron that dissociates from transferrin within the early endosome, while transferrin and its receptor are recycled to the cell surface where the iron-free transferrin dissociates again (Dautry-Varsat *et al.*, 1983). The EGF receptor differs yet again, first activating a cellular signalling response, then being irreversibly downregulated upon ligand binding, desensitising the cell to further signals (Sigismund *et al.*, 2008). EGF and its receptor is sorted to the late endosome, much like LDL and its bound cholesterol.

1.3.2.2 Exocytosis

The ER is a network of tubules surrounding the nucleus, and an extension of the outer nuclear membrane, central to protein and lipid synthesis as well as Ca²⁺ homeostasis. Newly synthesised proteins associated with the ER are passed on to the Golgi apparatus, a stack-like arrangement of flattened compartments. The Golgi acts as a site of oligo/polysaccharide synthesis, protein modification, and ultimately as an import / export hub, sorting products for their respective destinations.

1.3.3 Degradative Pathways

Lysosomes are the primary site of digestion within the cell, containing a myriad of digestive enzymes: proteases, lipases, nucleases, glycosidases, phosphatases, phospholipases and sulphatases, acid hydrolases requiring low pH for proteolytic activation and continued function. The lysosome maintains a low pH through the use of V-type ATPase, which pumps H^+ into the lumen, in a reversal of the method for cellular ATP synthesis, where H^+ gradient is used to form ATP (reviewed in Holliday 2014). Lysosomes are formed from the convergence of several pathways, and as such exhibit a somewhat heterogenous morphology (Warburton and Wynn 1976; Kelly *et al.*, 1989). Lysosomal hydrolase precursors are sourced from the secretory pathway, while membranes and digestion targets come from endocytosis, endosomal maturation or autophagy. New lysosomes are also 'seeded' by the hydrolases and undigested products of existing lysosomes. The progressive nature of lysosome formation and heterogeneity makes the distinction between late endosome and lysosome difficult, leading to the more general term "endolysosome".

Lysosomal activity attempts to digest material down to basic molecular building blocks, releasing them back into the cell for reuse (Sagné and Gasnier 2008). Some materials are resistant to lysosomal action and undergo successive cycles of degradation in endosomal compartments termed residual bodies. Residual, degradation resistant material must either be exocytosed or allowed to exist in the cytoplasm as lipofuscin granules (Schnitka 1965; Kerr 1970; Schellens 1974; Munnell and Cork 1980). Lysosomal dysfunction and exocytosis is an emerging area of interest, with an varied biological and clinical implications including Alzheimer's disease and Parkinson's disease (Annunziata *et al.*, 2013; Reviewed in Samie and Xu 2014; Zhang *et al.*, 2009). Melanin secretion is a specialised form of lysosomal exocytosis (Mishima 1967), and plasma membrane repair can rapidly take place upon lysosome/plasma membrane fusion (Reddy *et al.*, 2001), other more recent discoveries include a role in microglial signalling (Dou *et al.*, 2012), neurite outgrowth (Arantes and Andrews 2006) and phagocytic control (Samie *et al.*, 2013; Czibener *et al.*, 2006).

1.3.3.1 The Late Endosome

From the early endosome, materials not recycled or otherwise retrieved are destined for the lysosome for degradative processing. The cell must ensure membrane-bound material is collected within the endosomal space and does this by clustering membrane proteins, invaginating the membrane that contains them into the lumen of the endosome. The resulting intravesicular budding creates vesicles within the endosomal membrane which is now termed a 'multivesicular body' (Seglen and Bohley 1992). Subsequent lysosomal fusion allows digestion of both soluble and transmembrane material. The internal vesicles of multivesicular bodies are created using a specialised group of complexes: ESCRT-0,I,II,III (Babst *et al.*, 2002; Katzmann *et al.*, 2001). The ESCRT complexes recognise membrane proteins tagged for degradation by ubiquitin and progressively collect them, then sequesters these enriched vesicles into the endosomal lumen (Wollert *et al.*, 2009).

1.3.3.2 The Ubiquitin-Proteasome System

The ubiquitin-proteasome is responsible for the vast majority of protein degradation including damaged, abnormal, and heavily regulated proteins (Rock *et al.*, 1994). The ubiquitin-proteasome system degrades proteins by attaching ubiquitin, a 76 amino acid polypeptide to a target protein, this can lead to either deubiquitination, where the target protein is "rescued" from destruction, or it can continue to be ubiquitinated until destruction by the proteasome (Lilienbaum 2013; **Figure 9**). Proteasome based degradation is primarily carried out by the 26S proteasome complex, a 20S barrel shaped catalytic subcomplex made of proteases and a 19S regulatory subcomplex responsible for the capture, movement, and unfolding of the ubiquitinated protein (Groll and Huber 2003).

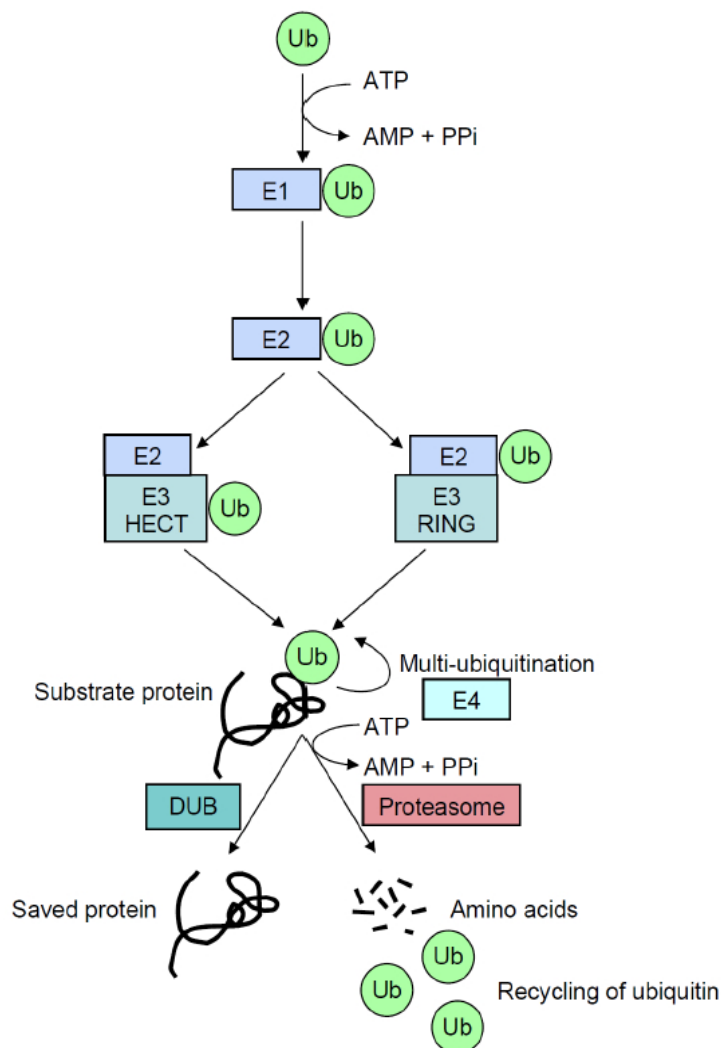


Figure 9.) The Ubiquitin-Proteasome System (from Lilienbaum 2013). Ubiquitin (Ub) is loaded onto an E1-activating enzyme (E1 enzyme) in an ATP-dependent manner, this "activated" ubiquitin is then translocated to E2-conjugating enzyme (E2 enzyme). E3 enzymes facilitate transfer to the substrate protein, this substrate protein can be rescued from the proteasome by deubiquitinating enzymes (DUB) or undergo subsequent rounds of ubiquitination. Further ubiquitination by E2/3 or rapid multiubiquitination by E4, commits the substrate to degradation by the proteasome, releasing amino acids and ubiquitin.

1.3.3.3 Autophagy

Autophagy is the process of destroying damaged and aggregated proteins, oxidised lipids, organelles and intracellular pathogens. The cell performs autophagy by manipulating internal membranes and the proteins that associate with them to form an autophagosome. An autophagosome is a double membraned vesicle that engulfs cellular material and degrades it upon fusion with acid hydrolase rich lysosomes.

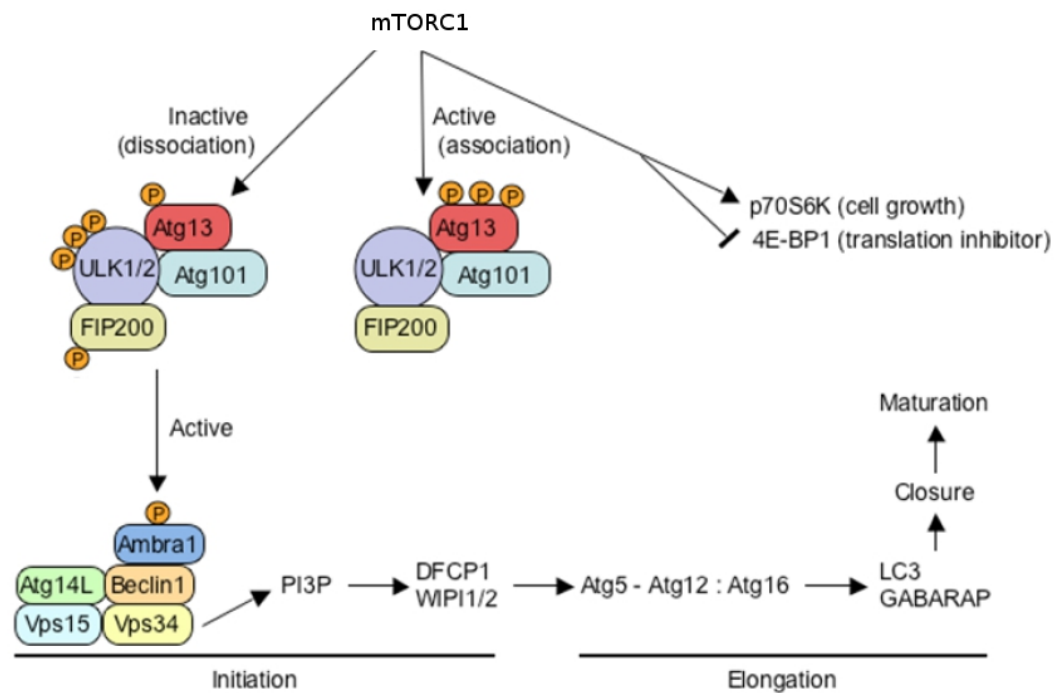


Figure 10.) Autophagosome Initiation Dependent on mTORC1 Inactivity (adapted from Lilienbaum 2013). Energy and stress signalling determines mTORC1 signalling – high energy, low stress means mTORC1 activity. Lack of mTORC1 signalling leads to dissociation from the ULK complex, subsequent activation of the Beclin-vps34 complex which initiates autophagosome development.

Autophagy initiation can be controlled by Unc-51 like autophagy activating kinase (ULK) complex, which is made up of an ULK protein (ULK1 or ULK2), Atg13, focal adhesion kinase-family interacting protein of 200kDa (FIP200) and Atg101 (Jung *et al.*, 2009; Mercer *et al.*, 2009). Under growth positive (high energy) conditions, autophagy is inhibited by mTORC1, which binds the ULK complex, phosphorylating Atg13 and deactivating it. Inactivity of mTORC1 leads to dissociation of mTORC1 from the ULK complex and eventual dephosphorylation of Atg13 (Chang *et al.*, 2009; Ganley *et al.*, 2009; Hosokawa *et al.*, 2009; Jung *et al.*, 2009). When active, ULK1 phosphorylates "activating molecule of Beclin 1-regulated autophagy 1" (Ambra1) of the Beclin1 complex (Kang *et al.*, 2011). The Beclin1 complex in turn associates with the class III phosphatidylinositol 3-kinase Vps34 (with other proteins including Atg14) to form the Beclin-Vps34 complex, capable of synthesising PI(3)P from phosphatidylinositol, which is key to the identity / development of the initial autophagosomal membrane, the phagophore (**Figure 10**; Kihara *et al.*, 2001; Funderburk *et al.*, 2010; Devereaux *et al.*, 2013; Lilienbaum 2013).

The phagophore (also known as the isolation membrane) is the initial nucleation point for the autophagosome which will eventually become the autolysosome (**Figure 11**; Longatti and Tooze 2009). The source of phagophore lipid membrane has been the subject of much debate, with contributions ranging from ER and Golgi to mitochondria (Hayashi-Nishino *et al.*, 2009; Yla-Anttila *et al.*, 2009; Hailey *et al.*, 2010; Mari *et al.*, 2011). Regardless of the source, the phagophore must elongate to form a mature autophagosome. This process is completed with the transmembrane protein Atg9, trafficked from the trans-Golgi network and late endosome, thought to act in lipid and protein recruitment (Kim *et al.*, 2002). A host of other proteins are recruited to the autophagosome by PI(3)P to aid in nucleation and elongation: WD-repeat domain phosphoinositide interacting proteins (WIPI1 and 2), double FYVE-containing protein (DFCP1), and autophagy linked FYVE protein (ALFY).



Figure 11.) Development of the Autophagosome (from Longatti and Tooze 2009). With the initial creation of the phagophore (IM/PAS) through ULK1 and the synthesis of PI(3)P, the membrane is expanded with the addition of lipidated LC3 and the Atg12-Atg5 system. Closure around the captured cell material creates an immature autophagosome (Avi) which eventually develops with the contribution of endosomal compartments and lysosomes (E/LY) into a degradative autophagosome (Avd), maturation leads to the fully functional autolysosome capable of destroying the cellular material captured within.

Two ubiquitin-like conjugation systems exist in the elongating phagophore. The Atg12-Atg5 system forms an E3-like (ubiquitin ligase-like) enzyme, while microtubule-associated protein light chain 3 (LC3) is reversibly sequestered from the cytoplasm. Sequestration occurs through processing and subsequent conjugation with phosphatidylethanolamine (PE) to form the lipidated "LC3-II" (the unlipidated form being termed "LC3-I") (Hanada *et al.*, 2007; Fujita *et al.*, 2008). Both LC3-II and the Atg12-Atg5 system contribute to the phagophore either by elongation or autophagosome closure (Hanada *et al.*, 2007; Xie *et al.*, 2008; Geng and Klionsky 2008). In addition to allowing autophagosome elongation, LC3 proteins make targeted autophagy possible by recruiting adaptor proteins such as p62 that in turn sequester cargos (ubiquitinated proteins in the case of p62) (Pankiv *et al.*, 2007; Shvets *et al.*, 2008).

After closure of the autophagosome, maturation occurs through fusion with early/late endocytic compartments (Liou *et al.*, 1997; Berg *et al.*, 1998). Lysosomal fusion completes maturation to a degradative autolysosome, allowing vacuolar V-ATPases and cathepsin hydrolases to work in tandem to acidify and proteolytically digest the contents, respectively (Lukacs *et al.*, 1990; Mullins and Bonifacino 2001). The products of completed autophagy eventually find their way back into cytoplasm to be recycled through the actions of permeases (Yang *et al.*, 2006), increasing the nutrient pool of the cell and subsequently restoring energy signalling.

1.4 The Mechanistic Target of Rapamycin

The mechanistic target of rapamycin (mTOR) is a large serine / threonine kinase, with orthologues existing down to the level of yeast (Kunz *et al.*, 1993). mTOR is named after the macrolide antibiotic and immunosuppressant rapamycin that led to its discovery.

mTOR acts as the linchpin of energy signalling within the cell, integrating internal and external energy cues such as insulin, amino acid abundance, AMP, oxygen, and growth factors. mTOR translates upstream energy signals into appropriate responses – blocking autophagy, encouraging mRNA translation, changing the level of lipid synthesis, mitochondrial proliferation and function (Reviewed in Zoncu *et al.*, 2011; Laplante and Sabatini 2012).

1.4.1 mTOR Structure

The mTOR protein itself is a 289kDa kinase subunit that exists in two distinct complexes, mTOR complex 1 and mTOR complex 2 (mTORC1 and mTORC2, respectively) (**Figure 12**; Loewith *et al.*, 2002). These complexes have structural overlaps; both containing the proteins mTOR, DEP domain containing mTOR interacting protein (DEPTOR) (Peterson *et al.*, 2009) and mammalian lethal with SEC13 protein 8 (mLST8) (Loewith *et al.*, 2002). Distinctions between the complexes include: regulatory associated protein of mTOR (RAPTOR) (Hara *et al.*, 2002) and 40kDa Pro-rich Akt substrate (PRAS40) (Sancak *et al.*, 2007) in mTORC1 and rapamycin insensitive companion of mTOR (RICTOR); mammalian stress activated MAP kinase interacting protein 1 (mSIN1) (Yang *et al.*, 2006); and protein observed with RICTOR (PROTOR) restricted to mTORC2 (Sarbasov *et al.*, 2004; Wullshleger *et al.*, 2005; Pearce *et al.*, 2007).

Many mTOR subunits beyond the kinase domain itself are primarily concerned with binding – the DEP and PDZ domains in DEPTOR, WD40 repeats of mLST8, RNC, HEAT repeats and WD40 repeats in RAPTOR, as well as the PH domain and RBD of mSIN1. The mTOR subunit also contains many domains concerned with binding, including HEAT repeats, FAT, FRB, and FATC domains. Elements of mTORC2 without obvious domains (RICTOR and PROTOR) stand out as likely structural scaffolds.

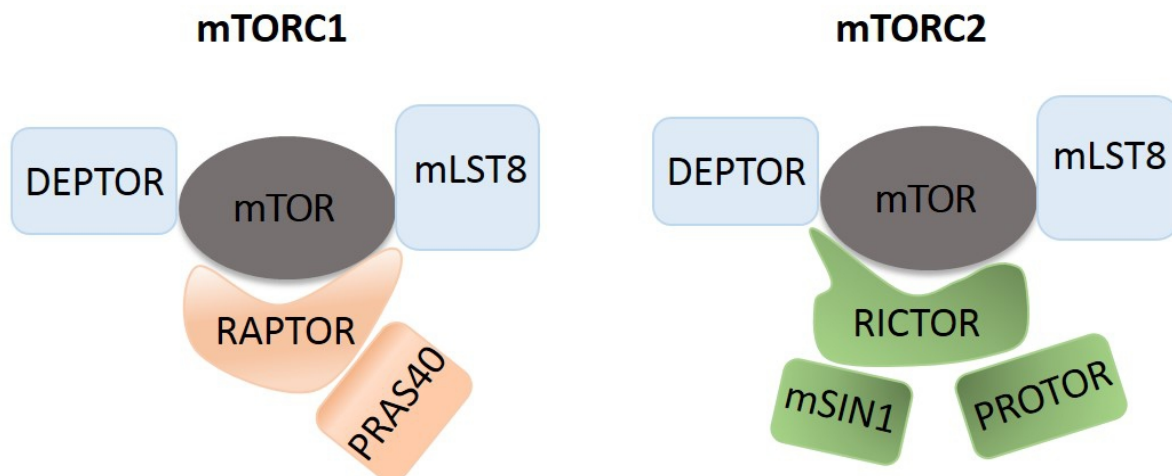


Figure 12.) The structure of mTORC1 and 2. mTORC1 and 2 have overlapping subunit members, mTORC1 contains the subunits mTOR, DEPTOR, mLST8, RAPTOR and PRAS40, while mTORC2 contains mTOR, DEPTOR, mLST8, RICTOR, mSIN1 and PROTOR. The mTOR kinase is shown in black, other shared subunits are shown in blue, with those unique to mTORC 1 and 2 are red and green respectively.

mTORC1 is perhaps the better understood complex, activated by growth factor receptors via the tuberous sclerosis complex and the monomeric GTPase Rheb. mTORC1 is also controlled by amino acid abundance via Rag-GTPases and the Ragulator complex (**Figure 13**; Garami *et al.*, 2003; Tee *et al.*, 2003; Sancak *et al.*, 2008; Sancak *et al.*, 2010)

mTORC1 Signalling

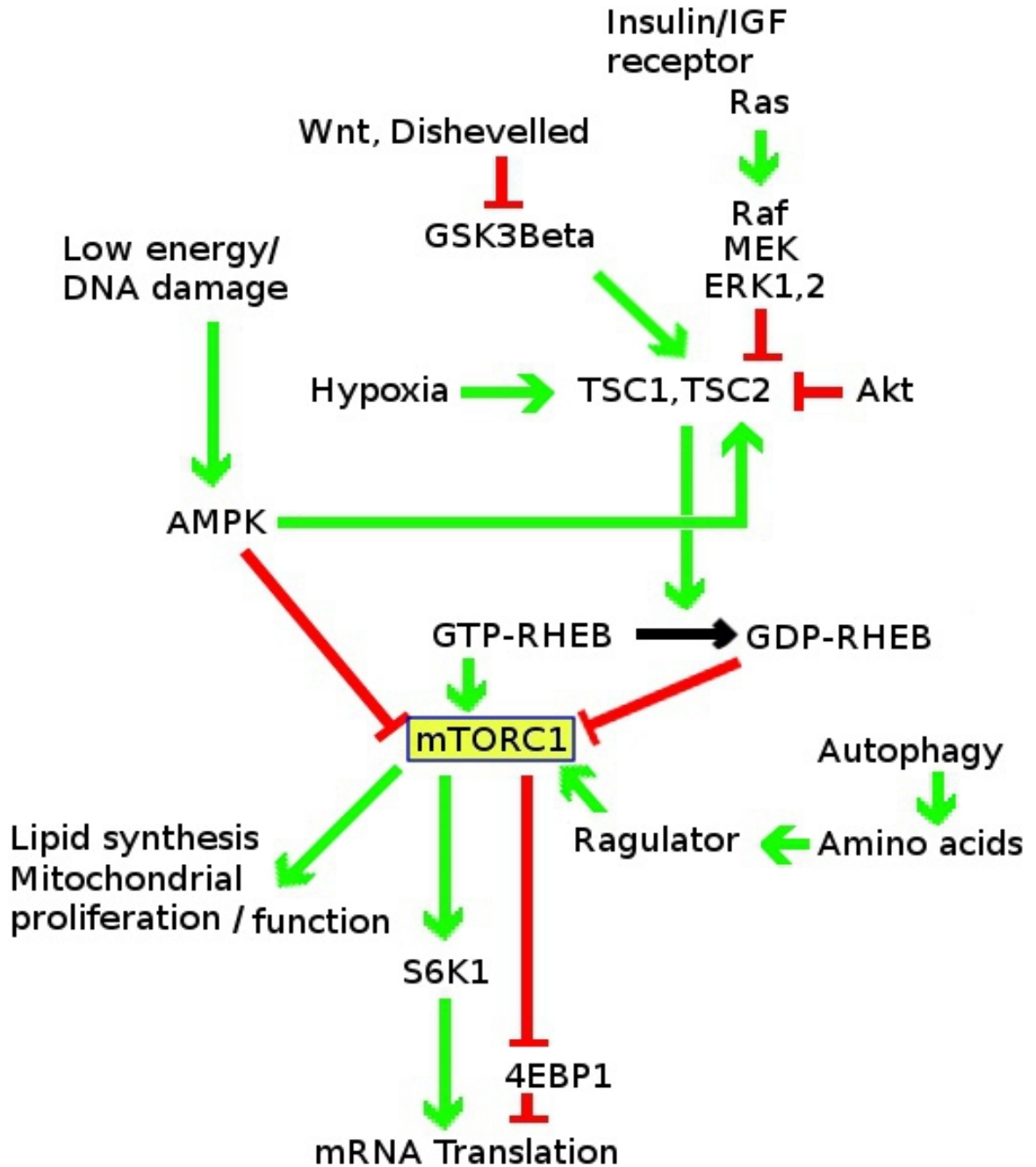


Figure 13.) mTORC1 signalling pathway. Energy signalling controls cell behavior, ensuring the correct response to high or low energy availability and stresses. Appropriate energy management is achieved through the interaction of induction or suppression signals (green and red arrows respectively). mTORC1 is a central point in energy signalling, integrating positive energy signals such as external signalling proteins and hormones (Wnt, insulin), growth factors (IGF), and nutrients (amino acids), or negative energy / stress signals such as AMP, hypoxia or DNA damage. mTORC1 turns the upstream signals into downstream effects through its action as a kinase on proteins such as S6K1 and 4EBP1. Control of mTORC1 is tightly linked to the state of the GTPase Rheb, which activates mTORC1 when GTP-bound, but not when converted to its GDP-bound state (black arrow).

mTORC2 Signalling

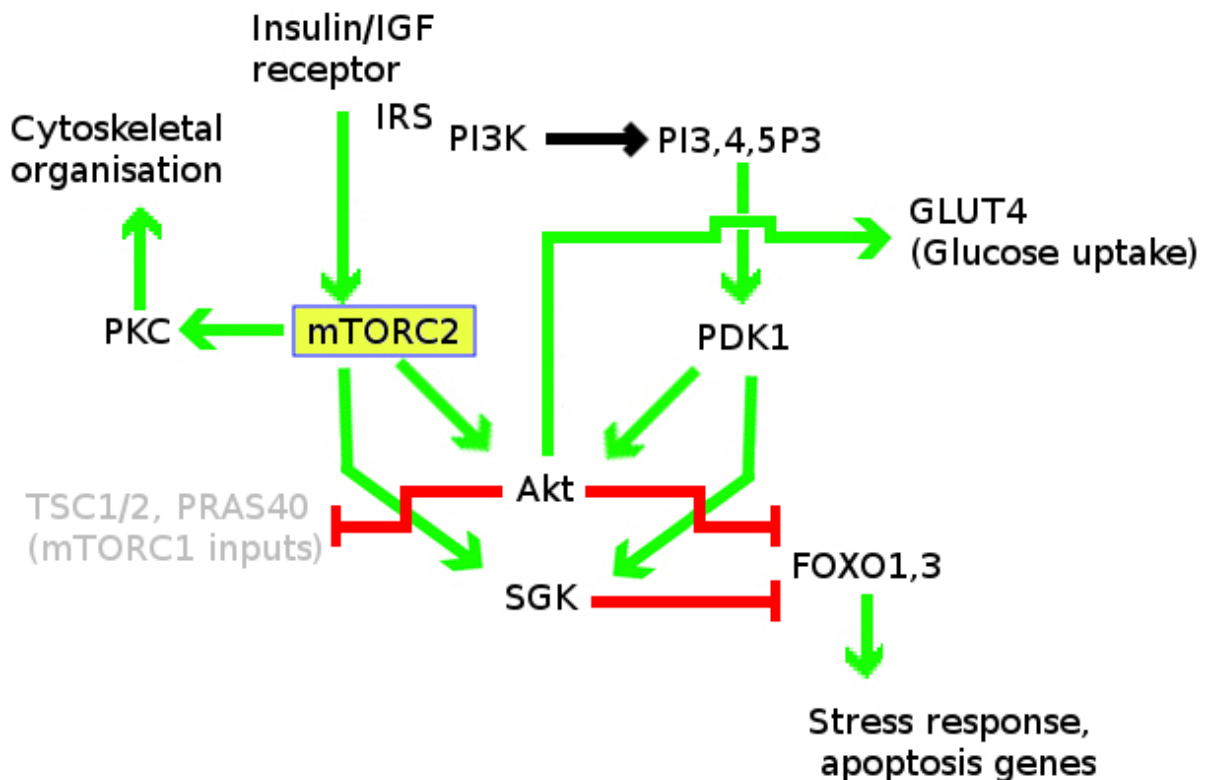


Figure 14.) mTORC2 signalling pathway. mTORC2, like mTORC1 helps achieve appropriate energy management through the interaction of induction or suppression signals (green and red arrows respectively). mTORC2 signalling overlaps with mTORC1, both of which integrate energy signals into cellular responses, however mTORC2 also has its own downstream effects. mTORC2, like mTORC1 is susceptible to insulin / growth factor signalling, and feeds into mTORC1 signalling via Akt phosphorylation of TSC1/2. mTORC2 controls apoptosis and stress response genes by targeting FOXO1/3 via SGK and Akt. Another established role for mTORC2 is the control of cytoskeletal reorganization via PKC and Rho GTPases.

mTORC2 is less well understood, but signals via growth factors to serum and glucocorticoid-regulated kinase (SGK) to regulate cell survival via fork head box protein O1 and 3 (FOXO1/3), protein kinase C (PKC) and Rho GTPases to control cytoskeleton organization, and Akt. Akt phosphorylation at Ser473 signals both mTORC1 via TSC1,2 and a second signal to FOXO1/3, promoting cell survival and cell cycle progression (**Figure 14**; Jacinto *et al.*, 2004; Guertin *et al.*, 2006; Shiota *et al.*, 2006; Garcia-martinez and Alessi 2008; Ikenoue *et al.*, 2008; Facchinetti *et al.*, 2008).

1.4.2 mTOR in Human Health

After first being pursued as an antibiotic (Vézina *et al.*, 1975; Sehgal *et al.*, 1975), rapamycin was found to be capable of preventing organ allograft rejection through suppression of mTOR mediated immune cell expansion (Calne *et al.*, 1989; Collier 1989; Thompson and Woo 1989; Tocci *et al.*, 1989). Further investigation into the mechanism of rapamycin revealed just how significant its action was on how a cell functions: having a role in the cell cycle (Heitman *et al.*, 1991; Brown *et al.*, 1994) including mammalian cells (Sabatini *et al.*, 1994; Sabers *et al.*, 1995), and involvement in translation initiation, transcription factor localisation and dependence on nutrient state (von Manteuffel *et al.*, 1997; Hara *et al.*, 1998; Wang *et al.*, 1998; Schmidt *et al.*, 1998; Beck *et al.*, 1999; Gingras *et al.*, 2001).

mTOR and insulin signalling are relevant to pathology in that insulin resistance can occur via an mTORC1 dependent feedback loop. The downstream target of mTORC1, S6K1 encourages mRNA translation but also phosphorylates IRS1, making the insulin receptor insensitive to further insulin signals (Um *et al.*, 2004). The reliance on an mTORC1 dependent feedback signal is key here – chronically high amino acid levels would signal insulin resistance, just as an insulin signal would, shutting down glucose uptake, but still signalling a ‘high energy state’ for the cell (Newgard *et al.*, 2009).

The wider biological context of mTOR signalling is primarily one of metabolic and proliferative control, but by extension, also one of ageing. Research has shown mTOR inactivation to be linked with longevity in yeast (Kaeberlein *et al.*, 2005), worms (Jia *et al.*, 2004), flies (Bjedov *et al.*, 2010), and possibly even in mammals (Neff *et al.*, 2013; Harrison *et al.*, 2009; Blagoskonny 2013; Ehninger and Neff 2014).

mTOR as a driver of ageing can be explained by several mechanisms. One factor that may play a role is stem cell exhaustion, where mTORC1 signalled proliferation pushes stem cells towards senescence, so that old cells can no longer be replaced (Janzen *et al.*, 2006;

Molofsky *et al.*, 2006). Damage to DNA and cellular components by reactive oxygen species (Reviewed in Cui *et al.*, 2011), may be relevant because of mTOR's proposed positive regulation of mitochondrial function and biogenesis (Cunningham *et al.*, 2007). The turnover of misfolded and damaged cellular components is a likely contributing factor to mTOR suppression dependent longevity. The importance of autophagy in longevity related to mTOR inhibition has been consistently reported (Hansen *et al.*, 2008; Toth *et al.*, 2008; Bjedov *et al.*, 2010) and changes in mRNA translation such as 60s ribosomal depletion or eIF4E modulation also appears to be intimately linked (Hansen *et al.*, 2007; Pan *et al.*, 2007; Syntichaki *et al.* 2007; Steffen *et al.*, 2008).

1.5 The Phosphoinositide Kinase

PIKfyve

The PIKfyve complex acts as a phosphoinositide kinase, phosphorylating the 5' position of PI3P to produce PI(3,5)P₂ which is also thought to act as a source of PI5P after phosphatase processing (Zolov *et al.*, 2012). The PIKfyve complex consists of the kinase PIKfyve itself, the scaffold protein Vac14, and Fig4, a 5' lipid phosphatase (regulating PI(3,5)P₂ production).

1.5.1 Structure

Structurally, the human PIKfyve kinase subunit contains several recognisable domains: a FYVE, DEP, HSP chaperonin-like domain (Cpn60_TCP1) and a CHK homology domain (containing many cysteine, histidine and lysine residues), as well as the catalytic PIP5K domain. The FYVE domain is crucial for binding the protein to target membranes containing PI3P, PIKfyve's substrate (Shisheva *et al.*, 1999; Sbrissa *et al.*, 2002a; Sbrissa *et al.*, 2002b; Rutherford *et al.*, 2006), while the role of the DEP, Cpn60_TCP1 and CHK domains are less clear. DEP domains are associated with binding stability and G-protein signalling in the context of other proteins (Wong *et al.*, 2000; Abramow-Newerly *et al.*, 2006; Ballon *et al.*, 2006), the CHK domain shows spectrin-like repeats that are implicated in cytoskeletal binding (Djinovic-Carugo *et al.*, 2002) and chaperonin-like domains classically relate to correct protein folding, but the one present in PIKfyve may to bind the Rab9 effector p40 (Ikononov *et al.*, 2003) and JLP (Ikononov *et al.*, 2009). The PIP5K (catalytic) domain is capable of phosphorylating PI(3)P at the 5' position to create PI(3,5)P₂, and has also been reported as a protein kinase *in vitro* (Sbrissa *et al.*, 2000; Ikononov *et al.*, 2003).

Beyond the kinase subunit, Vac14 stands out as containing many HEAT repeats that allow relevant protein-protein interactions (Dove *et al.*, 2002; Jin *et al.*, 2008) while Fig4 contains PIKfyve's regulatory 5' phosphatase.

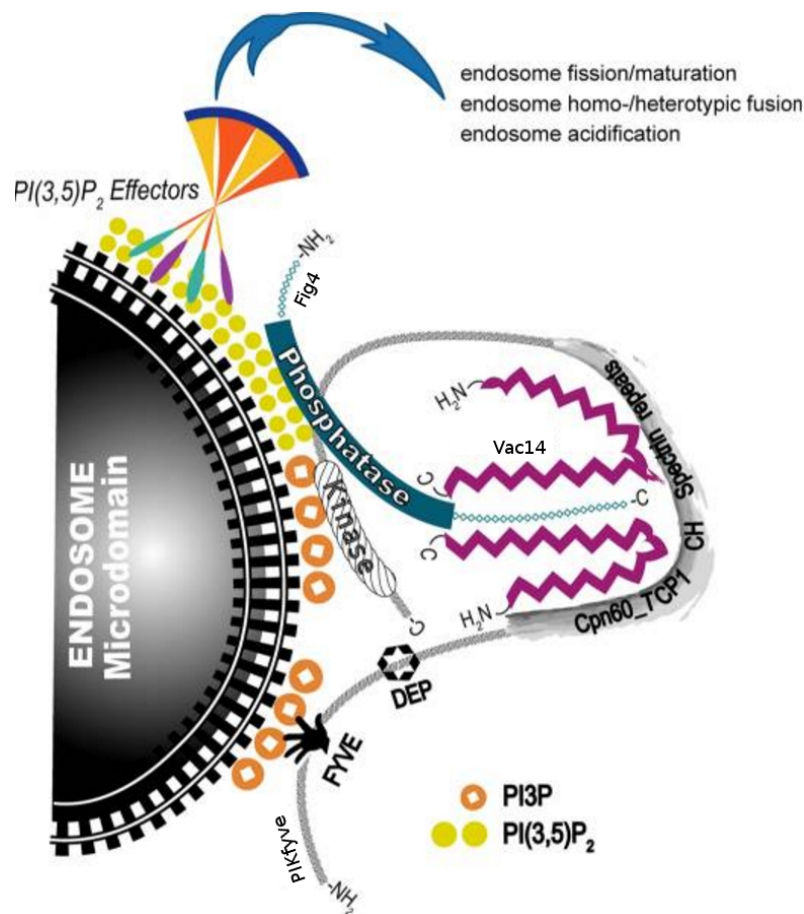


Figure 15.) Model of PIKfyve arrangement and binding (adapted from Ikonov *et al.*, 2009). PIKfyve is arranged around the binding of PI3P via its N-terminal FYVE domain, the C-terminal kinase domain and the Fig4 phosphatase. Structural support appears to be given by Vac14 binding Fig4 and PIKfyve.

In terms of organisation, the PIKfyve complex appears to be dependent on the multimerisation of Vac14 as a form of scaffold for the rest of the complex, with the HSP chaperonin-like domain presumed to lay in a way that allows both the N-terminal FYVE domain and the C-terminal kinase domain to bind and modify PI(3)P, respectively (**Figure 15**; Jin *et al.*, 2008; Sbrissa *et al.*, 2008; Ikonov *et al.*, 2009; Alghamdi *et al.*, 2013).

1.5.2 Function

PIKfyve is evolutionarily conserved and is found in yeast as Fab1. In yeast PI(3,5)P₂ levels spike rapidly upon exposure to hyperosmotic shock, but return close to basal levels within 30 minutes, suggesting a tightly regulated system and a role in stress response (Dove *et al.*, 1997; Bonangelino *et al.*, 2002; Cooke *et al.*, 1998). PI(3,5)P₂ depletion in yeast leads to swollen vacuoles, which are defective in retrograde trafficking with poor acidification. Study of mammalian PIKfyve has been aided by the creation of mouse mutants with defective

PIKfyve complex elements: perturbations in the effectiveness of PIKfyve lead to endosome enlargement / vacuolation in cells and embryonic lethality / neurodegeneration in mice (Chow *et al.*, 2007; Zhang *et al.*, 2007; Zolov *et al.*, 2012). Interestingly, while Fig4 antagonises the action of PIKfyve, it is also required for PIKfyve activation, making study of a PI(3,5)P₂ overabundant phenotype difficult.

In addition to the functions of PI(3,5)P₂, it should be noted that this phosphoinositide is capable of being modified by myotubularin related proteins (MTMRs) into PI(5)P, meaning PI(3,5)P₂ may contribute indirectly to the formation of PI(5)P within the cell (Berger *et al.*, 2002; Zolov *et al.*, 2012; Oppelt *et al.*, 2013).

PIKfyve exists in a cytosolic pool when inactive and is recruited to the site of action through association with the endosomal membrane (Shisheva *et al.*, 2001). The specific site of PIKfyve action has been somewhat controversial, however it is generally agreed that PIKfyve colocalises with primarily late endosomal and lysosomal markers, with some early endosomal involvement (Rutherford *et al.*, 2006). Mechanisms underlying the action of PIKfyve in mammals is unclear, however it appears to be required for the maintenance of endosomal trafficking, including that which is associated with the recruitment of ESCRT proteins and the formation of vesicles within multivesicular bodies, endosome-to-TGN transport and autophagy progression (Gary *et al.*, 1998; Odorizzi *et al.*, 1998; Whitley *et al.*, 2003; Rusten *et al.*, 2006; Rutherford *et al.*, 2006; Zhang *et al.*, 2007).

In spite of its relevance in cellular homeostasis and organism health, the PIKfyve signalled effectors remain poorly characterised. Interestingly, there appears to be a link between PIKfyve activity and mTOR, with PI(3,5)P₂ levels increased in cells upon addition of energy positive signals such as amino acids and insulin (Bridges *et al.*, 2012). Bridges *et al.* found that loss of a fully functional PIKfyve complex resulted in low phosphorylation of S6K1 (a primary downstream target of mTOR), and that the mTORC1 subunit RAPTOR binds PI(3,5)P₂. Subsequently, it was found that PIKfyve's effect on mTOR is reflected in yeast,

with the S6K1 homolog Sch9 recruited by PI(3,5)P₂ for TORC phosphorylation (Jin *et al.*, 2014). The channel mucolipin TRPML (Reviewed in Zeevi *et al.*, 2007) is another established effector of PI(3,5)P₂. PI(3,5)P₂ deficiency prevents TRPML activation, blocking Ca⁺ release from the endosomal lumen. Ca⁺ is required for endosomal / lysosomal fusion events, leading to lysosomal swelling (Dong *et al.*, 2010).

1.5.3 PIKfyve in Human Disease

A functioning PIKfyve complex is crucial to endosomal homeostasis and as such, defects can have a significant impact on the cell and organism as a whole. Studies in mice have shown similar themes in mutant or null copies of PIKfyve complex members, with vacuolation and neurodegeneration being the overarching phenotype (Chow *et al.*, 2007; Zhang *et al.*, 2007; Zolov *et al.*, 2012).

Corneal Fleck Dystrophy (CFD) is a condition linked to heterozygous null PIKfyve. CFD is characterised by visible white bodies within the cornea, thought to be distended keratocyte vacuoles (Li *et al.*, 2005). While Vac14 has not yet been conclusively linked to a specific human disease, it does appear to be down-regulated in those with chronic fatigue syndrome (Carmel *et al.*, 2006), and perhaps more significantly, Vac14 null mice show severe neuronal degeneration with perinatal death (Zhang *et al.*, 2007). Mutations in Fig4 cause Charcot-Marie-Tooth syndrome type 4J, a disease characterised by progressive peripheral neurodegeneration, including vacuolisation of sensory neurons and lysosomal storage dysfunction in motor neurons, with eventual demyelination leading to loss of sensation and muscle function (Zhang *et al.*, 2008; Chow *et al.*, 2009; Katona *et al.*, 2011; McCartney *et al.*, 2014; Nicholson *et al.*, 2011). A more severe form of disease occurs as Yunis-Varón syndrome, when homozygous or compound heterozygosity for a Fig4 null mutation leads to systemic defects, primarily presenting as central nervous system dysfunction and skeletal abnormalities (Campeau *et al.*, 2013).

1.6 Investigating Novel Interaction Partners of APP

Recent work aimed to establish APP interaction partners, specifically those that interact with APP's intracellular domain. An interactome was established using a proteo-liposome presenting method (Pocha *et al.*, 2011), followed by Label Free Quantification mass spectrometry (Hubner *et al.*, 2010).

Proteo-liposome presentation was performed by creating liposomes that include reactive maleimide-lipid anchors (**Figure 16A**). An N-terminal cysteine on bacterially expressed AICD couples the protein to the maleimide moiety of the lipid anchor producing AICD presented to the external environment (**Figure 16B**). AICD is presented in a similar manner to APP on an endosomal surface *in vivo*, which exposes its intracellular domain to the cytosol. The AICD-liposomes were incubated in pig brain cytosol, which acted as a protein pool from which AICD could pull interaction partners from (**Figure 16C**). After liposomes were washed and the attached proteins digested, the resulting peptides were identified and quantified by mass spectrometry to determine proteins interacting with AICD.

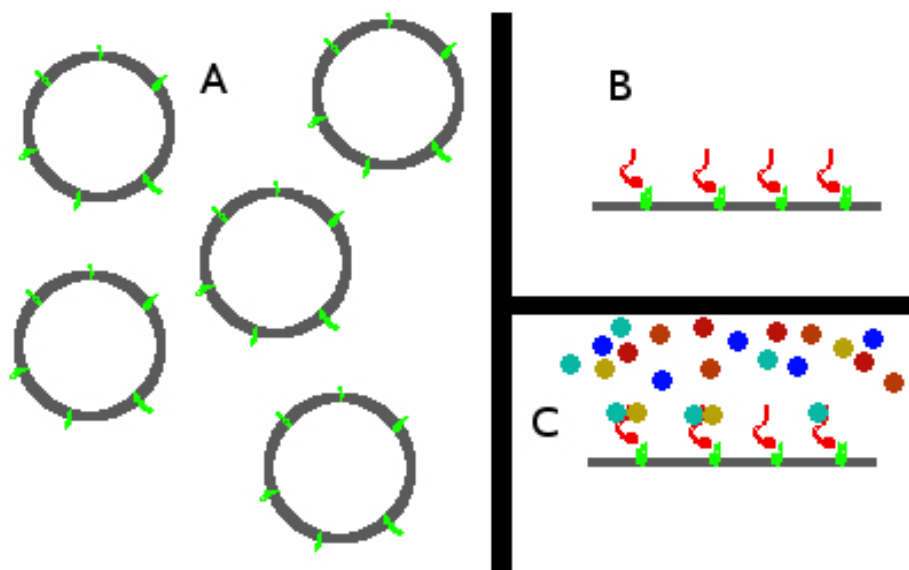


Figure 16.) AICD Proteo-liposome presentation method. A) Liposomes were created with reactive maleimide-lipid anchors embedded (green). **B)** AICD (red) was coupled to the lipid anchor. **C)** AICD proteo-liposomes were incubated in pig brain cytosol to provide a protein pool.

The proteo-liposome presentation method has the advantage of providing a 'membrane context', allowing interactions that require membrane interaction in addition to AICD. Mass spectrometry of bound proteins revealed 327 interaction partners significantly enriched over those from control proteo-liposomes in three replicate experiments. Among the enriched proteins were the established interaction partners Fe65, X11/Mint, SNX17 and Numb.

In addition to established AICD interactors, two candidate interactors of AICD that particularly stood out amongst those identified were the mTORC1 and PIKfyve complexes. Interestingly, in both cases multiple individual proteins from the complexes were enriched: mTOR, RAPTOR and mLST8 from mTORC1, and PIKfyve, Fig4 and Vac14 (all members) from the PIKfyve complex (unpublished dataset; Balklava *et al.*, 2015).

1.6.1 Confirming and Elaborating the Physical Interaction Between APP and mTOR

The interaction data must be interpreted with caution in light of the artificial, non-cellular conditions in which it is obtained. Building upon initial findings, Western blotting of AICD proteo-liposomes was performed, and confirmed the presence of mTOR and Raptor. Pulldown assays using AICD and HEK-293t lysates independently verified the mTOR interaction (unpublished dataset). Further experiments in HeLa cells showed strong colocalisation between mTOR, the late endosomal marker Lamp1 and either APP-GFP or AICD-GFP (unpublished dataset).

To elaborate the interaction, the respective requirements for binding were investigated. mTOR truncation, expression in *E. coli*, purification and AICD proteo-liposome recruitment showed AICD only binds to the kinase domain (R1955-W2549) (unpublished dataset). Subsequently, truncation of AICD showed the membrane proximal 10 amino acids (Truncation 4) to be necessary and sufficient for mTOR binding (unpublished dataset).

The experiments on APP-mTOR interaction described above appear to show that APP and mTOR bind through a direct protein-protein interaction between the kinase domain of mTOR and the 10 membrane proximal amino acids of AICD. The binding of AICD to the kinase domain of mTOR raises interesting questions about the nature of the interaction, in particular, if the kinase domain of mTOR is bound by AICD, what specific effect does that binding have? Does AICD alter mTOR signalling?

1.6.1.1 Biological Significance of the APP/mTOR Interaction

The plausibility of the interactions between APP and mTOR being of functional significance *in vivo* is supported by the fact that mTOR signalling has already been linked with Alzheimer's disease. Indeed, the role of increased mTOR signalling in Alzheimer's has already been reviewed in some detail, with discussions including research into dysfunctional protein synthesis, mTOR dependent tau phosphorylation and mTOR signaling dependent neurodegeneration (Pei and Hugon 2008).

1.6.2 Confirming and Elaborating the Physical Interaction Between APP and the PIKfyve Complex

As with the mTOR interaction, initial interaction data must be confirmed for further research to be justified. Western blotting of AICD proteo-liposomes was performed, and confirmed the presence of Vac14, a member of the PIKfyve complex, on proteoliposomes (Balklava *et al.*, 2015). Further experiments in HeLa cells showed colocalisation between Vac14-mCit, APP-CFP and either the early endosomal marker EEA1 or the late endosomal marker Lamp1 (Balklava *et al.*, 2015). Results also appear to align with previous research showing PIKfyve to be related to the endosomal sorting of receptors (Rutherford *et al.*, 2006).

Currinn *et al.* used truncation mutants to verify and elaborate on the requirements for interaction, pulldown of Vac14 was performed from HEK293 lysates using AICD or truncation mutants of AICD. Truncation of AICD showed that, in contrast to the requirements of mTOR

binding, the C-terminal (cytosolic) extremity of AICD is important to the binding of Vac14 (Currinn *et al.*, 2016).

The experiments described above demonstrated that the PIKfyve complex and APP interact via a direct protein-protein interaction between Vac14 and the C-terminus of AICD. An APP interaction with the PIKfyve complex is novel, and to our knowledge, no previous research directly indicates a link. Whether this interaction has biological significance requires experimental investigation.

1.6.3 Challenges in APP Family Research

When considering the practicalities of experiments involving APP manipulation, the potential pitfalls in experimental approach and interpretation must be considered. Perhaps the most overt challenge in APP research is the redundancy with other proteins within the APP family: APP, APLP1 and APLP2 have differing capacities to compensate for the loss of other members functions. In the case of APP, single knockout mice are viable and fertile, though they exhibit lower body and brain weight, impaired grip strength and altered behaviour as compared to wild type mice (Muller *et al.*, 1994; Zheng *et al.*, 1995; Li *et al.*, 1996; Magara *et al.*, 1999). APP/APLP1 double knockout mice are also viable (Heber *et al.*, 2000). In contrast APP/APLP2 and APLP1/APLP2 double knockout mice both exhibit perinatal lethality (von Koch *et al.*, 1997; Heber *et al.*, 2000). While APLP2 single knockout mice are viable, it appears that APLP2 is an absolute requirement for viability, suggesting perhaps that APLP2 is the exemplar of the APP family, rather than the more widely studied APP (**Table 3**; Heber *et al.*, 2000).

Table 3.) APP family: mouse knockouts and corresponding phenotypes (adapted from Heber *et al.*, 2000).

Knockout	Phenotype	Reference
APP	Viable, low body weight, poor grip strength, altered behaviour	Zheng <i>et al.</i> , 1995; Müller <i>et al.</i> , 1994; Li <i>et al.</i> , 1996; Tremml <i>et al.</i> , 1998
APLP1	Postnatal growth deficit	Heber <i>et al.</i> , 2000
APLP2	Viable, Normal	Von Koch <i>et al.</i> , 1997
APP+APLP1	Viable	Heber <i>et al.</i> , 2000
APP+ APLP2	Perinatally lethal	Von Koch <i>et al.</i> , 1997; Heber <i>et al.</i> , 2000
APLP1+ APLP2	Perinatally lethal	Heber <i>et al.</i> , 2000

An answer to investigational difficulties caused by functional redundancy may lie in simpler model organisms containing one APP orthologue, such as *C. elegans*. In addition, such simpler organisms can be a superior system that gives a high level of control over experimental conditions and potential confounding factors.

Mammalian cell lines can bridge the gap between an easily manipulated model and relevance in higher organisms, as an example, RNA interference (RNAi) can be used to knock down gene expression. One weakness of RNAi is the possibility of off-target effects, where the RNAi used targets other mRNA for destruction, however, this can be mitigated by using two different RNAi sequences for each target protein to identify target-specific effects.

With regards to the APP family, functional redundancy is problematic but is not insurmountable. Studying knockdown of APP family proteins simply requires a modified approach to the canonical single knockdown. The HeLa cell model may have advantages with regards to APP: according to expression data, HeLa cells do not express APLP1 (NCBI 2007; Scotto *et al.* 2008; NCBI 2008), although some companies selling polyclonal antibodies against APLP1 claim to detect it in HeLa cells (GeneTex 2013; Elabscience 2015). Lack of APLP1 drastically reduces the number of conditions required for study. Another challenge to studying AICD in particular is the small, transient nature of the protein; due to prompt destruction by the cell, it is particularly difficult to manipulate in a meaningful way through classical overexpression (Cupers *et al.*, 2001). GFP fusion is unlikely to overcome this issue – either interfering with interactions under investigation or otherwise failing to stabilise the protein enough to overcome this issue (Chang 2010). The challenge is to manipulate the level of AICD rapidly, in a reproducible manner.

1.6.4 Challenges in mTOR Research

While mTOR research is an established area of study, there are issues associated with it. mTOR signalling lies within a complicated network of cellular signalling, with a broad impact on major cellular functions in higher organisms. On a cellular level, mTOR controls many aspects of metabolism, stress response and proliferation, while on an organism wide scale,

mTOR impacts on aging and energy balance, in addition to its originally recognised role in immune responses (Heitman *et al.*, 1991; Brown *et al.*, 1994; Calne *et al.*, 1989; Collier 1989; Thompson and Woo 1989; Tocci *et al.*, 1989).

The systems used to study mTOR can be expected to have an effect on results, cultured cells in particular. In cell lines, the genetic background is already highly abnormal at the gene and chromosomal level, in order to enable continued culture. Characteristics required for prolonged and optimum culture include altered cell cycle controls, energy sensing and stress response, which of course are all within the domain of mTOR control. Furthermore, cell culture generally involves pushing cells into a growth state, be it through atmospheric oxygen concentrations, or the abundance of glucose and other nutrients, all of which are not representative of *in vivo* conditions (Schmelzle and Hall 2000; Pópulo *et al.*, 2012).

Interpreting results from cell culture becomes extremely difficult: are results due to experimental manipulation or are they an artifact of altered mTOR behaviour? With the weaknesses of studying mTOR in cell culture it is important to avoid or mitigate limitations by changing experimental conditions such as nutrient or growth factor availability. Furthermore, results should be supported using a system other than cell culture, for example with experiments performed in model organisms.

1.6.5 Challenges in PIKfyve Research

PIKfyve is a particularly challenging complex to study: PIKfyve's product, PI(3,5)P₂ is an extremely low abundance phosphoinositide, classically requiring specialist equipment and procedures to detect it. For example, doping target cells with tritiated inositol, extraction of lipids without degrading the target phosphoinositides, followed by HPLC/radionuclide detection (Dove *et al.*, 1997; Bonangelino *et al.*, 2002) or ³²P (Nocot *et al.*, 2006; Zhang *et al.*, 2007; Jefferies *et al.*, 2008). Biochemical quantification by classical methods is prohibitive

in terms of time, effort and equipment required, and as such has been a major roadblock in the field of PI(3,5)P₂ research. The ability to visualise PI(3,5)P₂ distribution would drastically improve PIKfyve research, allowing deeper dissection of the processes and interactions surrounding the complex.

1.6.5.1 Phosphoinositide Probes

Phosphoinositides provide a substrate capable of signalling the identity of a membrane, binding effectors that go on to enact the dynamic processes specific to that microenvironment. A variety of phosphoinositide binding sites have been discovered within proteins, including Pleckstrin Homology (PH), Phox Homology (PX) and FYVE domains (Cullen *et al.*, 2001; Itoh and Takenawa 2002; Lemmon 2003). These binding sites can be specific for certain phosphoinositides depending on sequence and have been used as the basis for specific probes. Phosphoinositide probes have been employed in research to elucidate the functions of inositides and characterise the processes of endosomal function and trafficking. Phosphoinositide specific probes are created by fusing the binding domain specific to the phosphoinositide of interest to a reporter such as GFP, examples of such probes include the FYVE domain of Early Endosome Antigen 1 (EEA1) for PI(3)P or the PH domain of phospholipase C for PI(4,5)P₂ (**Table 4**; Halet 2005). A PI(3,5)P₂ probe has the potential to open a variety of investigations which may otherwise be impossible with previously available techniques.

Table 4.) Phosphoinositide probes by *in vitro* specificity (from Halet 2005). A variety of phosphoinositide probes have been developed using binding domains shown to have specificity *in vitro* and used to study the endosome.

<i>In vitro</i> specificity	Protein Domain	Reference
PI(4,5)P ₂	PH _{PLCδ}	Lemmon <i>et al.</i> , 1995; Garcia <i>et al.</i> , 1995; Kavran <i>et al.</i> , 1998
PI(3,4,5)P ₃	PH _{Btk} PH _{CRP1} PH _{cytohesin} PH _{ARNO}	Rameh <i>et al.</i> , 1997; Kojima <i>et al.</i> , 1997; Klarlund <i>et al.</i> , 1997; Klarlund <i>et al.</i> , 1998; Venkateswarlu <i>et al.</i> , 1998a; Venkateswarlu <i>et al.</i> , 1998b; Venkateswarlu <i>et al.</i> , 1999
PI(3,4,5)P ₃ /PI(3,4)P ₂	PH _{PDK1} PH _{PKB}	French <i>et al.</i> , 1997; Stokoe <i>et al.</i> , 1997; Franke <i>et al.</i> , 1997; Kavran <i>et al.</i> , 1998
PI(3,4)P ₂	Pxp4/phox PH _{TAPP1/2}	Kanai <i>et al.</i> , 2001; Ellson <i>et al.</i> , 2001; Stahelin <i>et al.</i> , 2003; Dowler <i>et al.</i> , 2000; Thomas <i>et al.</i> , 2001; Watt <i>et al.</i> , 2004; Ago <i>et al.</i> , 2001; Zhan <i>et al.</i> , 2002
PI(3)P	FYVE _{EEA1} FYVE _{Hrs} PX _{p40phox}	Burd and Emr 1998; Gaullier <i>et al.</i> , 1998; Patki <i>et al.</i> , 1998; Gillooly <i>et al.</i> , 2000; Ellson <i>et al.</i> , 2001; Kanai <i>et al.</i> , 2001
PI(4)P	PH _{OSBP} PH _{FAPP1}	Levine and Munro 1998, 2002; Dowler <i>et al.</i> , 2000
PI(5)P	PHD _{ING2}	Gozani <i>et al.</i> , 2003

1.6.5.2 TRPML1 and the PI(3,5)P₂ Probe

The Transient Receptor Potential Mucolipin 1 (TRPML1) is a Ca²⁺ release channel specifically activated by PI(3,5)P₂, TRPML1 is a 65kDa protein, mutations of which are associated with type IV mucopolipidosis, a lysosomal storage disorder (Bargal *et al.*, 2000; Sun *et al.*, 2000; Dong *et al.*, 2010). ML1N, the N-terminal polybasic domain of TRPML is the binding domain of TRPML, specific for PI(3,5)P₂, because of its specificity, ML1N was an ideal candidate for development of a PI(3,5)P₂ probe. Li *et al.* developed ML1Nx2-GFP to facilitate identification of PI(3,5)P₂ positive vesicles (Dong *et al.*, 2010; Li *et al.*, 2013). This probe, if specific and as effective as reported, represents an advance in the investigative tools for the study of PI(3,5)P₂, and will be useful in the study of an APP/PIKfyve interaction.

1.6.6 Project Aims

Previous research has found a physical interaction between APP/mTOR and APP/PIKfyve.

This project aims to answer the following questions:

A) Does the physical interaction detected between APP and mTOR represent a functional relationship?

B) Does the physical interaction detected between APP and PIKfyve represent a functional relationship?

C) What is the nature of any functional relationship, specifically, how does this fit into the biology of the cell and relate to human disease?

Chapter 2

Materials and

Methods

2.1 Materials and Methods

2.1.1 Materials

Table 5. Protein Purification Solutions	
Wash buffer	50mM Potassium chloride (Fisher Scientific) 25mM HEPES (Fisher Scientific) 1mM Magnesium chloride (Fisher Scientific) pH7.0
Protein purification cell lysis buffer	150mM Sodium chloride (Fisher Scientific) 50mM Tris (Fisher Scientific) 10mM Imidazole (Sigma Aldrich) pH7.2
Elution Buffer	250mM Imidazole (Sigma Aldrich) 150mM Sodium chloride (Fisher Scientific) 50mM Tris (Fisher Scientific) pH7.2
Clearance buffer	500mM Sodium chloride (Fisher Scientific) 50mM TrisCl pH8.0 (Fisher Scientific) 10mM EDTA (Fisher Scientific)
Dialysis Buffer	125mM Potassium acetate (Fisher Scientific) 20mM HEPES (Fisher Scientific) 1mM EDTA (Fisher Scientific) pH7.2 (with KOH) (Fisher Scientific)

Table 6. Bacterial Culture Solutions and Media	
Lysogeny Broth (LB)	1L Distilled water 20g LB (Melford Bioscience) (autoclaved)
LB agar	1L Distilled water 37.5g LB agar (Fisher Scientific) (autoclaved)
Selective bacteriological media	LB agar or broth kanamycin (50µg/µl) (Sigma Aldrich) or ampicillin (100µg/µl) (Sigma Aldrich)
Nematode Growth Medium (NGM)	132ml K ₂ HPO ₄ (1M stock solution) (Fisher Scientific) 868ml KH ₂ PO ₄ (1M stock solution) (Fisher Scientific) 3g NaCl (Fisher Scientific) 2.5g Bacto peptone (Sigma Aldrich) 10g Agar (Sigma Aldrich) 10g Agarose (Fisher Scientific) After autoclaving: 1ml MgSO ₄ (1M stock solution, filter sterilised) (Fisher Scientific) 1ml CaCl ₂ (1M stock solution, filter sterilised) (Fisher Scientific) 1ml Cholesterol stock solution (5mg/mL in ethanol, filter sterilised) (Sigma Aldrich)

Table 7. Cloning	
10 x PCR buffer	500mM Potassium chloride (Fisher Scientific) 100mM Tris Cl pH8.8 (Fisher Scientific) 25mM Magnesium chloride (Fisher Scientific) 1% (v/v) Triton X-100 (Fisher Scientific)
Cloning PCR	40µl Sterile, distilled water 5µl 10x PCR buffer 1µl Primer 1 (10µM) 1µl Primer 2 (10µM) 1µl Taq polymerase (New England BioLabs) 1-2µl DNA template (1-10ng/µl)
Analytical PCR	16µl Sterile, distilled water 2µl 10x PCR buffer 0.4µl Primer 1 (10µM) 0.4µl Primer 2 (10µM) 0.4µl Taq polymerase (New England BioLabs) 0.5-1µl DNA template (1-10ng/µl)
Plasmid preparation solution 1	50 mM TrisCl pH 8.0 (Fisher Scientific) 10 mM EDTA (Fisher Scientific) 100µg/ml RNaseA (Fisher Scientific)
Plasmid preparation solution 2	200mM Sodium hydroxide (Fisher Scientific) 1% (w/v) SDS (Fisher Scientific)
Plasmid preparation solution 3	3M Potassium acetate pH5.5 (Fisher Scientific)
TAE buffer	40mM Tris (Fisher Scientific) 20mM Acetic acid (Fisher Scientific) 1mM EDTA (Fisher Scientific) pH8.0
TE buffer	10mM TrisCl pH8.0 (Fisher Scientific) 1mM EDTA (Fisher Scientific)

Table 8. Tissue Culture Solutions and Media	
Phosphate buffered saline (PBS)	137mM Sodium chloride (Fisher Scientific) 10mM Disodium phosphate (Fisher Scientific) 2.7mM Potassium chloride (Fisher Scientific) 1.8mM Potassium dihydrogen phosphate (Fisher Scientific) pH7.4
Cell culture medium: DMEM	Dulbecco's Modified Eagle Medium (DMEM) (Gibco) 10% (v/v) foetal calf serum (FCS) (Gibco) 1% (v/v) penicillin/streptomycin (Gibco)
Cell culture medium: RPMI 1640	Roswell Park Memorial Institute 1640 (RPMI 1640) medium (Gibco) 10% (v/v) FCS (Gibco) 1% (v/v) penicillin/streptomycin (Gibco)
Freezing medium	70% (v/v) cell culture medium 30% (v/v) FCS (Gibco) 10% (v/v) DMSO (Fisher Scientific)
4% Formaldehyde	4% formaldehyde from paraformaldehyde (w/v) (Fisher Scientific) dissolved in PBS (Fisher Scientific)
Mowiol mounting media	12.0ml 0.2M Tris Cl, pH8.5 (Fisher Scientific) 6.0ml H ₂ O 6.0g glycerol (Fisher Scientific) 2.4g Mowiol 4-88 (Sigma Aldrich) 2.5% (w/v) 1,4-diazobicyclo-[2.2.2]-octane (DABCO) (Sigma Aldrich)

Table 9. SDS-PAGE and Western Blotting Solutions	
Mammalian cell lysis buffer	150mM Sodium Chloride (Fisher Scientific) 50mM Tris pH 8.0 (Fisher Scientific) 1% (v/v) Triton-X100 (Fisher Scientific) 2.5mM β -glycerophosphate (Sigma Aldrich) 1mM EDTA (Fisher Scientific) 1mM NH ₄ F (Fisher Scientific) 1mM Vanadate (Sigma Aldrich) 1mM PMSF (Sigma Aldrich) 10mM Pyro-phosphate (Sigma Aldrich) 4 μ g/ml E-64 (Sigma Aldrich) 3.3 μ g/ml Aprotinin (Sigma Aldrich) 1 μ g/ml Pepstatin (Sigma Aldrich)
4x Laemmli buffer	200mM Tris pH 6.8 (Fisher Scientific) 40% (v/v) Glycerol (Fisher Scientific) 4% (w/v) SDS (Sodium dodecyl sulphate) (Fisher Scientific) 4% (v/v) β -mercaptoethanol (Fisher Scientific) 0.04% (w/v) Bromophenol blue (Fisher Scientific)
4x Separation gel buffer	1.5M Tris pH8.8 (Fisher Scientific)
4x Stacking gel buffer	0.5M Tris pH6.5 (Fisher Scientific)
SDS running buffer	190mM Glycine (Fisher Scientific) 25mM Tris (Fisher Scientific) 3.5mM SDS (Fisher Scientific)
10x Blotting buffer	1.9M Glycine (Fisher Scientific) 0.25M Tris base (Fisher Scientific) pH8.3
Blotting buffer	400mM Tris base (Fisher Scientific) 50mM Glycine (Fisher Scientific) 20% (v/v) Methanol (Fisher Scientific) pH8.3
10x TBS	1.5M Sodium chloride (Fisher Scientific) 0.2M Tris base (Fisher Scientific) pH7.5
TBSt	10% (v/v) 10x TBS 1% (v/v) Tween 20 (Fisher Scientific)
Blocking solution	TBSt 5% (w/v) Bovine serum albumin (BSA) (Fisher Scientific) 0.1% (v/v) Sodium azide (Fisher Scientific)
Enzyme substrate solution	100mM Tris pH 8.5 (Fisher Scientific) 1.25mM Luminol (Sigma Aldrich) 0.18mM Coumaric acid (Fisher Scientific) 0.01% (v/v) Hydrogen peroxide (added immediately before procedure) (Fisher Scientific)
X-ray film developer solution	Carestream® Kodak® autoradiography GBX developer/replenisher (Sigma Aldrich)
X-ray film fixer solution	Carestream® Kodak® autoradiography RP X-Omat LO fixer/replenisher (Sigma Aldrich)
Coomassie destain	70% (v/v) Distilled water 20% (v/v) Methanol (Fisher Scientific) 10% (v/v) Acetic acid (Fisher Scientific)
Coomassie stain	50% (v/v) Ethanol (Fisher Scientific) 40% (v/v) Distilled water 10% (v/v) Acetic acid (Fisher Scientific) 0.25% (w/v) Coomassie Brilliant Blue-R250 (Fisher Scientific)

Table 10. Antibodies				
Target	Company	Catalogue Number	Dilutions	Concentration
4EBP1 (rabbit IgG)	Cell Signaling Technology	9644	1:2000	Lot specific
4EBP1 Thr37/46 phospho-specific (rabbit IgG)	Cell Signaling Technology	2855	1:2000	Lot specific
4EBP1 Ser65 phospho-specific (rabbit IgG)	Cell Signaling Technology	13443	1:2000	Lot specific
4EBP1 Ser70 phospho-specific (rabbit)	Cell Signaling Technology	9455	1:2000	Lot specific
Akt (rabbit)	Cell Signaling Technology	9272	1:2000	Lot specific
Akt phospho-Ser473 phospho-specific (rabbit)	Cell Signaling Technology	9271	1:2000	Lot specific
Anti-mouse HRP (Horse IgG Secondary)	Cell Signaling Technology	7076	1:4000	Lot specific
Anti-rabbit HRP (Goat IgG Secondary)	Cell Signaling Technology	7074	1:4000	Lot specific
Anti-mouse Alexa 488 (Goat IgG F(ab') ₂ Secondary)	Cell Signaling Technology	4408	1:500	Lot specific
Anti-rabbit Alexa 488 (Goat IgG F(ab') ₂ Secondary)	Cell Signaling Technology	4412	1:500 (immunostain)	Lot specific
Anti-mouse Alexa 555 (Goat IgG F(ab') ₂ Secondary)	Cell Signaling Technology	4409	1:500	Lot specific
Anti-rabbit Alexa 555 (Goat IgG F(ab') ₂ Secondary)	Cell Signaling Technology	4413	1:500	Lot specific
APLP2 (rabbit IgG)	Abcam	ab140624	1:1000	Lot specific
APP (mouse IgG _{2b})	Santa Cruz Biotechnology	sc-53822	1:1000	200µg/ml
EEA1 (mouse IgG ₁)	BD Biosciences	610457	1:200	250µg/ml
eEF1A (mouse IgG1)	Upstate	05-235	1:2000	Lot specific
GFP (mouse IgG _{2b})	Santa Cruz Biotechnology	sc-81045	1:2000	100µg/ml
Lamp1 (mouse IgG ₁)	Santa Cruz Biotechnology	sc-20011	1:200	200µg/ml
MBP (mouse IgG1)	Cell Signaling Technology	2396	1:2000	Lot specific
mTOR (rabbit IgG)	Cell Signaling Technology	2983	1:2000	Lot specific
mTOR Ser2448 phospho-specific (rabbit)	Cell Signaling Technology	2971	1:2000	Lot specific
mTOR Ser2481 phospho-specific (rabbit)	Cell Signaling Technology	2974	1:2000	Lot specific
PIKfyve PIP5KIII (mouse IgG _{2a})	Santa Cruz Biotechnology	sc-100408	1:2000	100µg/ml
Raptor (mouse IgG ₁)	Santa Cruz Biotechnology	sc-81537	1:1000	100µg/ml
Rictor (rabbit IgG)	Cell Signaling Technology	9476	1:1000	Lot specific
S6K1 (rabbit)	Cell Signaling Technology	9202	1:2000	Lot specific
S6K1 phospho-Thr389 (phospho-specific) (rabbit)	Cell Signaling Technology	9205	1:2000	Lot specific
Tau (mouse IgG1)	Thermo Fisher	MN1000	1:2000	200µg/ml
Tubulin (rabbit IgG)	Abcam	ab125267	1:2000	0.5mg/ml
Vac14 (mouse IgG _{2b})	Santa Cruz Biotechnology	sc-271831	1:2000	200µg/ml

2.1.2 General Methods

2.1.2.1 Creation of Electrocompetent *E. coli*

E. coli (TOP10 / BL21DE3) overnight cultures were inoculated from frozen stocks into 2L conical flasks containing 500ml LB broth at a concentration of 1:100. Cultures were grown at 37°C in a 200rpm shaking incubator to 0.6 OD₆₀₀. The culture was chilled on ice for 20 minutes, then pelleted by centrifugation: 4000x g for 15 minutes at 4°C. Supernatant was removed, then cells resuspended in half the original culture's volume of ice cold, 10% (v/v) glycerol. The new suspension was centrifuged again (4000x g for 15 minutes at 4°C), then resuspended in 1/10th the previous volume of 10% glycerol. A final centrifugation was carried out, as above and the cells resuspended in a minimal volume of 10% glycerol, aliquoted into microcentrifuge tubes, then rapidly frozen in liquid nitrogen. Samples were stored at -80°C until used for transformation.

2.1.2.2 Bacterial Transformation of Electrocompetent *E. coli*

Bacterial transformation was performed by adding 100µl of electrocompetent bacteria and 5µl of the required plasmid into an electroporation cuvette. A pulse of 1.8kV was passed through the solution using a MicroPulser Electroporator (Bio Rad). and 1ml warm LB broth was immediately added. The transformed bacterial solution was incubated at 37°C for 1 hour, then inoculated onto an LB agar plate with added antibiotic (the antibiotic depending on the resistance found in the plasmid). Plates were incubated at 37°C for 24 hours prior to selection of transformed, antibiotic resistant clones. Clones were subsequently used for plasmid isolation, cloning or protein production.

2.1.2.3 Plasmid Isolation

Small volume, high quality plasmid preparation was performed using PeqGold plasmid miniprep kit (PeqLab) using the manufacturer's instructions.

Larger volumes of DNA were prepared by inoculating bacteria containing the required plasmid into 200ml LB broth plus an appropriate antibiotic. Cultures were grown overnight in

a 200rpm shaking incubator at 37°C, then centrifuged for 20 minutes at 2500x g and 4°C. Supernatant was discarded, then the pellet was resuspended in 5ml of 'solution 1' (50mM TrisCl, pH8.0, 10mM EDTA, 100µg/ml RNase A). 5ml 'solution 2' was added (200mM NaOH, 1% SDS), and the resulting mixture inverted then incubated for no more than 5 minutes at room temperature. 5ml solution 3 was added (3M potassium acetate, pH5.5), the mixture inverted repeatedly, then centrifuged for 20 minutes at 2500x g, 4°C. The floating debris layer was removed and discarded then the supernatant passed through a 0.45µm syringe filter. The filtered supernatant was combined with 15ml ice cold 100% isopropanol, mixed vigorously then incubated on ice for 15 minutes. The mixture was centrifuged as above once more and the supernatant removed, then the pellet washed with 70% ethanol and centrifuged again for 10 minutes. The supernatant was drained from the pellet, and the pellet dried through evaporation. The pellet was dissolved in an appropriate volume of TE buffer dependent on pellet size for further use.

2.1.2.4 Restriction Digests

For cloning purposes 10µg plasmid was added to 40µl sterile, distilled water with the correct buffer at the correct concentration, as per manufacturer instruction (New England BioLabs or Roche). 4µl of each relevant restriction enzyme was added, and the resulting mixture incubated at the required temperature suggested by the manufacturer.

2.1.2.5 Cloning

Agarose gels for DNA electrophoresis were made by dissolving 1% agarose (molecular biology grade) in TAE buffer and adding ethidium bromide to a final concentration of 0.01%. The solution was cooled at room temperature to roughly 60°C, poured into an appropriate gel cast / well comb combination, then left to set at room temperature. The first well was loaded with 5µl 0.1-10kb DNA marker (PeqLab) subsequent lanes were loaded with relevant DNA samples. Gels were run at 100V.

2.1.2.6 Polymerase Chain Reaction (PCR)

The DNA template to be used in the PCR reaction was diluted with distilled water to an appropriate concentration (plasmid DNA 1-10ng/ μ l, cDNA ~100ng/ μ l, genomic DNA 100-500ng/ μ l). Primers were diluted to a working concentration of 10 μ M, then the PCR reagents mixed on ice in PCR tubes with volumes dependent on whether PCR products are to be used for cloning or analytical purposes (**Table 11**).

Table 11. PCR Reagents cycle parameters were dependent on reaction requirements		
Volume (μ l) for cloning	Volume (μ l) for analytical purposes	Reagent
40	16	Sterile, distilled water
5	2	10x PCR buffer
1	0.4	dNTPs (10mM) (New England BioLabs)
1	0.4	Primer 1 (10 μ M)
1	0.4	Primer 2 (10 μ M)
1	0.4	Taq polymerase (New England BioLabs)
1-2 (1-10ng/ μ l)	0.5-1 (1-10ng/ μ l)	DNA template

PCR cycle programming was as follows:

- 1) 94°C, 1:30 minutes.
- 2) 94°C, 30 seconds.
- 3) 60°C, 30 seconds (annealing temperature, variable depending on primer length and composition).
- 4) 72°C, 1 minute per kilobase of PCR product.
- 5) Step 2-4 x35.
- 6) 72°C 10 minutes.
- 7) 4°C, ∞ minutes.

Mixed samples were sealed and inserted into the PCR machine with the tube surface in full contact with the sample holder and the PCR cycling started. Finished products were run on 1-2% agarose gels for analysis / purification.

2.1.2.7 Thawing Cell Stocks for Mammalian Tissue Culture

Inside a laminar flow cell culture cabinet, 10ml cell culture media (DMEM for HeLa cells, RPMI for SH-SY5Y) was dispensed into a sterile 15ml centrifuge tube and 5ml into a separate tube, both warmed in a 37°C waterbath. A vial of cells was removed from storage and thawed in the waterbath by gentle agitation, keeping the cap above the water to avoid contamination. The vial and 15ml tube of media were placed in a laminar flow cell culture cabinet and sprayed with 70% ethanol before the vial contents was added to the tube of media. The cell suspension was centrifuged at 300x g for 5 minutes to pellet cells, then the

supernatant was removed from the pellet and replaced with the remaining 5ml pre-warmed media. Cells were gently resuspended and added to a sterile T25 cell culture flask, then placed in a 5% CO₂ incubator at 37°C overnight. The following day old media was replaced with fresh, warmed media. Cells were passaged between 80-90% confluency.

2.1.2.8 Mammalian Tissue Culture Passage

Fresh cell culture media, sterile calcium/magnesium free PBS, and trypsin-EDTA was pre-warmed at 37°C in a waterbath, old media was removed and cells washed with PBS. PBS was removed and replaced with 1ml trypsin-EDTA, ensuring the cell covered surface of the flask was covered. The flask was incubated at 37°C and checked every 2 minutes for loss of cell adhesion. Once cells detached, 5ml fresh media was added and gently aspirated to dissociate clumps of cells. 50µl of cell suspension was removed and mixed with 450µl Trypan blue for counting. The volume required for the seeding density of the next passage was calculated using a haemocytometer (e.g. 2×10^4 cells/cm² x 25cm² for HeLa cells undergoing 4 days growth before passage), enough media to cover the surface of the new cell culture flask was used. The appropriate volume of cell suspension was mixed with warm cell culture media and seeded into a new cell culture flask. If growth is required for prolonged period, culture medium was replaced with fresh, warm media every 2 days.

2.1.2.9 Mammalian Tissue Culture Transfections

DMEM cultured HeLa cells were seeded at 100,000 cells per 0.5ml in 24 well plates containing sterile glass coverslips. For each well, on the following day 1µg of plasmid DNA was diluted in 50µl OptiMEM media (Gibco) and added to 2µl Lipofectamine 2000 (Invitrogen) diluted in 50µl OptiMEM media. After incubation (18 hours, 37°C, 5% CO₂) cells were washed twice with warm tissue culture medium and incubated overnight (37°C, 5% CO₂) prior to experimentation / fixation.

2.1.2.10 Preparation of Mammalian Tissue Culture Cells for Western Blotting

Cultures of HeLa or SH-SY5Y cells were seeded at 100,000 cells per 0.5ml in 24 well plates

and incubated overnight (37°C, 5% CO₂). Cell culture medium was removed and cells washed with ice cold PBS, 100µl mammalian cell lysis buffer was added per well, and the cells scraped and aspirated from the well using a micropipette. The lysate was centrifuged at maximum speed on a benchtop microcentrifuge for 15 minutes at 4°C and the resulting supernatant mixed with Laemmli buffer and heated to 95°C for 5 minutes.

2.1.2.11 Sodium Dodecyl Sulphate Polyacrylamide Gel Electrophoresis (SDS-PAGE)

Polyacrylamide gels were created by mixing appropriate ingredients in different amounts to create one section for adding and collecting protein above another section designed to resolve the proteins depending on molecular weight / charge. Higher percentage gels were used to resolve lower molecular weight proteins (and *vice versa*) as appropriate.

Gel Type	Tris	Glycerol	Bis/Acrylamide (40%)	SDS (10%)	APS (10%)	d.H ₂ O
Stacking (5%)	0.5ml (0.5M pH6.5)	0.4ml	0.25ml	20µl	10µl	0.82ml
Separation (8%)	1.25ml (1.5M, pH8.8)	1ml	1ml	100µl	50µl	1.6ml
Separation (10%)	1.25ml (1.5M, pH8.8)	1ml	1.25ml	100µl	50µl	1.35ml
Separation (15%)	1.25ml (1.5M, pH8.8)	1ml	1.88ml	100µl	50µl	0.73ml

Separation gel polymerisation was initiated by the addition of 2.5µl Tetramethylethylenediamine (TEMED), the solution was then briefly mixed, promptly added into gel-casting glass plates (BioRad) which were already sealed on the bottom and sides. The gel was overlaid with isopropanol and left to polymerise at room temperature for ~30 minutes. Isopropanol was rinsed off with water then allowed to drip dry. 1µl TEMED was introduced to the stacking gel, which was mixed and added on top of the separation gel, a well comb was placed in the stacking gel and the completed gel allowed to set.

A molecular weight marker was added to the first well (ColorPlus prestained protein ladder, broad range, New England BioLabs), and an appropriate volume of protein or lysate mixed with Laemmli buffer was added to subsequent wells. SDS-PAGE was run in SDS buffer,

passing 150V through the gel for ~1 hour or until adequate band resolution was obtained. When not used for western blotting, gels were stained with 400ml coomassie blue stain for 3-4hrs at room temperature, then proteins resolved with repeated coomassie destain application.

2.1.2.12 Western Blotting

Western blot cassettes were assembled, containing an outer layer of Whatman filter paper (8x6cm) with an electrophoresed protein containing SDS-PAGE gel and a methanol activated PVDF membrane (BioRad) cut to 8x5.7cm within. Cooling blocks were added to a western blotting tank, which was then filled with blotting buffer and set to mix at 200rpm using a magnetic bar. Protein transfer was performed at 200mA for 120 minutes. The resulting membrane was incubated in blocking solution for 1 hour at room temperature or overnight at 4°C. Blocking solution was removed and replaced with primary antibody solution, diluted as required in blocking solution and the membrane incubated in primary antibody for 1 hour at room temperature or overnight at 4°C. The primary antibody was removed, and the membrane washed three times for 10 minutes each in TBSt. The final wash of TBSt was replaced with the relevant HRP-conjugated secondary antibody, diluted as required in TBSt, the membrane was then incubated for 1-2 hours. Secondary antibody was removed and the membrane washed three times for 10 minutes each in TBSt. Membranes were incubated in 2.5ml enzyme substrate then sealed in cling film and allowed to expose X-ray film (RX NIF 130mm x 180mm Fujifilm, Fisher Scientific) in a dark room for varied time-points. The film was incubated in developer solution (Kodak) for up to 5 minutes, rinsed in running tap water, then incubated in fixer solution (Kodak) for approximately 5 minutes. Film was washed thoroughly in running tap water, then left to drip dry at room temperature.

2.1.2.13 Immunostaining

HeLa cells grown on coverslips in 24 well plates were washed in warm PBS, then fixed for 20 minutes in 4% formaldehyde fixative (4% formaldehyde from paraformaldehyde in PBS). Following two subsequent washes with PBS, cells were permeabilised using 0.1% Triton X-

100 in PBS for 4 minutes, followed by two more washes with PBS. Cells were incubated under 2% bovine serum albumin (BSA) in PBS for 15 minutes. Cells were exposed to the relevant primary antibody, diluted (1:100-1:300) with 2% BSA in PBS for 1 hour at room temperature. Coverslips were washed three times with PBS, then incubated with secondary, fluorophore-conjugated antibody diluted (1:500) with 2% BSA in PBS. Following a further three PBS washes, cells were mounted on slides using Mowiol.

2.1.2.14 Microscopy

Immunostained, BODIPY, and LysoTracker stained samples were imaged with confocal microscopy using a Leica Microsystems SP5 TCS II MP DM16000B microscope. Cells *in situ* were visualised and imaged under an inverted Nikon Eclipse TS100 microscope with 40x objective.

2.1.3 Investigation Specific Methods

2.1.3.1 Construction of AICD, TAT and TAT-AICD

pET28-MBP-AICD was created using AICD PCR amplified from pEGFP-n1-APP, in turn created from HeLa APP695 cDNA cloned into pEGFP-n1 (Clontech) (Currinn *et al.*, 2016). AICD encoding DNA was amplified with a TAT domain containing 5'-primer, and cloned into pET28-MBP-TEV (Pocha *et al.*, 2011) using 5' BamHI and 3' XhoI sites to make pET28-MBP-TAT-AICD. A HindIII site between TAT and AICD was used in conjunction with Pfu polymerase plus ligation resulting in a frame-shift introducing four bases after TAT, but eliminating AICD, creating pET28-MBP-TAT (Guscott *et al.*, 2016).

2.1.3.2 Protein Expression and Purification

10ml *E. coli* (BL21DE3) overnight cultures containing expression plasmids were inoculated into conical flasks containing 1L LB broth with 50µg/µl kanamycin. Cultures were grown at 37°C in a 200rpm shaking incubator to 0.6 OD₆₀₀. Protein expression was induced by adding 100µM IPTG and the culture incubated for a further 3 hours at 37°C in a 200rpm shaking incubator. Cultures were harvested by 2500x g centrifugation at 4°C for 20 minutes,

supernatant was drained and the resulting pellet stored overnight at -20°C.

Pellets were resuspended in 10ml lysis buffer plus the protease inhibitors E-64 (4µg/ml), aprotinin (3.2µg/ml), pepstatin (1µg/ml) and PMSF (1mM). Resuspension was aided with three cycles of 1 minute sonication followed by 3 minutes incubation on ice. Cell debris was cleared from the lysate using 10,000rpm centrifugation for 30 minutes at 4°C, then passed through a 0.45µm syringe filter.

A Ni-NTA agarose column (Pierce, Thermo Scientific) was equilibrated in protein purification lysis buffer, lysate passed through the column with flow through collected. The column was washed with 6x 10ml protein purification lysis buffer, then the bound protein was eluted using 5ml elution buffer, collected in five elution fractions of 1ml. 10µl samples of each elution fraction were mixed with Laemmli buffer and run on 10% SDS-PAGE to determine the elution fractions containing protein. Columns were cleared of residual protein using 10ml clearance buffer followed by a 10ml distilled water wash. Cleared columns were stored in 20% ethanol and reused by clearing the column of ethanol then washing with 5ml 100mM nickel sulphate.

14000 MWCO dialysis tubing was rinsed in distilled water, then dialysis buffer. Relevant elution fractions were pooled and sealed within the tubing, then incubated in 1L dialysis buffer overnight at 4°C with gentle stirring. Dialysis buffer was changed and the samples incubated again for a total of approximately 24 hours. Purified proteins were aliquoted and, after samples were taken for protein quantification, frozen for future use.

Protein quantification was performed by comparing test samples to bovine serum albumin solutions of known concentration. Triplicate samples were prepared, each with the following: 5µl of protein solution, 25µl BioRad DC protein assay reagent A, 200µl BioRad DC protein assay reagent B (BioRad). Samples were prepared in a 96 well plate and absorbance at 595nm was read for each well. Triplicates were averaged, and the resulting absorbances plotted against known protein concentration. Purified protein concentrations ranged from

2.5mg/ml to 3.5mg/ml.

2.1.3.3 TAT Uptake Assay

HeLa cells were grown on coverslips in 24 well plates, seeded at 50,000 cells/0.5ml two days prior to the experiment and transfected the day before experimentation. TAT uptake assay cells were transfected with pEGFP-c3-2xML1N using Lipofectamine 2000. Cells were treated with 350nM or 700nM MBP-TAT, MBP-AICD, or MBP-TAT-AICD. After incubation of up to 1 hour, cells were exposed to 4% formaldehyde, then immunostained for MBP (1:200 primary antibody dilution) as described in **2.1.2.13**.

2.1.3.4 RNAi Suppression

RNAi against two APP and APLP2 targets were used alone or in combination and compared to a luciferase targetting control: APPI, APPII, APLP2I, APLP2II, DoubleI (APPI+APLP2I), DoubleII (APPII+APLP2II) and Luci. (Luciferase). HeLa cells seeded at a density of 50,000 cells/0.5ml in a 24 well plate and incubated overnight. A transfection mix of 100µl OptiMEM, 12pmol RNAi and 3µl Interferin (PolyPlus) was mixed and incubated at room temperature for 20 minutes. Fresh media was added to cells, then the RNAi transfection mix was added to cells, for a 20nM final concentration. Cells were allowed to grow for 48-72 hours prior to fixation / lysis.

2.1.3.5 Vacuole Quantification

48-72 hours after RNAi transfection cells were imaged under an inverted Nikon Eclipse TS100 microscope with a 40x objective. A minimum of 25 cells per image were scored for the presence of vacuoles, counting the structures per cell for each condition.

2.1.3.6 Vacuole Quantification in PIKfyve Inhibitor Sensitised Cells

Cells were either RNAi suppressed against APP family members and luciferase (**2.1.3.4**), or treated with 350nM MBP-TAT, MBP-AICD or MBP-TAT-AICD, for 1 hour. PIKfyve inhibitor sensitisation was performed by adding 1µM YM201636 to cells for 45 minutes. After two

washes of warm PBS and fixation for 20 minutes with 4% formaldehyde, cells were imaged under an inverted Nikon Eclipse TS100 microscope with a 40x objective. The vacuoles in the first 5 cells per image, top left to right, were counted and used to quantify structures per cell for each condition. One-way ANOVAs ($\alpha=0.05$) were performed in GraphPad Prism 6 to compare vacuoles per cells.

2.1.3.7 APP Overexpression and mTOR Manipulation in HeLa and SH-SY5Y Cells

Plasmids for lentiviral transfection were PCR amplified and cloned into pEGFP-n1 and pmCherry-n1, then subcloned into pXLG3-GFP for lentiviral expression (Wassmer *et al.*, 2009), APP with or without Swedish mutation were obtained from Dr. Eric Hill (Aston University). Cell cultures expressing APP species or GFP controls (HeLa and SH-SY5Y) were cultured in RPMI plus 10% foetal bovine serum (FBS), seeded into 24 well plates at 50,000 cells/0.5ml and incubated overnight.

mTOR manipulation was carried out by washing a subset of cells with warm PBS and their media replaced with RPMI devoid of amino acids (US Biological) for 2 hours, with some then receiving essential and non-essential amino acids (PAA) for 30 minutes prior to lysis and western blotting for pmTOR-Ser2448, mTOR, APP, pS6K1-Thr389, S6K1, p4EBP1-Thr70, p4EBP1-Ser65, 4EBP1 and eEF1A (HeLa cells) and pmTOR-Ser2448, pmTOR-Ser2481, mTOR, APP, pS6K1-Thr389, p4EBP1-Ser65, pAkt-Ser473, Akt, Tau and eEF1A (SH-SY5Y cells).

2.1.3.8 *C. elegans* culture

C. elegans was maintained on NGM agar aseptically poured into petri dishes, allowed to cool, with 50 μ l *E.coli* OP50 liquid culture then added and grown overnight at 37°C. A scalpel was soaked in 70% ethanol, then the ethanol burned off through exposure to a bunsen flame, the now sterile scalpel was used to transfer a square of worm containing agar from an existing culture of worms to the new plate. Other worm manipulation such as the transfer of individual worms was performed with a 32 gauge platinum wire, sterilised in a bunsen flame,

visualised under a dissecting microscope.

2.1.3.9 Lipid Quantification in *C. elegans* by Oil Red O and BODIPY Staining

RNAi knockdown can be achieved in *C. elegans* by feeding with bacteria expressing dsRNA against the target genes (Kamath 2003). dsRNA for each of the gene was expressed in *E. coli* (HD115) by inserting a segment of coding region into a plasmid vector L4440 (pPD129.36), a cloning vector containing two T7 polymerase promoters in opposite orientation. (Timmons *et al.*, 2001; Timmons and Fire 1998). To perform RNAi, 3ml LB plus 100µg/ml ampicillin was inoculated with a single RNAi clone colony from a culture grown on LB agar plus 100µg/ml ampicillin and 12.5µg/ml tetracycline. Clones were grown in a shaker incubator at 37°C overnight and 100µl seeded onto 3cm NGM Lite agar plus 0.5mM IPTG. After overnight induction at room temperature, worms were transferred to induced plates and incubated until analysis.

C. elegans strains *lon-2(e678)* and *apl-1(yn5)* were obtained from the *C. elegans* stock collection (University of Minnesota) and Dr. Li (City College of New York), and grown on nematode growth medium (NGM) inoculated with a bacterial lawn of *E. coli* (OP50) (Brenner 1974). RNAi knockdown in controls (*lon-2(e678)*) or *apl-1(yn5)* (a mutant devoid of the intracellular domain of *apl-1*), was obtained by feeding *E. coli* (HD115) expressing dsRNA against either *daf-15*, *let-363* or a control vector (L4440) grown on NGM supplemented with IPTG (Timmons and Fire 1998).

Staining protocols were adapted from other publications (O'Rourke *et al.*, 2009; Klapper *et al.*, 2011). Animals for Oil Red O staining were washed in M9 buffer, fixed for 30 minutes in 4% formaldehyde, washed three times in PBS, then twice in 70% isopropanol, then stained for 30 minutes with 60% Oil Red O solution. Animals for BODIPY staining were washed in M9 buffer, fixed for 30 minutes in 4% formaldehyde, washed three times in PBS, then treated with a solution of 1µg/ml BODIPY 493/503 in PBS for 1 hour. Animals were mounted using Mowiol and visualised using compound light and confocal microscopy for Oil Red O and

BODIPY, respectively.

2.1.3.10 LysoTracker Staining

HeLa cells seeded in 24 well plates at 50,000 cells/0.5ml were incubated overnight. Cells were treated for 4 hours with either apilimod (0nM, 25nM, or 250nM), YM201636 (100nM or 1 μ M) or ammonium sulphate (10mM). 1 μ M LysoTracker Red DND-99 was added, and the plate incubated for 5 minutes before cells were washed with warm PBS and fixed using 4% formaldehyde. Cells were washed a further two times before being mounted on slides using Mowiol. Cells were imaged by confocal microscopy for the quantification of LysoTracker positive structures per cell and intensity per unit area.

2.1.3.11 Automated Vesicle Quantification

Using Fiji ImageJ, maximum projections of Z-plane stacks were created from confocal microscope images, whole cells in an image were cut and pasted into a new, black background image and exported for analysis with an individual identity. Each cell underwent automated Squassh analysis using the MOSAIC suite in ImageJ (Rizk *et al.*, 2014). Data was exported to LibreOffice Calc where a threshold was applied to remove background noise, excluding structures less than 1 pixel in size or 0.15 average intensity. One way ANOVA ($\alpha=0.05$) with Tukey's post-hoc test was performed in GraphPad Prism 6. Automated vesicle quantification was carried out to quantify GFP-ML1Nx2 structures per cell, GFP-ML1Nx2 area per μm^2 , lysotracker positive vesicles per cell, lysotracker intensity per unit area, Lampl vesicles per cell and area of Lampl per μm^2 .

Chapter 3

Results

3.1 TAT-AICD as a Biochemical Tool

3.1.1 Introduction

3.1.1.1 Manipulating APP

To investigate protein interactions it is important to A) have a method for manipulating the systems in question and B) have a way of detecting changes that have arisen from that manipulation.

Considering APP specifically, there are viable, classic tools to be used for manipulation such as overexpression via transfection or knockdown via RNA interference (RNAi), these can be used to test hypotheses about APP's behaviour. The hypothesis underlying this work is that APP's interaction with PIKfyve, as described (Balklava *et al.*, 2015) has a functional element, or, put simply: APP affects PIKfyve function. A second hypothesis stems from the same proteo-liposome data that discovered the APP/PIKfyve interaction, that of APP and mTOR or: APP alters mTOR function. While some aspects related to the manipulation of APP may be simple to perform, there are also many complications and potential pitfalls, requiring specialised approaches.

3.1.1.2 Challenges in Overexpressing AICD

AICD was found to interact with PIKfyve and mTOR, and as such it is worth studying in isolation from the rest of APP. AICD is a relatively small protein fragment of 47 amino acids and is prone to degradation (Cupers *et al.*, 2001). This rapid degradation presents difficulties for the study of APP biology: overexpression of AICD proves to be difficult; GFP on the N-terminal end is unlikely to be enough to prevent rapid degradation and C-terminal GFP would likely interfere with the action of the protein considering its proximity to binding and phosphorylation sites critical to trafficking and protein interaction (Chang and Suh 2010). Producing high levels of AICD rapidly within each and every cell in a population, on demand, would provide a powerful tool for revealing the intracellular outputs of APP.

3.1.1.3 TAT

The Trans-Activator of Transcription (TAT), a promoter of gene expression for the Human Immunodeficiency Virus was the first protein shown to spontaneously and efficiently cross the cell membrane in 1988 (Frankel and Pabo 1988; Green and Loewenstein 1988). Since then research into TAT's unusual behaviour and the promising possibility of a TAT based drug delivery platform led to further refinement, creating the shortest sequence preserving penetrative behaviour: TAT(48-60) peptide, a Cell Penetrating Peptide (CPP) (Ezhevsky *et al.*, 1997; Vivés *et al.*, 1997).

3.1.1.4 Mechanisms of TAT Entry

CPP mechanisms have been the subject of much discussion over the last 20 or so years (Reviewed by Bechara and Sagan 2013), with research focusing on whether uptake is temperature and energy independent (Derossi *et al.*, 1994) or clathrin mediated (Lundberg *et al.*, 2003). Positive charge is key in cellular uptake (Ryser and Hancock 1965), but more specifically to CPPs; the guanidinium headgroup of arginine is important: polyarginine was found to increase uptake beyond that of other polycationic moieties such as polylysine (Mitchell *et al.*, 2000), while alanine scanning of basic residues reduced uptake (Wender *et al.*, 2000).

With focus so heavily on positive charge, the first models developed for CPP internalisation involved the binding of positively charged residues on the CPP with negatively charged species on the cell surface such as the phosphates of phospholipids, leading to disrupted membrane integrity and translocation (**Figure 17**).

Complicating matters, later research noted flaws in previous work, where fixation artifacts could arise when studying CPPs using fluorophore tags (Lundberg *et al.*, 2003), leading to doubts about receptor independent internalisation.



Figure 17.) Examples of proposed CPP translocation mechanisms (from Bechara and Sagan 2013). A) Inverted micelle formation. B) Pore-formation. C) Adaptive translocation.

Evidence now exists for CPP internalisation via many pinocytotic methods: CPP uptake can be lowered by inhibiting clathrin mediated endocytosis with chlorpromazine, lipid raft import using M β CD and macropinocytosis using 5-(N-ethyl-N-isopropyl)amiloride (EIPA), (Duchart *et al.*, 2007) suggesting a promiscuous approach to cell entry. Interestingly, Duchart *et al.* also found that preference for uptake method was dependent on peptide concentration, with macropinocytosis prevailing under 10 μ M.

The original model for CPP uptake has been reinvigorated by several more recent studies: membrane translocation can occur at 4°C (Jiao *et al.*, 2009) and in a cell free membrane model devoid of endocytic machinery (Saalik *et al.*, 2011), while another group determined both passive and active internalisation occurs (Guterstam *et al.*, 2009).

Regardless of initial mechanism for translocation, it is accepted that CPPs find their way into the cytosolic space through direct translocation or endosomal escape (Guterstam *et al.*, 2009; Bechara and Sagan 2013). Importantly, as we know CPPs can gain access to the cytosolic milieu their potential as a tool in molecular biology starts to emerge.

3.1.1.5 Using TAT as a Tool in Molecular Biology

CPPs, simply put are peptides able to efficiently enter cells, with this in mind it presents an opportunity to study cell biology: a TAT-fusion can be used to produce an acute spike in the protein of interest within all cells exposed, with only minor modification to that protein and with easy control over magnitude. The use of CPPs overcomes the weaknesses of classic overexpression, which can result in variable expression.

By fusing TAT to AICD it should be possible to determine effects of acute AICD overexpression on the cell, giving us a unique opportunity to examine the validity and relevance of a PIKfyve/AICD and mTOR/AICD interaction. Previous results point towards AICD as having a positive influence on PIKfyve function (Balklava *et al.* 2015), assuming TAT-AICD mimics this effect, it opens possibilities for the use of TAT-AICD beyond the field of Alzheimer's research into endosomal / PIKfyve research. While PIKfyve function can be induced in yeast using osmotic stress (Dove *et al.*, 1997), with no reliable method of increasing PIKfyve activity, PIKfyve research has been limited to loss of function studies in higher organisms. TAT-AICD may be a novel method for increasing PIKfyve activity in mammalian cells. In short, the aim of creating TAT-AICD was to determine whether it is useful as a tool in PIKfyve research, capable of entering the cell and acting on prospective interactors of AICD.

3.1.2 Results

Before using TAT-AICD as a tool for studying the interactions and outputs of APP, it is important to characterise the behaviour of TAT-AICD and confirm its action as compared to relevant controls.

3.1.2.1 Confirmation and Characterisation of TAT Uptake

Confirming the viability and usefulness of TAT as a tool is crucial before investigating any specific interactions. Studying TAT-AICD requires proper controls that show any effect

observed is not due to the presence of A) protein added exogenously, and B) is not just the effect of the TAT sequence itself. Describing the cellular distribution of TAT-AICD over time is particularly important to determining possible AICD functions in the cell: where does AICD localise and over what timeframe upon addition to the cell?

Three proteins were created and produced bacterially: His-MBP-AICD and His-MBP-TAT as controls and His-MBP-TAT-AICD (“AICD”, “TAT” and “TAT-AICD”, respectively) for future use in studying AICD interactions (**Figure 18A**). Purified protein was found to run at 40-50kDa, with little degradation (**Figure 18B**).

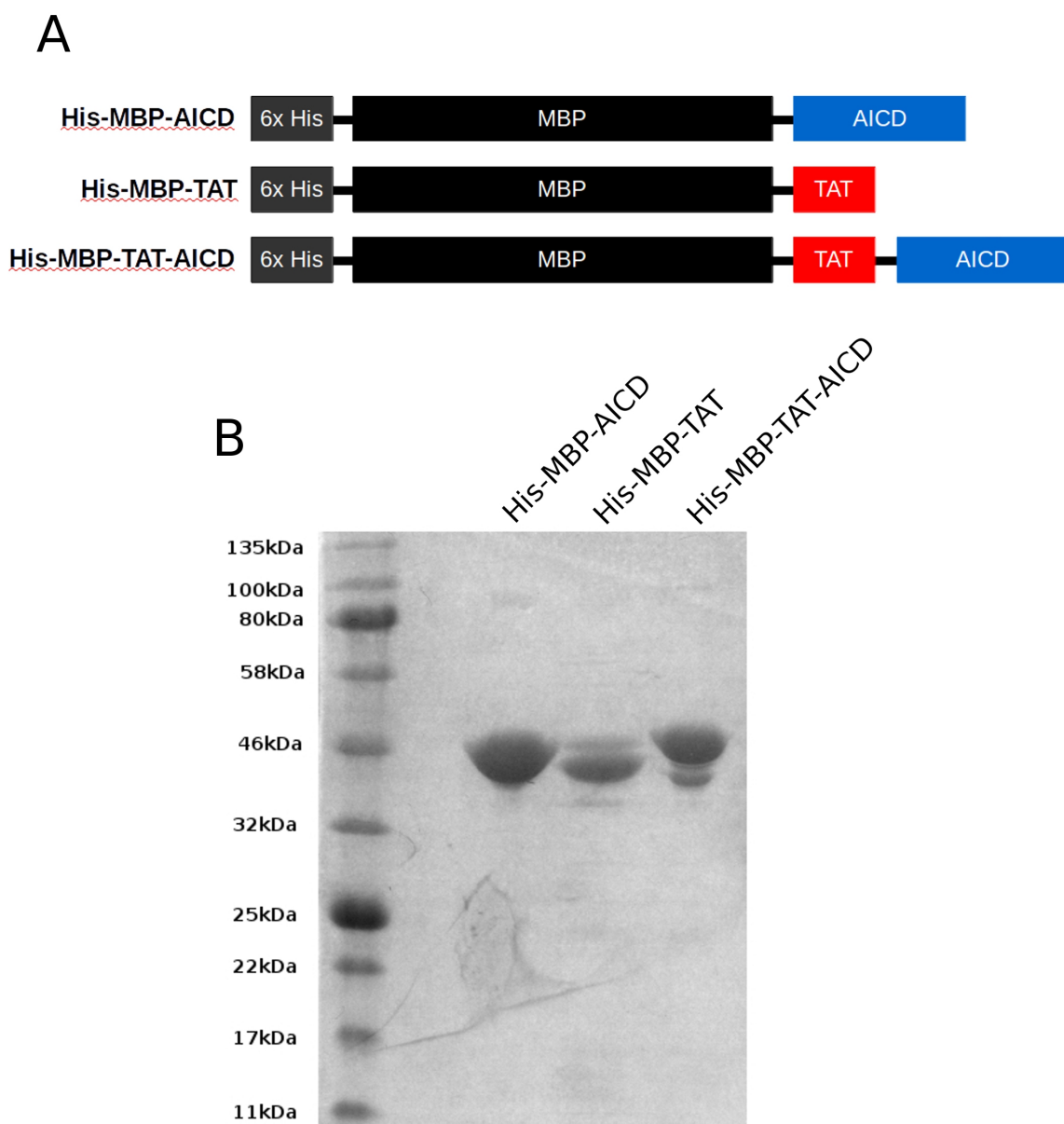
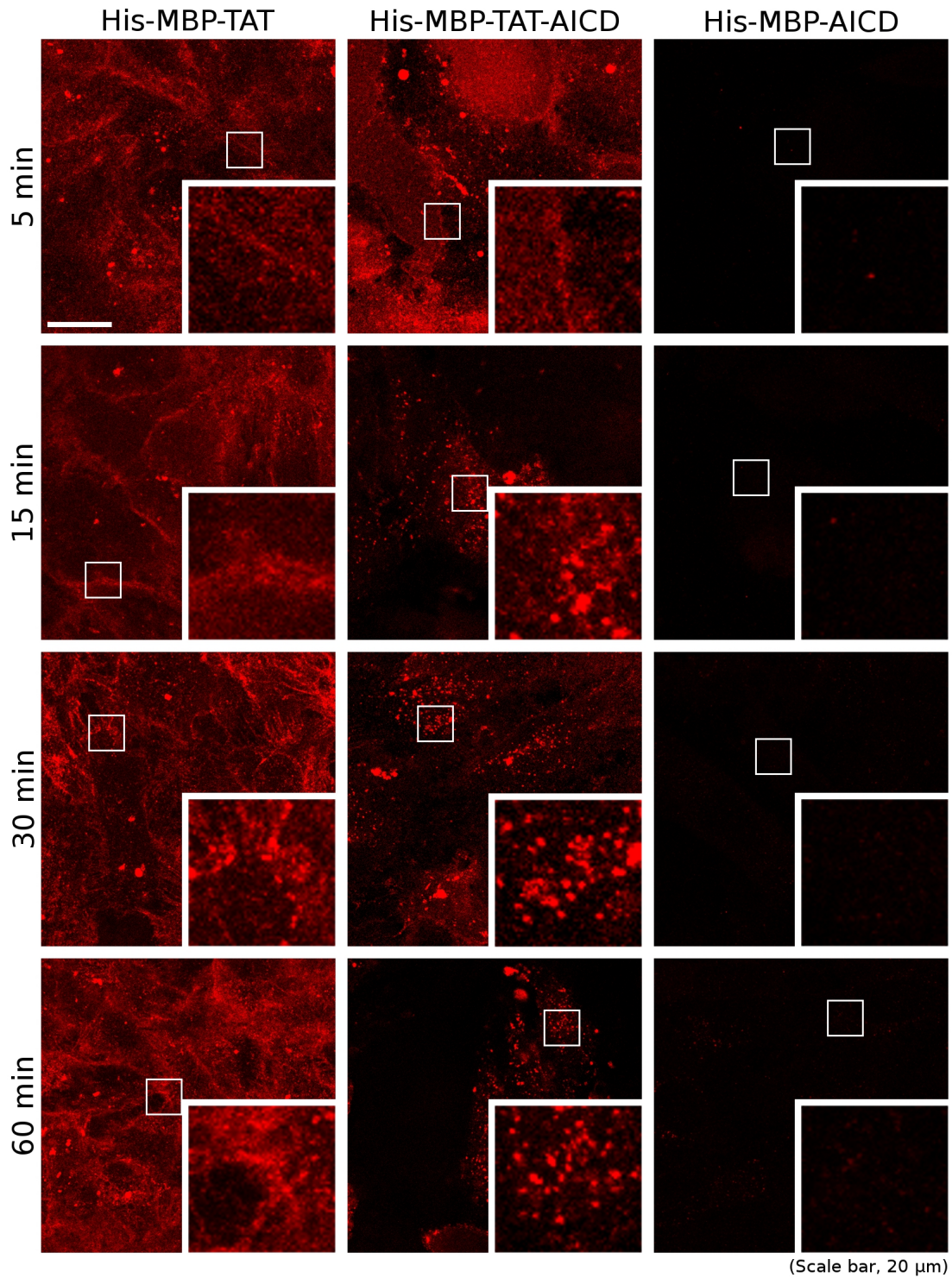


Figure 18.) Design Expression and Purification of TAT, TAT-AICD, AICD. A) Diagram showing layout of bacterially produced proteins for investigation of TAT-AICD. N-terminal to C-terminal layout left to right: Grey = 6x Histidine tag, Black = Maltose Binding Protein (MBP), Red = TAT peptide sequence, Blue = AICD. **B)** Purified proteins used in the investigation of TAT-AICD as seen on SDS-PAGE using Coomassie Brilliant Blue (~40-50kDa). Left to right: AICD, TAT, TAT-AICD. Note the minor degradation in TAT-AICD: full length TAT-AICD is indicated by higher molecular weight compared to controls.

One of the novel APP interaction partners under investigation is the PIKfyve complex, which creates PI(3,5)P₂ from PI(3)P. The PI(3,5)P₂ probe GFP-ML1Nx2 provides the ideal tool to investigate the sub-cellular sites of PIKfyve activity, by combining its expression with the immunostaining of MBP, the distribution of PIKfyve activity and TAT-AICD can be compared. To confirm and characterise TAT / TAT-AICD uptake in comparison to the distribution of PIKfyve activity, HeLa cells transfected with ML1Nx2-GFP were treated with 700nM of MBP-AICD, MBP-TAT or MBP-TAT-AICD protein for 5, 15, 30 or 60 minutes.

(**Figure 19**) shows MBP staining where exogenously produced protein has penetrated the cell and diffused throughout the cytoplasm. 700nM TAT or TAT-AICD penetrates the cell rapidly (with as little as 5 minutes incubation), while AICD alone does not penetrate to any appreciable degree. The distribution of MBP staining in TAT and TAT-AICD treated cells is similar at 5 minutes exposure, seen to highlight the cell surface but otherwise be diffuse throughout the cell. Interestingly, timepoints after 5 minutes begin to show a divergence in staining morphology: while TAT alone stays homogeneously distributed, TAT-AICD staining becomes progressively clustered and punctate.

The distribution of GFP-ML1Nx2 is notable when compared to that of MBP in TAT-AICD treated cells. (**Figure 20**) shows GFP-ML1Nx2 and MBP in TAT, TAT-AICD or AICD treated cells: Colocalisation is evident between MBP immunostain (red) and GFP-ML1Nx2 (green) in TAT-AICD treated cells, but not controls, showing TAT-AICD and the PI(3,5)P₂ probe can both be found associated with the same intracellular compartments at the same time.



(Scale bar, 20 μ m)

Figure 19.) Penetration and cellular distribution of MBP-TAT and MBP-TAT-AICD in GFP-ML1Nx2 transfected HeLa cells. MBP immunostaining in cells treated with 700nM TAT, TAT-AICD or AICD (left to right) for 5, 15, 30 or 60 minutes (top to bottom) TAT and TAT-AICD proteins were taken up and retained by cells, while AICD alone was not, showing TAT to be required for rapid cell penetration. TAT alone exhibits a diffuse staining pattern, while TAT-AICD appears to be primarily vesicular. Images representative of cells in n=3. Scale bar, 20 μ m.

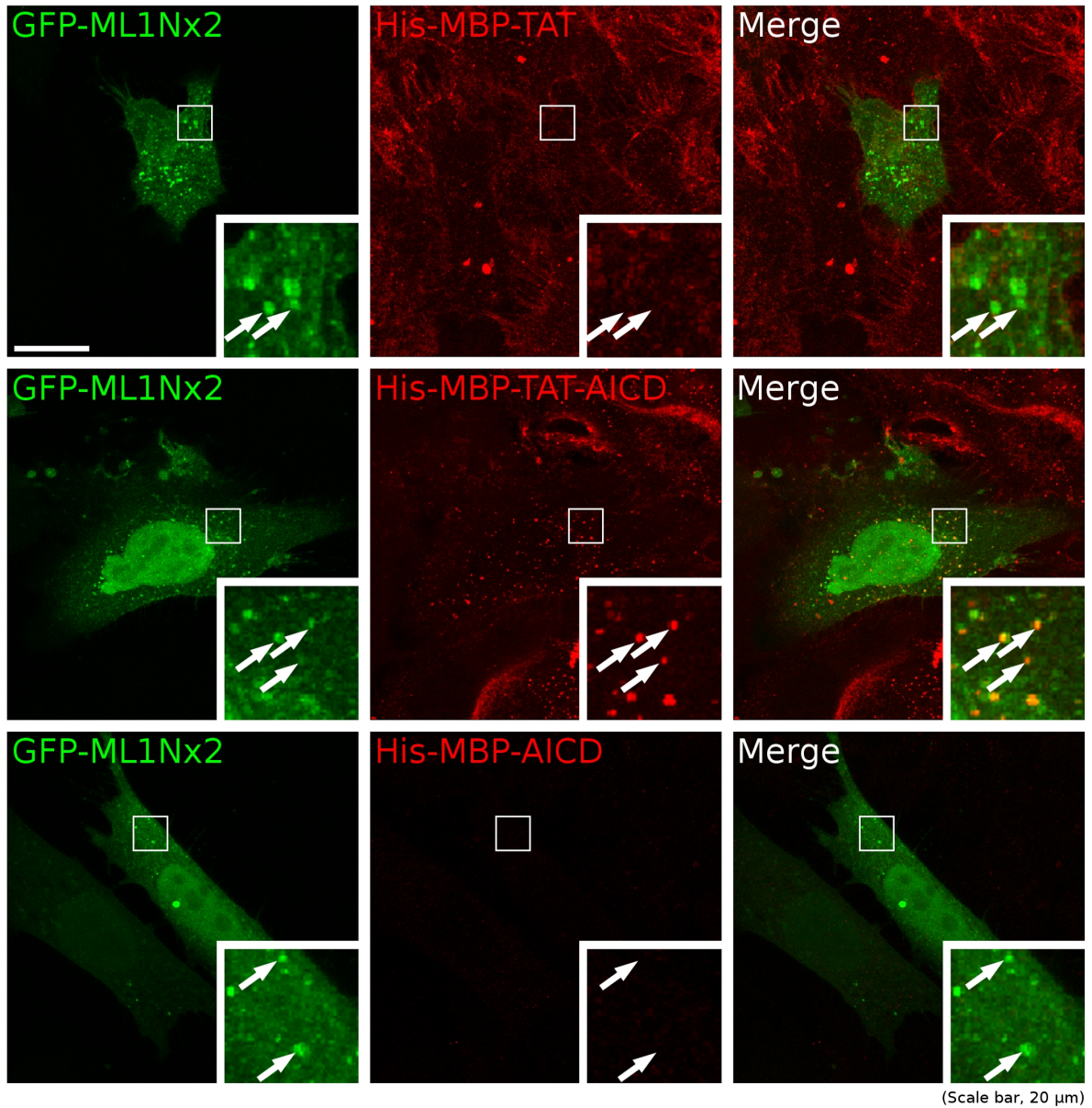


Figure 20.) Penetration and cellular distribution of MBP-TAT, MBP-TAT-AICD and GFP-ML1Nx2 in GFP-ML1Nx2 transfected HeLa cells. Distribution of the endogenously expressed PI(3,5)P₂ probe GFP-ML1Nx2, MBP immunostaining and merged GFP-ML1Nx2/MBP channel (left to right) in cells treated with 700nM TAT, TAT-AICD or AICD (top to bottom) for 30 minutes. GFP-ML1Nx2 colocalises with TAT-AICD but not TAT or AICD. Images representative of cells in n=3. Scale bar, 20μm.

3.1.2.2 TAT-AICD Appears to Increase PIKfyve Function

Combining the ability to tightly manipulate AICD levels in large numbers of cells, with the ability to detect changes in PI(3,5)P₂ metabolism is potentially useful. It would allow elucidation of a relationship between APP and the PIKfyve complex. The ability of AICD to influence PIKfyve function was investigated by treating cells with TAT-AICD and observing the abundance and size of GFP-ML1Nx2 positive vesicles or the abundance of vacuoles associated with PIKfyve inhibition.

Upon transfection with the PI(3,5)P₂ probe GFP-ML1Nx2, the GFP signal appears more pronounced and numerous in TAT-AICD treated cells (**Figure 21A**). TAT-AICD significantly increases the number (**Figure 21B**) and size (**Figure 21C**) of ML1Nx2-GFP positive structures within the cell compared to controls, as measured by automated Squash segmentation (Mosaic plugin for ImageJ).

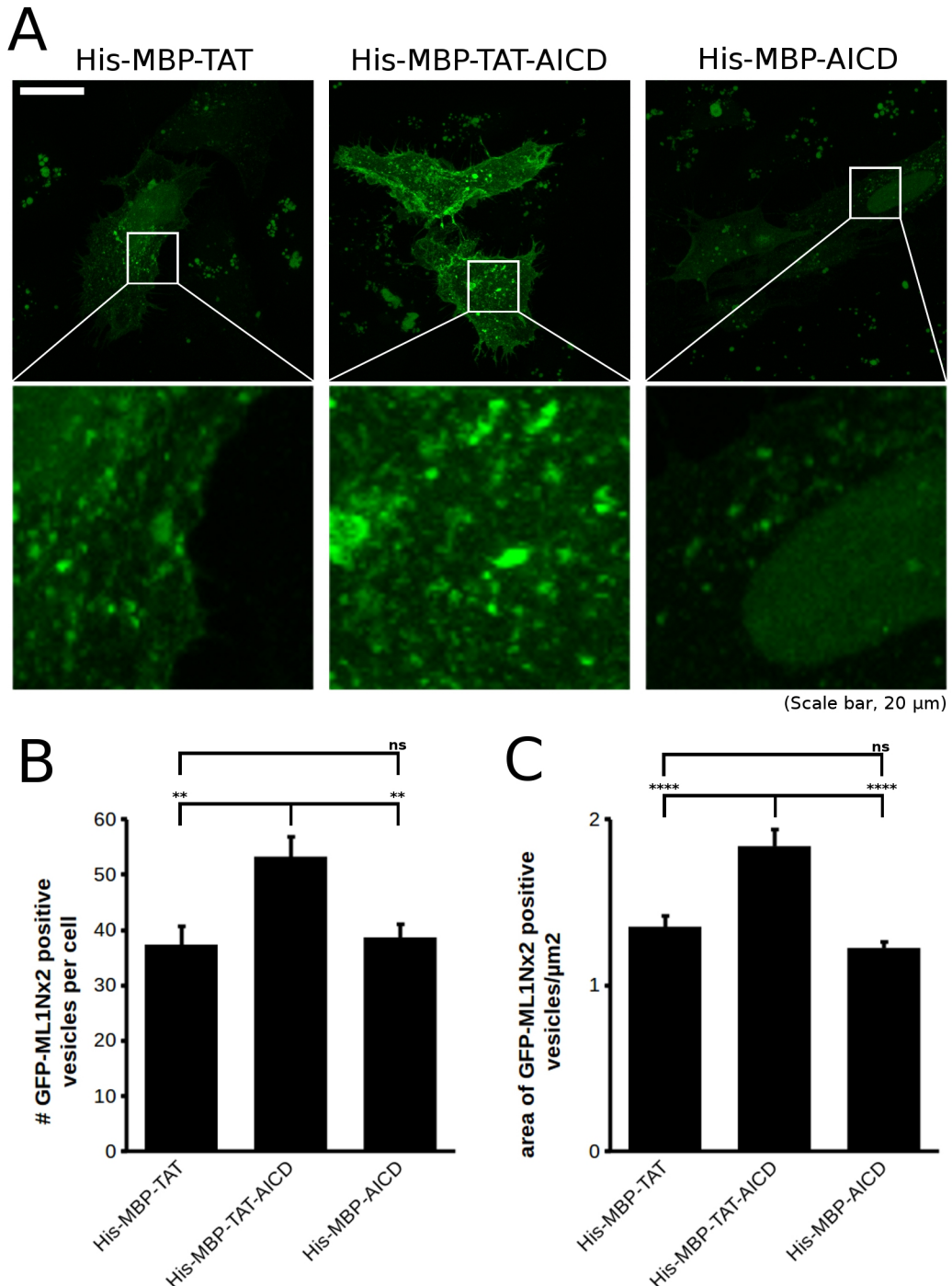


Figure 21.) The effect of TAT-AICD on ML1Nx2-GFP in HeLa cells. A) Distribution of GFP-ML1Nx2 in GFP-ML1Nx2 transfected cells treated with TAT, TAT-AICD or AICD (left to right) TAT-AICD treated cells appear to have altered ML1Nx2-GFP distribution. **B,C)** Number (per cell) and average area (μm²) of GFP-ML1Nx2 positive vesicles were significantly increased upon TAT-AICD treatment. Data was pooled from n=3. Cells analysed: TAT = 83, TAT-AICD = 68, AICD = 81. Statistical tests in B and C were performed using one-way ANOVA with Tukey's post-hoc test, α=0.05, *p<0.05, **p<0.01, ***p<0.001, ****p<0.0001. Error bars = SE. Scale bar, 20μm.

To determine if gross pathology of PIKfyve dysfunction could be influenced by TAT-AICD exposure, cells were treated with TAT-AICD then briefly challenged with a specific PIKfyve inhibitor (1 μ M YM201636, 45 minutes) and imaged by light microscopy (**Figure 22A**). TAT-AICD treatment was found to significantly mitigate cellular vacuolation caused by PIKfyve dysfunction as compared to controls (**Figure 22B**).

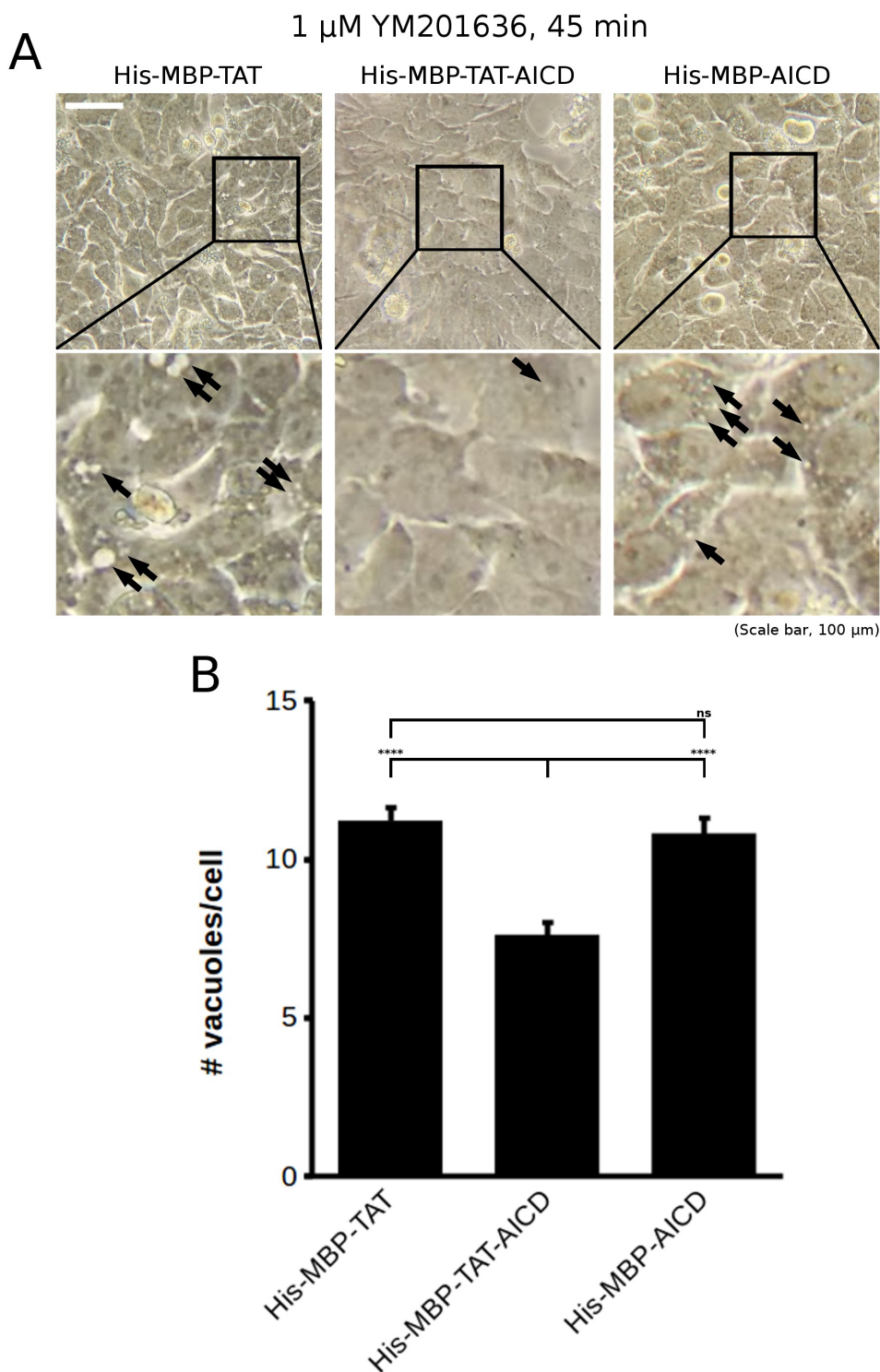


Figure 22.) The effect of TAT-AICD on PIKfyve inhibited HeLa cells. A) Vacuoles visible in cells (arrows) treated with 1 μ M YM201636 for 45 minutes after exposure to TAT, TAT-AICD or AICD (left to right). Scale bar 100 μ m. **B)** Number of vacuoles per cell in cells treated with 1 μ M YM201636 for 45 minutes after exposure to TAT, TAT-AICD or AICD (left to right). Cells treated with TAT-AICD exhibit lower vacuolation. Cells analysed: 150 per condition. Error bars = SE. Statistical tests in B, C and E were performed using one-way ANOVA with Tukey's post-hoc test, $\alpha=0.05$, * $p<0.05$, ** $p<0.01$, *** $p<0.001$, **** $p<0.0001$.

3.1.2.3 TAT-AICD and mTOR Substrates

Proteo-liposome recruitment lead to selection of two potential complexes as interacting with AICD: mTOR and PIKfyve. Previous results in mammalian tissue culture suggest a functional role for mTOR, therefore HeLa cells were treated with either AICD, TAT or TAT-AICD for 1 hour then lysed, western blotted and probed for the mTOR targets phospho-S6K1 Thr389 and phospho-4EBP1 Ser65. TAT-AICD as seen in (Figure 23) does not appear to modify the signalling of phospho-S6K1 Thr389 and phospho-4EBP1 Ser65.

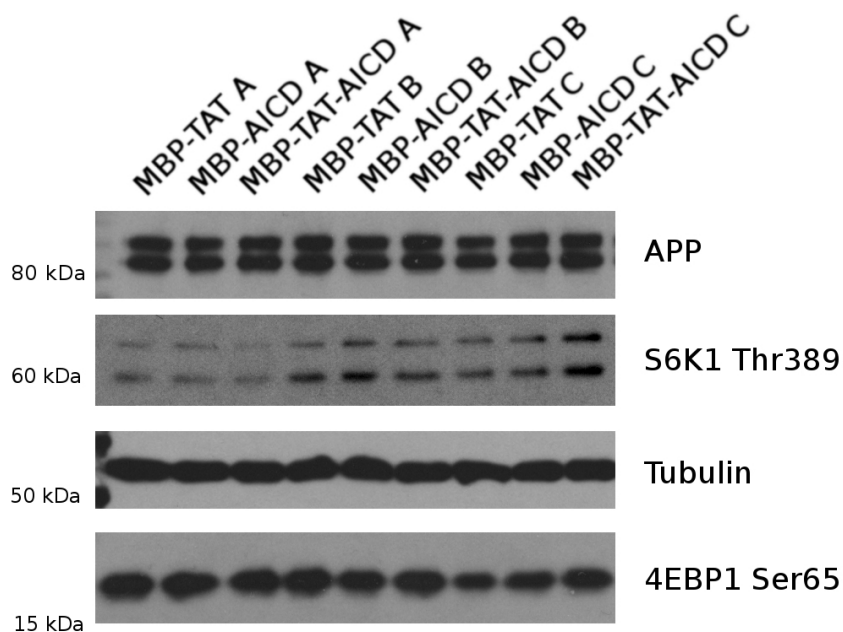


Figure 23.) mTOR signalling in HeLa cells upon treatment with TAT-AICD. Western blots showing APP, phospho-S6K1 Thr389, Tubulin, phospho-4EBP1 Ser65 levels (top to bottom) in cells treated with TAT, AICD or TAT-AICD (left to right in triplicate, A to C). No internally consistent change can be seen in the downstream mTOR targets S6K1 (Thr389) and 4EBP1 (Ser65).

3.1.3 Discussion

Studying the Intracellular domain of APP has previously been limited due to unreliable overexpression of fluorophore fused AICD and high turnover (Cupers *et al.*, 2001), while PIKfyve research is limited to loss of function due to a lack of reliable methods for increasing PI(3,5)P₂ levels. In this chapter the use of exogenous TAT-AICD is introduced as a tool for investigating interaction partners of the intracellular domain of APP and PIKfyve function.

3.1.3.1 Confirming and Describing TAT and TAT-AICD Cellular Uptake

Cellular uptake of TAT and TAT-AICD was confirmed by immunostaining for MBP after treating cells with increasing concentrations of protein for varying periods. Uptake of TAT constructs seem to occur rapidly with high cellular levels of MBP detected at 700nM after as little as 5 minutes.

Importantly TAT and TAT-AICD show very different cellular localisation profiles - TAT localisation was found to be homogenous in nature, while TAT-AICD was clearly concentrated in distinct punctae within the cell. TAT and TAT-AICD's only distinction is the presence of AICD, so any differential behaviour can be attributed to AICD; AICD is localising to these specific vesicles. The divergence in MBP stain distribution after 5 minute exposure between TAT versus TAT-AICD is significant. The staining at 5 minutes is consistent with TAT plasma membrane association and cytosol diffusion, while distinct TAT-AICD punctae development suggests some kind of interaction and sequestration.

3.1.3.2 TAT-AICD Colocalises with ML1Nx2-GFP

Interestingly, GFP-ML1Nx2, a probe for the PIKfyve product PI(3,5)P₂ colocalises substantially with TAT-AICD. When considering a PIKfyve/AICD interaction it is important to note overlap between one partner and the product of the other. Overlap of the PI(3,5)P₂ probe with TAT-AICD backs up initial data showing Vac14 colocalisation with APP (Balklava *et al.*, 2015), further suggesting an interaction between APP and the PIKfyve complex.

3.1.3.3 TAT-AICD Decreases Sensitivity to PIKfyve Inhibition in HeLa Cells

To investigate whether TAT-AICD impacts PIKfyve function, apilimod (a potent, specific PIKfyve inhibitor) was added briefly to TAT-AICD treated cells. By counting vacuolar structures in TAT-AICD treated versus control cells, TAT-AICD treatment imparted a partial resistance to vacuolation. The results suggest a functional link between PIKfyve and AICD/APP, but are indirect measures of PIKfyve dysfunction rather than a measure of PI(3,5)P₂, the lower vacuole count alone is far from conclusive. In combination with the wider body of evidence this experiment is more substantial, and together they strongly suggests AICD as being related to PI(3,5)P₂'s creation or turnover. This is not the only explanation of inhibited vacuole creation, but is perhaps the most obvious.

3.1.3.4 TAT-AICD Increases ML1Nx2-GFP Number and Size

Combining the acute treatment of exogenous TAT-AICD with the PI(3,5)P₂ probe provides unique and compelling evidence of an APP/PIKfyve interaction: application of TAT-AICD significantly increases both the number and size of ML1Nx2-GFP positive vesicles. While ML1Nx2-GFP is not a direct biochemical measurement of PI(3,5)P₂, changes in both the number and size of these vesicles upon TAT-AICD application are consistent with AICD increasing the amount of PI(3,5)P₂ within the cell.

3.1.3.5 TAT-AICD is a Novel Tool for the Manipulation of PIKfyve Function

Previous work has shown the intracellular domain of APP (AICD) interacts with PIKfyve. A bacterially produced fusion protein was created consisting of a Cell Penetrating Peptide (CPP) linked with AICD (TAT-AICD). TAT-AICD is capable of rapidly penetrating the cell, and importantly, colocalises with the PI(3,5)P₂ probe GFP-ML1Nx2, consistent with a AICD/PIKfyve interaction. Testing signs of PIKfyve function after TAT-AICD treatment shows that TAT-AICD appears to be capable of consistently increasing PIKfyve activity (**Figure 21-22**).

Beyond the initial significance to the understanding of an APP/PIKfyve relationship, PIKfyve research has previously been limited to studying purely loss of function in cells higher than yeast due to the lack of reliable methods of increasing PI(3,5)P₂ levels in mammalian cells. The ability of TAT-AICD to reliably increase PIKfyve activity may be useful as a tool in PIKfyve research, a field previously plagued by technical challenges.

In spite of the positive results, these findings have limitations. While it is clear that TAT enters the cell (**Figure 19-20**) the mechanism for that entrance is still debated; until that debate is settled some ambiguity will remain surrounding the interpretation of results, particularly considering many models include the involvement of endosomal processes, the very system this work tries to investigate.

3.1.3.6 TAT-AICD has no Discernable Effect on Several mTOR Substrates

Previous data suggests a link between mTOR/APP in *C. elegans* and mammalian cell culture (unpublished dataset). By treating cells with TAT-AICD it was expected that any mTOR interaction would become evident by western blotting treated cells then probing for changes in mTOR substrates. Interestingly, TAT-AICD appeared to have no effect on mTOR signalling to the substrates tested: phospho-4EBP1 Ser65 and phospho-S6K1 Thr389 (**Figure 23**). This negative result does raise questions about the nature of an mTOR/APP interaction: it is clear that any APP/mTOR relationship is more complicated than a simple up or downregulation, and some effort should be made to explore this complexity.

An important point is that some inherent property of the exogenous protein prevents it influencing mTOR in the way that endogenously produced protein does, while this may be the post-translational modification / phosphorylation state of AICD, the N-terminal placement of TAT-AICD's His and MBP tags may be a more compelling possibility, interfering with an mTOR interaction. Indeed, initial investigation of the AICD/mTOR interaction narrows down the interaction to the N-terminal extremity of AICD (unpublished dataset), where steric interference from MBP may be expected.

Using different experimental systems such as classical overexpression and the use of different cell models may shed light on an APP/mTOR interaction. mTOR is not an easy system to experiment with, particularly in immortalised mammalian cell culture: a system defined by genetic eccentricities related to cell proliferation and metabolic control (Hanahan and Weinberg 2011). Relating to this point, cell starvation prior to treatment may give a lower background and using a different cell system or testing other mTOR substrates may be useful.

3.2 Investigating a Functional Interaction Between APP and mTOR

3.2.1 Introduction

mTOR is central to energy signalling within the cells, integrating inputs such as glucose and amino acid abundance, stress signals such as AMP / hypoxia and DNA damage, then signalling appropriate downstream effects: either driving or inhibiting actions such as protein production, cell division, lipid biosynthesis, autophagy and apoptosis.

mTOR signalling alteration has been reported in an APP / Alzheimer's disease context. The nature of the alteration has been reviewed (Garellick and Kennedy 2011), with points in favour of each model reviewed by Sweitch and colleagues (Sweitch *et al.*, 2008). The interactions discussed and researched have often been framed as an indirect one. The specific nature of an APP/mTOR interaction has been debated as to whether mTOR signalling is upregulated or downregulated.

3.2.1.1 Evidence for mTOR Signalling Lowered in Alzheimer's Disease

Evidence for the lowering of mTOR signalling related to APP / Alzheimer's disease can be found from several laboratories. A decrease in the level of protein synthesis in diseased tissue has been detected in Alzheimer's disease affected brains (Langstrom *et al.*, 1989) which would imply inhibition of mTOR signalling. A β 42 exposure in neuronal cells, PS-1 / APP mutant, transgenic mice are reported as exhibiting reduced mTOR dependent (Thr389) phosphorylated p70S6K1. Interesting to note is that the mouse model, lowered mTOR signalling was only found in the cortex, not the cerebellum, a distribution that correlates with Alzheimer's disease pathology. Additionally, in the same paper, mTOR signalling was also lowered in the lymphocytes of Alzheimer's patients, an effect that correlated with the patient's mini mental status examination (MMSE) score (Lafay-Chebassier *et al.*, 2005).

Another approach that favours a decreased mTOR signalling model is that investigating long term potentiation (LTP), with evidence showing mTOR signalling inhibition correlates with impairment of synaptic plasticity in hippocampal slices of a mouse model for Alzheimer's disease. The same study found LTP inhibition upon application of A β 1-42 recovered when cells were exposed to the GSK3 β inhibitors lithium or kenpaullone (Ma *et al.*, 2010).

A paper describing the positive effect of presenilin-1 on PI3K signalling, with subsequent inactivation of GSK3 and reduced tau phosphorylation also supports a model of decreased mTOR signalling in Alzheimer's, as PS1 knockout mice show increased tau phosphorylation (Baki *et al.*, 2004).

At first the evidence for lowered mTOR signalling seems compelling, however it should be noted that the above publications rely upon data derived from patients, patient tissues or mouse models, where secondary pathology may be responsible for the prevailing signalling environment, for example amyloid induced toxicity, general cell health and the energy state of the patient or mouse cells at time of sampling / death and may not be representative of the disease's underlying molecular mechanisms.

3.2.1.2 Evidence for Upregulated mTOR Signalling in Alzheimer's Disease

Many groups conclude an increase in mTOR signalling in Alzheimer's disease (Pei and Hugon 2008), evidence supporting upregulated mTOR signalling includes mTOR phosphorylated at Ser 2481 correlating with total tau and phospho-4EBP1 at Ser 65 and Thr 70 being increased significantly in Alzheimer's brains (Li *et al.*, 2005). The phosphorylation of S6K1 at Thr 421 / Ser 424 has also been reported in relation to increased total and phosphor-tau (An *et al.*, 2003). A group studying a drosophila tauopathy model concluded that TOR mediated cell cycle progression caused neurodegeneration (Khurana *et al.*, 2006).

In addition to the above experimental evidence, rapamycin was described as preventing cognitive deficits (measured using the Morris water maze), decreasing the amount of A β 42 and increasing autophagy in PDAPP mice, an animal model of Alzheimer's (Spilman *et al.*, 2010). Similar results were obtained by another group (Caccamo *et al.*, 2010) in triple transgenic mice (APP^{swe}, PS1M146V, Tau P301L) (Oddo *et al.*, 2003). Caccamo *et al.* also claimed in the same 2010 paper that A β 42 increased mTOR signalling. mTOR signalling was enhanced in Alzheimer's patients (Pei and Hugon 2008) and APP overexpression shows similar changes (Caccamo *et al.*, 2011) in almost direct contradiction to Lafay-Chebassier and colleagues.

When considering the likelihood of an APP/mTOR interaction it is important to note existing research into the other APP family of proteins; APLP1 and APLP2 having been shown as important modulators in glucose / insulin homeostasis (Needham *et al.*, 2008), taken with the functional redundancy observed between the APP family of proteins, a role for APP in mTOR function is rational.

It is important to note the differences in research concluding either an "up" or "down" model – "down" evidence is reliant on late stage / established disease samples, which may hint at the findings being artifacts of widespread cell stress / death. Those concluding upregulated mTOR signalling in Alzheimer's disease have a lot more experimental control over conditions, manipulating simple systems and observing specific outcomes. To summarise, a model for increased mTOR signalling in Alzheimer's disease appears to be favoured by high quality, well controlled research, consistent with a possible direct interaction.

3.2.1.3 Investigating an APP/mTOR Interaction

The investigation of an interaction between APP and mTOR requires tackling the specific challenges associated with both proteins. Functional redundancy between the APP family proteins (APP, APLP1, APLP2) needs to be taken into account. Redundance can be accounted for by either studying in a more primitive system prior to divergence of orthologs

(*C. elegans* or *D. melanogaster*) or eliminating each protein alone or in combination, for example using RNAi in higher systems such as mammalian cells.

Studying mTOR specifically also has challenges associated with it. Tissue culture is a staple experimental system, but often involves cells derived from sources such as tumours where cellular controls of metabolism and cell division have been circumvented, the problem being that these are the very systems controlled by mTOR (Schmelzle and Hall 2000; Pópulo *et al.*, 2012). Beyond the genetic eccentricity found in tissue cultured cells, tissue culture media also adds to experimental ambiguity with glucose levels often far exceeding physiological levels; blood sugar levels are between 4-6.5mM in those with a high-starch diet (Daly *et al.*, 1998), while DMEM media may contain as much as 25mM glucose (Dulbecco and Freeman 1959; Morton 1970). The issues with tissue culture can be avoided by either experimenting in a model organism where physiological nutrient levels are present or accounting for the glucose experimentally (comparing “normal” cell culture conditions with depleted nutrients for example).

3.2.2 Results

3.2.2.1 APP Overexpression in HeLa and SH-SY5Y Cells Increases Downstream

Phosphorylation in Targets of mTORC1 and mTORC2

If APP does indeed interact functionally with mTOR, mTOR signalling changes may be expected upon alteration of APP. To test APP's effect on mTOR signalling APP-GFP was overexpressed in HeLa and SH-SY5Y cells and compared to GFP overexpression. To further investigate whether the presence and processing of full length APP is important in mTOR signalling, overexpression of AICD-GFP and APP-GFP with Swedish mutation (APP(Swe)) was performed, with subsequent western blotting of lysates for proteins and signalling outputs of interest. mTOR function is altered when nutrient abundance changes, to determine if APP affects this, mTOR substrates were tested for phosphorylation in basal, starved and recovering conditions.

HeLa cells overexpressing APP, APP(Swe) or AICD showed an apparent increase in mTORC1 substrate phosphorylation under basal conditions as compared to controls (GFP), this includes 4EBP1 phosphorylation at Ser65 and Thr70, and S6K1 at Thr389 (**Figure 24A**). Akt dependent phosphorylation of mTOR (Ser2448) also increases, pointing to elevated mTORC2 signalling. Interestingly, APP with Swedish mutation did not appear to enhance mTOR signalling any more than APP or AICD overexpression.

Densitometry was performed on HeLa lysate western blots, densitometry on APP blots demonstrates an increase in APP signal between GFP expressing controls and those expressing GFP-APP (**Figure 24B**). Densitometry also highlights that AICD-GFP expression is sufficient to increase mTORC target phosphorylation, both mTORC1 targets, as shown by pS6K1 Thr389 (**Figure 24C**) and mTORC2 targets, as shown by pmTOR Ser2448 (**Figure 24D**).

With a likely effect of APP on mTOR phosphorylation targets in HeLa cells, the relevance of this result in a neuronal system is worthwhile investigating when considering the implications in Alzheimer's disease, experiments were repeated in SH-SY5Y neuroblastoma cells.

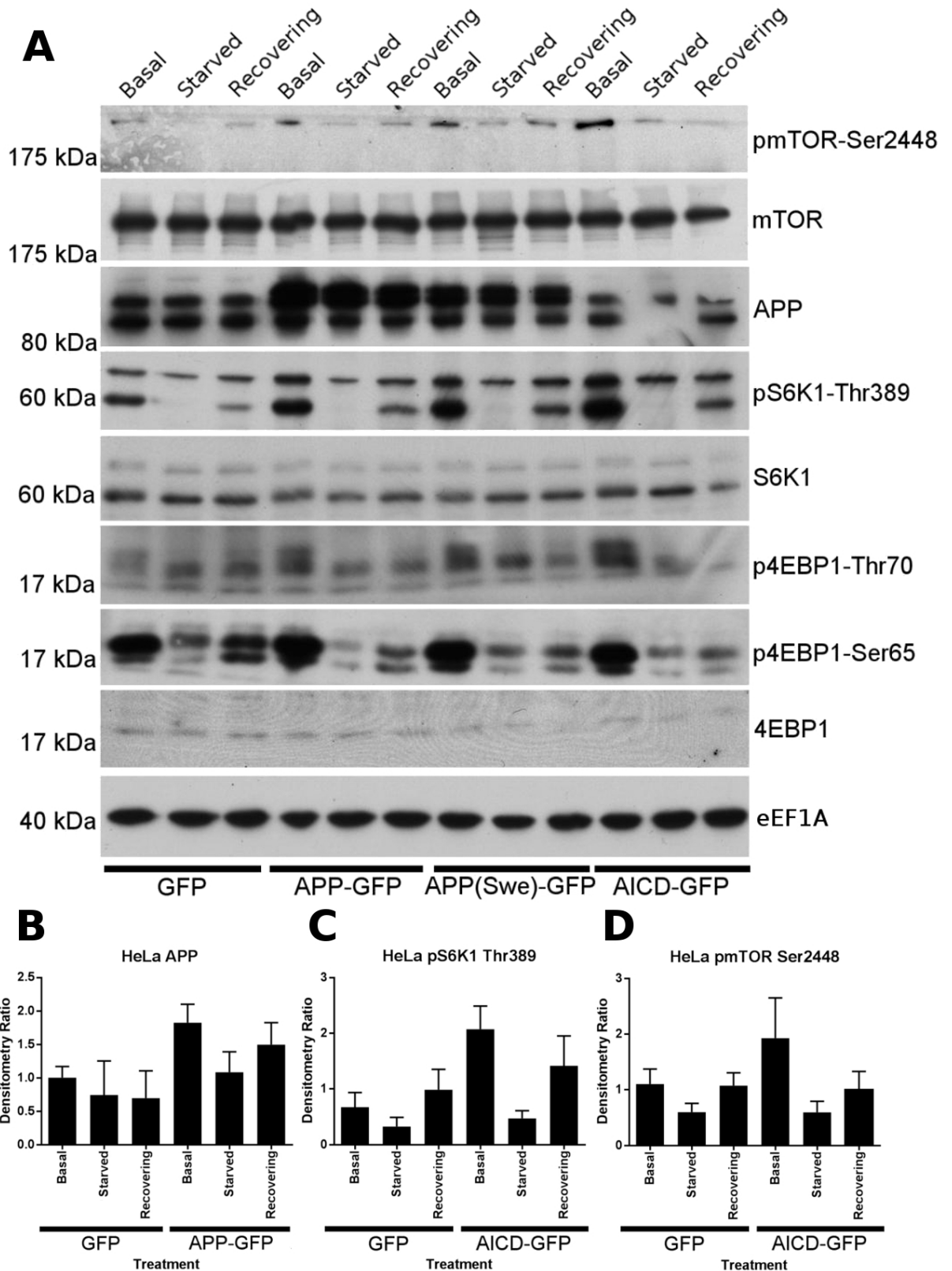


Figure 24.) APP drives mTOR signalling in HeLa cells. A) Lentiviral overexpression of APP (APP-GFP), APP containing the Swedish mutations (APP(Swe)-GFP) or AICD (AICD-GFP) leads to increased apparent phosphorylation of all measured downstream targets of mTOR compared to controls (GFP) in HeLa cells as shown by western blot. Blots demonstrate APP is capable of driving mTORC1 and 2 activity via its intracellular domain. To compare different cell energy states, cells were either given fresh media as a basal condition (Basal), starved of nutrients for 2 hours with amino acid deficient media (Starved) or starved then allowed to recover in fresh, complete media (Recovering). Samples were blotted for pmTOR-Ser2448, mTOR, APP, pS6K1-Thr389, S6K1, p4EBP1-Thr70, p4EBP1-Ser65, 4EBP1 and eEF1A (top to bottom). **B)** Densitometry on selected samples blotted for APP from **A** shows the apparent increase in detectable APP upon APP-GFP expression, and the possible loss of APP upon starvation. **C-D)** Densitometry on selected samples blotted for pS6K1 Thr389 (**C**) and pmTOR Ser2448 (**D**) from **A** shows AICD-GFP expression is sufficient to increase apparent basal, downstream phosphorylation of mTORC1 and mTORC2 targets respectively. **B-D)** Densitometry was performed in ImageJ from n=3, error bars= SE.

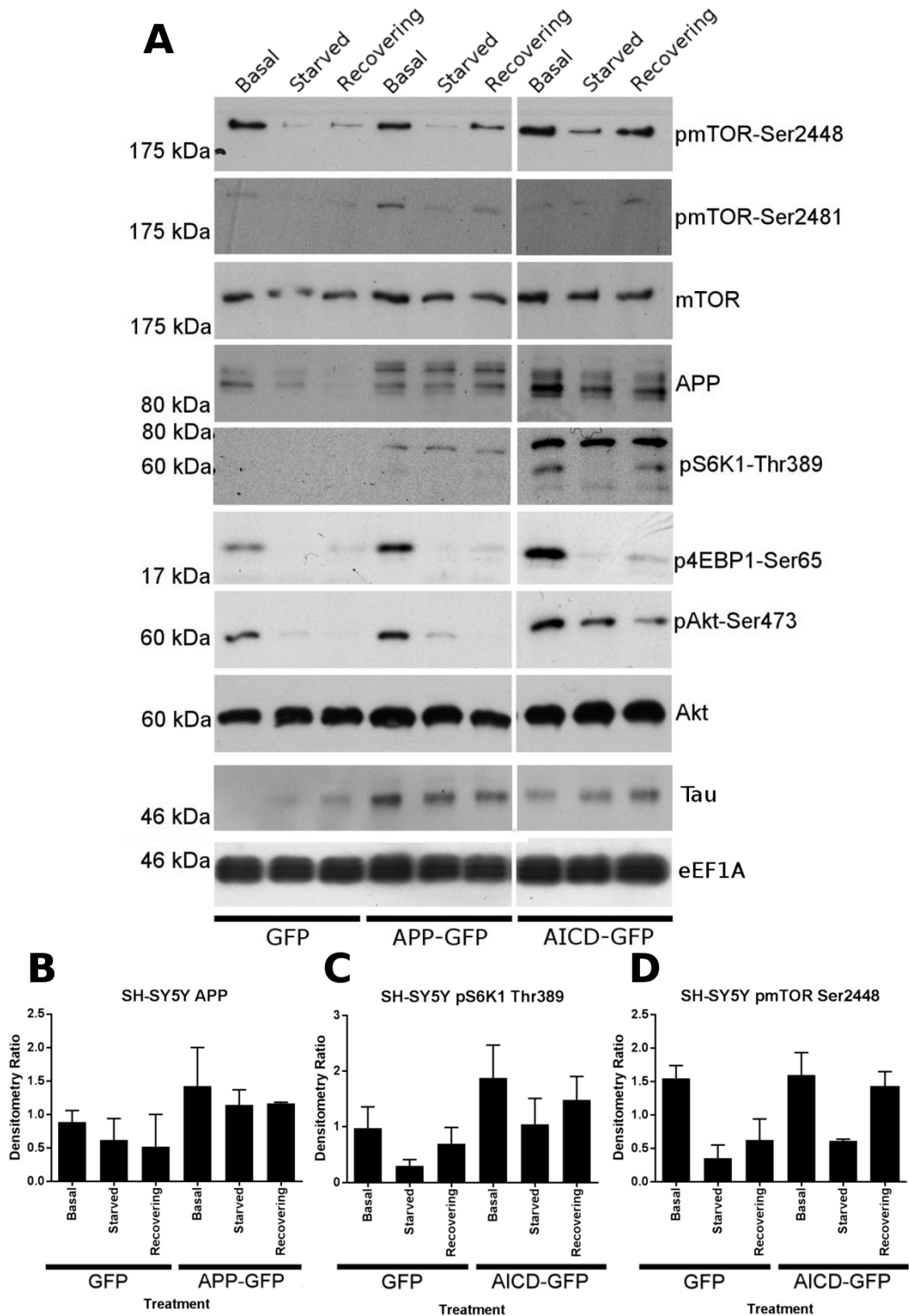


Figure 25.) APP drives mTOR signalling in SH-SY5Y cells. Lentiviral overexpression of APP (APP-GFP) or AICD (AICD-GFP) leads to increased phosphorylation of measured downstream targets of mTOR compared to controls (GFP) in SH-SY5Y neuroblastoma cells, as shown by western blot. Blots demonstrate APP is capable of driving mTORC1 and 2 activity via its intracellular domain. To compare different cell energy states, cells were either given fresh media as a basal condition (Basal), starved of nutrients for 2 hours with amino acid deficient media (Starved) or starved then allowed to recover in fresh, complete media (Recovering). Samples were blotted for pmTOR-Ser2448, pmTOR-Ser2481, mTOR, APP, pS6K1-Thr389, p4EBP1-Ser65, pAkt-Ser473, Akt, Tau and eEF1A (top to bottom). **B**) Densitometry on selected samples blotted for APP from **A** shows the apparent increase in detectable APP upon APP-GFP expression, and the possible loss of APP upon starvation. **C-D**) Densitometry on selected samples blotted for pS6K1 Thr389 (**C**) and pmTOR Ser2448 (**D**) from **A** shows AICD-GFP expression is sufficient to increase apparent basal, downstream phosphorylation of mTORC1 and mTORC2 targets respectively. **B-D**) Densitometry was performed in ImageJ from n=3, error bars= SE.

Data acquired in SH-SY5Y neuroblastoma supports that found in HeLa cells, showing APP and AICD increasing mTORC1 and mTORC2 signalling (**Figure 25A**). Basal, starved and resupplemented cells in APP and AICD overexpression appear to be increased over and above corresponding controls in phospho-mTOR Ser2448, phospho-S6K1 Thr389 and phospho-Akt Ser473.

Densitometry was performed on SH-SY5Y lysate western blots, as in HeLa cellsz densitometry on APP blots demonstrates an increase in APP signal between GFP expressing controls and those expressing GFP-APP (**Figure 25B**). Densitometry also highlights that AICD-GFP expression is sufficient to increase mTORC target phosphorylation, both mTORC1 targets, as shown by pS6K1 Thr389 (**Figure 25C**) and mTORC2 targets, as shown by pmTOR Ser2448 (**Figure 25D**).

3.2.2.2 APL-1 Mutation yn5 Creates an Additive Effect with daf-15 and let-363

Knockdown, Showing Fat Droplet Accumulation as Seen by Oil Red O and BODIPY Staining

The insulin receptor in *C. elegans* (DAF-2) controls fat metabolism, inhibition of this system, upstream of mTOR, has been reported to increase lipid droplet accumulation (Jia *et al.*, 2004; Palgunow *et al.*, 2012). To further establish whether a functional link exists between mTOR and APP, and whether such a link is conserved, lipid droplet accumulation was observed via Oil Red O staining (**Figure 26A**). Manipulation was performed using RNAi suppression of the mTOR ortholog gene *let-363* and the RAPTOR ortholog *daf-15*, alone or in combination with *C. elegans* carrying the APP ortholog C-terminal truncation, *apl-1(yn5)*. Suppression of DAF-15 / LET-363, or the *apl-1(yn5)* mutation produces mild accumulation of lipids, as seen by deeper Oil Red O staining. Combining suppression of DAF-15 or LET-363 with the *apl-1(yn5)* mutation produces profound lipid accumulation over and above any single condition, hinting at a conserved linked function for APP and mTOR.

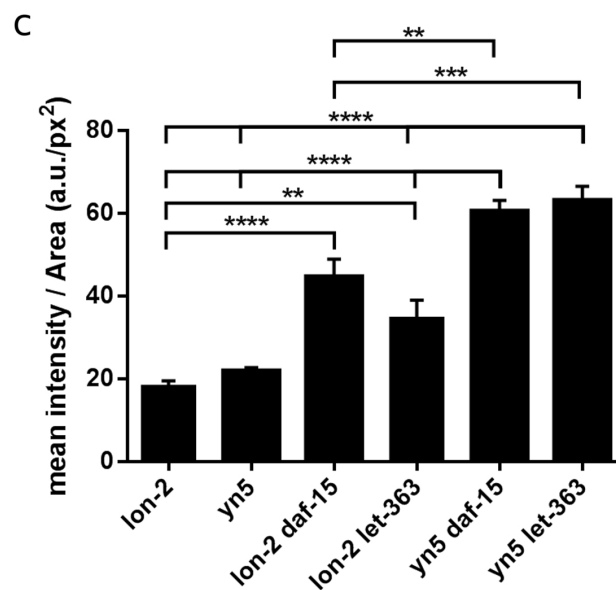
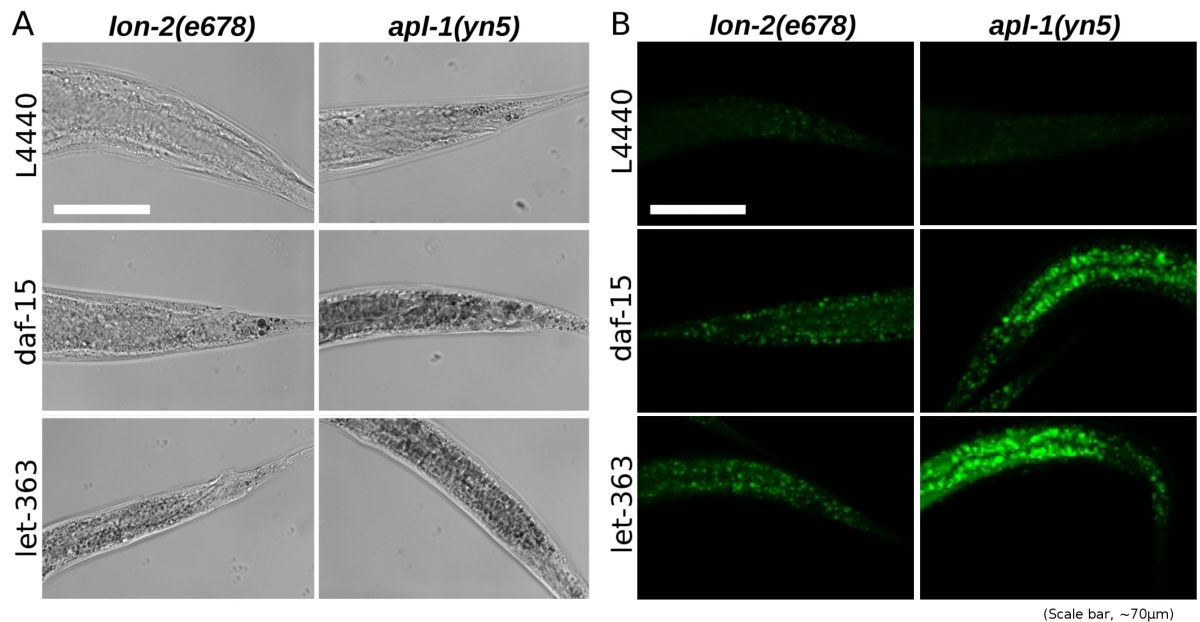


Figure 26.) Truncation of the intracellular domain from the *C. elegans* ortholog of APP, APL-1 (*apl-1(yn5)*) creates an increase in lipid deposition when combined with suppression of *C. elegans* mTOR function. Suppression of mTOR (LET-363) or RAPTOR (DAF-15) in *C. elegans* by feeding respective dsRNA expressing bacteria led to moderately increased lipid accumulation compared to empty L4440 plasmid expression. Lipid accumulation increased upon mTOR knockdown in *apl-1(yn5)* truncation mutants over *lon-2(e678)* controls. Changes in tail lipid accumulation were visualised by Oil Red O (A) and BODIPY staining (B). Using confocal z-stacks of BODIPY stained worm images, quantification of lipid accumulation was possible (C). Quantification showed a moderate but significant increase in lipid droplet staining upon LET-363 or DAF-15 suppression, but a large significant rise in lipid droplet staining when *apl-1(yn5)* is combined with LET-363 or DAF-15 suppression. Data was pooled from n=3, total worms analysed: *lon-2*= 53, *yn5*= 56, *lon-2 daf-15*= 67, *lon-2 let-363*= 45, *yn5 daf-15*= 52, *yn5 let-363*= 53. Analysis was performed using one-way ANOVA with Tukey's post-hoc test, $\alpha=0.05$, ** $p \leq 0.01$, *** $p \leq 0.001$, **** $p \leq 0.0001$. Error bars = SE. Scale bar, $\sim 70\mu\text{m}$.

Quantification was performed as an elaboration of the work of Palgunow *et al.* (Palgunow *et al.*, 2012). The effect of RNAi suppression of DAF-15, LET-363 levels and that of the *apl-1* truncation mutant *apl-1(yn5)* was evaluated, BODIPY 493/503 fluorescent dye was used to stain and quantify lipid droplets in the tail of each animal (Figure 26B/C). Intensity was significantly increased in the tails of worms upon knockdown of TOR signalling elements, but

even moreso when combining TOR suppression with *apl-1(yn5)* mutation (**Figure 26C**), showing a combination effect that would be expected from both proteins contributing to the same pathway.

3.2.2.3 Knockdown of APP Family Proteins, Alone or in Combination Fails to Alter mTOR Signalling

To investigate loss of APP function on mTOR in mammalian cells RNAi suppression was used in HeLa cells against relevant APP family members (note that APLP1 is not expressed in HeLa cells); APP and APLP2 were knocked down alone, or in combination as a double knockdown to allow for possible effects of functional redundance present in APP family proteins (Heber *et al.*, 2000).

APP, APLP2 and double knockdowns were confirmed by western blotting (**Figure 27A**), corresponding protein levels were successfully inhibited: APPI and APPII lowered levels of APP, APLP2I and APLP2II diminished APLP2, while DoubleI and DoubleII suppressed both APP and APLP2 levels.

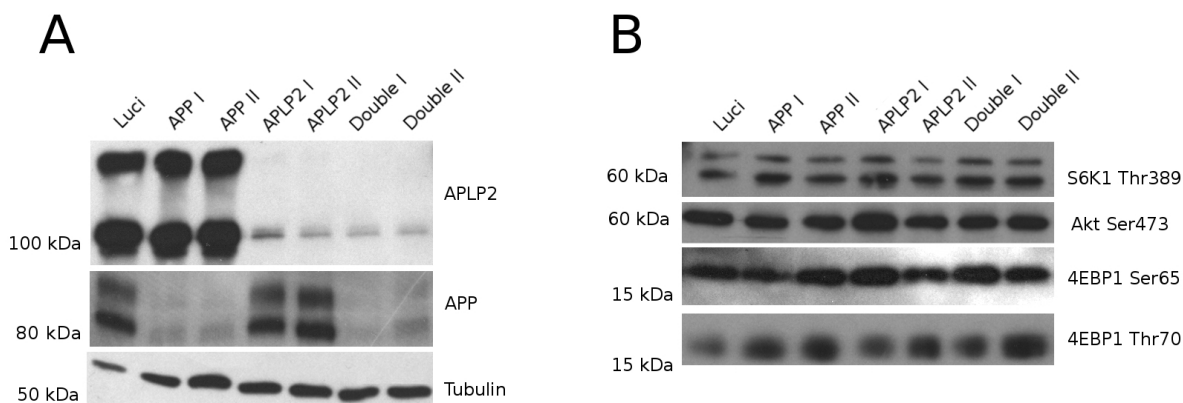


Figure 27.) Successful knockdown of APP family proteins in HeLa cells, alone or in combination, fails to alter mTOR signalling. RNAi suppression of the APP family proteins APP or APLP2 alone or in combination in HeLa cells, shows a substantial loss in the corresponding protein as shown in western blots. **(A)** APPI, APPII knockdown lowers APP, APLP2I, APLP2II, lowers APLP2 while DoubleI (APPI+APLP2I) and DoubleII (APPII+APLP2II) lower both APP and APLP2 levels showing successful knockdown. **(B)** Western blotting mTOR substrates (S6K1-Thr389, 4EBP1-Thr70, 4EBP1-Ser65) and mTOR complex 2 (Akt-Ser473) shows no discernible patterns as compared to each other and Luciferase (Luci.) controls.

APP family knockdowns were probed for mTOR dependent substrate phosphorylation to determine whether loss of APP is linked to mTOR in mammalian cells (**Figure 27B**). Surprisingly, no alteration in mTOR signalling was evident in any conditions.

3.2.3 Discussion

3.2.3.1 APP Overexpression in HeLa and SH-SY5Y Cells Increases Downstream

Phosphorylation in Targets of mTORC1 and mTORC2

By overexpressing APP-GFP, APP(Swe)-GFP and AICD-GFP in HeLa cells then probing for a wide range of mTOR substrates, increased mTOR signalling was detected, primarily in basal conditions. The increase was not only restricted to mTORC1, with Akt dependent phosphorylation of Ser2448 consistent with increased mTORC2 activity. In addition, no difference was detected between APP and APP containing the Swedish double mutation, a result that may not be expected if increased APP processing was directly linked with mTOR signalling. In all, these results show a clear role for APP in mTOR signaling in HeLa cells, providing a high energy / proliferative signal.

To test the significance of an APP/mTOR interaction across multiple tissue types SH-SY5Y neuroblastoma cells overexpressing APP/AICD were probed for changes in mTOR signalling. Results showed similar behaviour to HeLa cells overexpressing APP/AICD: mTOR signalling was increased across multiple substrates, including those of mTORC1 and mTORC2. Increased mTOR signalling in HeLas, in and of itself points to relevance in mammalian tissue, but with similar results in neuronal cell culture, a role in two very different tissue types is suggested, pointing to a significant role within the entire organism. The changes in mTOR signalling in SH-SY5Y cells in particular are significant, showing relevance specifically in neuronal context, which is potentially important when considering a role in the pathology of Alzheimer's disease as a neurodegenerative disorder.

3.2.3.2 APL-1 Mutation yn5 is Additive with daf-15 and let-363 Mutation, Showing Fat Droplet Accumulation as Seen by Oil Red O and BODIPY Staining

Evidence for APP's interaction with mTOR signalling in HeLa and SH-SY5Y cells does not necessarily translate *in vivo* or represent a conserved function of the APP protein and its orthologs. To investigate an *in vivo*, conserved role for APP, *C. elegans* was used as a model organism, genetic interaction was determined through knockdown of mTOR complex

orthologs and an intracellular domain free truncation mutation in the *C. elegans* ortholog of APP. Using previously established methodology (Jia *et al.*, 2004) Oil Red O was used to visualise lipid droplet accumulation, showing the accumulation of lipid droplets upon loss of mTOR function, which was potentiated by *apl-1* mutation. The relevance of this finding was that APL-1, the conserved ortholog of APP in *C. elegans* appears to regulate mTOR function, demonstrating a conserved interaction.

Oil Red O appeared to show regulation of mTOR by APL-1, however this method was difficult to quantify by conventional means, use of BODIPY shows more than twice the staining was apparent when APL-1 mutation was combined with mTOR knockdown. These data confirm and quantify the effects seen with Oil Red O, solidifying a role for APP in mTOR signalling throughout the metazoan phylum.

3.2.3.3 Successful Knockdown of APP Family Proteins, Alone or in Combination Fails to Alter mTOR Signalling

Overexpression data in mammalian cells appeared to clearly show APP increasing mTOR function. APP knockdowns were performed to determine effects related to loss of function. Surprisingly, while APP and APLP2 knockdown alone or in combination was successful, no consistent, discernible changes to mTOR signalling were detected.

Explaining these results are difficult, considering just how clear the *C. elegans* knockdown/mutation and mammalian overexpression data is. One possible justification of this result is that APP only contributes to mammalian mTOR signalling in a positive manner within this cell line, or that mammalian cancer cells are robust enough to normalise mTOR signalling even with a positive component dramatically reduced. HeLa cells are known to be defective in the tumour suppressor LKB1, which is upstream of AMPK within the mTOR signalling pathway (Shackleford and Shaw 2009; Wingo *et al.*, 2009), other genetic and epigenetic changes may be expected. While by no means fatal to the hypothesis of APP being linked to mTOR signalling, it does raise doubts or suggest a more complex interaction.

Future investigation is needed to elucidate the factors that influence APP/mTOR interaction in a way that explains the results. Performing knockdown in another cell line and measuring a wider range of mTOR outputs in varying nutrient states or after being sensitised by an mTORC inhibitor may help confirm APP involvement. If mammalian cells do indeed have a further mTOR compensatory mechanism beyond the APP family, it may be difficult to determine. The specific mechanism of compensation may be better understood via site directed mutagenesis of AICD or mTOR interaction sites, which would go a long way to characterise the interaction, with potential for relevant residues to be identified.

3.3 Investigating a Functional Interaction Between APP and the PIKfyve Complex

3.3.1 Introduction

The endosome is a dynamic system of compartments within the cell responsible for the import, sorting transport, destruction or export of cargoes. Each of the cargo fates require distinct behaviours from the cell, an endosomal compartment must be transported to the right location within the cell, the correct proteins must be recruited to the compartment's surface and fusion / fission events need to be undertaken. The identity and behaviour of endosomal compartments is underpinned by phosphoinositides – membrane integrated lipids with an inositol head capable of being phosphorylated into a vast array of molecules able to differentiate that surface from others.

PIKfyve is a phosphoinositide kinase, converting PI(3)P to PI(3,5)P₂. PI(3,5)P₂ is of much lower abundance than its precursor and is less well studied, but is clearly of significance to the endosome and the cell generally. Dysfunction of members within the PIKfyve complex leads to cellular vacuolation and neurodegeneration, for example Fig4 mutation causes pigmentation and neurodegenerative defects in mice and PIKfyve dysfunction is associated with human disease in the form of Charcot Marie Tooth 4J, Amyotrophic Lateral Sclerosis and Yunis-Varón Syndrome (Chow *et al.*, 2007; Zhang 2008; Chow *et al.*, 2009; Campeau *et al.*, 2013).

To date PI(3,5)P₂ has been shown as being responsible for the progression of the endosomal system to a late endosomal/lysosomal phenotype (Ikonomov *et al.*, 2002; Rutherford *et al.*, 2006; de Lartigue *et al.*, 2009) and linked to lysosomal action through interaction with

TRPML-1, a calcium channel which, when defective leads to mucopolipidosis type IV, a lysosomal storage disease (Bach *et al.*, 2010).

Alzheimer's disease can be easily framed as being related to endosomal dysfunction; enlarged endosomal compartments in the form of Granulovacuolar Degeneration (GVD) are a primary hallmark of Alzheimer's disease (Okamoto *et al.*, 1991), albeit one that is often overlooked in favour of plaques and tangles. In addition to being a feature of Alzheimer's pathology, the endosome is also an important system for the trafficking and processing of APP, being a location of high beta and gamma secretase action (Bhalla *et al.*, 2012).

Proteo-liposome analysis of AICD recently discovered that the PIKfyve complex interacts physically with the AICD via Vac14, that APP and Vac14 migrate together under live-cell imaging (Balklava *et al.*, 2015). Balklava *et al.* also began investigating the functional relationship between APP and PIKfyve using *C. elegans* as a model. The APP / PIKfyve ortholog interaction was elaborated, showing shared and additive pathology in the form of swollen hypodermal vacuoles upon loss of function in APL-1 or PPK-3 (APP and PIKfyve orthologs), where the protein functions are reduced alone or in combination. The vacuolation present in APL-1 or PPK-3 mutants was also identified as primarily RAB-7 and LMP-1 positive (late endosomal and lysosomal, respectively), indicating late endosomal / lysosomal disruption.

Further investigation should provide insight into whether this interaction has functional elements, whether the APP family has an effect on the function of PIKfyve, and if so, in what way, particularly as it relates to higher organisms.

3.3.2 Results

3.3.2.1 APP/APLP2 Double Knockdown Increases the Percentage of Cells with Vacuolar Structures in HeLa Cells Visible by Light Microscopy

To answer the question of whether the APP family has an effect on PIKfyve function, loss of APP function was performed using RNAi suppression in HeLa cells against relevant APP family members: APP and APLP2 were knocked down alone, or in combination as a double knockdown to cover possible effects of functional redundancy present in APP family proteins (Heber *et al.*, 2000).

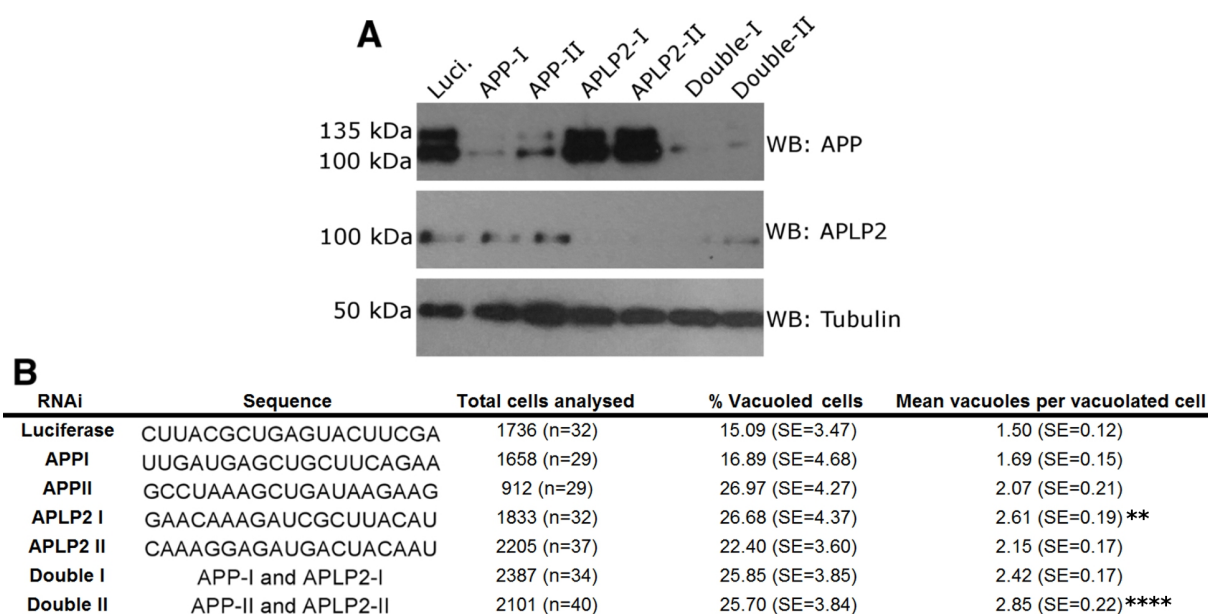


Figure 28.) APP family siRNA for the investigation of an APP/PIKfyve interaction. A) Confirmation of APP and APLP2 knockdown alone or in combination, by Western blotting. **B)** siRNA sequences for APP family members and analysis of vacuolation in HeLa cells. The total number of cells are shown (Total cells analysed), with the number of images the results were pooled from in brackets. The percentage HeLa cells in which vacuoles were observed (% Vacuolated cells) and the mean number of vacuoles per vacuolated cell (Mean vacuoles per vacuolated cell) were quantified manually, standard error is shown in brackets. The number of vacuoles appeared to increase upon suppression of both APP and APLP2, but analysis by ANOVA shows mixed results. Astrisks denote significantly different results to Luciferase control, with APLP2I and Double II showing significantly higher mean number of vacuoles per vacuolated cell. Data was pooled from n=4, analysis was performed using ANOVA with Tukey's post-hoc test, $\alpha=0.05$, ** $p\leq 0.01$, **** $p\leq 0.0001$.

PIKfyve inhibition creates gross cellular pathology in the form of vacuoles visible via light microscopy (Rutherford *et al.*, 2006; de Lartigue *et al.*, 2009). To investigate a relationship between APP family loss and PIKfyve function, cells were RNAi suppressed for APP, APLP2 or both APP and APLP2, then the cells with vacuolar structures were counted. APP, APLP2 and double knockdowns were confirmed by western blotting (**Figure 28A**), corresponding protein levels were successfully inhibited: APPI and APPII lowered levels of APP, APLP2I and

APLP2II diminished APLP2, while DoubleI and DoubleII suppressed both APP and APLP2 levels. The percentage of cells exhibiting vacuoles were counted for each condition, showing an apparent increase in the percentage of cells exhibiting vacuolar structures and the number of vacuoles per vacuolated cell (**Figure 28B**). Analysis gave mixed results, with only APLP2I and Double II achieving a significant difference from Luciferase controls.

3.3.2.2 APP/APLP2 Double Knockdown Increases Sensitivity to PIKfyve Inhibition in HeLa Cells

The RNAi suppression of APP or APLP2 appears to moderately increase vacuolation, but to a much lesser extent than PIKfyve RNAi, where cells appear to be filled with vacuoles (Rutherford *et al.*, 2006), suggesting a complementary, secondary role rather than being essential. To further test this phenomenon the same experiment was undertaken, but with cells exposed to chemical PIKfyve inhibition for only 45 minutes, the reasoning being that if APP family proteins contribute to PIKfyve function, loss may sensitise cells to PIKfyve inhibition, creating vacuolation earlier than fully competent cells.

Visually, double knockdowns appear more vacuolated (**Figure 29A**), quantification of these results show significantly higher vacuolation in double knockdowns as well as APLP2 duplex I (**Figure 29B**). These data show double RNAi suppression of APP and APLP2 sensitises cells to the depletion of PIKfyve activity, leading to increased vacuolation.

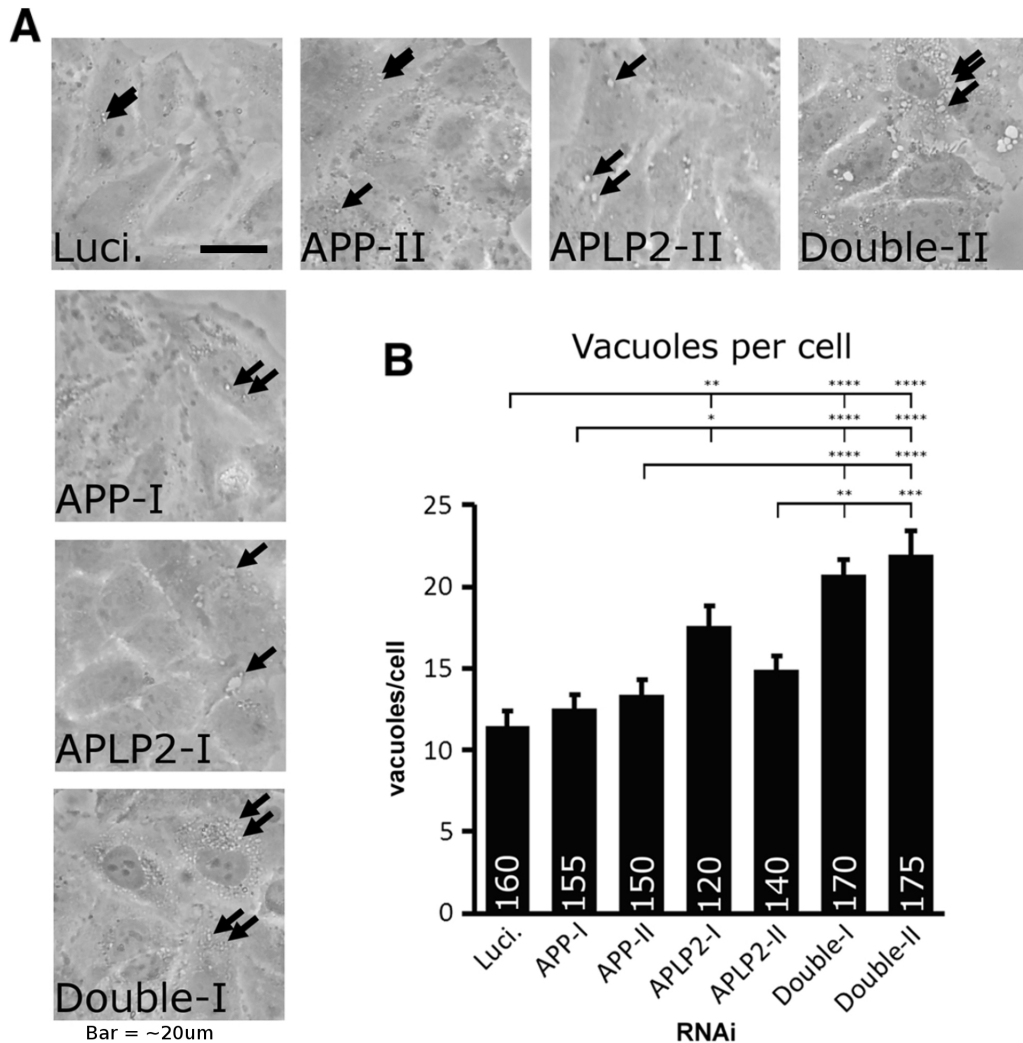


Figure 29.) RNAi suppression of APP and APLP2 increases the number of vacuoles per cell in PIKfyve inhibited HeLa cells. A) RNAi suppression of APP and APLP2 via two duplexes each (I and II) combined with limited PIKfyve inhibition (1 μ M YM201636, 45min) gave an apparent increase in vacuoles (arrows) over Luciferase RNAi control. **B)** Increase in vacuolation was confirmed by quantification. Data pooled from n=3. Statistical test using ANOVA with Tukey's post hoc analysis, $\alpha=0.05$, only significant differences are indicated, * $p\leq 0.05$, ** $p\leq 0.01$, *** $p\leq 0.001$, **** $p\leq 0.0001$. Total number of cells analysed per condition are indicated in each bar in the diagram. Error bars = SE.

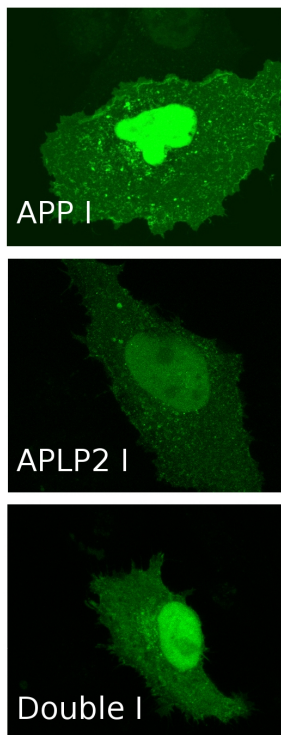
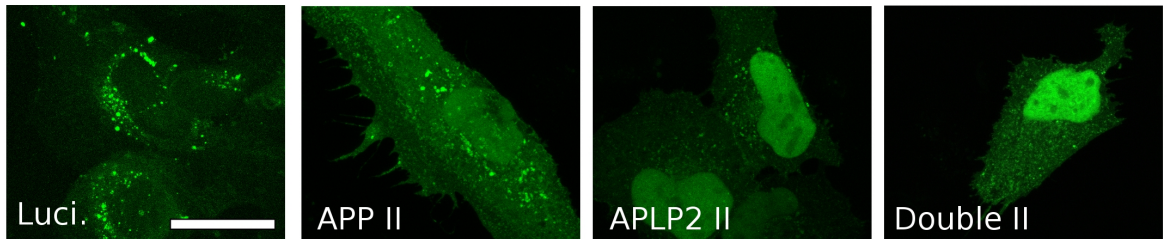
3.3.2.3 APP/APLP2 Double Knockdown Decreases the Number of ML1Nx2-GFP

Positive Vesicles in HeLa Cells

The ML1Nx2-GFP probe, a tandem repeat of TRPML-1 PI(3,5)P₂ binding domain fused to GFP, is a powerful new tool to measure a prospective link between APP family proteins and PIKfyve; able to detect the distribution of PI(3,5)P₂ within the cell. By transfecting ML1Nx2-GFP into HeLa cells then suppressing with RNAi against APP, APLP2 or both, the behaviour of PI(3,5)P₂ under APP family depletion was elucidated (**Figure 30A**). The number of PI(3,5)P₂ positive structures was quantified using the mosaic suite for ImageJ (Rizk *et al.*, 2014), providing automatic, unbiased segmentation and quantification of subcellular structures using Squash analysis.

Squash analysis showed a pronounced and significant drop in the number of ML1Nx2-GFP positive structures per cell between Luciferase controls and knockdowns, with the exception of APP duplex I (**Figure 30B**). Results show that suppression of APP family proteins does indeed impact the presence of PI(3,5)P₂.

A



Bar = ~20µm

B

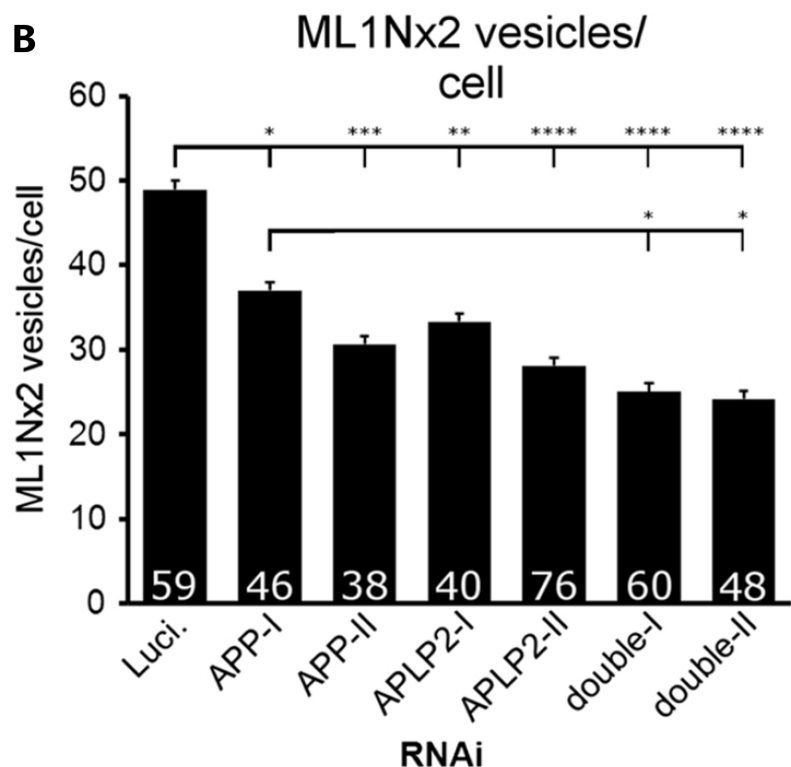


Figure 30.) APP and APLP2 suppression leads to the reduction of ML1Nx2-GFP positive vesicles. A) Single or double suppression of APP and APLP2 resulted in an apparent loss of ML1Nx2-GFP positive structures as compared to the Luciferase (Luci.) negative control. **B)** Loss of ML1N-GFP was confirmed by automatic segmentation and quantification using the mosaic plugin for ImageJ. Data pooled from n=3. Statistical testing was undertaken using ANOVA with Tukey's post hoc analysis, $\alpha=0.05$, only significant differences are indicated, * $p \leq 0.05$, ** $p \leq 0.01$, *** $p \leq 0.001$, **** $p \leq 0.0001$. Number of cells analysed per condition are indicated in each bar in the diagram. Error bars = SE. Scale bar, ~20µm.

3.3.3 Discussion

3.3.3.1 APP/APLP2 Double Knockdown Increases the Percentage of Cells with Intracellular Structures in HeLa Cells Visible by Light Microscopy

To determine whether the physical link between APP and PIKfyve is truly functional in nature requires that the presence or action of one protein be linked with that of the other. PIKfyve's function as a PIP kinase lead to the hypothesis that APP is the likely upstream effector, and as such APP family manipulation was the obvious choice for initial investigation. The output measurement of PIKfyve function is perhaps the most challenging part of determining a functional link; PIKfyve's product is extremely low abundance and labile, as such it requires specialised methods for measurement.

The morphology of cells deficient in PIKfyve function has been well documented (Rutherford *et al.*, 2006; Chow *et al.*, 2007; de Lartigue *et al.*, 2009), with widespread vacuolation obvious. **(Figure 29A)** appears to show the percentage of cells with vacuolar structures do indeed increase when APP family knockdown occurs, even if the effect is weak alone, the significance being that it suggests a functional link between APP and PIKfyve. In spite of the informative results, it is important to note that these do not conclusively show a functional link between APP and PIKfyve. The next step is to find whether APP dysfunction is linked directly to PIKfyve function or not.

3.3.3.2 APP/APLP2 Double Knockdown Increases Sensitivity to PIKfyve Inhibition in HeLa Cells

To link the loss of APP family proteins to PIKfyve function, cells were first sensitised with an inhibitor specific for PIKfyve; a decrease or non-significant change in vacuolation would suggest the APP dependent vacuolation was unrelated to PIKfyve function, while an increase vacuolation adds evidence that the two phenotypes are related or identical. **(Figure 30A)** shows substantial increase in the vacuolation phenotype and quantification of vacuole numbers. **(Figure 30B)** confirms significantly increased vacuolation in APP family

knockdowns, particularly double APP/APLP2 knockdowns. While far from conclusive when taken alone, this is indicative of APP family proteins having an effect on PIKfyve function.

3.3.3.3 APP/APLP2 Double Knockdown Decreases the Number of ML1Nx2-GFP

Positive Vesicles in HeLa Cells

The investigations of Li *et al.* (Li *et al.*, 2013) suggest the ML1Nx2 probe is specific to the presence of PI(3,5)P₂, our own independent investigations corroborate the idea that the ML1Nx2 probe is a reporter of PIKfyve function (Currinn *et al.*, 2016; Guscott *et al.*, 2016). Experiments detailed in Currinn *et al.* show that PIKfyve inhibition almost completely eliminates vesicular ML1Nx2-GFP. By knocking down APP family proteins and measuring the change in vesicular ML1Nx2-GFP we found more evidence for a functional link between APP and PIKfyve: loss of APP family proteins is associated with the significant loss of ML1Nx2-GFP positive vesicles, and by extension PIKfyve function.

In spite of the inherent difficulty of studying both APP and PIKfyve, the evidence taken together provides a growing case for an APP/PIKfyve relationship, which is not only physical, but functional in nature.

Further to the results above, investigations undertaken and published recently support and add to the findings, specifically that overexpression of APP or AICD was shown to stimulate the formation of ML1Nx2 positive structures (Currinn *et al.*, 2016).

3.4 APP and Lysosomal Acidification

3.4.1 Introduction

Previous chapters have dealt with the evidence of an AICD interaction with mTOR and the evidence for an interaction with PIKfyve. Both of these prospective interactors are particularly interesting in that they are thought to contribute to the same system: that of the autophagosome/lysosome (de Lartigue 2009; Jung *et al.*, 2010; Martin *et al.*, 2013).

mTOR is central to energy signalling within the cell and as such controls the processes of autophagy very carefully (Tokunaga *et al.*, 2004). Any disruption to mTOR signalling can in turn be expected to alter the capability for autophagy, this is seen with mTOR inhibition leading to energy conserving “housekeeping” responses such as lowered metabolism, lowered mRNA translation and increased autophagy (Glick *et al.*, 2010). This situation is reversed upon mTOR overactivation, with autophagy inhibited. Overactivation of mTOR is proposed to be a contributing factor to ageing related disorders, including Alzheimer’s (Zoncu *et al.*, 2011), making this system particularly interesting when investigating a functional APP interaction.

PIKfyve is known to drive progression of endosomes towards a late endosomal/lysosomal phenotype through the production of PI(3,5)P₂, additionally, recent debate has centred around possible V-ATPase regulation by PI(3,5)P₂ (Li *et al.*, 2014; Ho *et al.*, 2015). Experiments detailed in the previous chapter show APP to interact physically and functionally with PIKfyve, this leads naturally to the hypothesis that APP, through its interaction with PIKfyve supports lysosomal activity. Data from both an APP/mTOR and APP/PIKfyve interaction can be related to autophagy, making an opportunity to investigate this system particularly intriguing.

3.4.2 Results

3.4.2.1 Rapid Turnover of APP in SH-SY5Y Cells is Induced by Inhibition of mTOR Via Torin 1

When investigating the interaction of APP with mTOR in SH-SY5Y cells, a decrease in APP levels were noted upon serum or amino acid starvation (**Figure 24-25**), two manipulations which lower mTOR signalling. The loss of APP under starvation conditions raises the possibility that the amount of APP within the cell is tightly controlled by mTOR. The control of APP by mTOR was tested via the manipulation of mTOR signalling (**Figure 31**), manipulation was performed with amino acid starvation, or one of two mTORC inhibitors: rapamycin, an allosteric mTOR inhibitor known to suppress some mTORC1 functions (Loewith *et al.*, 2002; Sarbassov *et al.*, 2006) or Torin 1, an ATP competitive inhibitor capable of eliminating both mTORC1 and mTORC2 signals (Thoreen *et al.*, 2009). The results show that while amino acid starvation and Torin 1 treatment is able to diminish APP to a similar degree, rapamycin does not. Cellular APP levels are controlled by mTOR activity in a rapamycin insensitive manner.

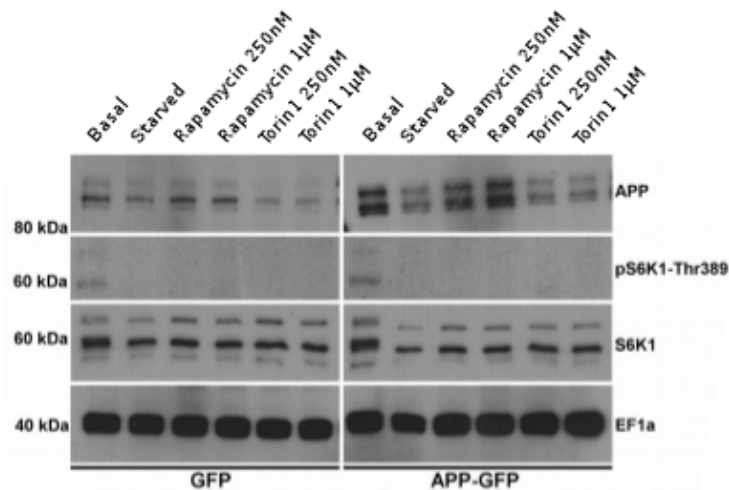


Figure 31.) APP abundance is dependent on mTOR catalytic activity in both SH-SY5Y cell controls and those lentivirally overexpressing APP. mTOR suppression with 2hr amino acid starvation (Starved) or 2hr Torin 1 application (Torin 1, 250nM or 1µM) lowers APP compared to basal nutrition (Basal) or 2hr rapamycin treatment (Rapamycin, 250nM or 1µM) in SH-SY5Y cells lentivirally overexpressing GFP (GFP) or APP (APP-GFP), as shown by western blot. Phosphorylation of S6K1 was used to indicate suppression of mTORC1, which occurred in all but basal conditions. Samples were blotted for APP, pS6K1-Thr389, S6K1 and eEF1A (top to bottom).

3.4.2.2 APP Turnover by Amino Acid Starvation is Halted by Lysosomal Inhibition

Enhanced endosomal sorting for lysosomal degradation is the classical route for transmembrane receptor downregulation (Katzmann *et al.*, 2001), making this the likely route for APP turnover. Degradative sorting can be prevented via pH quenching of endosomes (Oda *et al.*, 1991; Yoshimuri *et al.*, 1991) or the inhibition of PI(3)P dependent sorting (Futter *et al.*, 2001). To test the dependence of rapid APP removal by endosomal sorting/lysosomal degradation, cells were amino acid starved alone or in combination with inhibitors: chloroquine, ammonium chloride or wortmannin, then probed for APP levels (**Figure 32**). APP was found to be rapidly removed upon amino acid starvation, but preserved by inhibition of lysosomal acidification or PI(3)P dependent endosomal sorting.

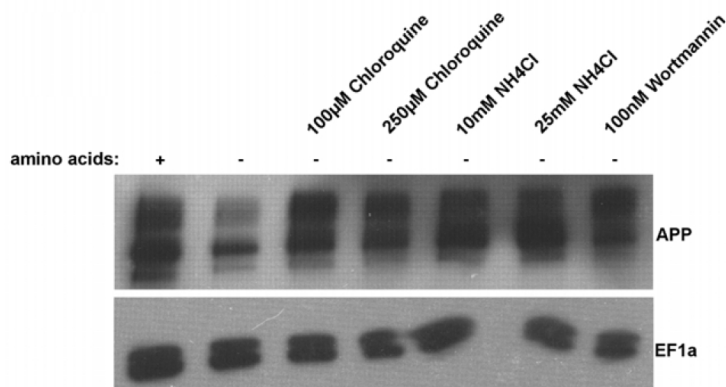


Figure 32.) mTOR inhibition-induced downregulation of APP is mediated by lysosomal degradation in HeLa cells. Loss of APP is induced upon removal of amino acids for 2 hrs (amino acids -), as compared to basal control (amino acid +). Suppression of endosomal acidification with using the pH quenchers chloroquine (100µM, 250µM Chloroquine) or ammonium chloride (10mM, 25mM NH₄Cl) prevents starvation dependent APP loss. Suppression of membrane sorting into intraluminal vesicles using the PI3K inhibitor Wortmannin (100nM Wortmannin), a PI3K inhibitor is also capable of preventing amino acid starvation induced APP loss. Samples were blotted for APP and eEF1A (top to bottom).

3.4.2.3 PIKfyve Inhibition Lowers the Number of LysoTracker Positive Structures

Mimicking Inhibited Lysosomal Acidification

To determine PIKfyve's relationship to acidic organelles, LysoTracker was used to measure vesicular pH changes upon PIKfyve inhibition as compared to compounds known to alter vesicular pH. PIKfyve was inhibited with YM201636 and compared to control cells: untreated HeLa cells or those treated with ammonium sulphate, an inhibitor of lysosomal acidity (**Figure 33**). Staining cells with LysoTracker revealed the number of LysoTracker positive structures were significantly reduced upon PIKfyve inhibition compared to untreated HeLa cells. Positive control cells (ammonium sulphate treated) show a similar effect, reducing LysoTracker staining substantially.

PIKfyve inhibition using YM201636 reduced the average number of acidified vesicles in cells. Inhibition of acidification also reduced the number of LysoTracker positive vesicles, suggesting that the LysoTracker probe utilised indeed reflected acidification.

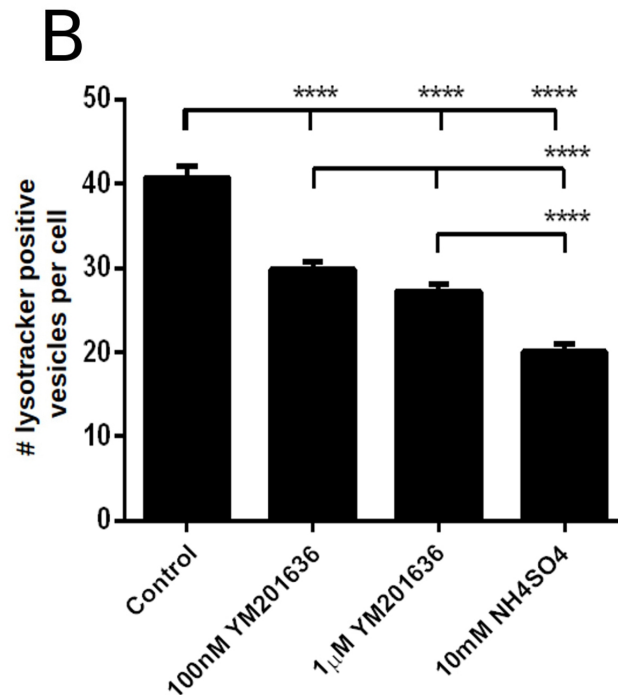
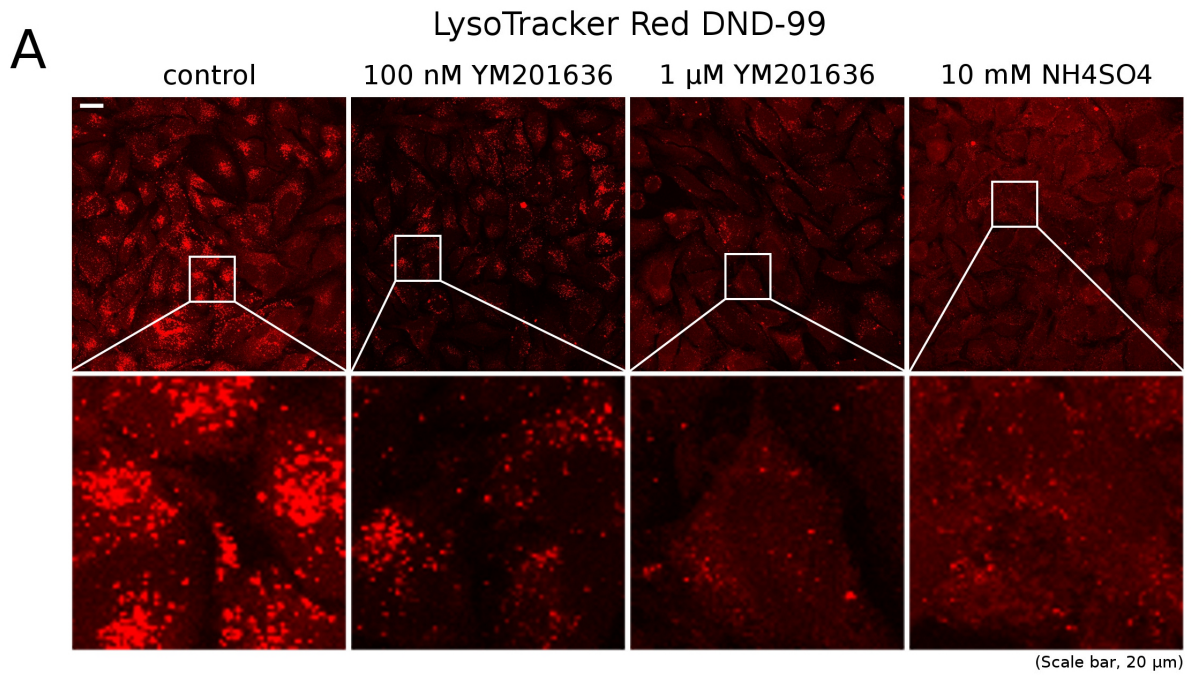


Figure 33.) PIKfyve inhibition using YM201636 lowers the number of acidic vesicles. Loss of vesicular acidification lowers lysotracker staining, as such the number of acidified vesicles can be determined. **A)** Comparing LysoTracker staining of control cells against those pH quenched with ammonium sulphate (NH₄SO₄) demonstrated that a loss of acidification translates into a loss of LysoTracker staining positive vesicles. Inhibition of PIKfyve activity (100nM, 1 μ M YM201636) showed an apparent loss of lysotracker staining, demonstrating that PIKfyve plays a role in acidifying cellular compartments. **B)** Quantification confirms NH₄SO₄ treatment or PIKfyve inhibition significantly suppresses acidification of cellular compartments as measured by the average number of lysotracker positive vesicles per cell. Data was pooled from n=3. Cells analysed: ≥ 104 per condition. Quantification was performed using automatic segmentation with the mosaic plugin for ImageJ. Statistical analysis was performed using one way ANOVA with Tukey's post-hoc test, $\alpha=0.05$, *** $p \leq 0.001$, **** $p \leq 0.0001$. Error bars = SE. Scale bar, 20 μ m.

3.4.2.4 PIKfyve Inhibition Using Apilimod Reduces Lysotracker and Lamp1 Positive Vesicles

PIKfyve inhibition is known to create cellular vacuolation (Rutherford *et al.*, 2006; de Lartigue *et al.*, 2009), and has also been linked to suppressed endosomal acidification (Li *et al.*, 2014). Lysotracker Red, a pH sensitive fluorescent dye useful for examining abnormalities in lysosomal acidification is able to detect the number and distribution of lysosomal structures (Colvin *et al.*, 2010; Fonseca *et al.*, 2012). Lysotracker has also been used quantitatively (Xu *et al.*, 2014), detecting lysosomal storage diseases through measurement of “Total Organelle Intensity” by multiplying average vesicle intensity with the structure size.

To determine the suitability of Lysotracker in detecting PIKfyve dysfunction and to clarify the relationship between PIKfyve dysfunction and late endosomal behaviour, HeLa cells were treated with the specific PIKfyve inhibitor Apilimod and either stained with Lysotracker or immunostained for Lamp1. (**Figure 34A**) shows an apparent lowering in the number of Lysotracker positive vesicles and intensity, with segmentation confirming this loss (**Figure 34B/C**). (**Figure 35A**) shows a change in Lamp1 staining; Lamp1 positive vesicles appear to be larger but less numerous. Segmentation verifies the visual findings with PIKfyve significantly lowering the number of Lamp1 positive vesicles, but significantly increasing their size in a concentration dependent manner (**Figure 35B/C**).

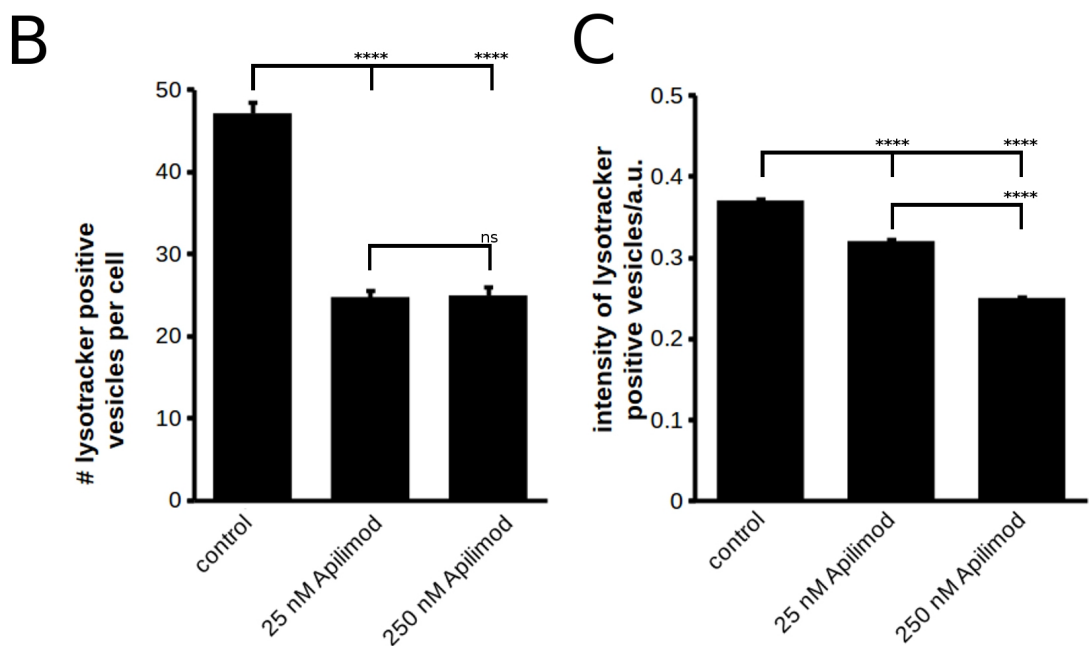
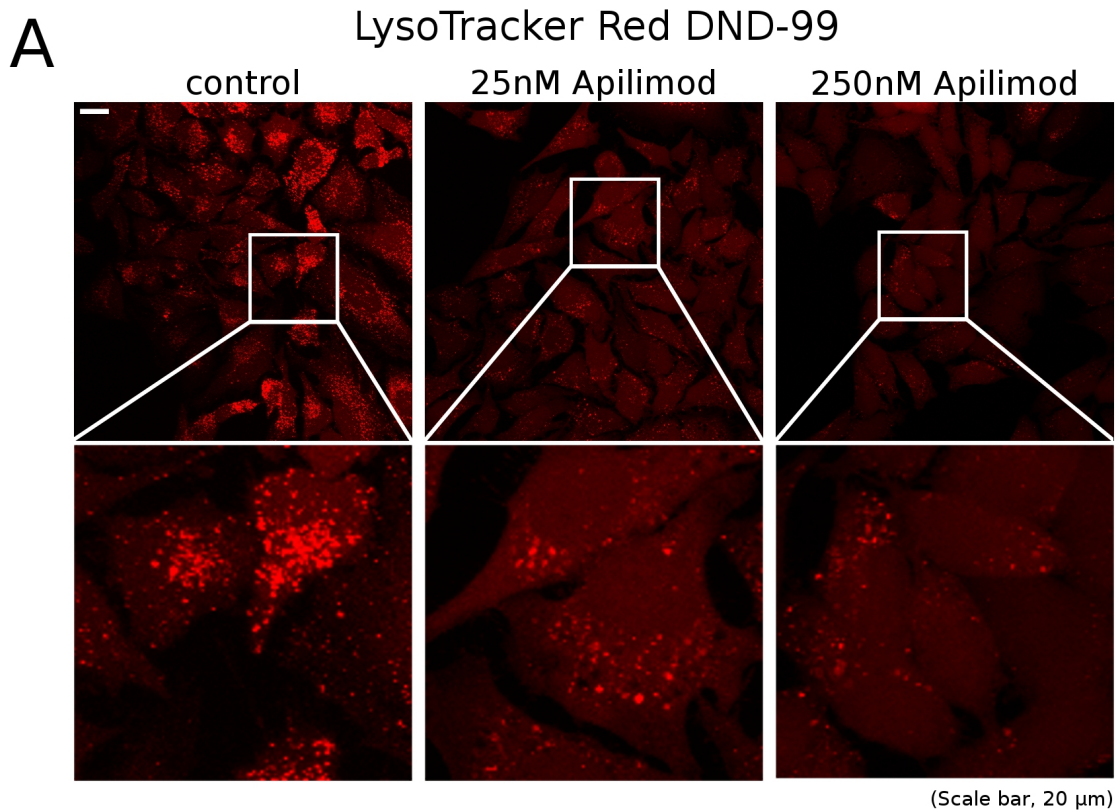


Figure 34.) Inhibition of PIKfyve using apilimod affects acidified organelles. A) Inhibition of PIKfyve using 25nM or 250nM apilimod led to a decrease of the number and intensity of acidified organelles labelled with LysoTracker. **B)** Quantification of the average number of LysoTracker positive vesicles per cell, measured using the mosaic plugin for ImageJ. Both apilimod concentrations significantly reduced the number of LysoTracker positive vesicles. **C)** Quantification of average vesicular LysoTracker intensity showed a significant, apilimod concentration dependent reduction of vesicular LysoTracker staining. **A-C)** Data were pooled from $n=3$. Cells analysed: ≥ 309 cells per condition. **B-C)** was performed using one-way ANOVA with Tukey's post-hoc test, $\alpha=0.05$, **** $p \leq 0.0001$. Error bars = SE. Scale bar, 20 μ m.

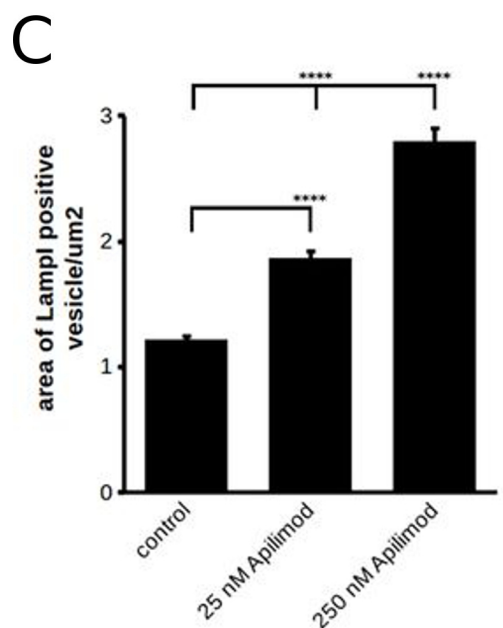
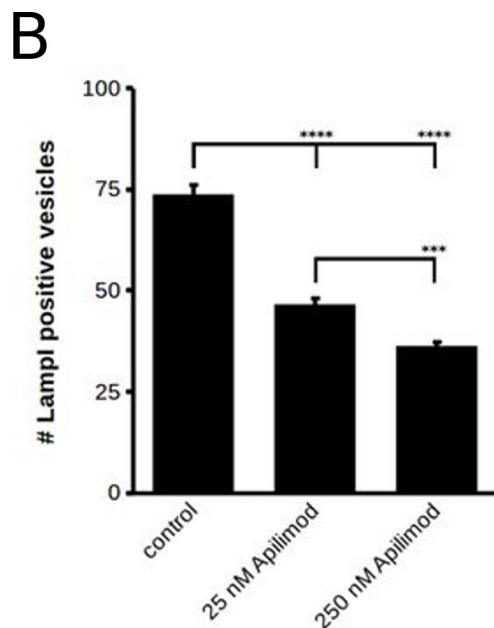
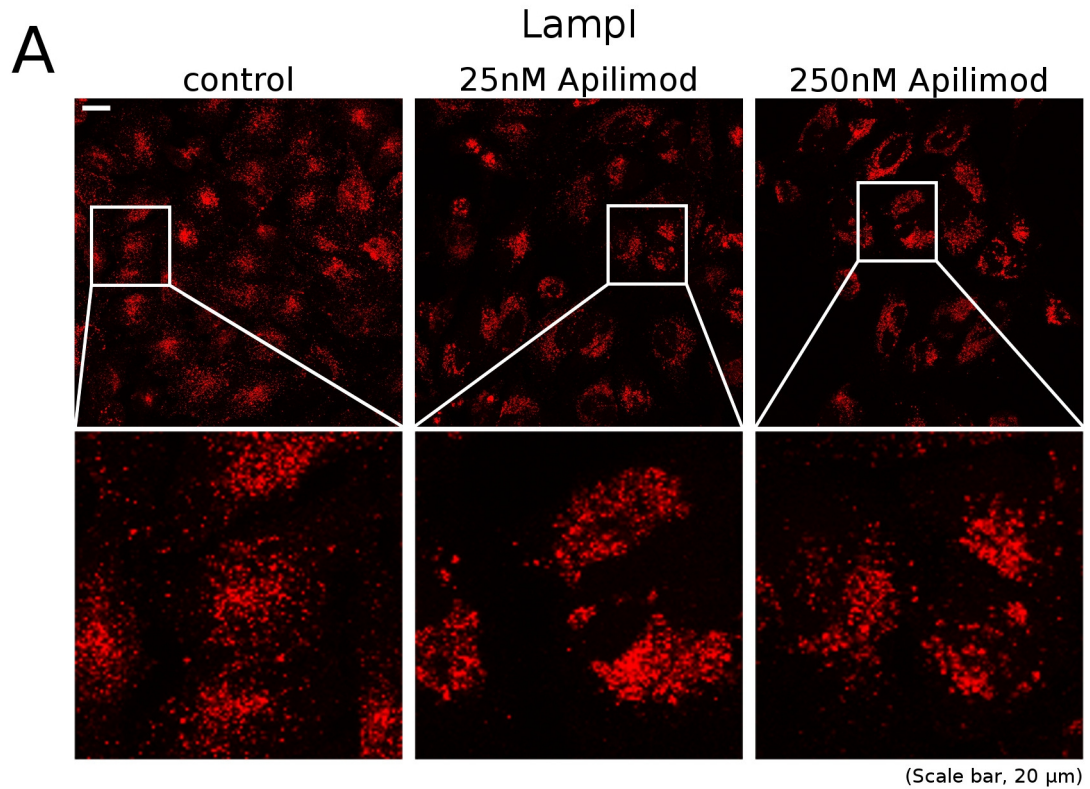


Figure 35.) Inhibition of PIKfyve using apilimod affects late endosomes/lysosomes. A) Lamp1 positive compartment immunostaining upon PIKfyve inhibition. Apilimod appeared to alter the morphology and distribution of Lamp1 positive vesicles within the cell, producing fewer, larger late endosomal / lysosomal structures. **B)** Quantification of Lamp1 positive vesicles showed that PIKfyve inhibition reduced the number of Lamp1 positive late endosomes and lysosomes in a way that was dependent on apilimod concentration. **C)** Analysis of late endosome/lysosomal structures showed that while the number of Lamp1 vesicles per cell was reduced, their size increased, suggesting swelling or aggregation of the compartment. Data was pooled from n=3. Cells analysed: 240 per condition. **B-C)** was performed using one-way ANOVA with Tukey's post-hoc test, $\alpha=0.05$, *** $p \leq 0.001$, **** $p \leq 0.0001$. Error bars are SE. Scale bar, 20 μ m.

3.4.3 Discussion

In this chapter APP was shown to be rapidly removed and that turnover is dependent on mTOR, but in a rapamycin resistant manner. The turnover of APP is dependent on lysosomal function, being halted by lysosomal inhibitors, including chloroquine and wortmannin.

Staining of cells with LysoTracker, a pH sensitive probe, was determined to be quantifiable in relation to lysosomal function; changes in PIKfyve function can be detected as LysoTracker positive structures are lost upon PIKfyve inhibition, albeit to a lesser degree than full V-ATPase inhibition, while mTOR suppression appears to increase the number of LysoTracker positive structures.

To test a link between PIKfyve function and lysosomal function, cells treated with PIKfyve inhibitor were stained with LysoTracker and others immunostained for Lamp1 (**Figure 33-35**), each compared to controls, showing an increase in structure intensity consistent with an increase in PIKfyve activity.

mTOR and PIKfyve have roles in lysosomal function. Evidence for an AICD interaction with mTOR and PIKfyve raises the intriguing possibility that APP may be linked to lysosomal / autophagy function. The investigation of APP in lysosomal function drew from observations that APP turnover was tightly controlled by mTOR signalling - starvation seemed to rapidly degrade APP levels, most noticeably in SH-SY5Y neuroblastoma cells. Rapid turnover would be expected from a protein requiring tight control, so is significant in and of itself, but is more interesting considering the implication of APP in human pathology: amyloid deposition is a result of inappropriate protein processing, be it high abundance, altered secretase action or low lysosomal destruction (Hardy and Higgins 1992), if APP removal is rapid and alters the very system that controls its turnover, the nature of APP involvement in lysosomal function has significant consequences for our understanding of Alzheimer's disease.

3.4.3.1 Rapid Turnover of APP in SH-SY5Y Cells is Induced by Inhibition of mTOR Via Torin 1

Demonstration of rapid APP turnover upon starvation / mTOR inhibition was a significant finding, highlighting APP as requiring tight control within the cell. Highly controlled APP levels are in keeping with an important cellular role, or one where the rapid increase of that protein is itself important, e.g. p53 (Lane and Lavine 2010). It is energetically expensive to have a protein constantly made and destroyed and would be evolutionarily disadvantageous if its removal were not absolutely necessary for the correct, healthy function of the cell.

Combining what we now know about APP turnover with the nature of APP as a protein liable to produce an aggregation prone peptide product (A β), leads to the lysosome being an important area of APP study: Alzheimer's disease can be easily framed as a disease of dysfunctional protein processing, a mechanism intricately linked with endosomal sorting and lysosomal function.

3.4.3.2 Amino Acid Starvation Dependent APP Turnover is Halted by Lysosomal Inhibition

As shown previously, APP removal is rapid upon starvation, showing autophagy as a primary controller of APP abundance. To confirm the dependence on the lysosome for the primary control of APP, lysosomal inhibition was used: the rapid turnover of APP was halted by disruption of lysosomal progression and maturation. By knowing how APP is controlled within the cell, further research can be geared towards how the lysosome may play a role in APP homeostasis and by extension, Alzheimer's disease. Now that APP destruction is found to be reliant on the correct function of mTOR and the lysosome, the ability for APP to influence those very systems becomes hugely relevant.

3.4.3.3 PIKfyve Inhibition Lowers the Number of LysoTracker Positive Structures

Mimicking Inhibited Lysosomal Acidification

An ongoing discussion in PIKfyve research has been whether PIKfyve is involved in lysosomal acidification (Li *et al.*, 2014; Ho *et al.*, 2015). The relationship of PIKfyve to vesicular acidification was determined by comparing LysoTracker staining in untreated cells, to those exposed to YM201636 or ammonium sulphate. PIKfyve inhibition was found to mimic the inhibition of lysosomal acidification, with greatly reduced lysoTracker positive structures. The results suggest a role for PIKfyve in endosomal acidification.

3.4.3.4 PIKfyve Inhibition Using Apilimod Reduces LysoTracker and Lamp1 Positive Vesicles

As an extension of showing PIKfyve inhibition mimicking the inhibition of lysosomal acidification, the effect of PIKfyve inhibition on the late endosomal structures was used to determine the extent of PIKfyve's influence.

LysoTracker staining clearly shows a loss of acidification as measured by both the intensity of LysoTracker positive vesicles and the number of those vesicles per cell when cells are treated with the specific PIKfyve inhibitor, apilimod. PIKfyve inhibition also lead to the number of Lamp1 positive structures decreasing, but their size increasing, suggesting aggregation or swelling of these compartments. Much like the loss of acidic structures, changes in Lamp1 are indicative of an alteration in endo/lysosomal function, indeed PIKfyve has been suggested to control early to late endosome maturation and their fission / fusion (Zou *et al.*, 2015; Miller *et al.*, 2015; Dong *et al.*, 2010). Unlike the work of other groups, the findings above are not meant to differentiate which mechanism may be responsible, be it directly on V-ATPase or indirectly via TRPML. The aim here is to confirm PIKfyve has a role in endosomal acidification.

PIKfyve being shown as a substantial player in endo/lysosomal function is potentially significant for our understanding of APP, particularly as it relates to pathology. If APP

activates PIKfyve and PIKfyve is needed for lysosomal function, a model can be formulated wherein a change to the processing of APP can lead to vacuolation / neurodegeneration through depletion of PI(3,5)P₂.

3.4.3.5 Further Evidence for APP/PIKfyve Interdependence

The results from this project complement those published in Currinn *et al.* (2016), where the interdependence of APP and PIKfyve was investigated in some depth. PIKfyve was found to be required for the correct trafficking of APP. By inhibiting PIKfyve with either YM201636 or apilimod in cells containing fluorescent tagged APP, then immunostaining for the markers EEA1 (early endosome), Lamp1 (late endosome / lysosomal) and GM130 (Golgi), a marked APP redistribution was found. APP accumulated in EEA1 positive structures, while Lamp1 and GM130 positive pools diminished as compared to non-inhibited controls, where APP is found abundantly in each.

The experiment showed APP becoming trapped in early endosome derived vesicles upon PIKfyve inhibition, suggesting that some function of PIKfyve is required for APP trafficking, be it the control over endosomal acidification or sorting more generally. APP was also found to increase PIKfyve activity in the Currinn *et al.* 2016 publication. The effect of APP on PIKfyve activity was determined by transfecting cells with an ML1Nx2 probe alongside different forms of APP/AICD, and quantifying the number of ML1Nx2 positive vesicles in each case with or without PIKfyve inhibition. The number of ML1Nx2 positive vesicles was significantly higher in cells transfected with APP, AICD or AICD with an N-terminal (membrane adjacent) truncation, but not in APP lacking AICD (APPΔAICD) or APP with C-terminal truncations. PIKfyve inhibition with YM201636 lowered the number of ML1Nx2 positive vesicles in all cases to a similar level.

Taken together there appears to be evidence for the presence of APP influencing PIKfyve activity and PIKfyve activity in turn being required for the correct determination of APP's fate in the cell.

Chapter 4

Discussion

4.1 Discussion

This project aimed to determine whether interactions detected between APP and either PIKfyve or mTOR are functional as well as physical and if so, the nature of these relationships.

4.1.1 Summary of Findings

4.1.1.1 Creation and use of TAT-AICD as a Biochemical Tool

Challenges in the investigation of AICD interaction led to the creation of TAT-AICD, a cell permeable biochemical tool intended for the acute, controlled exposure of cells to AICD. This was used to test for changes in PIKfyve and mTOR outputs: the ML1Nx2-GFP PI(3,5)P₂ probe or PIKfyve inhibitor sensitised cell vacuolation for PIKfyve and mTOR substrate phosphorylation state for mTOR. Results showed TAT-AICD was capable of rapidly penetrating cells unlike AICD alone, and with a clustered cellular distribution differing from TAT alone.

TAT-AICD was found to co-localise with the PI(3,5)P₂ probe, which may be expected if AICD interacts with PIKfyve, as indicated by previous *in vitro* findings (Balklava *et al.*, 2015). Treating GFP-ML1Nx2 expressing cells with TAT-AICD increased the number and area of PI(3,5)P₂ positive structures over TAT or AICD treatment alone which could be a sign of increased PI(3,5)P₂ production. TAT-AICD treatment was also found to moderate vacuolation in cells subject to brief PIKfyve inhibition, which would be expected if PI(3,5)P₂ was more abundant in TAT-AICD treated cells.

Treating cells with TAT-AICD did not appear to create any consistent change in mTOR signalling as shown by western blot detection of S6K1 Thr389 and 4EBP1 Ser65 phosphorylation, downstream targets of mTOR. Unpublished data suggests AICD/mTOR interaction occurs on the N-terminal extremity of AICD, in the case of TAT-AICD, this area

may be sterically hindered by MBP, which would explain the lack of effect on mTOR signalling.

4.1.1.2 Testing Prospective APP Interaction Partners

The APP/mTOR interaction was primarily investigated using mammalian tissue culture and *C. elegans*. In mammalian tissue culture APP overexpression or APP family knockdown was used, paired with detection of mTOR substrate phosphorylation. In *C. elegans*, mutants with truncated APP ortholog were compared and combined with mTOR ortholog subunit knockdown, measured using lipid accumulation as an output. The APP/PIKfyve interaction was investigated using APP family knockdown, with outputs measured using vacuolation upon PIKfyve inhibition or a PI(3,5)P₂ detecting probe.

APP overexpression showed that mTOR substrates appeared to be more strongly phosphorylated in APP expressing cells, be they HeLa or SH-SY5Y. However, knockdown of APP family proteins failed to noticeably or consistently alter mTOR substrate phosphorylation. Truncation of the *C. elegans* APP ortholog led to visible, albeit subtle fat droplet accumulation, a sign of mTOR dysfunction (as shown by mTOR ortholog knockdown). This effect was compounded by combining mTOR ortholog knockdowns with APP ortholog truncation to create a measurable, significant level of lipid accumulation.

Investigation of an APP/PIKfyve interaction using APP family knockdown resulted in a higher percentage of double knockdown cells with vacuolation and sensitising cells with a PIKfyve inhibitor lead to a significantly increased number of vacuoles per cell in double knockdowns. Using the PI(3,5)P₂ probe ML1Nx2-GFP, double knockdown of APP family proteins led to a decrease in ML1Nx2-GFP positive vesicles, indicating an impact on the presence of PI(3,5)P₂.

An APP/mTOR interaction produced compelling, but sometimes unclear results, while APP/PIKfyve results were overwhelmingly positive. The results led to the conclusion that

while the PIKfyve function is positively influenced by APP, an APP/mTOR interaction may be more complex, requiring further study to understand.

4.1.1.3 The Relevance of APP in the Endosome: A Result Driven Investigation

A profound change in APP levels was noticed upon mTOR inhibition during previous experiments on mTOR substrates. This was investigated in SH-SY5Y cells using starvation, rapamycin or Torin 1 and observing changes in APP levels. The investigation found that APP was less abundant in cells that have undergone either starvation or full chemical inhibition of mTOR's catalytic function: APP's presence and turnover appeared to be intimately linked to the function of mTOR.

To elaborate on the cellular impact of APP's interaction with mTOR or PIKfyve, autophagy was a prime candidate for study, particularly considering its correlation with mTOR activity. To confirm whether or not APP turnover is dependent on lysosomal activity, APP levels were detected under amino acid starvation with or without lysosomal inhibition. Results showed starvation dependent APP turnover clearly requiring lysosomal acidification.

In light of APP being under tight lysosomal control, and appearing to have a clear positive impact on PIKfyve, determining PIKfyve's role in this system becomes particularly interesting. The nature of PIKfyve's involvement in the acidification of endo/lysosomes is beginning to be explored, but is still somewhat unclear, particularly concerning mammalian systems (Li *et al.*, 2013; Ho *et al.*, 2015).

To better understand PIKfyve's role in acidification, cells were treated with PIKfyve specific inhibitors or a pH quencher and compared to controls using the pH sensitive dye LysoTracker. PIKfyve inhibition led to a significantly lower number of LysoTracker positive structures, while not completely eliminating them. This might be explained by a reduction in the acidification of endo/lysosomes or a reduction in the number of these structures. Further testing cells for pH or the late endosomal / lysosomal marker Lamp1 showed that PIKfyve inhibition was

decreasing both the number and intensity of LysoTracker positive structures, while decreasing the number and increasing the area of Lamp1 positive structures – indicating a less acidic, swelling/aggregating phenotype. The results point to PIKfyve as having a role in the formation / maintenance of acidic compartments.

4.1.1.4 Summary

In summary, while attempts to determine the nature of an APP-mTOR interaction gave results indicating a complex relationship; a consistent functional interaction between the intracellular domain of APP and PIKfyve was found, where AICD was capable of promoting PIKfyve activity. Investigating the relevance of the endo/lysosomal system, APP downregulation was found to be dependent on both lysosomal acidification and loss of mTOR signalling. Further study found that PIKfyve function was important in maintaining the morphology and pH of late endosomal processes, suggesting an interplay between APP and the lysosome which could be relevant to our understanding of cell biology and disease.

4.1.2 Significance

4.1.2.1 A Tool for Mammalian PIKfyve and AICD Research

The increase of PI(3,5)P₂ in mammalian cells has been a manipulation absent in the toolbox of PIKfyve researchers. It is significant in and of itself, with studies of mammalian PIKfyve limited to loss of function up until now. The creation of a tool for the rapid manipulation of PIKfyve function has the potential for wide application in the field of PIKfyve research, but also highlights the capability of cell penetrating peptides in biochemical research.

More generally, TAT-AICD benefits from being a simple to use tool that lends itself to large replicate statistical analysis. TAT-AICD is able to acutely raise the internal pool of a specific protein (in this case AICD). The benefit for AICD specifically is that the chronic effects of exposure are avoided, including long-term transcriptional alteration and AICD downregulation.

The experiments undertaken with TAT-AICD in this project were quite broad in scope, primarily looking at vacuolation and PI(3,5)P₂ distribution. However, future study should investigate biochemical changes in the cell with more detail. Modification of the TAT-AICD construct may also be useful for investigating site specific changes to AICD and their effect on the cell.

In summary, TAT-AICD avoids the downsides of other techniques, allowing greater control over AICD experiments than has previously been possible and has a high potential for future use.

4.1.2.2 Clues for APP's Role in Cellular Physiology

APP's capability of pushing PIKfyve or mTOR activity is intriguing when framed in what we know about APP. Research focusing on the extracellular domains of APP family proteins have pointed towards likely roles in cell-cell adhesion and growth factor like behaviour (Rossjohn *et al.*, 1999; Hoefgen *et al.*, 2014). An endosomal APP function has given clues to possible downstream behaviour beyond secretase driven, Fe65 partnered nuclear translocation.

Degradative pathways in the cell are dependent on the proper control of PIKfyve and mTOR. This project determined that these very pathways are affected by the intracellular domain of APP. Unusually, the presence of APP appears to be capable of promoting both a high energy, anti-degradative state through mTOR and the progression of degradative pathways via PIKfyve. The cellular context under which these signalling events occur is yet to be elucidated. One possibility is that extracellular cleavage of dimerised APP may act as a signal for either cell activity and division or activation of degradative pathways within the cell. In light of results implicating APP in mTOR and PIKfyve activity, development of a more complete model for APP's role in the cell may be possible with further study.

4.1.2.3 Ageing and Human Disease

Results showing APP as relevant in mTOR and PIKfyve activity are particularly interesting for APP's role in ageing and human disease. Control of energy and stress signals; destruction of damaged, surplus or aggregating protein is key to longterm health of a cell, and the remit of mTOR and PIKfyve. Having APP as such a pronounced effector raises the possibility that changes in the processing of APP may affect the ability of the cell to maintain good housekeeping generally and even the turnover of APP itself. Impact on cell health and APP turnover is of direct relevance to ageing and Alzheimer's disease.

Increased mTOR signalling in Alzheimer's has been described (Pei and Hugon 2008). In a *Drosophila* model of tauopathy for instance, mTOR mediated cell cycle activation was found to potentiate tau toxicity (Khurana *et al.*, 2006), whilst in tissue from brains of Alzheimer's patients mTOR activity appears to correlate with total tau levels (Li *et al.*, 2005). The fact that APP was found in the interaction studies to bind to a catalytically active site in mTOR (the kinase domain), suggested it might influence mTOR activity. This is supported by existing evidence that APP overexpression in mammalian cells and murine models results in mTOR signalling. More generally, mTOR signalling pushes protein synthesis and suppresses degradative pathways which are important to cellular health (**Figure 31-33**; Hansen *et al.*, 2008; Toth *et al.*, 2008; Bjedov *et al.*, 2010; Wu *et al.*, 2013).

A significant aspect of PIKfyve dysfunction is cellular vacuolation, where late endosomal compartments swell due to a breakdown in endosomal sorting. Granulovacuolar degeneration (GVD) is a vacuolar phenotype present in the hippocampus and other areas of Alzheimer's disease affected brains (Ball 1978); the swelling of Rab5 and Rab7 positive endosomes and lysosomal accumulation has also been implicated in Alzheimer's disease (Cataldo *et al.*, 2008).

GVD bodies are basophilic and, like PIKfyve deficient cell vacuoles, are derived from late-stage endosomal membranes (Funk *et al.*, 2011). The processes underlying GVD are poorly

understood, but defects in endosomal sorting and lysosomal integrity play a role in Alzheimer's disease (Lee *et al.*, 2011; Muhammad *et al.*, 2008; Nixon 2007; Wolfe *et al.*, 2013).

Interestingly, GVD bodies have been found to contain phosphorylated ribosomal protein S6 (pS6), the substrate of S6K, which is in turn a primary target of mTOR (Castellani *et al.*, 2011). pS6 is thought to have a role in RNA storage, degradation and translation, but is a hallmark of stress granules. Stress granules are transient, intracellular aggregations of protein and RNA that respond to oxidative stress and inappropriate transcription (Anderson and Kedersha 2008). Similarities between PIKfyve dysfunction and the GVD bodies of Alzheimer's disease in conjunction with possible overactivation of mTOR may be explained by APP signalling inappropriately.

4.1.3 Challenges and Limitations

Significance of the project's findings should not be understated, however the weaknesses inherent in the investigations should be discussed.

4.1.3.1 Consoling mTOR and PIKfyve Activation

Activation of PIKfyve by APP appears to be well supported using the evidence from this project. Although evidence for mTOR functional involvement was less consistent, some results still support activation by APP.

PIKfyve and mTOR activities are linked: PI(3,5)P₂ can act to recruit mTORC1 to membranes by directly binding RAPTOR and is also required in yeast, binding of Sch9, the yeast homolog of S6K (Bridges *et al.*, 2012; Jin *et al.*, 2014). On the surface, these findings appear to point to an mTOR activating role for PIKfyve, which would inhibit autophagy, while results of this project as well as other publications clearly show PIKfyve's importance for a functional lysosome. To console this apparent contradiction it is perhaps better to think of PI(3,5)P₂ as being contributing, but not sufficient for mTORC1 activity. Many more signals go

into the activation of mTOR than membrane recruitment by PI(3,5)P₂.

In the context of a functional APP interaction, it is difficult to delineate mTOR from PIKfyve. An interaction of APP with PIKfyve may potentiate a membrane to enable higher mTOR activity or facilitate autophagy.

4.1.3.2 New Tools: The ML1Nx2-GFP Probe

Li *et al.* published the development of the probe ML1Nx2-GFP, claiming it to have high specificity for PI(3,5)P₂ (Li *et al.*, 2013). This tool is potentially useful and indeed vesicular staining correlates with expected PI(3,5)P₂ levels and distribution. Just how closely ML1Nx2-GFP signal reflects the abundance and distribution of PI(3,5)P₂ specifically is difficult to validate in a cellular environment. The lack of comparable PI(3,5)P₂ measuring tools contributes, but also the difficulty of measuring cross-reactivity in the cell. In spite of questions revolving around specificity and result interpretation, the probe remains a unique tool, albeit one that would be served by further investigation. Results obtained with ML1Nx2-GFP should be considered as a relatively new addition to the PIKfyve researcher's toolbox, experiments utilising ML1Nx2-GFP should be considered as adding to a body of evidence and not as a magic bullet for PI(3,5)P₂ detection.

4.1.3.3 New Tools: TAT-AICD

While cell penetrating peptides have been known for many years (Frankel and Pabo 1988; Green and Loewenstein 1988), their mechanism of action has been widely debated (Reviewed by Bechara and Sagan 2013). As such, cell penetrating peptides have not seen extensive use in biochemical investigation, researchers preferring the more "tried and true" method of transfection. Results obtained should be viewed in the light of the unclear mechanism of action. In spite of this, TAT fusion does hold potential benefits over other methods in its ease of use, repeatability, small molecular weight and the sheer number of cells that can be analysed with it.

4.1.4 The Future of Alzheimer's Therapy and Research

Research into Alzheimer's disease therapy has been plagued by late phase clinical trial failure, with major issues in efficacy and / or safety. Examples include γ -secretase inhibitor semagacestat (Doody *et al.*, 2013), where interference of Notch signalling was heavily impacting participants (Henley *et al.*, 2014), and the beta amyloid clearing monoclonal antibody bapineuzumab (Miles *et al.*, 2013) that failed to improve clinical outcome in two phase III trials (Salloway *et al.*, 2014). Both of these therapies focused on the prevention of amyloid beta production or its clearing.

In spite of the continued failure to address pathology by focusing on amyloid beta, efforts are still being made to push development of similar drugs such as solanezumab that has already been shown to fail at improving cognition and functional ability (Doody *et al.*, 2014). One drug that does appear promising is masitinib (Piette *et al.*, 2011; Folch *et al.*, 2015). Masitinib inhibits c-Kit (CD117) and Fyn kinases, masitinib's mechanism of action is to dampen the body's immune reaction to amyloid through suppression of mast cells and inhibiting pathways to tau pathology. Interestingly, the Fyn kinase also contributes a significant signal to mTOR, indeed, when overactivated it can induce cell death through endoplasmic reticulum stress (Wang *et al.*, 2015). In addition to contributing to tauopathy, c-Kit also feeds a positive signal to mTOR through PI3K, and is key in cancer cell survival. The drug has been associated with slowing of cognitive decline in adjunct therapy and has successfully completed futility testing in phase III trials, showing it to be capable of reaching its efficacy objective (Airiau *et al.*, 2013).

In summary, targeting the body's reaction to amyloid beta, preventing tau phosphorylation and excitotoxicity may help slow Alzheimer's disease in comparison to targetting amyloid beta alone (Nygaard *et al.*, 2014).

4.1.4.1 Approaches to APP Research

APP research has received a huge amount of attention due to its involvement in Alzheimer's disease, attention that is only growing with an ageing population and the healthcare / social impacts entailed. The drive for effective Alzheimer's therapies has in turn impacted how research is conducted. APP research has overwhelmingly focused on its place in human disease, revolving around amyloid beta to the point where other research is perhaps overshadowed or underfunded. It can be argued that a "race for the cure" has been a major stumbling block in its own success, with laboratories focused on late pathological processes before properly understanding the underlying biology of the molecules in question. Escaping the disease fixation in APP research allows focus on incremental elucidation of APP functions which can then inform intelligent drug / therapy design where all previous amyloid beta targeting approaches have failed.

4.1.4.2 Next Steps in APP Research

Prioritising the cellular roles and context of APP family proteins may lead to a clearer picture for future Alzheimer's therapy. Previous research sees the APP extracellular domain as acting in cell-cell adhesion or with growth factor like behaviour (Rossjohn *et al.*, 1999; Hoefgen *et al.*, 2014) and the intracellular domain performing a role in nuclear signalling upon secretase processing (Cao and Sudhof 2001). This project has found a role for the intracellular domain of APP in the endo / lysosome.

Future research questions should address how the functions attributed to APP may fit together. Although this seems a simple question, it becomes complex considering the myriad variables. Variables include: cell type, the intracellular location of APP at any one time, phosphorylation of sites on AICD, preferential secretase activity. Beyond this, extracellular dimerisation and behaviour upon secretase release, isoform type, and the importance of anchored versus free AICD must all be considered.

Knowing the specific circumstances required for the positive effect of APP on mTOR would greatly benefit from further investigation.

Considering the APP-PIKfyve interaction specifically, further work surrounding the structural biology of the physical interaction may be helpful: discovering which specific residues are important on both molecules would go a long way to solidifying the interaction of AICD with Vac14 as the basis for increased PIKfyve activity.

References

- Abramow-Newerly, M., Ming, H., & Chidiac, P. (2006). Modulation of subfamily B/R4 RGS protein function by 14-3-3 proteins. *Cell Signal*, *18*(12), 2209-2222. doi:10.1016/j.cellsig.2006.05.011
- Abramow-Newerly, M., Roy, A. A., Nunn, C., & Chidiac, P. (2006). RGS proteins have a signalling complex: interactions between RGS proteins and GPCRs, effectors, and auxiliary proteins. *Cell Signal*, *18*(5), 579-591. doi:10.1016/j.cellsig.2005.08.010
- Ago, T., Takeya, R., Hiroaki, H., Kuribayashi, F., Ito, T., Kohda, D., & Sumimoto, H. (2001). The PX domain as a novel phosphoinositide-binding module. *Biochem Biophys Res Commun*, *287*(3), 733-738. doi:10.1006/bbrc.2001.5629
- Airiau, K., Mahon, F.-X., Josselin, M., Jeanneteau, M., Belloc, F. (2013) PI3K/mTOR pathway inhibitors sensitize chronic myeloid leukemia stem cells to nilotinib and restore the response of progenitors to nilotinib in the presence of stem cell factor. *Cell Death Dis.*, *4*:e827. Doi:10.1038/cddis.2013.309
- Akhtar, M. W., Kim, M. S., Adachi, M., Morris, M. J., Qi, X., Richardson, J. A., . . . Monteggia, L. M. (2012). In vivo analysis of MEF2 transcription factors in synapse regulation and neuronal survival. *PLoS One*, *7*(4), e34863. doi:10.1371/journal.pone.0034863
- Alberts, B., Johnson, A., Lewis, J., Raff, M., Walter, P. (2007) *Molecular Biology of the Cell*. 5th edition. New York: Garland Science. ISBN:9780815341055.
- Alghamdi, T. A., Ho, C. Y., Mrakovic, A., Taylor, D., Mao, D., & Botelho, R. J. (2013). Vac14 protein multimerization is a prerequisite step for Fab1 protein complex assembly and function. *J Biol Chem*, *288*(13), 9363-9372. doi:10.1074/jbc.M113.453712
- Allinson, T. M., Parkin, E. T., Turner, A. J., & Hooper, N. M. (2003). ADAMs family members as amyloid precursor protein alpha-secretases. *J Neurosci Res*, *74*(3), 342-352. doi:10.1002/jnr.10737
- An, W. L., Cowburn, R. F., Li, L., Braak, H., Alafuzoff, I., Iqbal, K., . . . Pei, J. J. (2003). Up-regulation of phosphorylated/activated p70 S6 kinase and its relationship to neurofibrillary pathology in Alzheimer's disease. *Am J Pathol*, *163*(2), 591-607. doi:10.1016/s0002-9440(10)63687-5
- Andersen, O. M., Reiche, J., Schmidt, V., Gotthardt, M., Spoelgen, R., Behlke, J., . . . Willnow, T. E. (2005). Neuronal sorting protein-related receptor sorLA/LR11 regulates processing of the amyloid precursor protein. *Proc Natl Acad Sci U S A*, *102*(38), 13461-13466. doi:10.1073/pnas.0503689102
- Anderson, P., & Kedersha, N. (2007). Stress granules: the Tao of RNA triage. *Trends in Biochemical Sciences*, *33*(3), 141-150. doi:10.1016/j.tibs.2007.12.003
- Anderson, R. G., Brown, M. S., & Goldstein, J. L. (1977). Role of the coated endocytic vesicle in the uptake of receptor-bound low density lipoprotein in human fibroblasts. *Cell*, *10*(3), 351-364. Retrieved from <http://www.ncbi.nlm.nih.gov/pubmed/191195>
- Annunziata, I., Patterson, A., Danielle, H., Hu, H., Moshiah, S., Gomero, E., . . . d'Azzo, A., al. (2013). Lysosomal NEU1 deficiency affects amyloid precursor protein levels and amyloid- β secretion via deregulated lysosomal exocytosis. *Nat Commun.*, *4*:2734. doi:10.1038/ncomms3734.
- Arantes, R. M., & Andrews, N. W. (2006). A role for synaptotagmin VII-regulated exocytosis of lysosomes in neurite outgrowth from primary sympathetic neurons. *J Neurosci*, *26*(17), 4630-4637. doi:10.1523/JNEUROSCI.0009-06.2006
- Ashley, J., Packard, M., Ataman, B., & Budnik, V. (2005). Fasciclin II signals new synapse formation through amyloid precursor protein and the scaffolding protein dX11/Mint. *J Neurosci*, *25*(25), 5943-5955. doi:10.1523/jneurosci.1144-05.2005
- Babst, M., Katzmann, D. J., Snyder, W. B., Wendland, B., & Emr, S. D. (2002). Endosome-associated complex, ESCRT-II, recruits transport machinery for protein sorting at the multivesicular body. *Dev Cell*, *3*(2), 283-289. Retrieved from <http://www.ncbi.nlm.nih.gov/pubmed/12194858>
- Bach, G., Zeevi, David A., Frumkin, A., & Kogot-Levin, A. (2010). Mucopolipidosis type IV and the mucopolipins. *Biochemical Society Transactions*, *38*(6), 1432-1435. doi:10.1042/bst0381432
- Baki, L., Shioi, J., Wen, P., Shao, Z., Schwarzman, A., Gama-Sosa, M., . . . Robakis, N. K.

- (2004). PS1 activates PI3K thus inhibiting GSK-3 activity and tau overphosphorylation: effects of FAD mutations. *EMBO J*, 23(13), 2586-2596. doi:10.1038/sj.emboj.7600251
- Balklava, Z., Niehage, C., Currinn, H., Mellor, L., Guscott, B., Poulin, G., . . . Wassmer, T. (2015). The Amyloid Precursor Protein Controls PIKfyve Function. *PLoS One*, 10(6), e0130485. doi:10.1371/journal.pone.0130485
- Ball, M. J. (1978). Topographic distribution of neurofibrillary tangles and granulovacuolar degeneration in hippocampal cortex of aging and demented patients. A quantitative study. *Acta Neuropathologica*, 42(2), 73-80. doi:10.1007/bf00690970
- Ballon, D. R., Flanary, P. L., Gladue, D. P., Konopka, J. B., Dohlman, H. G., & Thorner, J. (2006). DEP-domain-mediated regulation of GPCR signaling responses. *Cell*, 126(6), 1079-1093. doi:10.1016/j.cell.2006.07.030
- Bamberger, M. E., & Landreth, G. E. (2001). Microglial interaction with beta-amyloid: implications for the pathogenesis of Alzheimer's disease. *Microsc Res Tech*, 54(2), 59-70. doi:10.1002/jemt.1121
- Bargal, R., Avidan, N., Ben-Asher, E., Olender, Z., Zeigler, M., Frumkin, A., . . . Bach, G. (2000). Identification of the gene causing mucopolidosis type IV. *Nat Genet*, 26(1), 118-123. doi:10.1038/79095
- Barlowe, C., Orci, L., Yeung, T., Hosobuchi, M., Hamamoto, S., Salama, N., . . . Schekman, R. (1994). COPII: a membrane coat formed by Sec proteins that drive vesicle budding from the endoplasmic reticulum. *Cell*, 77(6), 895-907. Retrieved from <http://www.ncbi.nlm.nih.gov/pubmed/8004676>
- Barnham, K. J., McKinsty, W. J., Multhaup, G., Galatis, D., Morton, C. J., Curtain, C. C., . . . Cappai, R. (2003). Structure of the Alzheimer's disease amyloid precursor protein copper binding domain. A regulator of neuronal copper homeostasis. *J Biol Chem*, 278(19), 17401-17407. doi:10.1074/jbc.M300629200
- Baumkotter, F., Wagner, K., Eggert, S., Wild, K., & Kins, S. (2012). Structural aspects and physiological consequences of APP/APLP trans-dimerization. *Exp Brain Res*, 217(3-4), 389-395. doi:10.1007/s00221-011-2878-6
- Bayascas, J. R., Wullschleger, S., Sakamoto, K., Garcia-Martinez, J. M., Clacher, C., Komander, D., . . . Alessi, D. R. (2008). Mutation of the PDK1 PH domain inhibits protein kinase B/Akt, leading to small size and insulin resistance. *Mol Cell Biol*, 28(10), 3258-3272. doi:10.1128/MCB.02032-07
- Bechara, C., & Sagan, S. (2013). Cell-penetrating peptides: 20 years later, where do we stand? *FEBS Letters*, 587(12), 1693-1702. doi:http://dx.doi.org/10.1016/j.febslet.2013.04.031
- Beck, T., & Hall, M. N. (1999). The TOR signalling pathway controls nuclear localization of nutrient-regulated transcription factors. *Nature*, 402(6762), 689-692. doi:10.1038/45287
- Berg, T. O., Fengsrud, M., Strømhaug, P. E., Berg, T., & Seglen, P. O. (1998). Isolation and Characterization of Rat Liver Amphisomes: EVIDENCE FOR FUSION OF AUTOPHAGOSOMES WITH BOTH EARLY AND LATE ENDOSOMES. *Journal of Biological Chemistry*, 273(34), 21883-21892. doi:10.1074/jbc.273.34.21883
- Berger, P., Bonneick, S., Willi, S., Wymann, M., & Suter, U. (2002). Loss of phosphatase activity in myotubularin-related protein 2 is associated with Charcot-Marie-Tooth disease type 4B1. *Hum Mol Genet*, 11(13), 1569-1579. Retrieved from <http://www.ncbi.nlm.nih.gov/pubmed/12045210>
- Bhalla, A., Vetanovetz, C. P., Morel, E., Chamoun, Z., Paolo, G. D., & Small, S. A. (2012). Characterizing the location and trafficking routes of the neuronal retromer and its role in amyloid precursor protein transport. *Neurobiology of disease*, 47(1), 126-134. doi:10.1016/j.nbd.2012.03.030
- Bjedov, I., Toivonen, J. M., Kerr, F., Slack, C., Jacobson, J., Foley, A., & Partridge, L. (2010). Mechanisms of life span extension by rapamycin in the fruit fly *Drosophila melanogaster*. *Cell Metab*, 11(1), 35-46. doi:10.1016/j.cmet.2009.11.010
- Blagosklonny, M. V. (2013). Rapamycin extends life- and health span because it slows aging. *Aging (Albany NY)*, 5(8), 592-598.
- Bonangelino, C. J., Nau, J. J., Duex, J. E., Brinkman, M., Wurmser, A. E., Gary, J. D., . . . Weisman, L. S. (2002). Osmotic stress-induced increase of phosphatidylinositol 3,5-bisphosphate requires Vac14p, an activator of the lipid kinase Fab1p. *J Cell Biol*, 156(6), 1015-1028. doi:10.1083/jcb.200201002

- Bonifacino, J. S., & Glick, B. S. (2004). The Mechanisms of Vesicle Budding and Fusion. *Cell*, 116(2), 153-166. doi:10.1016/S0092-8674(03)01079-1
- Bonifacino, J. S., & Lippincott-Schwartz, J. (2003). Coat proteins: shaping membrane transport. *Nat Rev Mol Cell Biol*, 4(5), 409-414. doi:10.1038/nrm1099
- Bonifacino, J. S., & Traub, L. M. (2003). Signals for sorting of transmembrane proteins to endosomes and lysosomes. *Annu Rev Biochem*, 72, 395-447. doi:10.1146/annurev.biochem.72.121801.161800
- Borg, J. P., Ooi, J., Levy, E., & Margolis, B. (1996). The phosphotyrosine interaction domains of X11 and FE65 bind to distinct sites on the YENPTY motif of amyloid precursor protein. *Mol Cell Biol*, 16(11), 6229-6241. Retrieved from <http://www.ncbi.nlm.nih.gov/pubmed/8887653>
- Boucrot, E., Saffarian, S., Zhang, R., & Kirchhausen, T. (2010). Roles of AP-2 in clathrin-mediated endocytosis. *PLoS One*, 5(5), e10597. doi:10.1371/journal.pone.0010597
- Braak, H., & Braak, E. (1991). Neuropathological staging of Alzheimer-related changes. *Acta Neuropathol*, 82(4), 239-259. Retrieved from <http://www.ncbi.nlm.nih.gov/pubmed/1759558>
- Brenner, S. (1974). The genetics of *Caenorhabditis elegans*. *Genetics*, 77(1), 71-94.
- Bridges, D., Ma, J. T., Park, S., Inoki, K., Weisman, L. S., & Saltiel, A. R. (2012). Phosphatidylinositol 3,5-bisphosphate plays a role in the activation and subcellular localization of mechanistic target of rapamycin 1. *Mol Biol Cell*, 23(15), 2955-2962. doi:10.1091/mbc.E11-12-1034
- Bridges, D., & Saltiel, A. R. (2012). Phosphoinositides in insulin action and diabetes. *Curr Top Microbiol Immunol*, 362, 61-85. doi:10.1007/978-94-007-5025-8_3
- Brouillet, E., Trembleau, A., Galanaud, D., Volovitch, M., Bouillot, C., Valenza, C., . . . Allinquant, B. (1999). The amyloid precursor protein interacts with Go heterotrimeric protein within a cell compartment specialized in signal transduction. *J Neurosci*, 19(5), 1717-1727. Retrieved from <http://www.ncbi.nlm.nih.gov/pubmed/10024358>
- Brown, E. J., Albers, M. W., Shin, T. B., Ichikawa, K., Keith, C. T., Lane, W. S., & Schreiber, S. L. (1994). A mammalian protein targeted by G1-arresting rapamycin-receptor complex. *Nature*, 369(6483), 756-758. doi:10.1038/369756a0
- Brown, J., Smith, S., Brun, A., Collinge, J., Gydesen, S., Hardy, J., . . . Goate, A. (1991). Genetic characterization of a novel familial dementia. *Ann N Y Acad Sci*, 640, 181-183. Retrieved from <http://www.ncbi.nlm.nih.gov/pubmed/1776737>
- Burd, C. G., & Emr, S. D. (1998). Phosphatidylinositol(3)-phosphate signaling mediated by specific binding to RING FYVE domains. *Mol Cell*, 2(1), 157-162. Retrieved from <http://www.ncbi.nlm.nih.gov/pubmed/9702203>
- Bush, A. I., Beyreuther, K., & Masters, C. L. (1993). The beta A4 amyloid protein precursor in human circulation. *Ann N Y Acad Sci*, 695, 175-182. Retrieved from <http://www.ncbi.nlm.nih.gov/pubmed/8239279>
- Bush, A. I., Martins, R. N., Rumble, B., Moir, R., Fuller, S., Milward, E., . . . et al. (1990). The amyloid precursor protein of Alzheimer's disease is released by human platelets. *J Biol Chem*, 265(26), 15977-15983. Retrieved from <http://www.ncbi.nlm.nih.gov/pubmed/2118534>
- Bush, A. I., Multhaup, G., Moir, R. D., Williamson, T. G., Small, D. H., Rumble, B., . . . Masters, C. L. (1993). A novel zinc(II) binding site modulates the function of the beta A4 amyloid protein precursor of Alzheimer's disease. *J Biol Chem*, 268(22), 16109-16112. Retrieved from <http://www.ncbi.nlm.nih.gov/pubmed/8344894>
- Caccamo, A., Majumder, S., Richardson, A., Strong, R., & Oddo, S. (2010). Molecular interplay between mammalian target of rapamycin (mTOR), amyloid-beta, and Tau: effects on cognitive impairments. *J Biol Chem*, 285(17), 13107-13120. doi:10.1074/jbc.M110.100420
- Caccamo, A., Maldonado, M. A., Majumder, S., Medina, D. X., Holbein, W., Magri, A., & Oddo, S. (2011). Naturally secreted amyloid-beta increases mammalian target of rapamycin (mTOR) activity via a PRAS40-mediated mechanism. *J Biol Chem*, 286(11), 8924-8932. doi:10.1074/jbc.M110.180638
- Calne, R. Y., Collier, D. S., Lim, S., Pollard, S. G., Samaan, A., White, D. J., & Thiru, S. (1989). Rapamycin for immunosuppression in organ allografting. *Lancet*, 2(8656), 227. Retrieved from <http://www.ncbi.nlm.nih.gov/pubmed/2568561>

- Campeau, P. M., Lenk, G. M., Lu, J. T., Bae, Y., Burrage, L., Turnpenny, P., . . . Lee, B. H. (2013). Yunis-Varon syndrome is caused by mutations in FIG4, encoding a phosphoinositide phosphatase. *Am J Hum Genet*, *92*(5), 781-791. doi:10.1016/j.ajhg.2013.03.020
- Cao, X., & Sudhof, T. C. (2001). A transcriptionally [correction of transcriptively] active complex of APP with Fe65 and histone acetyltransferase Tip60. *Science*, *293*(5527), 115-120. doi:10.1126/science.1058783
- Caricasole, A., Copani, A., Caruso, A., Caraci, F., Iacovelli, L., Sortino, M. A., . . . Nicoletti, F. (2003). The Wnt pathway, cell-cycle activation and beta-amyloid: novel therapeutic strategies in Alzheimer's disease? *Trends Pharmacol Sci*, *24*(5), 233-238. Retrieved from <http://www.ncbi.nlm.nih.gov/pubmed/12767722>
- Carmel, L., Efroni, S., White, P. D., Aslakson, E., Vollmer-Conna, U., & Rajeevan, M. S. (2006). Gene expression profile of empirically delineated classes of unexplained chronic fatigue. *Pharmacogenomics*, *7*(3), 375-386. doi:10.2217/14622416.7.3.375
- Castellani, R. J., Gupta, Y., Sheng, B., Siedlak, S. L., Harris, P. L. R., Coller, J. M., . . . Zhu, X. (2011). A novel origin for granulovacuolar degeneration in aging and Alzheimer's disease: parallels to stress granules. *Lab Invest*, *91*(12), 1777-1786. Retrieved from <http://dx.doi.org/10.1038/labinvest.2011.149>
- Cataldo, A. M., Mathews, P. M., Boiteau, A. B., Hassinger, L. C., Peterhoff, C. M., Jiang, Y., . . . Nixon, R. A. (2008). Down Syndrome Fibroblast Model of Alzheimer-Related Endosome Pathology : Accelerated Endocytosis Promotes Late Endocytic Defects. *The American Journal of Pathology*, *173*(2), 370-384. doi:10.2353/ajpath.2008.071053
- Chandra, V., Bharucha, N. E., & Schoenberg, B. S. (1986). Conditions associated with Alzheimer's disease at death: case-control study. *Neurology*, *36*(2), 209-211. Retrieved from <http://www.ncbi.nlm.nih.gov/pubmed/3945392>
- Chang, K. A., & Suh, Y. H. (2010). Possible roles of amyloid intracellular domain of amyloid precursor protein. *BMB Rep*, *43*(10), 656-663. doi:10.5483/BMBRep.2010.43.10.656
- Chang, Y. Y., & Neufeld, T. P. (2009). An Atg1/Atg13 complex with multiple roles in TOR-mediated autophagy regulation. *Mol Biol Cell*, *20*(7), 2004-2014. doi:10.1091/mbc.E08-12-1250
- Chang-Ileto, B., Frere, S. G., Chan, R. B., Voronov, S. V., Roux, A., & Di Paolo, G. (2011). Synaptojanin 1-mediated PI(4,5)P2 hydrolysis is modulated by membrane curvature and facilitates membrane fission. *Dev Cell*, *20*(2), 206-218. doi:10.1016/j.devcel.2010.12.008
- Chartier-Harlin, M. C., Crawford, F., Hamandi, K., Mullan, M., Goate, A., Hardy, J., . . . Broeckhoven, C. V. (1991). Screening for the beta-amyloid precursor protein mutation (APP717: Val---Ile) in extended pedigrees with early onset Alzheimer's disease. *Neurosci Lett*, *129*(1), 134-135. Retrieved from <http://www.ncbi.nlm.nih.gov/pubmed/1922963>
- Chartier-Harlin, M. C., Crawford, F., Houlden, H., Warren, A., Hughes, D., Fidani, L., . . . et al. (1991). Early-onset Alzheimer's disease caused by mutations at codon 717 of the beta-amyloid precursor protein gene. *Nature*, *353*(6347), 844-846. doi:10.1038/353844a0
- Chen, W. J., Goldstein, J. L., & Brown, M. S. (1990). NPXY, a sequence often found in cytoplasmic tails, is required for coated pit-mediated internalization of the low density lipoprotein receptor. *J Biol Chem*, *265*(6), 3116-3123.
- Cheret, C., Willem, M., Fricker, F. R., Wende, H., Wulf-Goldenberg, A., Tahirovic, S., . . . Birchmeier, C. (2013). Bace1 and Neuregulin-1 cooperate to control formation and maintenance of muscle spindles. *EMBO J*, *32*(14), 2015-2028. doi:10.1038/emboj.2013.146
- Chow, C. Y., Landers, J. E., Bergren, S. K., Sapp, P. C., Grant, A. E., Jones, J. M., . . . Meisler, M. H. (2009). Deleterious variants of FIG4, a phosphoinositide phosphatase, in patients with ALS. *Am J Hum Genet*, *84*(1), 85-88. doi:10.1016/j.ajhg.2008.12.010
- Chow, C. Y., Zhang, Y., Dowling, J. J., Jin, N., Adamska, M., Shiga, K., . . . Meisler, M. H. (2007). Mutation of FIG4 causes neurodegeneration in the pale tremor mouse and patients with CMT4J. *Nature*, *448*(7149), 68-72. doi:10.1038/nature05876
- Clarris, H. J., Cappai, R., Heffernan, D., Beyreuther, K., Masters, C. L., & Small, D. H. (1997). Identification of heparin-binding domains in the amyloid precursor protein of Alzheimer's disease by deletion mutagenesis and peptide mapping. *J Neurochem*, *68*(3), 1164-1172. Retrieved from <http://www.ncbi.nlm.nih.gov/pubmed/9048763>
- Colvin, R. A., Means, T. K., Diefenbach, T. J., Moita, L. F., Friday, R. P., Sever, S., . . . Luster,

- A. D. (2010). Synaptotagmin-mediated vesicle fusion regulates cell migration. *Nat Immunol*, 11(6), 495-502.
doi:http://www.nature.com/nijournal/v11/n6/supinfo/ni.1878_S1.html
- Cooke, F. T., Dove, S. K., McEwen, R. K., Painter, G., Holmes, A. B., Hall, M. N., . . . Parker, P. J. (1998). The stress-activated phosphatidylinositol 3-phosphate 5-kinase Fab1p is essential for vacuole function in *S. cerevisiae*. *Curr Biol*, 8(22), 1219-1222. Retrieved from <http://www.ncbi.nlm.nih.gov/pubmed/9811604>
- Corder, E. H., & Woodbury, M. A. (1993). Genetic heterogeneity in Alzheimer's disease: a grade of membership analysis. *Genet Epidemiol*, 10(6), 495-499.
doi:10.1002/gepi.1370100628
- Crawford, F., Hardy, J., Mullan, M., Goate, A., Hughes, D., Fidani, L., . . . Chartier-Harlin, M. C. (1991). Sequencing of exons 16 and 17 of the beta-amyloid precursor protein gene in 14 families with early onset Alzheimer's disease fails to reveal mutations in the beta-amyloid sequence. *Neurosci Lett*, 133(1), 1-2. Retrieved from <http://www.ncbi.nlm.nih.gov/pubmed/1791986>
- Cremona, O., Di Paolo, G., Wenk, M. R., Luthi, A., Kim, W. T., Takei, K., . . . De Camilli, P. (1999). Essential role of phosphoinositide metabolism in synaptic vesicle recycling. *Cell*, 99(2), 179-188. Retrieved from <http://www.ncbi.nlm.nih.gov/pubmed/10535736>
- Crews, L., Rockenstein, E., Masliah, E. (2010). APP transgenic modeling of Alzheimer's disease: mechanisms of neurodegeneration and aberrant neurogenesis. *Brain Struct Funct.*, 214(2-3), 111-126.
- Cui, H., Kong, Y., & Zhang, H. (2012). Oxidative stress, mitochondrial dysfunction, and aging. *J Signal Transduct*, 2012, 646354. doi:10.1155/2012/646354
- Cullen, P. J., Cozier, G. E., Banting, G., & Mellor, H. (2001). Modular phosphoinositide-binding domains--their role in signalling and membrane trafficking. *Curr Biol*, 11(21), R882-893.
- Cunningham, J. T., Rodgers, J. T., Arlow, D. H., Vazquez, F., Mootha, V. K., & Puigserver, P. (2007). mTOR controls mitochondrial oxidative function through a YY1-PGC-1alpha transcriptional complex. *Nature*, 450(7170), 736-740. doi:10.1038/nature06322
- Cupers, P., Orlans, I., Craessaerts, K., Annaert, W., & De Strooper, B. (2001). The amyloid precursor protein (APP)-cytoplasmic fragment generated by γ -secretase is rapidly degraded but distributes partially in a nuclear fraction of neurones in culture. *Journal of Neurochemistry*, 78(5), 1168-1178. doi:10.1046/j.1471-4159.2001.00516.x
- Currinn, H., Guscott, B., Balklava, Z., Rothnie, A., & Wassmer, T. (2016). APP controls the formation of PI(3,5)P(2) vesicles through its binding of the PIKfyve complex. *Cellular and Molecular Life Sciences*, 73, 393-408. doi:10.1007/s00018-015-1993-0
- Czibener, C., Sherer, N. M., Becker, S. M., Pypaert, M., Hui, E., Chapman, E. R., . . . Andrews, N. W. (2006). Ca²⁺ and synaptotagmin VII-dependent delivery of lysosomal membrane to nascent phagosomes. *J Cell Biol*, 174(7), 997-1007.
doi:10.1083/jcb.200605004
- Dahms, S. O., Konnig, I., Roeser, D., Guhrs, K. H., Mayer, M. C., Kaden, D., . . . Than, M. E. (2012). Metal binding dictates conformation and function of the amyloid precursor protein (APP) E2 domain. *J Mol Biol*, 416(3), 438-452. doi:10.1016/j.jmb.2011.12.057
- Daigle, I., & Li, C. (1993). apl-1, a *Caenorhabditis elegans* gene encoding a protein related to the human beta-amyloid protein precursor. *Proc Natl Acad Sci U S A*, 90(24), 12045-12049. Retrieved from <http://www.ncbi.nlm.nih.gov/pubmed/8265668>
- Daly, M. E., Vale, C., Walker, M., Littlefield, A., Alberti, K. G., & Mathers, J. C. (1998). Acute effects on insulin sensitivity and diurnal metabolic profiles of a high-sucrose compared with a high-starch diet. *Am J Clin Nutr*, 67(6), 1186-1196.
- Dautry-Varsat, A., Ciechanover, A., & Lodish, H. F. (1983). pH and the recycling of transferrin during receptor-mediated endocytosis. *Proc Natl Acad Sci U S A*, 80(8), 2258-2262. Retrieved from <http://www.ncbi.nlm.nih.gov/pubmed/6300903>
- de la Monte, S. M., Hutchins, G. M., & Moore, G. W. (1989). Racial differences in the etiology of dementia and frequency of Alzheimer lesions in the brain. *J Natl Med Assoc*, 81(6), 644-652. Retrieved from <http://www.ncbi.nlm.nih.gov/pubmed/2746686>
- de la Monte, S. M., Wells, S. E., Hedley-Whyte, T., & Growdon, J. H. (1989). Neuropathological distinction between Parkinson's dementia and Parkinson's plus Alzheimer's disease. *Ann Neurol*, 26(3), 309-320. doi:10.1002/ana.410260302

- de Lartigue, J., Polson, H., Feldman, M., Shokat, K., Tooze, S. A., Urbe, S., & Clague, M. J. (2009). PIKfyve regulation of endosome-linked pathways. *Traffic*, *10*(7), 883-893.
- Del Villar, K., & Miller, C. A. (2004). Down-regulation of DENN/MADD, a TNF receptor binding protein, correlates with neuronal cell death in Alzheimer's disease brain and hippocampal neurons. *Proc Natl Acad Sci U S A*, *101*(12), 4210-4215. doi:10.1073/pnas.0307349101
- Derossi, D., Joliot, A. H., Chassaing, G., & Prochiantz, A. (1994). The third helix of the Antennapedia homeodomain translocates through biological membranes. *J Biol Chem*, *269*(14), 10444-10450.
- Devereaux, K., Dall'Armi, C., Alcazar-Roman, A., Ogasawara, Y., Zhou, X., Wang, F., . . . Di Paolo, G. (2013). Regulation of mammalian autophagy by class II and III PI 3-kinases through PI3P synthesis. *PLoS One*, *8*(10), e76405. doi:10.1371/journal.pone.0076405
- Di Paolo, G., & De Camilli, P. (2006). Phosphoinositides in cell regulation and membrane dynamics. *Nature*, *443*(7112), 651-657. Retrieved from <http://dx.doi.org/10.1038/nature05185>
- Djinovic-Carugo, K., Gautel, M., Ylanne, J., & Young, P. (2002). The spectrin repeat: a structural platform for cytoskeletal protein assemblies. *FEBS Lett*, *513*(1), 119-123. Retrieved from <http://www.ncbi.nlm.nih.gov/pubmed/11911890>
- Dong, X. P., Shen, D., Wang, X., Dawson, T., Li, X., Zhang, Q., . . . Xu, H. (2010). PI(3,5)P(2) controls membrane trafficking by direct activation of mucolipin Ca(2+) release channels in the endolysosome. *Nat Commun*, *1*, 38. doi:10.1038/ncomms1037
- Doody, R. S., Raman, R., Farlow, M., Iwatsubo, T., Vellas, B., Joffe, S., . . . Mohs, R. (2013). A phase 3 trial of semagacestat for treatment of Alzheimer's disease. *N Engl J Med*, *369*(4), 341-350. doi:10.1056/NEJMoa1210951
- Dos, D. S., Ali, S. M., Kim, D.-H., Guertin, D. A., Latek, R. R., Erdjument-Bromage, H., . . . Sabatini, D. M. (2004). Rictor, a Novel Binding Partner of mTOR, Defines a Rapamycin-Insensitive and Raptor-Independent Pathway that Regulates the Cytoskeleton. *Current Biology*, *14*(14), 1296-1302. doi:10.1016/j.cub.2004.06.054
- Dou, Y., Wu, H. J., Li, H. Q., Qin, S., Wang, Y. E., Li, J., . . . Duan, S. (2012). Microglial migration mediated by ATP-induced ATP release from lysosomes. *Cell Res*, *22*(6), 1022-1033. doi:10.1038/cr.2012.10
- Dove, S. K., Cooke, F. T., Douglas, M. R., Sayers, L. G., Parker, P. J., & Michell, R. H. (1997). Osmotic stress activates phosphatidylinositol-3,5-bisphosphate synthesis. *Nature*, *390*(6656), 187-192. Retrieved from <http://dx.doi.org/10.1038/36613>
- Dove, S. K., McEwen, R. K., Mayes, A., Hughes, D. C., Beggs, J. D., & Michell, R. H. (2002). Vac14 controls PtdIns(3,5)P(2) synthesis and Fab1-dependent protein trafficking to the multivesicular body. *Curr Biol*, *12*(11), 885-893. Retrieved from <http://www.ncbi.nlm.nih.gov/pubmed/12062051>
- Dowler, S., Currie, R. A., Campbell, D. G., Deak, M., Kular, G., Downes, C. P., & Alessi, D. R. (2000). Identification of pleckstrin-homology-domain-containing proteins with novel phosphoinositide-binding specificities. *Biochem J*, *351*(Pt 1), 19-31. Retrieved from <http://www.ncbi.nlm.nih.gov/pubmed/11001876>
- Duchardt, F., Fotin-Mleczek, M., Schwarz, H., Fischer, R., & Brock, R. (2007). A comprehensive model for the cellular uptake of cationic cell-penetrating peptides. *Traffic*, *8*(7), 848-866. doi:10.1111/j.1600-0854.2007.00572.x
- Dulbecco, R., & Freeman, G. (1959). Plaque production by the polyoma virus. *Virology*, *8*(3), 396-397.
- Duriez, B., Duquesnoy, P., Escudier, E., Bridoux, A. M., Escalier, D., Rayet, I., . . . Amselem, S. (2007). A common variant in combination with a nonsense mutation in a member of the thioredoxin family causes primary ciliary dyskinesia. *Proc Natl Acad Sci U S A*, *104*(9), 3336-3341. doi:10.1073/pnas.0611405104
- Ehninger, D., Neff, F., & Xie, K. (2014). Longevity, aging and rapamycin. *Cell Mol Life Sci*, *71*(22), 4325-4346. doi:10.1007/s00018-014-1677-1
- Elabscience Biotechnology. (2015) APLP1 polyclonal antibody EAP2000. Retrieved from <http://www.elabscience.com/Manual/Antibody/EAP2000.pdf>
- Ellson, C. D., Gobert-Gosse, S., Anderson, K. E., Davidson, K., Erdjument-Bromage, H., Tempst, P., . . . Stephens, L. R. (2001). PtdIns(3)P regulates the neutrophil oxidase complex by binding to the PX domain of p40(phox). *Nat Cell Biol*, *3*(7), 679-682. doi:10.1038/35083076

- Ezhevsky, S. A., Nagahara, H., Vocero-Akbani, A. M., Gius, D. R., Wei, M. C., & Dowdy, S. F. (1997). Hypo-phosphorylation of the retinoblastoma protein (pRb) by cyclin D:Cdk4/6 complexes results in active pRb. *Proceedings of the National Academy of Sciences of the United States of America*, *94*(20), 10699-10704. Retrieved from <http://www.ncbi.nlm.nih.gov/pmc/articles/PMC23451/>
- Facchinetti, V., Ouyang, W., Wei, H., Soto, N., Lazorchak, A., Gould, C., . . . Jacinto, E. (2008). The mammalian target of rapamycin complex 2 controls folding and stability of Akt and protein kinase C. *EMBO J*, *27*(14), 1932-1943. doi:10.1038/emboj.2008.120
- Ferguson, S. S., Barak, L. S., Zhang, J., & Caron, M. G. (1996). G-protein-coupled receptor regulation: role of G-protein-coupled receptor kinases and arrestins. *Can J Physiol Pharmacol*, *74*(10), 1095-1110.
- Fidani, L., Rooke, K., Chartier-Harlin, M. C., Hughes, D., Tanzi, R., Mullan, M., . . . Goate, A. (1992). Screening for mutations in the open reading frame and promoter of the beta-amyloid precursor protein gene in familial Alzheimer's disease: identification of a further family with APP717 Val-->Ile. *Hum Mol Genet*, *1*(3), 165-168. Retrieved from <http://www.ncbi.nlm.nih.gov/pubmed/1303172>
- Folch, J., Petrov, D., Ettcheto, M., Pedros, I., Abad, S., Beas-Zarate, C., . . . Camins, A. (2015). Masitinib for the treatment of mild to moderate Alzheimer's disease. *Expert Rev Neurother*, *15*(6), 587-596. doi:10.1586/14737175.2015.1045419
- Fonseca, B. D., Diering, G. H., Bidinosti, M. A., Dalal, K., Alain, T., Balgi, A. D., . . . Roberge, M. (2012). Structure-Activity Analysis of Niclosamide Reveals Potential Role for Cytoplasmic pH in Control of Mammalian Target of Rapamycin Complex 1 (mTORC1) Signaling. *The Journal of Biological Chemistry*, *287*(21), 17530-17545. doi:10.1074/jbc.M112.359638
- Franke, T. F., Kaplan, D. R., Cantley, L. C., & Toker, A. (1997). Direct regulation of the Akt proto-oncogene product by phosphatidylinositol-3,4-bisphosphate. *Science*, *275*(5300), 665-668. Retrieved from <http://www.ncbi.nlm.nih.gov/pubmed/9005852>
- Frankel, A. D., & Pabo, C. O. (1988). Cellular uptake of the tat protein from human immunodeficiency virus. *Cell*, *55*(6), 1189-1193. doi:10.1016/0092-8674(88)90263-2
- French, P. J., Bijman, J., Bot, A. G., Boomaars, W. E., Scholte, B. J., & de Jonge, H. R. (1997). Genistein activates CFTR Cl⁻ channels via a tyrosine kinase- and protein phosphatase-independent mechanism. *Am J Physiol*, *273*(2 Pt 1), C747-753. Retrieved from <http://www.ncbi.nlm.nih.gov/pubmed/9277373>
- Fujita, N., Itoh, T., Omori, H., Fukuda, M., Noda, T., & Yoshimori, T. (2008). The Atg16L complex specifies the site of LC3 lipidation for membrane biogenesis in autophagy. *Mol Biol Cell*, *19*(5), 2092-2100. doi:10.1091/mbc.E07-12-1257
- Funderburk, S. F., Wang, Q. J., & Yue, Z. (2010). The Beclin 1-VPS34 complex--at the crossroads of autophagy and beyond. *Trends Cell Biol*, *20*(6), 355-362. doi:10.1016/j.tcb.2010.03.002
- Funk, K. E., Mrak, R. E., & Kuret, J. (2011). Granulovacuolar Degeneration Bodies of Alzheimer's Disease Resemble Late-stage Autophagic Organelles. *Neuropathology and applied neurobiology*, *37*(3), 295-306. doi:10.1111/j.1365-2990.2010.01135.x
- Futter, C. E., Collinson, L. M., Backer, J. M., & Hopkins, C. R. (2001). Human VPS34 is required for internal vesicle formation within multivesicular endosomes. *The Journal of Cell Biology*, *155*(7), 1251-1264. doi:10.1083/jcb.200108152
- Gallo, J. M., & Spickett, C. (2010). The role of CELF proteins in neurological disorders. *RNA Biol*, *7*(4), 474-479. Retrieved from <http://www.ncbi.nlm.nih.gov/pubmed/20622515>
- Ganley, I. G., Lam du, H., Wang, J., Ding, X., Chen, S., & Jiang, X. (2009). ULK1.ATG13.FIP200 complex mediates mTOR signaling and is essential for autophagy. *J Biol Chem*, *284*(18), 12297-12305. doi:10.1074/jbc.M900573200
- Garami, A., Zwartkruis, F. J., Nobukuni, T., Joaquin, M., Rocco, M., Stocker, H., . . . Thomas, G. (2003). Insulin activation of Rheb, a mediator of mTOR/S6K/4E-BP signaling, is inhibited by TSC1 and 2. *Mol Cell*, *11*(6), 1457-1466. Retrieved from <http://www.ncbi.nlm.nih.gov/pubmed/12820960>
- Garcia, P., Gupta, R., Shah, S., Morris, A. J., Rudge, S. A., Scarlata, S., . . . Rebecchi, M. J. (1995). The pleckstrin homology domain of phospholipase C-delta 1 binds with high affinity to phosphatidylinositol 4,5-bisphosphate in bilayer membranes. *Biochemistry*, *34*(49), 16228-16234. Retrieved from <http://www.ncbi.nlm.nih.gov/pubmed/8519781>

- Garcia-Martinez, J. M., & Alessi, D. R. (2008). mTOR complex 2 (mTORC2) controls hydrophobic motif phosphorylation and activation of serum- and glucocorticoid-induced protein kinase 1 (SGK1). *Biochem J*, *416*(3), 375-385. doi:10.1042/BJ20081668
- Gardella, J. E., Ghiso, J., Gorgone, G. A., Marratta, D., Kaplan, A. P., Frangione, B., & Gorevic, P. D. (1990). Intact Alzheimer amyloid precursor protein (APP) is present in platelet membranes and is encoded by platelet mRNA. *Biochem Biophys Res Commun*, *173*(3), 1292-1298. Retrieved from <http://www.ncbi.nlm.nih.gov/pubmed/1702629>
- Garelick, M. G., & Kennedy, B. K. (2011). TOR on the Brain. *Experimental gerontology*, *46*(2-3), 155-163. doi:10.1016/j.exger.2010.08.030
- Garrett, M. D., Zahner, J. E., Cheney, C. M., & Novick, P. J. (1994). GDI1 encodes a GDP dissociation inhibitor that plays an essential role in the yeast secretory pathway. *EMBO J*, *13*(7), 1718-1728. Retrieved from <http://www.ncbi.nlm.nih.gov/pubmed/8157010>
- Gary, J. D., Wurmser, A. E., Bonangelino, C. J., Weisman, L. S., & Emr, S. D. (1998). Fab1p is essential for PtdIns(3)P 5-kinase activity and the maintenance of vacuolar size and membrane homeostasis. *J Cell Biol*, *143*(1), 65-79.
- Gaullier, J. M., Simonsen, A., D'Arrigo, A., Bremnes, B., Stenmark, H., & Aasland, R. (1998). FYVE fingers bind PtdIns(3)P. *Nature*, *394*(6692), 432-433. doi:10.1038/28767
- Geng, J., & Klionsky, D. J. (2008). The Atg8 and Atg12 ubiquitin-like conjugation systems in macroautophagy. 'Protein modifications: beyond the usual suspects' review series. *EMBO Rep*, *9*(9), 859-864. doi:10.1038/embor.2008.163
- GeneTex. (2013) APLP1 antibody GTX30055. Retrieved from <http://www.genetex.com/APLP1-antibody-GTX30055.html>
- Georgakopoulos, A., Litterst, C., Ghersi, E., Baki, L., Xu, C., Serban, G., & Robakis, N. K. (2006). Metalloproteinase/Presenilin1 processing of ephrinB regulates EphB-induced Src phosphorylation and signaling. *EMBO J*, *25*(6), 1242-1252. doi:10.1038/sj.emboj.7601031
- Gertz, H. J., Xuereb, J., Huppert, F., Brayne, C., McGee, M. A., Paykel, E., . . . Wischik, C. M. (1998). Examination of the validity of the hierarchical model of neuropathological staging in normal aging and Alzheimer's disease. *Acta Neuropathol*, *95*(2), 154-158. Retrieved from <http://www.ncbi.nlm.nih.gov/pubmed/9498050>
- Ghosal, K., Vogt, D. L., Liang, M., Shen, Y., Lamb, B. T., & Pimplikar, S. W. (2009). Alzheimer's disease-like pathological features in transgenic mice expressing the APP intracellular domain. *Proc Natl Acad Sci U S A*, *106*(43), 18367-18372. doi:10.1073/pnas.0907652106
- Gillooly, D. J., Morrow, I. C., Lindsay, M., Gould, R., Bryant, N. J., Gaullier, J. M., . . . Stenmark, H. (2000). Localization of phosphatidylinositol 3-phosphate in yeast and mammalian cells. *EMBO J*, *19*(17), 4577-4588. doi:10.1093/emboj/19.17.4577
- Gingras, A. C., Raught, B., & Sonenberg, N. (2001). Control of translation by the target of rapamycin proteins. *Prog Mol Subcell Biol*, *27*, 143-174. Retrieved from <http://www.ncbi.nlm.nih.gov/pubmed/11575159>
- Glick, D., Barth, S., & Macleod, K. F. (2010). Autophagy: cellular and molecular mechanisms. *J Pathol*, *221*(1), 3-12. doi:10.1002/path.2697
- Goate, A., Chartier-Harlin, M. C., Mullan, M., Brown, J., Crawford, F., Fidani, L., . . . et al. (1991). Segregation of a missense mutation in the amyloid precursor protein gene with familial Alzheimer's disease. *Nature*, *349*(6311), 704-706. doi:10.1038/349704a0
- Goedert, M., Wischik, C. M., Crowther, R. A., Walker, J. E., & Klug, A. (1988). Cloning and sequencing of the cDNA encoding a core protein of the paired helical filament of Alzheimer disease: identification as the microtubule-associated protein tau. *Proc Natl Acad Sci U S A*, *85*(11), 4051-4055. Retrieved from <http://www.ncbi.nlm.nih.gov/pubmed/3131773>
- Goodman, Y., Steiner, M. R., Steiner, S. M., & Mattson, M. P. (1994). Nordihydroguaiaretic acid protects hippocampal neurons against amyloid beta-peptide toxicity, and attenuates free radical and calcium accumulation. *Brain Res*, *654*(1), 171-176. Retrieved from <http://www.ncbi.nlm.nih.gov/pubmed/7982093>
- Gozani, O., Karuman, P., Jones, D. R., Ivanov, D., Cha, J., Lugovskoy, A. A., . . . Yuan, J. (2003). The PHD finger of the chromatin-associated protein ING2 functions as a nuclear phosphoinositide receptor. *Cell*, *114*(1), 99-111. Retrieved from <http://www.ncbi.nlm.nih.gov/pubmed/12859901>
- Green, M., & Loewenstein, P. M. (1988). Autonomous functional domains of chemically

- synthesized human immunodeficiency virus tat trans-activator protein. *Cell*, 55(6), 1179-1188. doi:[http://dx.doi.org/10.1016/0092-8674\(88\)90262-0](http://dx.doi.org/10.1016/0092-8674(88)90262-0)
- Groll, M., & Huber, R. (2003). Substrate access and processing by the 20S proteasome core particle. *Int J Biochem Cell Biol*, 35(5), 606-616. Retrieved from <http://www.ncbi.nlm.nih.gov/pubmed/12672453>
- Grosshans, B. L., Ortiz, D., & Novick, P. (2006). Rabs and their effectors: achieving specificity in membrane traffic. *Proc Natl Acad Sci U S A*, 103(32), 11821-11827. doi:10.1073/pnas.0601617103
- Gruenberg, J., & Stenmark, H. (2004). The biogenesis of multivesicular endosomes. *Nat Rev Mol Cell Biol*, 5(4), 317-323. doi:10.1038/nrm1360
- Guerreiro, R., Wojtas, A., Bras, J., Carrasquillo, M., Rogaeva, E., Majounie, E., . . . Alzheimer Genetic Analysis, G. (2013). TREM2 variants in Alzheimer's disease. *N Engl J Med*, 368(2), 117-127. doi:10.1056/NEJMoa1211851
- Guertin, D. A., Stevens, D. M., Thoreen, C. C., Burds, A. A., Kalaany, N. Y., Moffat, J., . . . Sabatini, D. M. (2006). Ablation in mice of the mTORC components raptor, rictor, or mLST8 reveals that mTORC2 is required for signaling to Akt-FOXO and PKCalpha, but not S6K1. *Dev Cell*, 11(6), 859-871. doi:10.1016/j.devcel.2006.10.007
- Guscott, B., Balklava, Z., Safrany, S. T., & Wassmer, T. (2016). A cell-permeable tool for analysing APP intracellular domain function and manipulation of PIKfyve activity. *Bioscience Reports*. doi:10.1042/bsr20160040
- Guterstam, P., Madani, F., Hirose, H., Takeuchi, T., Futaki, S., El Andaloussi, S., . . . Langel, U. (2009). Elucidating cell-penetrating peptide mechanisms of action for membrane interaction, cellular uptake, and translocation utilizing the hydrophobic counter-anion pyrenebutyrate. *Biochim Biophys Acta*, 1788(12), 2509-2517. doi:10.1016/j.bbamem.2009.09.014
- Hailey, D. W., Rambold, A. S., Satpute-Krishnan, P., Mitra, K., Sougrat, R., Kim, P. K., & Lippincott-Schwartz, J. (2010). Mitochondria supply membranes for autophagosome biogenesis during starvation. *Cell*, 141(4), 656-667. doi:10.1016/j.cell.2010.04.009
- Halet, G. (2005). Imaging phosphoinositide dynamics using GFP-tagged protein domains. *Biol Cell*, 97(7), 501-518. doi:10.1042/BC20040080
- Hanada, T., Noda, N. N., Satomi, Y., Ichimura, Y., Fujioka, Y., Takao, T., . . . Ohsumi, Y. (2007). The Atg12-Atg5 conjugate has a novel E3-like activity for protein lipidation in autophagy. *J Biol Chem*, 282(52), 37298-37302. doi:10.1074/jbc.C700195200
- Hanahan, D., & Weinberg, R. A. (2011). Hallmarks of cancer: the next generation. *Cell*, 144(5), 646-674. doi:10.1016/j.cell.2011.02.013
- Hansen, M., Chandra, A., Mitic, L. L., Onken, B., Driscoll, M., & Kenyon, C. (2008). A role for autophagy in the extension of lifespan by dietary restriction in *C. elegans*. *PLoS Genet*, 4(2), e24. doi:10.1371/journal.pgen.0040024
- Hansen, M., Taubert, S., Crawford, D., Libina, N., Lee, S. J., & Kenyon, C. (2007). Lifespan extension by conditions that inhibit translation in *Caenorhabditis elegans*. *Aging Cell*, 6(1), 95-110. doi:10.1111/j.1474-9726.2006.00267.x
- Hara, K., Maruki, Y., Long, X., Yoshino, K., Oshiro, N., Hidayat, S., . . . Yonezawa, K. (2002). Raptor, a binding partner of target of rapamycin (TOR), mediates TOR action. *Cell*, 110(2), 177-189. Retrieved from <http://www.ncbi.nlm.nih.gov/pubmed/12150926>
- Hara, K., Yonezawa, K., Weng, Q. P., Kozlowski, M. T., Belham, C., & Avruch, J. (1998). Amino acid sufficiency and mTOR regulate p70 S6 kinase and eIF-4E BP1 through a common effector mechanism. *J Biol Chem*, 273(23), 14484-14494.
- Hardy, J., & Allsop, D. (1991). Amyloid deposition as the central event in the aetiology of Alzheimer's disease. *Trends Pharmacol Sci*, 12(10), 383-388. Retrieved from <http://www.ncbi.nlm.nih.gov/pubmed/1763432>
- Hardy, J., & Higgins, G. (1992). Alzheimer's disease: the amyloid cascade hypothesis. *Science*, 256(5054), 184-185. doi:10.1126/science.1566067
- Harold, D., Abraham, R., Hollingworth, P., Sims, R., Gerrish, A., Hamshere, M. L., . . . Williams, J. (2009). Genome-wide association study identifies variants at CLU and PICALM associated with Alzheimer's disease. *Nat Genet*, 41(10), 1088-1093. doi:10.1038/ng.440
- Harrison, D. E., Strong, R., Sharp, Z. D., Nelson, J. F., Astle, C. M., Flurkey, K., . . . Miller, R. A. (2009). Rapamycin fed late in life extends lifespan in genetically heterogeneous mice.

- Nature*, 460(7253), 392-395. doi:10.1038/nature08221
- Hayashi-Nishino, M., Fujita, N., Noda, T., Yamaguchi, A., Yoshimori, T., & Yamamoto, A. (2009). A subdomain of the endoplasmic reticulum forms a cradle for autophagosome formation. *Nat Cell Biol*, 11(12), 1433-1437. doi:10.1038/ncb1991
- He, F., Umehara, T., Saito, K., Harada, T., Watanabe, S., Yabuki, T., . . . Muto, Y. (2010). Structural insight into the zinc finger CW domain as a histone modification reader. *Structure*, 18(9), 1127-1139. doi:10.1016/j.str.2010.06.012
- Heber, S., Herms, J., Gajic, V., Hainfellner, J., Aguzzi, A., Rulicke, T., . . . Muller, U. (2000). Mice with combined gene knock-outs reveal essential and partially redundant functions of amyloid precursor protein family members. *J Neurosci*, 20(21), 7951-7963.
- Heitman, J., Movva, N. R., & Hall, M. N. (1991). Targets for cell cycle arrest by the immunosuppressant rapamycin in yeast. *Science*, 253(5022), 905-909.
- Henley, D. B., Sundell, K. L., Sethuraman, G., Dowsett, S. A., & May, P. C. (2014). Safety profile of semagacestat, a gamma-secretase inhibitor: IDENTITY trial findings. *Current Medical Research and Opinion*, 30(10), 2021-2032. doi:10.1185/03007995.2014.939167
- Henne, W. M., Boucrot, E., Meinecke, M., Evergren, E., Vallis, Y., Mittal, R., & McMahon, H. T. (2010). FCHO proteins are nucleators of clathrin-mediated endocytosis. *Science*, 328(5983), 1281-1284. doi:10.1126/science.1188462
- Ho, C. Y., Choy, C. H., Wattson, C. A., Johnson, D. E., & Botelho, R. J. (2015). The Fab1/PIKfyve phosphoinositide phosphate kinase is not necessary to maintain the pH of lysosomes and of the yeast vacuole. *J Biol Chem*, 290(15), 9919-9928. doi:10.1074/jbc.M114.613984
- Hoefgen, S., Coburger, I., Roeser, D., Schaub, Y., Dahms, S. O., & Than, M. E. (2014). Heparin induced dimerization of APP is primarily mediated by E1 and regulated by its acidic domain. *Journal of Structural Biology*, 187(1), 30-37. doi:http://dx.doi.org/10.1016/j.jsb.2014.05.006
- Hoefgen, S., Dahms, S. O., Oertwig, K., & Than, M. E. (2015). The amyloid precursor protein shows a pH-dependent conformational switch in its E1 domain. *J Mol Biol*, 427(2), 433-442. doi:10.1016/j.jmb.2014.12.005
- Holliday, L. S. (2014). Vacuolar H⁺-ATPase: An Essential Multitasking Enzyme in Physiology and Pathophysiology. *New Journal of Science*, 2014, 21. doi:10.1155/2014/675430
- Holling, T. M., Schooten, E., & van Den Elsen, P. J. (2004). Function and regulation of MHC class II molecules in T-lymphocytes: of mice and men. *Hum Immunol*, 65(4), 282-290. doi:10.1016/j.humimm.2004.01.005
- Hollingworth, P., Harold, D., Sims, R., Gerrish, A., Lambert, J. C., Carrasquillo, M. M., . . . Williams, J. (2011). Common variants at ABCA7, MS4A6A/MS4A4E, EPHA1, CD33 and CD2AP are associated with Alzheimer's disease. *Nat Genet*, 43(5), 429-435. doi:10.1038/ng.803
- Holmes, C., Boche, D., Wilkinson, D., Yadegarfar, G., Hopkins, V., Bayer, A., . . . Nicoll, J. A. (2008). Long-term effects of Abeta42 immunisation in Alzheimer's disease: follow-up of a randomised, placebo-controlled phase I trial. *Lancet*, 372(9634), 216-223. doi:10.1016/S0140-6736(08)61075-2
- Hosokawa, N., Hara, T., Kaizuka, T., Kishi, C., Takamura, A., Miura, Y., . . . Mizushima, N. (2009). Nutrient-dependent mTORC1 association with the ULK1-Atg13-FIP200 complex required for autophagy. *Mol Biol Cell*, 20(7), 1981-1991. doi:10.1091/mbc.E08-12-1248
- Hubner, N. C., & Mann, M. (2011). Extracting gene function from protein-protein interactions using Quantitative BAC InteraCtomics (QUBIC). *Methods*, 53(4), 453-459. doi:10.1016/j.ymeth.2010.12.016
- Huotari, J., & Helenius, A. (2011). Endosome maturation. *EMBO J*, 30(17), 3481-3500. doi:10.1038/emboj.2011.286
- Iida, K., Mornaghi, R., & Nussenzweig, V. (1982). Complement receptor (CR1) deficiency in erythrocytes from patients with systemic lupus erythematosus. *J Exp Med*, 155(5), 1427-1438.
- Ikenoue, T., Inoki, K., Yang, Q., Zhou, X., & Guan, K. L. (2008). Essential function of TORC2 in PKC and Akt turn motif phosphorylation, maturation and signalling. *EMBO J*, 27(14), 1919-1931. doi:10.1038/emboj.2008.119
- Ikonomov, O. C., Fligger, J., Sbrissa, D., Dondapati, R., Mlak, K., Deeb, R., & Shisheva, A. (2009). Kinesin adapter JLP links PIKfyve to microtubule-based endosome-to-trans-Golgi

- network traffic of furin. *J Biol Chem*, 284(6), 3750-3761. doi:10.1074/jbc.M806539200
- Ikonomov, O. C., Sbrissa, D., Mlak, K., Deeb, R., Fligger, J., Soans, A., . . . Shisheva, A. (2003). Active PIKfyve associates with and promotes the membrane attachment of the late endosome-to-trans-Golgi network transport factor Rab9 effector p40. *J Biol Chem*, 278(51), 50863-50871. doi:10.1074/jbc.M307260200
- Ikonomov, O. C., Sbrissa, D., Mlak, K., Kanzaki, M., Pessin, J., & Shisheva, A. (2002). Functional dissection of lipid and protein kinase signals of PIKfyve reveals the role of PtdIns 3,5-P2 production for endomembrane integrity. *J Biol Chem*, 277(11), 9206-9211. doi:10.1074/jbc.M108750200
- Itoh, T., & De Camilli, P. (2006). BAR, F-BAR (EFC) and ENTH/ANTH domains in the regulation of membrane-cytosol interfaces and membrane curvature. *Biochim Biophys Acta*, 1761(8), 897-912. doi:10.1016/j.bbali.2006.06.015
- Itoh, T., & Takenawa, T. (2002). Phosphoinositide-binding domains: Functional units for temporal and spatial regulation of intracellular signalling. *Cell Signal*, 14(9), 733-743.
- Iwatsubo, T. (2004). The gamma-secretase complex: machinery for intramembrane proteolysis. *Curr Opin Neurobiol*, 14(3), 379-383. doi:10.1016/j.conb.2004.05.010
- Iwatsubo, T. (2004). [Pathogenesis of Alzheimer's disease: implications from amyloid research front]. *Rinsho Shinkeigaku*, 44(11), 768-770. Retrieved from <http://www.ncbi.nlm.nih.gov/pubmed/15651286>
- Jacinto, E., Loewith, R., Schmidt, A., Lin, S., Rugg, M. A., Hall, A., & Hall, M. N. (2004). Mammalian TOR complex 2 controls the actin cytoskeleton and is rapamycin insensitive. *Nat Cell Biol*, 6(11), 1122-1128. doi:10.1038/ncb1183
- Jahn, R., & Scheller, R. H. (2006). SNAREs--engines for membrane fusion. *Nat Rev Mol Cell Biol*, 7(9), 631-643. doi:10.1038/nrm2002
- Janzen, V., Forkert, R., Fleming, H. E., Saito, Y., Waring, M. T., Dombkowski, D. M., . . . Scadden, D. T. (2006). Stem-cell ageing modified by the cyclin-dependent kinase inhibitor p16INK4a. *Nature*, 443(7110), 421-426. doi:10.1038/nature05159
- Jefferies, H. B., Cooke, F. T., Jat, P., Boucheron, C., Koizumi, T., Hayakawa, M., . . . Parker, P. J. (2008). A selective PIKfyve inhibitor blocks PtdIns(3,5)P(2) production and disrupts endomembrane transport and retroviral budding. *EMBO Rep*, 9(2), 164-170. doi:10.1038/sj.embor.7401155
- Jia, K., Chen, D., & Riddle, D. L. (2004). The TOR pathway interacts with the insulin signaling pathway to regulate *C. elegans* larval development, metabolism and life span. *Development*, 131(16), 3897-3906. doi:10.1242/dev.01255
- Jiang, L., Zhong, J., Dou, X., Cheng, C., Huang, Z., & Sun, X. (2015). Effects of ApoE on intracellular calcium levels and apoptosis of neurons after mechanical injury. *Neuroscience*, 301, 375-383. doi:10.1016/j.neuroscience.2015.06.005
- Jiao, C. Y., Delarochette, D., Burlina, F., Alves, I. D., Chassaing, G., & Sagan, S. (2009). Translocation and endocytosis for cell-penetrating peptide internalization. *J Biol Chem*, 284(49), 33957-33965. doi:10.1074/jbc.M109.056309
- Jin, N., Chow, C. Y., Liu, L., Zolov, S. N., Bronson, R., Davisson, M., . . . Weisman, L. S. (2008). VAC14 nucleates a protein complex essential for the acute interconversion of PI3P and PI(3,5)P(2) in yeast and mouse. *EMBO J*, 27(24), 3221-3234. doi:10.1038/emboj.2008.248
- Jin, N., Mao, K., Jin, Y., Tevzadze, G., Kauffman, E. J., Park, S., . . . Weisman, L. S. (2014). Roles for PI(3,5)P(2) in nutrient sensing through TORC1. *Molecular Biology of the Cell*, 25(7), 1171-1185. doi:10.1091/mbc.E14-01-0021
- Jun, G., Naj, A. C., Beecham, G. W., Wang, L. S., Buros, J., Gallins, P. J., . . . Schellenberg, G. D. (2010). Meta-analysis confirms CR1, CLU, and PICALM as alzheimer disease risk loci and reveals interactions with APOE genotypes. *Arch Neurol*, 67(12), 1473-1484. doi:10.1001/archneurol.2010.201
- Jung, C. H., Jun, C. B., Ro, S. H., Kim, Y. M., Otto, N. M., Cao, J., . . . Kim, D. H. (2009). ULK-Atg13-FIP200 complexes mediate mTOR signaling to the autophagy machinery. *Mol Biol Cell*, 20(7), 1992-2003. doi:10.1091/mbc.E08-12-1249
- Jung, C. H., Ro, S. H., Cao, J., Otto, N. M., & Kim, D. H. (2010). mTOR regulation of autophagy. *FEBS Lett*, 584(7), 1287-1295. doi:10.1016/j.febslet.2010.01.017
- Jung, H. S., & Lee, M. S. (2009). Macroautophagy in homeostasis of pancreatic beta-cell. *Autophagy*, 5(2), 241-243. Retrieved from <http://www.ncbi.nlm.nih.gov/pubmed/19066457>

- Kaduszkiewicz, H., Zimmermann, T., Beck-Bornholdt, H.-P., & van den Bussche, H. (2005). Cholinesterase inhibitors for patients with Alzheimer's disease: systematic review of randomised clinical trials. *BMJ*, *331*(7512), 321-327. doi:10.1136/bmj.331.7512.321
- Kaeberlein, M., Powers, R. W., 3rd, Steffen, K. K., Westman, E. A., Hu, D., Dang, N., . . . Kennedy, B. K. (2005). Regulation of yeast replicative life span by TOR and Sch9 in response to nutrients. *Science*, *310*(5751), 1193-1196. doi:10.1126/science.1115535
- Kaether, C., Schmitt, S., Willem, M., & Haass, C. (2006). Amyloid precursor protein and Notch intracellular domains are generated after transport of their precursors to the cell surface. *Traffic*, *7*(4), 408-415. doi:10.1111/j.1600-0854.2006.00396.x
- Kamada, Y., Fujioka, Y., Suzuki, N. N., Inagaki, F., Wullschleger, S., Loewith, R., . . . Ohsumi, Y. (2005). Tor2 directly phosphorylates the AGC kinase Ypk2 to regulate actin polarization. *Mol Cell Biol*, *25*(16), 7239-7248. doi:10.1128/MCB.25.16.7239-7248.2005
- Kamath, R. S., Fraser, A. G., Dong, Y., Poulin, G., Durbin, R., Gotta, M., . . . Ahringer, J. (2003). Systematic functional analysis of the *Caenorhabditis elegans* genome using RNAi. *Nature*, *421*(6920), 231-237. doi:http://www.nature.com/nature/journal/v421/n6920/supinfo/nature01278_S1.html
- Kaminski, W. E., Orso, E., Diederich, W., Klucken, J., Drobnik, W., & Schmitz, G. (2000). Identification of a novel human sterol-sensitive ATP-binding cassette transporter (ABCA7). *Biochem Biophys Res Commun*, *273*(2), 532-538. doi:10.1006/bbrc.2000.2954
- Kaminski, W. E., Piehler, A., & Schmitz, G. (2000). Genomic organization of the human cholesterol-responsive ABC transporter ABCA7: tandem linkage with the minor histocompatibility antigen HA-1 gene. *Biochem Biophys Res Commun*, *278*(3), 782-789. doi:10.1006/bbrc.2000.3880
- Kanai, F., Liu, H., Field, S. J., Akbary, H., Matsuo, T., Brown, G. E., . . . Yaffe, M. B. (2001). The PX domains of p47phox and p40phox bind to lipid products of PI(3)K. *Nat Cell Biol*, *3*(7), 675-678. doi:10.1038/35083070
- Kang, R., Zeh, H. J., Lotze, M. T., & Tang, D. (2011). The Beclin 1 network regulates autophagy and apoptosis. *Cell Death Differ*, *18*(4), 571-580. doi:10.1038/cdd.2010.191
- Karas, G. B., Burton, E. J., Rombouts, S. A., van Schijndel, R. A., O'Brien, J. T., Scheltens, P., . . . Barkhof, F. (2003). A comprehensive study of gray matter loss in patients with Alzheimer's disease using optimized voxel-based morphometry. *Neuroimage*, *18*(4), 895-907. Retrieved from <http://www.ncbi.nlm.nih.gov/pubmed/12725765>
- Karran, E., Mercken, M., & De Strooper, B. (2011). The amyloid cascade hypothesis for Alzheimer's disease: an appraisal for the development of therapeutics. *Nat Rev Drug Discov*, *10*(9), 698-712. doi:10.1038/nrd3505
- Katona, I., Zhang, X., Bai, Y., Shy, M. E., Guo, J., Yan, Q., . . . Li, J. (2011). Distinct pathogenic processes between Fig4-deficient motor and sensory neurons. *Eur J Neurosci*, *33*(8), 1401-1410. doi:10.1111/j.1460-9568.2011.07651.x
- Katzmann, D. J., Babst, M., & Emr, S. D. (2001). Ubiquitin-dependent sorting into the multivesicular body pathway requires the function of a conserved endosomal protein sorting complex, ESCRT-I. *Cell*, *106*(2), 145-155. Retrieved from <http://www.ncbi.nlm.nih.gov/pubmed/11511343>
- Katzmann, D. J., Odorizzi, G., & Emr, S. D. (2002). Receptor downregulation and multivesicular-body sorting. *Nat Rev Mol Cell Biol*, *3*(12), 893-905. doi:10.1038/nrm973
- Kavran, J. M., Klein, D. E., Lee, A., Falasca, M., Isakoff, S. J., Skolnik, E. Y., & Lemmon, M. A. (1998). Specificity and promiscuity in phosphoinositide binding by pleckstrin homology domains. *J Biol Chem*, *273*(46), 30497-30508. Retrieved from <http://www.ncbi.nlm.nih.gov/pubmed/9804818>
- Kelly, B. M., Waheed, A., Etten, R., & Chang, P. L. (1989). Heterogeneity of lysosomes in human fibroblasts. *Molecular and Cellular Biochemistry*, *87*(2), 171-183. doi:10.1007/bf00219260
- Keyel, P. A., Mishra, S. K., Roth, R., Heuser, J. E., Watkins, S. C., & Traub, L. M. (2006). A single common portal for clathrin-mediated endocytosis of distinct cargo governed by cargo-selective adaptors. *Mol Biol Cell*, *17*(10), 4300-4317. doi:10.1091/mbc.E06-05-0421
- Kerr, J. F. R. (1970). Liver cell defecation; an electron microscope study of the discharge of lysosomal residual bodies into the intercellular space. *Amer. J. Pathol.*, *100*,99-103
- Khera, R., & Das, N. (2009). Complement Receptor 1: disease associations and therapeutic

- implications. *Mol Immunol*, 46(5), 761-772. doi:10.1016/j.molimm.2008.09.026
- Khurana, V., Lu, Y., Steinhilb, M. L., Oldham, S., Shulman, J. M., & Feany, M. B. (2006). TOR-Mediated Cell-Cycle Activation Causes Neurodegeneration in a Drosophila Tauopathy Model. *Current Biology*, 16(3), 230-241. doi:<http://dx.doi.org/10.1016/j.cub.2005.12.042>
- Kidd, M. (1963). Paired helical filaments in electron microscopy of Alzheimer's disease. *Nature*, 197, 192-193. Retrieved from <http://www.ncbi.nlm.nih.gov/pubmed/14032480>
- Kihara, A., Kabeya, Y., Ohsumi, Y., & Yoshimori, T. (2001). Beclin-phosphatidylinositol 3-kinase complex functions at the trans-Golgi network. *EMBO Rep*, 2(4), 330-335. doi:10.1093/embo-reports/kve061
- Kim, J., Huang, W. P., Stromhaug, P. E., & Klionsky, D. J. (2002). Convergence of multiple autophagy and cytoplasm to vacuole targeting components to a perivacuolar membrane compartment prior to de novo vesicle formation. *J Biol Chem*, 277(1), 763-773. doi:10.1074/jbc.M109134200
- Kim, T. W., Wu, K., Xu, J. L., McAuliffe, G., Tanzi, R. E., Wasco, W., & Black, I. B. (1995). Selective localization of amyloid precursor-like protein 1 in the cerebral cortex postsynaptic density. *Brain Res Mol Brain Res*, 32(1), 36-44. Retrieved from <http://www.ncbi.nlm.nih.gov/pubmed/7494461>
- King, G. D., Cherian, K., & Turner, R. S. (2004). X11alpha impairs gamma- but not beta-cleavage of amyloid precursor protein. *J Neurochem*, 88(4), 971-982. Retrieved from <http://www.ncbi.nlm.nih.gov/pubmed/14756819>
- King, G. D., & Scott Turner, R. (2004). Adaptor protein interactions: modulators of amyloid precursor protein metabolism and Alzheimer's disease risk? *Exp Neurol*, 185(2), 208-219. Retrieved from <http://www.ncbi.nlm.nih.gov/pubmed/14736502>
- Kirsch, K. H., Georgescu, M. M., Ishimaru, S., & Hanafusa, H. (1999). CMS: an adapter molecule involved in cytoskeletal rearrangements. *Proc Natl Acad Sci U S A*, 96(11), 6211-6216. Retrieved from <http://www.ncbi.nlm.nih.gov/pubmed/10339567>
- Kitaguchi, N., Takahashi, Y., Tokushima, Y., Shiojiri, S., & Ito, H. (1988). Novel precursor of Alzheimer's disease amyloid protein shows protease inhibitory activity. *Nature*, 331(6156), 530-532. doi:10.1038/331530a0
- Klapper, M., Ehmke, M., Palgunow, D., Böhme, M., Matthäus, C., Bergner, G., . . . Döring, F. (2011). Fluorescence-based fixative and vital staining of lipid droplets in *Caenorhabditis elegans* reveal fat stores using microscopy and flow cytometry approaches. *Journal of Lipid Research*, 52(6), 1281-1293. doi:10.1194/jlr.D011940
- Klarlund, J. K., Guilherme, A., Holik, J. J., Virbasius, J. V., Chawla, A., & Czech, M. P. (1997). Signaling by phosphoinositide-3,4,5-trisphosphate through proteins containing pleckstrin and Sec7 homology domains. *Science*, 275(5308), 1927-1930. Retrieved from <http://www.ncbi.nlm.nih.gov/pubmed/9072969>
- Klarlund, J. K., Guilherme, A., Holik, J. J., Virbasius, J. V., Chawla, A., & Czech, M. P. (1997). Signaling by phosphoinositide-3,4,5-trisphosphate through proteins containing pleckstrin and Sec7 homology domains. *Science*, 275(5308), 1927-1930.
- Klarlund, J. K., Rameh, L. E., Cantley, L. C., Buxton, J. M., Holik, J. J., Sakelis, C., . . . Czech, M. P. (1998). Regulation of GRP1-catalyzed ADP ribosylation factor guanine nucleotide exchange by phosphatidylinositol 3,4,5-trisphosphate. *J Biol Chem*, 273(4), 1859-1862.
- Koch, H. J., Uyanik, G., & Fischer-Barnicol, D. (2005). Memantine: a therapeutic approach in treating Alzheimer's and vascular dementia. *Curr Drug Targets CNS Neurol Disord*, 4(5), 499-506.
- Kojima, T., Fukuda, M., Watanabe, Y., Hamazato, F., & Mikoshiba, K. (1997). Characterization of the pleckstrin homology domain of Btk as an inositol polyphosphate and phosphoinositide binding domain. *Biochem Biophys Res Commun*, 236(2), 333-339. doi:10.1006/bbrc.1997.6947
- Koltai, T. (2014). Clusterin: a key player in cancer chemoresistance and its inhibition. *Oncotargets Ther*, 7, 447-456. doi:10.2147/OTT.S58622
- Krauß, M., & Haucke, V. (2007). Phosphoinositide-metabolizing enzymes at the interface between membrane traffic and cell signalling. *EMBO Reports*, 8(3), 241-246. doi:10.1038/sj.embor.7400919
- Kunz, J., Henriquez, R., Schneider, U., Deuter-Reinhard, M., Movva, N. R., & Hall, M. N.

- (1993). Target of rapamycin in yeast, TOR2, is an essential phosphatidylinositol kinase homolog required for G1 progression. *Cell*, 73(3), 585-596. Retrieved from <http://www.ncbi.nlm.nih.gov/pubmed/8387896>
- Lafay-Chebassier, C., Paccalin, M., Page, G., Barc-Pain, S., Perault-Pochat, M. C., Gil, R., . . . Hugon, J. (2005). mTOR/p70S6k signalling alteration by A β exposure as well as in APP-PS1 transgenic models and in patients with Alzheimer's disease. *Journal of Neurochemistry*, 94(1), 215-225. doi:10.1111/j.1471-4159.2005.03187.x
- Lai, A., Sisodia, S. S., & Trowbridge, I. S. (1995). Characterization of sorting signals in the beta-amyloid precursor protein cytoplasmic domain. *J Biol Chem*, 270(8), 3565-3573. Retrieved from <http://www.ncbi.nlm.nih.gov/pubmed/7876092>
- Lambert, J. C., Heath, S., Even, G., Campion, D., Sleegers, K., Hiltunen, M., . . . Amouyel, P. (2009). Genome-wide association study identifies variants at CLU and CR1 associated with Alzheimer's disease. *Nat Genet*, 41(10), 1094-1099. doi:10.1038/ng.439
- Lambert, J. C., Ibrahim-Verbaas, C. A., Harold, D., Naj, A. C., Sims, R., Bellenguez, C., . . . Amouyel, P. (2013). Meta-analysis of 74,046 individuals identifies 11 new susceptibility loci for Alzheimer's disease. *Nat Genet*, 45(12), 1452-1458. doi:10.1038/ng.2802
- Lammich, S., Okochi, M., Takeda, M., Kaether, C., Capell, A., Zimmer, A. K., . . . Haass, C. (2002). Presenilin-dependent intramembrane proteolysis of CD44 leads to the liberation of its intracellular domain and the secretion of an Abeta-like peptide. *J Biol Chem*, 277(47), 44754-44759. doi:10.1074/jbc.M206872200
- Lane, D., & Levine, A. (2010). p53 Research: the past thirty years and the next thirty years. *Cold Spring Harb Perspect Biol*, 2(12), a000893. doi:10.1101/cshperspect.a000893
- Laplante, M., & Sabatini, D. M. (2012). mTOR signaling in growth control and disease. *Cell*, 149(2), 274-293. doi:10.1016/j.cell.2012.03.017
- Lee, S., Sato, Y., & Nixon, R. A. (2011). Lysosomal proteolysis inhibition selectively disrupts axonal transport of degradative organelles and causes an Alzheimer's-like axonal dystrophy. *The Journal of Neuroscience*, 31(21), 7817-7830. doi:10.1523/JNEUROSCI.6412-10.2011
- Leissring, M. A., Murphy, M. P., Mead, T. R., Akbari, Y., Sugarman, M. C., Jannatipour, M., . . . LaFerla, F. M. (2002). A physiologic signaling role for the gamma -secretase-derived intracellular fragment of APP. *Proc Natl Acad Sci U S A*, 99(7), 4697-4702. doi:10.1073/pnas.072033799
- Lemmon, M. A. (2003). Phosphoinositide recognition domains. *Traffic*, 4(4), 201-213.
- Lemmon, M. A., Ferguson, K. M., O'Brien, R., Sigler, P. B., & Schlessinger, J. (1995). Specific and high-affinity binding of inositol phosphates to an isolated pleckstrin homology domain. *Proc Natl Acad Sci U S A*, 92(23), 10472-10476. Retrieved from <http://www.ncbi.nlm.nih.gov/pubmed/7479822>
- Lemmon, M. A., & Schlessinger, J. (2010). Cell signaling by receptor tyrosine kinases. *Cell*, 141(7), 1117-1134. doi:10.1016/j.cell.2010.06.011
- Letourneur, F., Gaynor, E. C., Hennecke, S., Demolliere, C., Duden, R., Emr, S. D., . . . Cosson, P. (1994). Coatamer is essential for retrieval of dilysine-tagged proteins to the endoplasmic reticulum. *Cell*, 79(7), 1199-1207. Retrieved from <http://www.ncbi.nlm.nih.gov/pubmed/8001155>
- Lev, S., Moreno, H., Martinez, R., Canoll, P., Peles, E., Musacchio, J. M., . . . Schlessinger, J. (1995). Protein tyrosine kinase PYK2 involved in Ca(2+)-induced regulation of ion channel and MAP kinase functions. *Nature*, 376(6543), 737-745. doi:10.1038/376737a0
- Levine, T. P., & Munro, S. (1998). The pleckstrin homology domain of oxysterol-binding protein recognises a determinant specific to Golgi membranes. *Curr Biol*, 8(13), 729-739. Retrieved from <http://www.ncbi.nlm.nih.gov/pubmed/9651677>
- Lewis, F., Schaffer, S.K., Sussex, J., O'Neill, P., Cockroft, L. The trajectory of dementia in the UK – making a difference. Alzheimer's Research UK and Office of Health Economics. Retrieved from <http://www.alzheimersresearchuk.org/wp-content/uploads/2015/01/OHE-report-Full.pdf>
- Li, S., Tiab, L., Jiao, X., Munier, F. L., Zografos, L., Frueh, B. E., . . . Schorderet, D. F. (2005). Mutations in PIP5K3 are associated with Francois-Neetens mouchettee fleck corneal dystrophy. *Am J Hum Genet*, 77(1), 54-63. doi:10.1086/431346
- Li, S. C., Diakov, T. T., Xu, T., Tarsio, M., Zhu, W., Couoh-Cardel, S., . . . Kane, P. M. (2014). The signaling lipid PI(3,5)P(2) stabilizes V(1)–V(o) sector interactions and activates the V-

- ATPase. *Molecular Biology of the Cell*, 25(8), 1251-1262. doi:10.1091/mbc.E13-10-0563
- Li, X., Alafuzoff, I., Soininen, H., Winblad, B., & Pei, J.-J. (2005). Levels of mTOR and its downstream targets 4E-BP1, eEF2, and eEF2 kinase in relationships with tau in Alzheimer's disease brain. *FEBS Journal*, 272(16), 4211-4220. doi:10.1111/j.1742-4658.2005.04833.x
- Li, X., Alafuzoff, I., Soininen, H., Winblad, B., & Pei, J. J. (2005). Levels of mTOR and its downstream targets 4E-BP1, eEF2, and eEF2 kinase in relationships with tau in Alzheimer's disease brain. *FEBS J*, 272(16), 4211-4220. doi:10.1111/j.1742-4658.2005.04833.x
- Li, X., Wang, X., Zhang, X., Zhao, M., Tsang, W. L., Zhang, Y., . . . Xu, H. (2013). Genetically encoded fluorescent probe to visualize intracellular phosphatidylinositol 3,5-bisphosphate localization and dynamics. *Proceedings of the National Academy of Sciences*, 110(52), 21165-21170. doi:10.1073/pnas.1311864110
- Li, Z. W., Stark, G., Götz, J., Rülcke, T., Gschwind, M., Huber, G., . . . Weissmann, C. (1996). Generation of mice with a 200-kb amyloid precursor protein gene deletion by Cre recombinase-mediated site-specific recombination in embryonic stem cells. *Proceedings of the National Academy of Sciences of the United States of America*, 93(12), 6158-6162. Retrieved from <http://www.ncbi.nlm.nih.gov/pmc/articles/PMC39206/>
- Liao, F., Zhang, T. J., Jiang, H., Lefton, K. B., Robinson, G. O., Vassar, R., . . . Holtzman, D. M. (2015). Murine versus human apolipoprotein E4: differential facilitation of and co-localization in cerebral amyloid angiopathy and amyloid plaques in APP transgenic mouse models. *Acta Neuropathol Commun*, 3, 70. doi:10.1186/s40478-015-0250-y
- Lida, S., Marcoli, R., & Bickle, T. A. (1982). Phenotypic reversion of an IS1-mediated deletion mutation: a combined role for point mutations and deletions in transposon evolution. *EMBO J*, 1(6), 755-759. Retrieved from <http://www.ncbi.nlm.nih.gov/pubmed/6329702>
- Lilienbaum, A. (2013). Relationship between the proteasomal system and autophagy. *Int J Biochem Mol Biol*, 4(1), 1-26. Retrieved from <http://www.ncbi.nlm.nih.gov/pubmed/23638318>
- Liou, W., Geuze, H. J., Geelen, M. J., & Slot, J. W. (1997). The autophagic and endocytic pathways converge at the nascent autophagic vacuoles. *J Cell Biol*, 136(1), 61-70. Retrieved from <http://www.ncbi.nlm.nih.gov/pubmed/9008703>
- Liu, S., Breitbart, A., Sun, Y., Mehta, P. D., Boutajangout, A., Scholtzova, H., & Wisniewski, T. (2014). Blocking the apolipoprotein E/amyloid beta interaction in triple transgenic mice ameliorates Alzheimer's disease related amyloid beta and tau pathology. *J Neurochem*, 128(4), 577-591. doi:10.1111/jnc.12484
- Lo, A. C., Thinakaran, G., Slunt, H. H., & Sisodia, S. S. (1995). Metabolism of the amyloid precursor-like protein 2 in MDCK cells. Polarized trafficking occurs independent of the chondroitin sulfate glycosaminoglycan chain. *J Biol Chem*, 270(21), 12641-12645. Retrieved from <http://www.ncbi.nlm.nih.gov/pubmed/7759513>
- Loewith, R., Jacinto, E., Wullschleger, S., Lorberg, A., Crespo, J. L., Bonenfant, D., . . . Hall, M. N. (2002). Two TOR complexes, only one of which is rapamycin sensitive, have distinct roles in cell growth control. *Mol Cell*, 10(3), 457-468. Retrieved from <http://www.ncbi.nlm.nih.gov/pubmed/12408816>
- Longatti, A., & Tooze, S. A. (2009). Vesicular trafficking and autophagosome formation. *Cell Death Differ*, 16(7), 956-965. doi:10.1038/cdd.2009.39
- Lopez-Sanchez, N., Muller, U., & Frade, J. M. (2005). Lengthening of G2/mitosis in cortical precursors from mice lacking beta-amyloid precursor protein. *Neuroscience*, 130(1), 51-60. doi:10.1016/j.neuroscience.2004.09.020
- Lorent, K., Overbergh, L., Moechars, D., De Strooper, B., Van Leuven, F., & Van den Berghe, H. (1995). Expression in mouse embryos and in adult mouse brain of three members of the amyloid precursor protein family, of the alpha-2-macroglobulin receptor/low density lipoprotein receptor-related protein and of its ligands apolipoprotein E, lipoprotein lipase, alpha-2-macroglobulin and the 40,000 molecular weight receptor-associated protein. *Neuroscience*, 65(4), 1009-1025. Retrieved from <http://www.ncbi.nlm.nih.gov/pubmed/7542371>
- Lukacs, G. L., Rotstein, O. D., & Grinstein, S. (1990). Phagosomal acidification is mediated by a vacuolar-type H(+)-ATPase in murine macrophages. *J Biol Chem*, 265(34), 21099-21107. Retrieved from <http://www.ncbi.nlm.nih.gov/pubmed/2147429>

- Lundberg, M., Wikstrom, S., & Johansson, M. (2003). Cell surface adherence and endocytosis of protein transduction domains. *Mol Ther*, *8*(1), 143-150.
- Lundmark, R., & Carlsson, S. R. (2010). Driving membrane curvature in clathrin-dependent and clathrin-independent endocytosis. *Semin Cell Dev Biol*, *21*(4), 363-370. doi:10.1016/j.semcdb.2009.11.014
- Lunnon, K., Sattlecker, M., Furney, S. J., Coppola, G., Simmons, A., Proitsi, P., . . . dNeuroMed, C. (2013). A blood gene expression marker of early Alzheimer's disease. *J Alzheimers Dis*, *33*(3), 737-753. doi:10.3233/JAD-2012-121363
- Lustbader, J. W., Cirilli, M., Lin, C., Xu, H. W., Takuma, K., Wang, N., . . . Wu, H. (2004). ABAD directly links Abeta to mitochondrial toxicity in Alzheimer's disease. *Science*, *304*(5669), 448-452. doi:10.1126/science.1091230
- Lyckman, A. W., Confaloni, A. M., Thinakaran, G., Sisodia, S. S., & Moya, K. L. (1998). Post-translational processing and turnover kinetics of presynaptically targeted amyloid precursor superfamily proteins in the central nervous system. *J Biol Chem*, *273*(18), 11100-11106. Retrieved from <http://www.ncbi.nlm.nih.gov/pubmed/9556595>
- Ma, T., Hoeffler, C. A., Capetillo-Zarate, E., Yu, F., Wong, H., Lin, M. T., . . . Gouras, G. K. (2010). Dysregulation of the mTOR pathway mediates impairment of synaptic plasticity in a mouse model of Alzheimer's disease. *PLoS One*, *5*(9). doi:10.1371/journal.pone.0012845
- Mackenzie, I. R., Hao, C., & Munoz, D. G. (1995). Role of microglia in senile plaque formation. *Neurobiol Aging*, *16*(5), 797-804. Retrieved from <http://www.ncbi.nlm.nih.gov/pubmed/8532113>
- Mackenzie, I. R., Hao, C., & Munoz, D. G. (1995). Role of microglia in senile plaque formation. *Neurobiol Aging*, *16*(5), 797-804.
- Magara, F., Müller, U., Li, Z.-W., Lipp, H.-P., Weissmann, C., Stagljar, M., & Wolfer, D. P. (1999). Genetic background changes the pattern of forebrain commissure defects in transgenic mice underexpressing the β -amyloid-precursor protein. *Proceedings of the National Academy of Sciences*, *96*(8), 4656-4661. doi:10.1073/pnas.96.8.4656
- Mant, R., Parfitt, E., Hardy, J., & Owen, M. (1991). Mononucleotide repeat polymorphism in the APP gene. *Nucleic Acids Res*, *19*(16), 4572. Retrieved from <http://www.ncbi.nlm.nih.gov/pubmed/1909436>
- Marambaud, P., Wen, P. H., Dutt, A., Shioi, J., Takashima, A., Siman, R., & Robakis, N. K. (2003). A CBP binding transcriptional repressor produced by the PS1/epsilon-cleavage of N-cadherin is inhibited by PS1 FAD mutations. *Cell*, *114*(5), 635-645. Retrieved from <http://www.ncbi.nlm.nih.gov/pubmed/13678586>
- March, M. E., Lucas, D. M., Aman, M. J., & Ravichandran, K. S. (2000). p135 src homology 2 domain-containing inositol 5'-phosphatase (SHIPbeta) isoform can substitute for p145 SHIP in fcgamma RIIB1-mediated inhibitory signaling in B cells. *J Biol Chem*, *275*(39), 29960-29967. doi:10.1074/jbc.M003714200
- Mari, M., Tooze, S. A., & Reggiori, F. (2011). The puzzling origin of the autophagosomal membrane. *F1000 Biol Rep*, *3*, 25. doi:10.3410/b3-25
- Martin, S., Harper, C. B., May, L. M., Coulson, E. J., Meunier, F. A., & Osborne, S. L. (2013). Inhibition of PIKfyve by YM-201636 Dysregulates Autophagy and Leads to Apoptosis-Independent Neuronal Cell Death. *PLoS One*, *8*(3), e60152. doi:10.1371/journal.pone.0060152
- Matsuda, S., Yasukawa, T., Homma, Y., Ito, Y., Niikura, T., Hiraki, T., . . . Nishimoto, I. (2001). c-Jun N-terminal kinase (JNK)-interacting protein-1b/islet-brain-1 scaffolds Alzheimer's amyloid precursor protein with JNK. *J Neurosci*, *21*(17), 6597-6607. Retrieved from <http://www.ncbi.nlm.nih.gov/pubmed/11517249>
- McMahon, H. T., & Boucrot, E. (2011). Molecular mechanism and physiological functions of clathrin-mediated endocytosis. *Nat Rev Mol Cell Biol*, *12*(8), 517-533. doi:http://www.nature.com/nrm/journal/v12/n8/supinfo/nrm3151_S1.html
- McMahon, H. T., & Boucrot, E. (2015). Membrane curvature at a glance. *Journal of Cell Science*, *128*(6), 1065-1070. doi:10.1242/jcs.114454
- McMahon, H. T., Wigge, P., & Smith, C. (1997). Clathrin interacts specifically with amphiphysin and is displaced by dynamin. *FEBS Lett*, *413*(2), 319-322. Retrieved from <http://www.ncbi.nlm.nih.gov/pubmed/9280305>
- McNew, J. A., Parlati, F., Fukuda, R., Johnston, R. J., Paz, K., Paumet, F., . . . Rothman, J. E.

- (2000). Compartmental specificity of cellular membrane fusion encoded in SNARE proteins. *Nature*, 407(6801), 153-159. doi:10.1038/35025000
- Mercer, C. A., Kaliappan, A., & Dennis, P. B. (2009). A novel, human Atg13 binding protein, Atg101, interacts with ULK1 and is essential for macroautophagy. *Autophagy*, 5(5), 649-662. Retrieved from <http://www.ncbi.nlm.nih.gov/pubmed/19287211>
- Miles, L. A., Crespi, G. A., Doughty, L., & Parker, M. W. (2013). Bapineuzumab captures the N-terminus of the Alzheimer's disease amyloid-beta peptide in a helical conformation. *Sci Rep*, 3, 1302. doi:10.1038/srep01302
- Miller, A., Schafer, J., Upchurch, C., Spooner, E., Huynh, J., Hernandez, S., . . . Fares, H. (2015). Mucopolipidosis type IV protein TRPML1-dependent lysosome formation. *Traffic*, 16(3), 284-297. doi:10.1111/tra.12249
- Mishima, Y. (1967). Lysosomes in melanin phagocytosis and synthesis. *Nature*, 216(5110), 67. Retrieved from <http://www.ncbi.nlm.nih.gov/pubmed/6050674>
- Mitchell, D. J., Kim, D. T., Steinman, L., Fathman, C. G., & Rothbard, J. B. (2000). Polyarginine enters cells more efficiently than other polycationic homopolymers. *J Pept Res*, 56(5), 318-325.
- Morton, H. J. (1970). A survey of commercially available tissue culture media. *In Vitro*, 6(2), 89-108.
- Muhammad, A., Flores, I., Zhang, H., Yu, R., Staniszewski, A., Planel, E., . . . Small, S. A. (2008). Retromer deficiency observed in Alzheimer's disease causes hippocampal dysfunction, neurodegeneration, and A β accumulation. *Proceedings of the National Academy of Sciences*, 105(20), 7327-7332. doi:10.1073/pnas.0802545105
- Mullan, M., Crawford, F., Axelman, K., Houlden, H., Lilius, L., Winblad, B., & Lannfelt, L. (1992). A pathogenic mutation for probable Alzheimer's disease in the APP gene at the N-terminus of beta-amyloid. *Nat Genet*, 1(5), 345-347. doi:10.1038/ng0892-345
- Mullan, M., Houlden, H., Windelspecht, M., Fidani, L., Lombardi, C., Diaz, P., . . . et al. (1992). A locus for familial early-onset Alzheimer's disease on the long arm of chromosome 14, proximal to the alpha 1-antichymotrypsin gene. *Nat Genet*, 2(4), 340-342. doi:10.1038/ng1292-340
- Müller, U., Cristina, N., Li, Z.-W., Wolfer, D. P., Lipp, H.-P., Rülcke, T., . . . Weissmann, C. (1994). Behavioral and anatomical deficits in mice homozygous for a modified β -amyloid precursor protein gene. *Cell*, 79(5), 755-765. doi:10.1016/0092-8674(94)90066-3
- Mullins, C., & Bonifacino, J. S. (2001). The molecular machinery for lysosome biogenesis. *Bioessays*, 23(4), 333-343. doi:10.1002/bies.1048
- Multhaup, G., Schlicksupp, A., Hesse, L., Beher, D., Ruppert, T., Masters, C. L., & Beyreuther, K. (1996). The amyloid precursor protein of Alzheimer's disease in the reduction of copper(II) to copper(I). *Science*, 271(5254), 1406-1409. Retrieved from <http://www.ncbi.nlm.nih.gov/pubmed/8596911>
- Munter, L. M., Voigt, P., Harmeier, A., Kaden, D., Gottschalk, K. E., Weise, C., . . . Multhaup, G. (2007). GxxxG motifs within the amyloid precursor protein transmembrane sequence are critical for the etiology of A β 42. *EMBO J*, 26(6), 1702-1712. doi:10.1038/sj.emboj.7601616
- Munnell, J. F., Cork, L. C. (1980). Exocytosis of residual bodies in a lysosomal storage disease. *Am J Pathol.*, 98(2):385-394.
- Murrell, J., Farlow, M., Ghetti, B., & Benson, M. D. (1991). A mutation in the amyloid precursor protein associated with hereditary Alzheimer's disease. *Science*, 254(5028), 97-99.
- Naj, A. C., Jun, G., Beecham, G. W., Wang, L. S., Vardarajan, B. N., Buross, J., . . . Schellenberg, G. D. (2011). Common variants at MS4A4/MS4A6E, CD2AP, CD33 and EPHA1 are associated with late-onset Alzheimer's disease. *Nat Genet*, 43(5), 436-441. doi:10.1038/ng.801
- National centre for Biotechnology Information. Cervical cancer tumourigenesis (GDS3233 / 209462_at). Retrieved from http://www.ncbi.nlm.nih.gov/geo/tools/profileGraph.cgi?ID=GDS3233:209462_at
- National centre for Biotechnology Information. Epidermal growth factor effect on cervical carcinoma cell line: timecourse (GDS2623 / 209462_at). Retrieved from http://www.ncbi.nlm.nih.gov/geo/tools/profileGraph.cgi?ID=GDS2623:209462_at
- Needham, B. E., Wlodek, M. E., Ciccotosto, G. D., Fam, B. C., Masters, C. L., Proietto,

- J., . . . Cappai, R. (2008). Identification of the Alzheimer's disease amyloid precursor protein (APP) and its homologue APLP2 as essential modulators of glucose and insulin homeostasis and growth. *J Pathol*, 215(2), 155-163. doi:10.1002/path.2343
- Neff, F., Flores-Dominguez, D., Ryan, D. P., Horsch, M., Schroder, S., Adler, T., . . . Ehninger, D. (2013). Rapamycin extends murine lifespan but has limited effects on aging. *J Clin Invest*, 123(8), 3272-3291. doi:10.1172/jci67674
- Newgard, C. B., An, J., Bain, J. R., Muehlbauer, M. J., Stevens, R. D., Lien, L. F., . . . Svetkey, L. P. (2009). A branched-chain amino acid-related metabolic signature that differentiates obese and lean humans and contributes to insulin resistance. *Cell Metab*, 9(4), 311-326. doi:10.1016/j.cmet.2009.02.002
- Nicholson, G., Lenk, G. M., Reddel, S. W., Grant, A. E., Towne, C. F., Ferguson, C. J., . . . Meisler, M. H. (2011). Distinctive genetic and clinical features of CMT4J: a severe neuropathy caused by mutations in the PI(3,5)P(2) phosphatase FIG4. *Brain*, 134(Pt 7), 1959-1971. doi:10.1093/brain/awr148
- Nicot, A. S., Fares, H., Payraastre, B., Chisholm, A. D., Labouesse, M., & Laporte, J. (2006). The phosphoinositide kinase PIKfyve/Fab1p regulates terminal lysosome maturation in *Caenorhabditis elegans*. *Mol Biol Cell*, 17(7), 3062-3074. doi:10.1091/mbc.E06-12-1120
- Nicot, A.-S., Toussaint, A., Tosch, V., Kretz, C., Wallgren-Pettersson, C., Iwarsson, E., . . . Laporte, J. (2007). Mutations in amphiphysin 2 (BIN1) disrupt interaction with dynamin 2 and cause autosomal recessive centronuclear myopathy. *Nat Genet*, 39(9), 1134-1139. doi:http://www.nature.com/ng/journal/v39/n9/suppinf/ng2086_S1.html
- Nielsen, E., Severin, F., Backer, J. M., Hyman, A. A., & Zerial, M. (1999). Rab5 regulates motility of early endosomes on microtubules. *Nat Cell Biol*, 1(6), 376-382. doi:http://www.nature.com/ncb/journal/v1/n6/suppinf/ncb1099_376_S1.html
- Ninomiya, H., Roch, J. M., Sundsmo, M. P., Otero, D. A., & Saitoh, T. (1993). Amino acid sequence RERMS represents the active domain of amyloid beta/A4 protein precursor that promotes fibroblast growth. *J Cell Biol*, 121(4), 879-886. Retrieved from <http://www.ncbi.nlm.nih.gov/pubmed/8491779>
- Nishimoto, I., Okamoto, T., Matsuura, Y., Takahashi, S., Okamoto, T., Murayama, Y., & Ogata, E. (1993). Alzheimer amyloid protein precursor complexes with brain GTP-binding protein G(o). *Nature*, 362(6415), 75-79. doi:10.1038/362075a0
- Nixon, R. A. (2007). Autophagy, amyloidogenesis and Alzheimer disease. *Journal of Cell Science*, 120(23), 4081-4091. doi:10.1242/jcs.019265
- Nygaard, H. B., van Dyck, C. H., & Strittmatter, S. M. (2014). Fyn kinase inhibition as a novel therapy for Alzheimer's disease. *Alzheimer's Research & Therapy*, 6(1), 8-8. doi:10.1186/alzrt238
- O'Rourke, E. J., Soukas, A. A., Carr, C. E., & Ruvkun, G. (2009). *C. elegans* Major Fats Are Stored in Vesicles Distinct from Lysosome-Related Organelles. *Cell metabolism*, 10(5), 430-435. doi:10.1016/j.cmet.2009.10.002
- Oda, K., Nishimura, Y., Ikehara, Y., & Kato, K. (1991). Bafilomycin A1 inhibits the targeting of lysosomal acid hydrolases in cultured hepatocytes. *Biochem Biophys Res Commun*, 178(1), 369-377.
- Oddo, S., Caccamo, A., Kitazawa, M., Tseng, B. P., & LaFerla, F. M. (2003). Amyloid deposition precedes tangle formation in a triple transgenic model of Alzheimer's disease. *Neurobiol Aging*, 24(8), 1063-1070.
- Odorizzi, G., Babst, M., & Emr, S. D. (1998). Fab1p PtdIns(3)P 5-kinase function essential for protein sorting in the multivesicular body. *Cell*, 95(6), 847-858. Retrieved from <http://www.ncbi.nlm.nih.gov/pubmed/9865702>
- Ogoshi, K., Hashimoto, S., Nakatani, Y., Qu, W., Oshima, K., Tokunaga, K., . . . Matsushima, K. (2011). Genome-wide profiling of DNA methylation in human cancer cells. *Genomics*, 98(4), 280-287. doi:10.1016/j.ygeno.2011.07.003
- Ohno, M., Sametsky, E. A., Younkin, L. H., Oakley, H., Younkin, S. G., Citron, M., . . . Disterhoft, J. F. (2004). BACE1 deficiency rescues memory deficits and cholinergic dysfunction in a mouse model of Alzheimer's disease. *Neuron*, 41(1), 27-33. Retrieved from <http://www.ncbi.nlm.nih.gov/pubmed/14715132>
- Okamoto, K., Hirai, S., Iizuka, T., Yanagisawa, T., & Watanabe, M. (1991). Reexamination of granulovacuolar degeneration. *Acta Neuropathol*, 82(5), 340-345.
- Opattova, A., Cente, M., Novak, M., & Filipcik, P. (2015). The ubiquitin proteasome system as

- a potential therapeutic target for treatment of neurodegenerative diseases. *Gen Physiol Biophys*, 34(4), 337-352. doi:10.4149/gpb_2015024
- Oppelt, A., Lobert, V. H., Haglund, K., Mackey, A. M., Rameh, L. E., Liestol, K., . . . Wesche, J. (2013). Production of phosphatidylinositol 5-phosphate via PIKfyve and MTMR3 regulates cell migration. *EMBO Rep*, 14(1), 57-64. doi:10.1038/embor.2012.183
- Palgunow, D., Klapper, M., & Döring, F. (2012). Dietary Restriction during Development Enlarges Intestinal and Hypodermal Lipid Droplets in *Caenorhabditis elegans*. *PLoS One*, 7(11), e46198. doi:10.1371/journal.pone.0046198
- Pan, K. Z., Palter, J. E., Rogers, A. N., Olsen, A., Chen, D., Lithgow, G. J., Kapahi, P. (2007). Inhibition of mRNA translation extends lifespan in *Caenorhabditis elegans*. *Aging Cell*, 6(1):111-9. doi:10.1111/j.1474-9726.2006.00266.x
- Pankiv, S., Clausen, T. H., Lamark, T., Brech, A., Bruun, J. A., Outzen, H., . . . Johansen, T. (2007). p62/SQSTM1 binds directly to Atg8/LC3 to facilitate degradation of ubiquitinated protein aggregates by autophagy. *J Biol Chem*, 282(33), 24131-24145. doi:10.1074/jbc.M702824200
- Patki, V., Lawe, D. C., Corvera, S., Virbasius, J. V., & Chawla, A. (1998). A functional PtdIns(3)P-binding motif. *Nature*, 394(6692), 433-434. doi:10.1038/28771
- Paul, S. P., Taylor, L. S., Stansbury, E. K., & McVicar, D. W. (2000). Myeloid specific human CD33 is an inhibitory receptor with differential ITIM function in recruiting the phosphatases SHP-1 and SHP-2. *Blood*, 96(2), 483-490. Retrieved from <http://www.ncbi.nlm.nih.gov/pubmed/10887109>
- Pearce, L. R., Huang, X., Boudeau, J., Pawlowski, R., Wullschleger, S., Deak, M., . . . Alessi, D. R. (2007). Identification of Protor as a novel Rictor-binding component of mTOR complex-2. *Biochem J*, 405(3), 513-522. doi:10.1042/BJ20070540
- Pearse, B. M. (1976). Clathrin: a unique protein associated with intracellular transfer of membrane by coated vesicles. *Proceedings of the National Academy of Sciences of the United States of America*, 73(4), 1255-1259. Retrieved from <http://www.ncbi.nlm.nih.gov/pmc/articles/PMC430241/>
- Pearse, B. M. (1987). Clathrin and coated vesicles. *The EMBO Journal*, 6(9), 2507-2512. Retrieved from <http://www.ncbi.nlm.nih.gov/pmc/articles/PMC553666/>
- Pei, J.-J., & Hugon, J. (2008). mTOR-dependent signalling in Alzheimer's disease. *Journal of Cellular and Molecular Medicine*, 12(6b), 2525-2532. doi:10.1111/j.1582-4934.2008.00509.x
- Pereira-Leal, J. B., & Seabra, M. C. (2001). Evolution of the Rab family of small GTP-binding proteins. *J Mol Biol*, 313(4), 889-901. doi:10.1006/jmbi.2001.5072
- Perez, R. G., Soriano, S., Hayes, J. D., Ostaszewski, B., Xia, W., Selkoe, D. J., . . . Koo, E. H. (1999). Mutagenesis identifies new signals for beta-amyloid precursor protein endocytosis, turnover, and the generation of secreted fragments, including Abeta42. *J Biol Chem*, 274(27), 18851-18856. Retrieved from <http://www.ncbi.nlm.nih.gov/pubmed/10383380>
- Perl, D. P. (2010). Neuropathology of Alzheimer's Disease. *The Mount Sinai Journal of Medicine, New York*, 77(1), 32-42. doi:10.1002/msj.20157
- Peterson, T. R., Laplante, M., Thoreen, C. C., Sancak, Y., Kang, S. A., Kuehl, W. M., . . . Sabatini, D. M. (2009). DEPTOR is an mTOR inhibitor frequently overexpressed in multiple myeloma cells and required for their survival. *Cell*, 137(5), 873-886. doi:10.1016/j.cell.2009.03.046
- Pfeffer, S. R. (1999). Transport-vesicle targeting: tethers before SNAREs. *Nat Cell Biol*, 1(1), E17-22. doi:10.1038/8967
- Piette, F., Belmin, J., Vincent, H., Schmidt, N., Pariel, S., Verny, M., . . . Hermine, O. (2011). Masitinib as an adjunct therapy for mild-to-moderate Alzheimer's disease: a randomised, placebo-controlled phase 2 trial. *Alzheimer's Research & Therapy*, 3(2), 1-11. doi:10.1186/alzrt75
- Pluskota, E., Dowling, J. J., Gordon, N., Golden, J. A., Szpak, D., West, X. Z., . . . Plow, E. F. (2011). The integrin coactivator Kindlin-2 plays a critical role in angiogenesis in mice and zebrafish. *Blood*, 117(18), 4978-4987. doi:10.1182/blood-2010-11-321182
- Pocha, S. M., & Wassmer, T. (2011). A novel role for retromer in the control of epithelial cell polarity. *Communicative & Integrative Biology*, 4(6), 749-751. Retrieved from <http://www.ncbi.nlm.nih.gov/pmc/articles/PMC3306349/>

- Podlisny, M. B., Tolan, D. R., & Selkoe, D. J. (1991). Homology of the amyloid beta protein precursor in monkey and human supports a primate model for beta amyloidosis in Alzheimer's disease. *Am J Pathol*, *138*(6), 1423-1435. Retrieved from <http://www.ncbi.nlm.nih.gov/pubmed/1905108>
- Ponte, P., Gonzalez-DeWhitt, P., Schilling, J., Miller, J., Hsu, D., Greenberg, B., . . . Fuller, F. (1988). A new A4 amyloid mRNA contains a domain homologous to serine proteinase inhibitors. *Nature*, *331*(6156), 525-527. doi:10.1038/331525a0
- Populo, H., Lopes, J. M., & Soares, P. (2012). The mTOR signalling pathway in human cancer. *Int J Mol Sci*, *13*(2), 1886-1918. doi:10.3390/ijms13021886
- Proitsi, P., Lee, S. H., Lunnon, K., Keohane, A., Powell, J., Troakes, C., . . . AddNeuroMed, C. (2014). Alzheimer's disease susceptibility variants in the MS4A6A gene are associated with altered levels of MS4A6A expression in blood. *Neurobiol Aging*, *35*(2), 279-290. doi:10.1016/j.neurobiolaging.2013.08.002
- Rak, A., Pylypenko, O., Durek, T., Watzke, A., Kushnir, S., Brunsveld, L., . . . Alexandrov, K. (2003). Structure of Rab GDP-dissociation inhibitor in complex with prenylated YPT1 GTPase. *Science*, *302*(5645), 646-650. doi:10.1126/science.1087761
- Rameh, L. E., Arvidsson, A., Carraway, K. L., 3rd, Couvillon, A. D., Rathbun, G., Crompton, A., . . . Cantley, L. C. (1997). A comparative analysis of the phosphoinositide binding specificity of pleckstrin homology domains. *J Biol Chem*, *272*(35), 22059-22066. Retrieved from <http://www.ncbi.nlm.nih.gov/pubmed/9268346>
- Ravetch, J. V., & Kinetic, J. P. (1991). Fc receptors. *Annu Rev Immunol*, *9*, 457-492. doi:10.1146/annurev.iy.09.040191.002325
- Reddy, A., Caler, E. V., & Andrews, N. W. (2001). Plasma membrane repair is mediated by Ca(2+)-regulated exocytosis of lysosomes. *Cell*, *106*(2), 157-169. Retrieved from <http://www.ncbi.nlm.nih.gov/pubmed/11511344>
- Ring, S., Weyer, S. W., Kilian, S. B., Waldron, E., Pietrzik, C. U., Filippov, M. A., . . . Muller, U. C. (2007). The secreted beta-amyloid precursor protein ectodomain APPs alpha is sufficient to rescue the anatomical, behavioral, and electrophysiological abnormalities of APP-deficient mice. *J Neurosci*, *27*(29), 7817-7826. doi:10.1523/JNEUROSCI.1026-07.2007
- Rizk, A., Paul, G., Incardona, P., Bugarski, M., Mansouri, M., Niemann, A., . . . Sbalzarini, I. F. (2014). Segmentation and quantification of subcellular structures in fluorescence microscopy images using Squassh. *Nat. Protocols*, *9*(3), 586-596. doi:10.1038/nprot.2014.037
<http://www.nature.com/nprot/journal/v9/n3/abs/nprot.2014.037.html#supplementary-information>
- Roch, J. M., Masliah, E., Roch-Levecq, A. C., Sundsmo, M. P., Otero, D. A., Veinbergs, I., & Saitoh, T. (1994). Increase of synaptic density and memory retention by a peptide representing the trophic domain of the amyloid beta/A4 protein precursor. *Proc Natl Acad Sci U S A*, *91*(16), 7450-7454.
- Rock, K. L., Gramm, C., Rothstein, L., Clark, K., Stein, R., Dick, L., . . . Goldberg, A. L. (1994). Inhibitors of the proteasome block the degradation of most cell proteins and the generation of peptides presented on MHC class I molecules. *Cell*, *78*(5), 761-771. doi:10.1016/S0092-8674(94)90462-6
- Rock, K. L., York, I. A., & Goldberg, A. L. (2004). Post-proteasomal antigen processing for major histocompatibility complex class I presentation. *Nat Immunol*, *5*(7), 670-677. doi:10.1038/ni1089
- Rogaev, E. I., Sherrington, R., Rogaeva, E. A., Levesque, G., Ikeda, M., Liang, Y., . . . et al. (1995). Familial Alzheimer's disease in kindreds with missense mutations in a gene on chromosome 1 related to the Alzheimer's disease type 3 gene. *Nature*, *376*(6543), 775-778. doi:10.1038/376775a0
- Rogawski, M. A., & Wenk, G. L. (2003). The neuropharmacological basis for the use of memantine in the treatment of Alzheimer's disease. *CNS Drug Rev*, *9*(3), 275-308. Retrieved from <http://www.ncbi.nlm.nih.gov/pubmed/14530799>
- Rohan de Silva, H. A., Jen, A., Wickenden, C., Jen, L. S., Wilkinson, S. L., & Patel, A. J. (1997). Cell-specific expression of beta-amyloid precursor protein isoform mRNAs and proteins in neurons and astrocytes. *Brain Res Mol Brain Res*, *47*(1-2), 147-156. Retrieved from <http://www.ncbi.nlm.nih.gov/pubmed/9221912>

- Rosen, D. R., Martin-Morris, L., Luo, L. Q., & White, K. (1989). A *Drosophila* gene encoding a protein resembling the human beta-amyloid protein precursor. *Proc Natl Acad Sci U S A*, *86*(7), 2478-2482. Retrieved from <http://www.ncbi.nlm.nih.gov/pubmed/2494667>
- Rosenberg, R. N., Green, J. B., White, C. L., 3rd, Sparkman, D. R., DeArmond, S. J., & Kepes, J. J. (1989). Dominantly inherited dementia and parkinsonism, with non-Alzheimer amyloid plaques: a new neurogenetic disorder. *Ann Neurol*, *25*(2), 152-158. doi:10.1002/ana.410250208
- Rossjohn, J., Cappai, R., Feil, S. C., Henry, A., McKinstry, W. J., Galatis, D., . . . Parker, M. W. (1999). Crystal structure of the N-terminal, growth factor-like domain of Alzheimer amyloid precursor protein. *Nat Struct Mol Biol*, *6*(4), 327-331. Retrieved from <http://dx.doi.org/10.1038/7562>
- Rusten, T. E., Rodahl, L. M., Pattni, K., Englund, C., Samakovlis, C., Dove, S., . . . Stenmark, H. (2006). Fab1 phosphatidylinositol 3-phosphate 5-kinase controls trafficking but not silencing of endocytosed receptors. *Mol Biol Cell*, *17*(9), 3989-4001. doi:10.1091/mbc.E06-03-0239
- Rutherford, A. C., Traer, C., Wassmer, T., Pattni, K., Bujny, M. V., Carlton, J. G., . . . Cullen, P. J. (2006). The mammalian phosphatidylinositol 3-phosphate 5-kinase (PIKfyve) regulates endosome-to-TGN retrograde transport. *J Cell Sci*, *119*(Pt 19), 3944-3957. doi:10.1242/jcs.03153
- Ryser, H. J., & Hancock, R. (1965). Histones and basic polyamino acids stimulate the uptake of albumin by tumor cells in culture. *Science*, *150*(3695), 501-503.
- Saalik, P., Niinep, A., Pae, J., Hansen, M., Lubenets, D., Langel, U., & Pooga, M. (2011). Penetration without cells: membrane translocation of cell-penetrating peptides in the model giant plasma membrane vesicles. *J Control Release*, *153*(2), 117-125. doi:10.1016/j.jconrel.2011.03.011
- Sabatini, D. M., Erdjument-Bromage, H., Lui, M., Tempst, P., & Snyder, S. H. (1994). RAFT1: a mammalian protein that binds to FKBP12 in a rapamycin-dependent fashion and is homologous to yeast TORs. *Cell*, *78*(1), 35-43. Retrieved from <http://www.ncbi.nlm.nih.gov/pubmed/7518356>
- Sabers, C. J., Martin, M. M., Brunn, G. J., Williams, J. M., Dumont, F. J., Wiederrecht, G., & Abraham, R. T. (1995). Isolation of a protein target of the FKBP12-rapamycin complex in mammalian cells. *J Biol Chem*, *270*(2), 815-822. Retrieved from <http://www.ncbi.nlm.nih.gov/pubmed/7822316>
- Sagne, C., & Gasnier, B. (2008). Molecular physiology and pathophysiology of lysosomal membrane transporters. *J Inherit Metab Dis*, *31*(2), 258-266. doi:10.1007/s10545-008-0879-9
- Sakamuro, D., Elliott, K. J., Wechsler-Reya, R., & Prendergast, G. C. (1996). BIN1 is a novel MYC-interacting protein with features of a tumour suppressor. *Nat Genet*, *14*(1), 69-77. doi:10.1038/ng0996-69
- Salloway, S., Sperling, R., Fox, N. C., Blennow, K., Klunk, W., Raskind, M., . . . Brashear, H. R. (2014). Two Phase 3 Trials of Bapineuzumab in Mild-to-Moderate Alzheimer's Disease. *New England Journal of Medicine*, *370*(4), 322-333. doi:10.1056/NEJMoa1304839
- Samie, M., Wang, X., Zhang, X., Goschka, A., Li, X., Cheng, X., . . . Xu, H. (2013). A TRP channel in the lysosome regulates large particle phagocytosis via focal exocytosis. *Dev Cell*, *26*(5), 511-524. doi:10.1016/j.devcel.2013.08.003
- Samie, M., Xu, H. (2014). Lysosomal exocytosis and lipid storage disorders. *J Lipid Res.*, *55*(6):995-1009. doi:10.1194/jlr.R046896.
- Sancak, Y., Bar-Peled, L., Zoncu, R., Markhard, A. L., Nada, S., & Sabatini, D. M. (2010). Regulator-Rag complex targets mTORC1 to the lysosomal surface and is necessary for its activation by amino acids. *Cell*, *141*(2), 290-303. doi:10.1016/j.cell.2010.02.024
- Sancak, Y., Peterson, T. R., Shaul, Y. D., Lindquist, R. A., Thoreen, C. C., Bar-Peled, L., & Sabatini, D. M. (2008). The Rag GTPases bind raptor and mediate amino acid signaling to mTORC1. *Science*, *320*(5882), 1496-1501. doi:10.1126/science.1157535
- Sancak, Y., Thoreen, C. C., Peterson, T. R., Lindquist, R. A., Kang, S. A., Spooner, E., . . . Sabatini, D. M. (2007). PRAS40 is an insulin-regulated inhibitor of the mTORC1 protein kinase. *Mol Cell*, *25*(6), 903-915. doi:10.1016/j.molcel.2007.03.003
- Sansanwal, P., Li, L., & Sarwal, M. M. (2015). Inhibition of intracellular clusterin attenuates

- cell death in nephropathic cystinosis. *J Am Soc Nephrol*, 26(3), 612-625.
doi:10.1681/ASN.2013060577
- Santolini, E., Puri, C., Salcini, A. E., Gagliani, M. C., Pelicci, P. G., Tacchetti, C., & Di Fiore, P. P. (2000). Numb is an endocytic protein. *J Cell Biol*, 151(6), 1345-1352. Retrieved from <http://www.ncbi.nlm.nih.gov/pubmed/11121447>
- Sarbassov, D. D., Ali, S. M., Sengupta, S., Sheen, J.-H., Hsu, P. P., Bagley, A. F., . . . Sabatini, D. M. (2006). Prolonged Rapamycin Treatment Inhibits mTORC2 Assembly and Akt/PKB. *Molecular Cell*, 22(2), 159-168.
doi:http://dx.doi.org/10.1016/j.molcel.2006.03.029
- Sbrissa, D., Ikononov, O. C., Deeb, R., & Shisheva, A. (2002). Phosphatidylinositol 5-phosphate biosynthesis is linked to PIKfyve and is involved in osmotic response pathway in mammalian cells. *J Biol Chem*, 277(49), 47276-47284. doi:10.1074/jbc.M207576200
- Sbrissa, D., Ikononov, O. C., & Shisheva, A. (1999). PIKfyve, a mammalian ortholog of yeast Fab1p lipid kinase, synthesizes 5-phosphoinositides. Effect of insulin. *J Biol Chem*, 274(31), 21589-21597. Retrieved from <http://www.ncbi.nlm.nih.gov/pubmed/10419465>
- Sbrissa, D., Ikononov, O. C., & Shisheva, A. (2000). PIKfyve lipid kinase is a protein kinase: downregulation of 5'-phosphoinositide product formation by autophosphorylation. *Biochemistry*, 39(51), 15980-15989. Retrieved from <http://www.ncbi.nlm.nih.gov/pubmed/11123925>
- Sbrissa, D., Ikononov, O. C., & Shisheva, A. (2002). Phosphatidylinositol 3-phosphate-interacting domains in PIKfyve. Binding specificity and role in PIKfyve. Endomembrane localization. *J Biol Chem*, 277(8), 6073-6079. doi:10.1074/jbc.M110194200
- Sbrissa, D., Ikononov, O. C., Fenner, H., Shisheva, A. (2008). ArPIKfyve homomeric and heteromeric interactions scaffold PIKfyve and Sac3 in a complex to promote PIKfyve activity and functionality. *J Mol Biol*, 384(4):766-79. doi:10.1016/j.jmb.2008.10.009
- Schellens, J. P. M. (1974). Ageing of mouse liver lysosomes an experimental study using indigestible marker substances. *Cell Tissue Res.*, 155:455. doi:10.1007/BF00227009
- Schmelzle, T., & Hall, M. N. (2000). TOR, a central controller of cell growth. *Cell*, 103(2), 253-262.
- Schmid, S. L., Braell, W. A., Schlossman, D. M., & Rothman, J. E. (1984). A role for clathrin light chains in the recognition of clathrin cages by 'uncoating ATPase'. *Nature*, 311(5983), 228-231. Retrieved from <http://www.ncbi.nlm.nih.gov/pubmed/6148701>
- Schmidt, A., Bickle, M., Beck, T., & Hall, M. N. (1997). The yeast phosphatidylinositol kinase homolog TOR2 activates RHO1 and RHO2 via the exchange factor ROM2. *Cell*, 88(4), 531-542. Retrieved from <http://www.ncbi.nlm.nih.gov/pubmed/9038344>
- Schnitka, T. K. (1965). Pinocytotic labeling of liver-cell lysosomes with colloidal gold: observations on the uptake of the marker, and its subsequent discharge into bile canaliculi. *Fed Proc* 24:556
- Scotto, L., Narayan, G., Nandula, S. V., Arias-Pulido, H., Subramaniam, S., Schneider, A., . . . Murty, V. V. (2008). Identification of copy number gain and overexpressed genes on chromosome arm 20q by an integrative genomic approach in cervical cancer: potential role in progression. *Genes Chromosomes Cancer*, 47(9)755-65. doi:10.1002/gcc.20577
- Seglen, P. O., & Bohley, P. (1992). Autophagy and other vacuolar protein degradation mechanisms. *Experientia*, 48(2), 158-172.
- Sehgal, S. N., Baker, H., & Vezina, C. (1975). Rapamycin (AY-22,989), a new antifungal antibiotic. II. Fermentation, isolation and characterization. *J Antibiot (Tokyo)*, 28(10), 727-732. Retrieved from <http://www.ncbi.nlm.nih.gov/pubmed/1102509>
- Seshadri, S., Fitzpatrick, A. L., Ikram, M. A., DeStefano, A. L., Gudnason, V., Boada, M., . . . Consortium, E. (2010). Genome-wide analysis of genetic loci associated with Alzheimer disease. *JAMA*, 303(18), 1832-1840. doi:10.1001/jama.2010.574
- Shackelford, D. B., Shaw, R. J. (2009). The LKB1-AMPK pathway: metabolism and growth control in tumour suppression. *Nat Rev Cancer.*, 9(8), 563-575. doi:10.1038/nrc2676
- Shaked, G. M., Chauv, S., Ubhi, K., Hansen, L. A., & Masliah, E. (2009). Interactions between the amyloid precursor protein C-terminal domain and G proteins mediate calcium dysregulation and amyloid beta toxicity in Alzheimer's disease. *FEBS J*, 276(10), 2736-2751. doi:10.1111/j.1742-4658.2009.06997.x
- Shariati, S. A., & De Strooper, B. (2013). Redundancy and divergence in the amyloid precursor protein family. *FEBS Lett*, 587(13), 2036-2045.

- doi:10.1016/j.febslet.2013.05.026
- Sherrington, R., Rogaev, E. I., Liang, Y., Rogaeva, E. A., Levesque, G., Ikeda, M., . . . St George-Hyslop, P. H. (1995). Cloning of a gene bearing missense mutations in early-onset familial Alzheimer's disease. *Nature*, *375*(6534), 754-760. doi:10.1038/375754a0
- Sherva, R., Baldwin, C. T., Inzelberg, R., Vardarajan, B., Cupples, L. A., Lunetta, K., . . . Farrer, L. A. (2011). Identification of novel candidate genes for Alzheimer's disease by autozygosity mapping using genome wide SNP data. *J Alzheimers Dis*, *23*(2), 349-359. doi:10.3233/JAD-2010-100714
- Shiota, C., Woo, J. T., Lindner, J., Shelton, K. D., & Magnuson, M. A. (2006). Multiallelic disruption of the rictor gene in mice reveals that mTOR complex 2 is essential for fetal growth and viability. *Dev Cell*, *11*(4), 583-589. doi:10.1016/j.devcel.2006.08.013
- Shisheva, A. (2001). PIKfyve: the road to PtdIns 5-P and PtdIns 3,5-P(2). *Cell Biol Int*, *25*(12), 1201-1206. doi:10.1006/cbir.2001.0803
- Shisheva, A., Sbrissa, D., & Ikononov, O. (1999). Cloning, characterization, and expression of a novel Zn²⁺-binding FYVE finger-containing phosphoinositide kinase in insulin-sensitive cells. *Mol Cell Biol*, *19*(1), 623-634. Retrieved from <http://www.ncbi.nlm.nih.gov/pubmed/9858586>
- Sigismund, S., Argenzio, E., Tosoni, D., Cavallaro, E., Polo, S., & Di Fiore, P. P. (2008). Clathrin-mediated internalization is essential for sustained EGFR signaling but dispensable for degradation. *Dev Cell*, *15*(2), 209-219. doi:10.1016/j.devcel.2008.06.012
- Sisodia, S. S., Koo, E. H., Hoffman, P. N., Perry, G., & Price, D. L. (1993). Identification and transport of full-length amyloid precursor proteins in rat peripheral nervous system. *J Neurosci*, *13*(7), 3136-3142. Retrieved from <http://www.ncbi.nlm.nih.gov/pubmed/8331390>
- Slunt, H. H., Thinakaran, G., Von Koch, C., Lo, A. C., Tanzi, R. E., & Sisodia, S. S. (1994). Expression of a ubiquitous, cross-reactive homologue of the mouse beta-amyloid precursor protein (APP). *J Biol Chem*, *269*(4), 2637-2644. Retrieved from <http://www.ncbi.nlm.nih.gov/pubmed/8300594>
- Small, D. H., Nurcombe, V., Reed, G., Clarris, H., Moir, R., Beyreuther, K., & Masters, C. L. (1994). A heparin-binding domain in the amyloid protein precursor of Alzheimer's disease is involved in the regulation of neurite outgrowth. *J Neurosci*, *14*(4), 2117-2127. Retrieved from <http://www.ncbi.nlm.nih.gov/pubmed/8158260>
- Soba, P., Eggert, S., Wagner, K., Zentgraf, H., Siehl, K., Kreger, S., . . . Beyreuther, K. (2005). Homo- and heterodimerization of APP family members promotes intercellular adhesion. *EMBO J*, *24*(20), 3624-3634. doi:10.1038/sj.emboj.7600824
- Soldati, T., Rancano, C., Geissler, H., & Pfeffer, S. R. (1995). Rab7 and Rab9 are recruited onto late endosomes by biochemically distinguishable processes. *J Biol Chem*, *270*(43), 25541-25548. Retrieved from <http://www.ncbi.nlm.nih.gov/pubmed/7592724>
- Soldati, T., Shapiro, A. D., & Pfeffer, S. R. (1995). Reconstitution of Rab9 endosomal targeting and nucleotide exchange using purified Rab9-GDP dissociation inhibitor complexes and endosome-enriched membranes. *Methods Enzymol*, *257*, 253-259. Retrieved from <http://www.ncbi.nlm.nih.gov/pubmed/8583928>
- Sollner, T., Bennett, M. K., Whiteheart, S. W., Scheller, R. H., & Rothman, J. E. (1993). A protein assembly-disassembly pathway in vitro that may correspond to sequential steps of synaptic vesicle docking, activation, and fusion. *Cell*, *75*(3), 409-418. Retrieved from <http://www.ncbi.nlm.nih.gov/pubmed/8221884>
- Spilman, P., Podlitskaya, N., Hart, M. J., Debnath, J., Gorostiza, O., Bredesen, D., . . . Galvan, V. (2010). Inhibition of mTOR by rapamycin abolishes cognitive deficits and reduces amyloid-beta levels in a mouse model of Alzheimer's disease. *PLoS One*, *5*(4), e9979. doi:10.1371/journal.pone.0009979
- Stahelin, R. V., Burian, A., Bruzik, K. S., Murray, D., & Cho, W. (2003). Membrane binding mechanisms of the PX domains of NADPH oxidase p40phox and p47phox. *J Biol Chem*, *278*(16), 14469-14479. doi:10.1074/jbc.M212579200
- Stashenko, P., Nadler, L. M., Hardy, R., & Schlossman, S. F. (1981). Expression of cell surface markers after human B lymphocyte activation. *Proc Natl Acad Sci U S A*, *78*(6), 3848-3852. Retrieved from <http://www.ncbi.nlm.nih.gov/pubmed/6973760>
- Steffen, K. K., MacKay, V. L., Kerr, E. O., Tsuchiya, M., Hu, D., Fox, L. A., . . . Kaeberlein, M. (2008). Yeast life span extension by depletion of 60s ribosomal subunits is mediated by

- Gcn4. *Cell*, 133(2), 292-302. doi:10.1016/j.cell.2008.02.037
- Stelzmann, R. A., Norman Schnitzlein, H., & Reed Murtagh, F. (1995). An english translation of alzheimer's 1907 paper, "über eine eigenartige erkankung der hirnrinde". *Clinical Anatomy*, 8(6), 429-431. doi:10.1002/ca.980080612
- Stokoe, D., Stephens, L. R., Copeland, T., Gaffney, P. R., Reese, C. B., Painter, G. F., . . . Hawkins, P. T. (1997). Dual role of phosphatidylinositol-3,4,5-trisphosphate in the activation of protein kinase B. *Science*, 277(5325), 567-570. Retrieved from <http://www.ncbi.nlm.nih.gov/pubmed/9228007>
- Stowell, M. H., Marks, B., Wigge, P., & McMahon, H. T. (1999). Nucleotide-dependent conformational changes in dynamin: evidence for a mechanochemical molecular spring. *Nat Cell Biol*, 1(1), 27-32. doi:10.1038/8997
- Stromhaug, P. E., Berg, T. O., Fengsrud, M., & Seglen, P. O. (1998). Purification and characterization of autophagosomes from rat hepatocytes. *Biochem J*, 335 (Pt 2), 217-224. Retrieved from <http://www.ncbi.nlm.nih.gov/pubmed/9761717>
- Sugarman, M. C., Yamasaki, T. R., Oddo, S., Echegoyen, J. C., Murphy, M. P., Golde, T. E., . . . LaFerla, F. M. (2002). Inclusion body myositis-like phenotype induced by transgenic overexpression of beta APP in skeletal muscle. *Proc Natl Acad Sci U S A*, 99(9), 6334-6339. doi:10.1073/pnas.082545599
- Sulem, P., Gudbjartsson, D. F., Stacey, S. N., Helgason, A., Rafnar, T., Magnusson, K. P., . . . Stefansson, K. (2007). Genetic determinants of hair, eye and skin pigmentation in Europeans. *Nat Genet*, 39(12), 1443-1452. doi:10.1038/ng.2007.13
- Sun, H., & Wolfe, J. H. (2000). Characterization of an unusual variant mRNA of human lysosomal alpha-mannosidase. *Exp Mol Med*, 32(4), 187-192. doi:10.1038/emm.2000.30
- Sun, S., Fu, J., Chen, J., Pang, W., Hu, R., Li, H., . . . Jiang, Y. (2015). ApoE type 4 allele affects cognitive function of aged population in Tianjin City, China. *Am J Alzheimers Dis Other Demen*, 30(5), 503-507. doi:10.1177/1533317514566114
- Sutton, R. B., Fasshauer, D., Jahn, R., & Brunger, A. T. (1998). Crystal structure of a SNARE complex involved in synaptic exocytosis at 2.4 Å resolution. *Nature*, 395(6700), 347-353. doi:10.1038/26412
- Svedruzic, Z. M., Popovic, K., & Sendula-Jengic, V. (2013). Modulators of gamma-secretase activity can facilitate the toxic side-effects and pathogenesis of Alzheimer's disease. *PLoS One*, 8(1), e50759. doi:10.1371/journal.pone.0050759
- Sweitzer, S. M., & Hinshaw, J. E. (1998). Dynamin undergoes a GTP-dependent conformational change causing vesiculation. *Cell*, 93(6), 1021-1029. Retrieved from <http://www.ncbi.nlm.nih.gov/pubmed/9635431>
- Swiech, L., Perycz, M., Malik, A., & Jaworski, J. (2008). Role of mTOR in physiology and pathology of the nervous system. *Biochim Biophys Acta*, 1784(1), 116-132. doi:10.1016/j.bbapap.2007.08.015
- Syntichaki, P., Troulinaki, K., Tavernarakis, N. (2007). eIF4E function in somatic cells modulates ageing in *Caenorhabditis elegans*. *Nature*, 445(7130):922-6. doi:10.1038/nature05603
- Tanzi, R. E., & Bertram, L. (2005). Twenty years of the Alzheimer's disease amyloid hypothesis: a genetic perspective. *Cell*, 120(4), 545-555. doi:10.1016/j.cell.2005.02.008
- Tanzi, R. E., McClatchey, A. I., Lamperti, E. D., Villa-Komaroff, L., Gusella, J. F., & Neve, R. L. (1988). Protease inhibitor domain encoded by an amyloid protein precursor mRNA associated with Alzheimer's disease. *Nature*, 331(6156), 528-530. doi:10.1038/331528a0
- Tebar, F., Bohlander, S. K., & Sorkin, A. (1999). Clathrin assembly lymphoid myeloid leukemia (CALM) protein: localization in endocytic-coated pits, interactions with clathrin, and the impact of overexpression on clathrin-mediated traffic. *Mol Biol Cell*, 10(8), 2687-2702. Retrieved from <http://www.ncbi.nlm.nih.gov/pubmed/10436022>
- Tee, A. R., Manning, B. D., Roux, P. P., Cantley, L. C., & Blenis, J. (2003). Tuberous sclerosis complex gene products, Tuberin and Hamartin, control mTOR signaling by acting as a GTPase-activating protein complex toward Rheb. *Curr Biol*, 13(15), 1259-1268.
- Thinakaran, G., Kitt, C. A., Roskams, A. J., Slunt, H. H., Masliah, E., von Koch, C., . . . et al. (1995). Distribution of an APP homolog, APLP2, in the mouse olfactory system: a potential role for APLP2 in axogenesis. *J Neurosci*, 15(10), 6314-6326. Retrieved from <http://www.ncbi.nlm.nih.gov/pubmed/7472397>
- Thomas, C. C., Dowler, S., Deak, M., Alessi, D. R., & van Aalten, D. M. (2001). Crystal

- structure of the phosphatidylinositol 3,4-bisphosphate-binding pleckstrin homology (PH) domain of tandem PH-domain-containing protein 1 (TAPP1): molecular basis of lipid specificity. *Biochem J*, 358(Pt 2), 287-294. Retrieved from <http://www.ncbi.nlm.nih.gov/pubmed/11513726>
- Thomson, A. W., & Woo, J. (1989). Immunosuppressive properties of FK-506 and rapamycin. *Lancet*, 2(8660), 443-444.
- Thoreen, C. C., Kang, S. A., Chang, J. W., Liu, Q., Zhang, J., Gao, Y., . . . Gray, N. S. (2009). An ATP-competitive mammalian target of rapamycin inhibitor reveals rapamycin-resistant functions of mTORC1. *J Biol Chem*, 284(12), 8023-8032. doi:10.1074/jbc.M900301200
- Timmons, L., Court, D. L., & Fire, A. (2001). Ingestion of bacterially expressed dsRNAs can produce specific and potent genetic interference in *Caenorhabditis elegans*. *Gene*, 263(1-2), 103-112.
- Timmons, L., & Fire, A. (1998). Specific interference by ingested dsRNA. *Nature*, 395(6705), 854-854. Retrieved from <http://dx.doi.org/10.1038/27579>
- Tocci, M. J., Matkovich, D. A., Collier, K. A., Kwok, P., Dumont, F., Lin, S., . . . Hutchinson, N. I. (1989). The immunosuppressant FK506 selectively inhibits expression of early T cell activation genes. *J Immunol*, 143(2), 718-726. Retrieved from <http://www.ncbi.nlm.nih.gov/pubmed/2472451>
- Tokunaga, C., Yoshino, K.-i., & Yonezawa, K. (2004). mTOR integrates amino acid- and energy-sensing pathways. *Biochemical and Biophysical Research Communications*, 313(2), 443-446. doi:<http://dx.doi.org/10.1016/j.bbrc.2003.07.019>
- Torii, M., Hashimoto-Torii, K., Levitt, P., & Rakic, P. (2009). Integration of neuronal clones in the radial cortical columns by EphA and ephrin-A signalling. *Nature*, 461(7263), 524-528. doi:10.1038/nature08362
- Toth, M. L., Sigmond, T., Borsos, E., Barna, J., Erdelyi, P., Takacs-Vellai, K., . . . Vellai, T. (2008). Longevity pathways converge on autophagy genes to regulate life span in *Caenorhabditis elegans*. *Autophagy*, 4(3), 330-338. Retrieved from <http://www.ncbi.nlm.nih.gov/pubmed/18219227>
- Tóth, M. L., Sigmond, T., Borsos, É., Barna, J., Erdélyi, P., Takács-Vellai, K., . . . Vellai, T. (2008). Longevity pathways converge on autophagy genes to regulate life span in *Caenorhabditis elegans*. *Autophagy*, 4(3), 330-338. doi:10.4161/auto.5618
- Traub, L. M., & Wendland, B. (2010). Cell biology: How to don a coat. *Nature*, 465(7298), 556-557. Retrieved from <http://dx.doi.org/10.1038/465556a>
- Tremml, P., Lipp, H.-P., Müller, U., Ricceri, L., & P. Wolfer, D. (1998). Neurobehavioral development, adult openfield exploration and swimming navigation learning in mice with a modified β -amyloid precursor protein gene. *Behavioural Brain Research*, 95(1), 65-76. doi:[http://dx.doi.org/10.1016/S0166-4328\(97\)00211-8](http://dx.doi.org/10.1016/S0166-4328(97)00211-8)
- Ullrich, O., Horiuchi, H., Bucci, C., & Zerial, M. (1994). Membrane association of Rab5 mediated by GDP-dissociation inhibitor and accompanied by GDP/GTP exchange. *Nature*, 368(6467), 157-160. doi:10.1038/368157a0
- Ullrich, O., Stenmark, H., Alexandrov, K., Huber, L. A., Kaibuchi, K., Sasaki, T., . . . Zerial, M. (1993). Rab GDP dissociation inhibitor as a general regulator for the membrane association of rab proteins. *J Biol Chem*, 268(24), 18143-18150. Retrieved from <http://www.ncbi.nlm.nih.gov/pubmed/8349690>
- Um, S. H., Frigerio, F., Watanabe, M., Picard, F., Joaquin, M., Sticker, M., . . . Thomas, G. (2004). Absence of S6K1 protects against age- and diet-induced obesity while enhancing insulin sensitivity. *Nature*, 431(7005), 200-205. doi:10.1038/nature02866
- Van Broeck, B., Chen, J. M., Treton, G., Desmidt, M., Hopf, C., Ramsden, N., . . . Rowley, A. (2011). Chronic treatment with a novel gamma-secretase modulator, JNJ-40418677, inhibits amyloid plaque formation in a mouse model of Alzheimer's disease. *Br J Pharmacol*, 163(2), 375-389. doi:10.1111/j.1476-5381.2011.01207.x
- van der Bliek, A. M., Redelmeier, T. E., Damke, H., Tisdale, E. J., Meyerowitz, E. M., & Schmid, S. L. (1993). Mutations in human dynamin block an intermediate stage in coated vesicle formation. *J Cell Biol*, 122(3), 553-563.
- van Duijn, C. M., Hendriks, L., Cruts, M., Hardy, J. A., Hofman, A., & Van Broeckhoven, C. (1991). Amyloid precursor protein gene mutation in early-onset Alzheimer's disease. *Lancet*, 337(8747), 978. Retrieved from <http://www.ncbi.nlm.nih.gov/pubmed/1678057>
- Van Nostrand, W. E., Farrow, J. S., Wagner, S. L., Bhasin, R., Goldgaber, D., Cotman, C. W.,

- & Cunningham, D. D. (1991). The predominant form of the amyloid beta-protein precursor in human brain is protease nexin 2. *Proc Natl Acad Sci U S A*, *88*(22), 10302-10306. Retrieved from <http://www.ncbi.nlm.nih.gov/pubmed/1946448>
- Van Nostrand, W. E., Schmaier, A. H., Farrow, J. S., Cines, D. B., & Cunningham, D. D. (1991). Protease nexin-2/amyloid beta-protein precursor in blood is a platelet-specific protein. *Biochem Biophys Res Commun*, *175*(1), 15-21. Retrieved from <http://www.ncbi.nlm.nih.gov/pubmed/1900151>
- Van Nostrand, W. E., Schmaier, A. H., Farrow, J. S., & Cunningham, D. D. (1990). Protease nexin-II (amyloid beta-protein precursor): a platelet alpha-granule protein. *Science*, *248*(4956), 745-748. Retrieved from <http://www.ncbi.nlm.nih.gov/pubmed/2110384>
- Van Nostrand, W. E., Schmaier, A. H., Farrow, J. S., & Cunningham, D. D. (1991). Platelet protease nexin-2/amyloid beta-protein precursor. Possible pathologic and physiologic functions. *Ann N Y Acad Sci*, *640*, 140-144. Retrieved from <http://www.ncbi.nlm.nih.gov/pubmed/1776731>
- Van Nostrand, W. E., Wagner, S. L., Farrow, J. S., & Cunningham, D. D. (1990). Immunopurification and protease inhibitory properties of protease nexin-2/amyloid beta-protein precursor. *J Biol Chem*, *265*(17), 9591-9594. Retrieved from <http://www.ncbi.nlm.nih.gov/pubmed/2112543>
- Vassar, R. (2004). BACE1: the beta-secretase enzyme in Alzheimer's disease. *J Mol Neurosci*, *23*(1-2), 105-114. doi:10.1385/JMN:23:1-2:105
- Venkateswarlu, K., Gunn-Moore, F., Oatey, P. B., Tavare, J. M., & Cullen, P. J. (1998). Nerve growth factor- and epidermal growth factor-stimulated translocation of the ADP-ribosylation factor-exchange factor GRP1 to the plasma membrane of PC12 cells requires activation of phosphatidylinositol 3-kinase and the GRP1 pleckstrin homology domain. *Biochem J*, *335* (Pt 1), 139-146. Retrieved from <http://www.ncbi.nlm.nih.gov/pubmed/9742223>
- Venkateswarlu, K., Gunn-Moore, F., Tavare, J. M., & Cullen, P. J. (1999). EGF-and NGF-stimulated translocation of cytohesin-1 to the plasma membrane of PC12 cells requires PI 3-kinase activation and a functional cytohesin-1 PH domain. *J Cell Sci*, *112* (Pt 12), 1957-1965.
- Venkateswarlu, K., Oatey, P. B., Tavare, J. M., & Cullen, P. J. (1998). Insulin-dependent translocation of ARNO to the plasma membrane of adipocytes requires phosphatidylinositol 3-kinase. *Curr Biol*, *8*(8), 463-466.
- Vezina, C., Kudelski, A., & Sehgal, S. N. (1975). Rapamycin (AY-22,989), a new antifungal antibiotic. I. Taxonomy of the producing streptomycete and isolation of the active principle. *J Antibiot (Tokyo)*, *28*(10), 721-726. Retrieved from <http://www.ncbi.nlm.nih.gov/pubmed/1102508>
- Vives, E., Brodin, P., & Lebleu, B. (1997). A truncated HIV-1 Tat protein basic domain rapidly translocates through the plasma membrane and accumulates in the cell nucleus. *J Biol Chem*, *272*(25), 16010-16017.
- von Koch, C. S., Zheng, H., Chen, H., Trumbauer, M., Thinakaran, G., van der Ploeg, L. H. T., . . . Sisodia, S. S. (1997). Generation of APLP2 KO Mice and Early Postnatal Lethality in APLP2/APP Double KO Mice. *Neurobiology of Aging*, *18*(6), 661-669. doi:10.1016/S0197-4580(97)00151-6
- von Manteuffel, S. R., Dennis, P. B., Pullen, N., Gingras, A. C., Sonenberg, N., & Thomas, G. (1997). The insulin-induced signalling pathway leading to S6 and initiation factor 4E binding protein 1 phosphorylation bifurcates at a rapamycin-sensitive point immediately upstream of p70s6k. *Mol Cell Biol*, *17*(9), 5426-5436.
- Wang, J., Ikonen, S., Gurevicius, K., Van Groen, T., & Tanila, H. (2003). Altered auditory-evoked potentials in mice carrying mutated human amyloid precursor protein and presenilin-1 transgenes. *Neuroscience*, *116*(2), 511-517. Retrieved from <http://www.ncbi.nlm.nih.gov/pubmed/12559106>
- Wang, X., Campbell, L. E., Miller, C. M., & Proud, C. G. (1998). Amino acid availability regulates p70 S6 kinase and multiple translation factors. *Biochem J*, *334* (Pt 1), 261-267.
- Wang, Y., Yamada, E., Zong, Haihong, Z., Pessin, J. E. (2015). Fyn Activation of mTORC1 stimulate the IRE1a-JNK pathway leading to cell death. *J Biol Chem.*, *290*(41):24772-83. doi:10.1074/jbc.M115.687020
- Warburton, M. J., & Wynn, C. H. (1976). Characterisation of the lysosomal heterogeneity in

- Chinese-hamster fibroblasts. *Eur J Biochem*, 65(2), 341-348.
- Wasco, W., Pettingell, W. P., Jondro, P. D., Schmidt, S. D., Gurubhagavatula, S., Rodes, L., . . . et al. (1995). Familial Alzheimer's chromosome 14 mutations. *Nat Med*, 1(9), 848. Retrieved from <http://www.ncbi.nlm.nih.gov/pubmed/7585193>
- Wassmer, T., Attar, N., Harterink, M., van Weering, J. R. T., Traer, C. J., Oakley, J., . . . Cullen, P. J. (2009). The Retromer Coat Complex Coordinates Endosomal Sorting and Dynein-Mediated Transport, with Carrier Recognition by the trans-Golgi Network. *Developmental Cell*, 17(1), 110-122. doi:10.1016/j.devcel.2009.04.016
- Waters, M. G., & Pfeffer, S. R. (1999). Membrane tethering in intracellular transport. *Curr Opin Cell Biol*, 11(4), 453-459. Retrieved from <http://www.ncbi.nlm.nih.gov/pubmed/10449330>
- Waters, M. G., Serafini, T., & Rothman, J. E. (1991). 'Coatomer': a cytosolic protein complex containing subunits of non-clathrin-coated Golgi transport vesicles. *Nature*, 349(6306), 248-251. doi:10.1038/349248a0
- Watt, S. A., Kimber, W. A., Fleming, I. N., Leslie, N. R., Downes, C. P., & Lucocq, J. M. (2004). Detection of novel intracellular agonist responsive pools of phosphatidylinositol 3,4-bisphosphate using the TAPP1 pleckstrin homology domain in immunoelectron microscopy. *Biochem J*, 377(Pt 3), 653-663. doi:10.1042/bj20031397
- Wender, P. A., Mitchell, D. J., Pattabiraman, K., Pelkey, E. T., Steinman, L., & Rothbard, J. B. (2000). The design, synthesis, and evaluation of molecules that enable or enhance cellular uptake: peptoid molecular transporters. *Proc Natl Acad Sci U S A*, 97(24), 13003-13008. doi:10.1073/pnas.97.24.13003
- Wenk, G. L. (2003). Neuropathologic changes in Alzheimer's disease. *J Clin Psychiatry*, 64 Suppl 9, 7-10. Retrieved from <http://www.ncbi.nlm.nih.gov/pubmed/12934968>
- West, M. J., Coleman, P. D., Flood, D. G., & Troncoso, J. C. (1994). Differences in the pattern of hippocampal neuronal loss in normal ageing and Alzheimer's disease. *Lancet*, 344(8925), 769-772. Retrieved from <http://www.ncbi.nlm.nih.gov/pubmed/7916070>
- Whitley, P., Reaves, B. J., Hashimoto, M., Riley, A. M., Potter, B. V., & Holman, G. D. (2003). Identification of mammalian Vps24p as an effector of phosphatidylinositol 3,5-bisphosphate-dependent endosome compartmentalization. *J Biol Chem*, 278(40), 38786-38795. doi:10.1074/jbc.M306864200
- Wigge, P., Kohler, K., Vallis, Y., Doyle, C. A., Owen, D., Hunt, S. P., & McMahon, H. T. (1997). Amphiphysin heterodimers: potential role in clathrin-mediated endocytosis. *Mol Biol Cell*, 8(10), 2003-2015. Retrieved from <http://www.ncbi.nlm.nih.gov/pubmed/9348539>
- Willem, M., Garratt, A. N., Novak, B., Citron, M., Kaufmann, S., Rittger, A., . . . Haass, C. (2006). Control of peripheral nerve myelination by the beta-secretase BACE1. *Science*, 314(5799), 664-666. doi:10.1126/science.1132341
- Wingo, S. N., Gallardo, T. D., Akbay, E. A., Liang, M., Contreras, C. M., Boren, T., . . . Castrillion, D. H. (2009). Somatic LKB1 mutations promote cervical cancer progression. *PloS ONE*, 4(4), e5137. doi:10.1371/journal.pone.0005137
- Wischik, C. M., Novak, M., Edwards, P. C., Klug, A., Tichelaar, W., & Crowther, R. A. (1988). Structural characterization of the core of the paired helical filament of Alzheimer disease. *Proc Natl Acad Sci U S A*, 85(13), 4884-4888. Retrieved from <http://www.ncbi.nlm.nih.gov/pubmed/2455299>
- Wischik, C. M., Novak, M., Thogersen, H. C., Edwards, P. C., Runswick, M. J., Jakes, R., . . . Klug, A. (1988). Isolation of a fragment of tau derived from the core of the paired helical filament of Alzheimer disease. *Proc Natl Acad Sci U S A*, 85(12), 4506-4510. Retrieved from <http://www.ncbi.nlm.nih.gov/pubmed/3132715>
- Wolfe, D. M., Lee, J.-h., Kumar, A., Lee, S., Orenstein, S. J., & Nixon, R. A. (2013). Autophagy failure in Alzheimer's disease and the role of defective lysosomal acidification. *The European journal of neuroscience*, 37(12), 1949-1961. doi:10.1111/ejn.12169
- Wolfson, C., Wolfson, D. B., Asgharian, M., M'Lan, C. E., Ostbye, T., Rockwood, K., Hogan, D. B. (2001). A reevaluation of the duration of survival after the onset of dementia. *J Engl J Med*, 344(15):1111-6. doi:10.1056/NEJM200104123441501
- Wollert, T., Wunder, C., Lippincott-Schwartz, J., & Hurley, J. H. (2009). Membrane scission by the ESCRT-III complex. *Nature*, 458(7235), 172-177. doi:10.1038/nature07836
- Wong, H. C., Mao, J., Nguyen, J. T., Srinivas, S., Zhang, W., Liu, B., . . . Zheng, J. (2000). Structural basis of the recognition of the dishevelled DEP domain in the Wnt signaling

- pathway. *Nat Struct Biol*, 7(12), 1178-1184. doi:10.1038/82047
- Wu, J. J., Liu, J., Chen, E. B., Wang, J. J., Cao, L., Narayan, N., . . . Finkel, T. (2013). Increased mammalian lifespan and a segmental and tissue-specific slowing of aging following genetic reduction of mTOR expression. *Cell reports*, 4(5), 913-920. doi:10.1016/j.celrep.2013.07.030
- Wullschleger, S., Loewith, R., Oppliger, W., & Hall, M. N. (2005). Molecular organization of target of rapamycin complex 2. *J Biol Chem*, 280(35), 30697-30704. doi:10.1074/jbc.M505553200
- Xie, L., Helmerhorst, E., Taddei, K., Plewright, B., Van Bronswijk, W., & Martins, R. (2002). Alzheimer's beta-amyloid peptides compete for insulin binding to the insulin receptor. *J Neurosci*, 22(10), RC221. doi:20026383
- Xu, M., Liu, K., Swaroop, M., Sun, W., Dehdashti, S. J., McKew, J. C., & Zheng, W. (2014). A phenotypic compound screening assay for lysosomal storage diseases. *J Biomol Screen*, 19(1), 168-175. doi:10.1177/1087057113501197
- Yang, Q., Inoki, K., Ikenoue, T., & Guan, K. L. (2006). Identification of Sin1 as an essential TORC2 component required for complex formation and kinase activity. *Genes Dev*, 20(20), 2820-2832. doi:10.1101/gad.1461206
- Yang, Z., Huang, J., Geng, J., Nair, U., & Klionsky, D. J. (2006). Atg22 recycles amino acids to link the degradative and recycling functions of autophagy. *Mol Biol Cell*, 17(12), 5094-5104. doi:10.1091/mbc.E06-06-0479
- Yla-Anttila, P., Vihinen, H., Jokitalo, E., & Eskelinen, E. L. (2009). Monitoring autophagy by electron microscopy in Mammalian cells. *Methods Enzymol*, 452, 143-164. doi:10.1016/S0076-6879(08)03610-0
- Yoshimori, T., Yamamoto, A., Moriyama, Y., Futai, M., & Tashiro, Y. (1991). Bafilomycin A1, a specific inhibitor of vacuolar-type H(+)-ATPase, inhibits acidification and protein degradation in lysosomes of cultured cells. *J Biol Chem*, 266(26), 17707-17712.
- Zeevi, D. A., Frumkin, A., & Bach, G. (2007). TRPML and lysosomal function. *Biochim Biophys Acta*, 1772(8), 851-858. doi:10.1016/j.bbadis.2007.01.004
- Zhan, Y., Virbasius, J. V., Song, X., Pomerleau, D. P., & Zhou, G. W. (2002). The p40phox and p47phox PX domains of NADPH oxidase target cell membranes via direct and indirect recruitment by phosphoinositides. *J Biol Chem*, 277(6), 4512-4518. doi:10.1074/jbc.M109520200
- Zhang, L., Sheng, R., Qin, Z. (2009). The lysosome and neurodegenerative diseases. *Acta Biochim Biophys Sin*, 41(6):437-45. doi:10.1093/abbs/gmp031.
- Zhang, X., Chow, C. Y., Sahenk, Z., Shy, M. E., Meisler, M. H., & Li, J. (2008). Mutation of FIG4 causes a rapidly progressive, asymmetric neuronal degeneration. *Brain*, 131(Pt 8), 1990-2001. doi:10.1093/brain/awn114
- Zhang, Y., Zolov, S. N., Chow, C. Y., Slutsky, S. G., Richardson, S. C., Piper, R. C., . . . Weisman, L. S. (2007). Loss of Vac14, a regulator of the signaling lipid phosphatidylinositol 3,5-bisphosphate, results in neurodegeneration in mice. *Proc Natl Acad Sci U S A*, 104(44), 17518-17523. doi:10.1073/pnas.0702275104
- Zheng, H., Jiang, M., Trumbauer, M. E., Sirinathsinghji, D. J., Hopkins, R., Smith, D. W., . . . Van der Ploeg, L. H. (1995). beta-Amyloid precursor protein-deficient mice show reactive gliosis and decreased locomotor activity. *Cell*, 81(4), 525-531.
- Zhou, L., Chavez-Gutierrez, L., Bockstael, K., Sannerud, R., Annaert, W., May, P. C., . . . De Strooper, B. (2011). Inhibition of beta-secretase in vivo via antibody binding to unique loops (D and F) of BACE1. *J Biol Chem*, 286(10), 8677-8687. doi:10.1074/jbc.M110.194860
- Zolov, S. N., Bridges, D., Zhang, Y., Lee, W. W., Riehle, E., Verma, R., . . . Weisman, L. S. (2012). In vivo, Pikfyve generates PI(3,5)P₂, which serves as both a signaling lipid and the major precursor for PI5P. *Proc Natl Acad Sci U S A*, 109(43), 17472-17477. doi:10.1073/pnas.1203106109
- Zoncu, R., Efeyan, A., & Sabatini, D. M. (2011). mTOR: from growth signal integration to cancer, diabetes and ageing. *Nat Rev Mol Cell Biol*, 12(1), 21-35. doi:10.1038/nrm3025
- Zou, J., Hu, B., Arpag, S., Yan, Q., Hamilton, A., Zeng, Y. S., . . . Li, J. (2015). Reactivation of Lysosomal Ca²⁺ Efflux Rescues Abnormal Lysosomal Storage in FIG4-Deficient Cells. *J Neurosci*, 35(17), 6801-6812. doi:10.1523/jneurosci.4442-14.2015